A Transcription Factor Guided Approach to the Generation of Pancreatic Endocrine-like Cells from Stem Cells

by

Blair Kenneth Gage

B.Sc. Honours in Biotechnology, The University of British Columbia and
The British Columbia Institute of Technology, May 2008

A THESIS SUBMITTED IN PARTIAL FULFILLMENT OF
THE REQUIREMENTS FOR THE DEGREE OF

DOCTOR OF PHILOSOPHY

in

THE FACULTY OF GRADUATE AND POSTDOCTORAL STUDIES
(Cell and Developmental Biology)

THE UNIVERSITY OF BRITISH COLUMBIA
(Vancouver)

August 2014

Abstract

Diabetes mellitus results in elevated blood glucose levels due to an insufficiency of the glucose lowering hormone insulin. In type 1 diabetes, insulin loss is due to an autoimmune destruction of the insulin producing pancreatic β-cells. One treatment for type 1 diabetes is the transplantation of cadaveric islets, although this process is limited by a lack of donor tissue. We and others are examining factors that influence the generation of new β-cells from stem cells. Specifically, the aims of this thesis were to examine the role of transcription factors in the formation of endocrine cells from stem cells. To do this, we developed a high content screening approach in human amniotic fluid stem cells to assess the effect of six pancreatic transcription factors on insulin expression. From this screen and subsequent studies, we observed that while transcription factor overexpression was capable of driving insulin expression, the resulting cells were unable to reverse diabetic hyperglycemia upon transplantation. Given the well-established developmental capacity of human embryonic stem cells (hESCs), we next characterized a novel hESC line (CA1S), which is amenable to high throughput screening and pancreatic differentiation. Using these cells, we found that the number of cells seeded into a culture system had a significant effect on the formation of endodermal, pancreatic progenitor and pancreatic endocrine cells. This effect correlated with hESC cell cycle status and resulted in the formation cells co-expressing insulin, glucagon and somatostatin. We next examined the effects of the transcription factors PAX4 and ARX on pancreatic endocrine specification. We revealed that increased PAX4 expression reduced ARX and glucagon expression leaving insulin positive cells. Reduced ARX expression by genomic editing resulted in fewer glucagon positive cells and increased PAX4 levels. Loss of ARX was also associated with an abundance of somatostatin positive cells and a partial reduction in insulin, which was rescued with re-expression of ARX adenoviral gene delivery methods. Collectively, the data presented in this thesis emphasise the role of transcription factor expression as a primary control point for the possible generation of β-cells from stem cells, which represents a potential cellular therapy for type 1 diabetes.

Preface

All studies in this thesis were conceived and designed by BK Gage, MJ Riedel, NJ Caron, JM Piret and TJ Kieffer. Portions of Chapters 1 and 7 were adapted from the following published book chapter: Gage BK, Wideman RD, Kieffer TJ (2014) Generating Pancreatic Endocrine Cells from Pluripotent Stem Cells. *Islets of Langerhans*, (2014), 2nd edn. Springer Netherlands (1). This work was written by BK Gage with revisions by RD Wideman and TJ Kieffer. SA White generated components of Figure 1.1 and JE Bruin, SE Erener, and A Asadi provided some of the images used in Figures 1.2 and 1.3.

Studies from Chapter 2 are published in the following article: Gage BK*, Riedel MJ*, Karanu F, Rezania A, Fujita Y, Webber TD, Baker RK, Wideman RD, Kieffer TJ (2010) Cellular reprogramming of human amniotic fluid cells to express insulin. *Differentiation* 80 (2-3):130-139 (2). * These authors contributed equally to this work. This work was written by MJ Riedel and BK Gage with revisions by RD Wideman and TJ Kieffer. Experiments were performed by BK Gage and MJ Riedel with assistance from TD Webber. Transplantation and tracking during *in vivo* testing of human amniotic fluid cells was performed by MJ Riedel and RD Wideman. Generation of recombinant adenoviral vectors was performed by Y Fujita, RK Baker, and TD Webber.

Studies from Chapter 3 are published in the following article: Caron NJ*, Gage BK*, O'Connor MD, Eaves CJ, Kieffer TJ, Piret JM (2013) A human embryonic stem cell line adapted for high throughput screening. *Biotechnol Bioeng* 110 (10):2706-2716 (3). * These authors contributed equally to this work. This work was written by NJ Caron and BK Gage with revisions by JM Piret, MD O'Connor, CJ Eaves and TJ Kieffer. CA1S cells were generated in the lab of Dr. James Piret. Figures 3.1 and 3.2 were generated solely by NJ Caron. Experiments associated with Figures 3.4, 3.5, 3.6 and 3.7 were performed by BK Gage.

Studies from Chapter 4 are published in the following article: Gage BK, Webber TD, Kieffer TJ (2013) Initial Cell Seeding Density Influences Pancreatic Endocrine Development During in vitro Differentiation of Human Embryonic Stem Cells. *PLoS ONE* 8 (12):e82076 (4). This work was written by BK Gage and revised by TJ Kieffer. Experiments associated with this chapter were performed by BK Gage with assistance from TD Webber. Transplantation experiments were performed with assistance from JE Bruin and JK Fox.

Studies from Chapter 5 are published in the following article: Gage BK, Baker RK, Kieffer TJ (2014) Overexpression of PAX4 Reduces Glucagon Expression in Differentiating hESCs. *Islets* (6):e29236 (5). This work was written by BK Gage with revisions by RK Baker and TJ Kieffer. Experiments associated with this chapter were performed by BK Gage. RK Baker generated the adenoviral construct.

Studies from Chapter 6 were performed by BK Gage with assistance from A Asadi. RK Baker generated the adenoviral construct. Transplantation experiments were performed with assistance from M Mojibian and S O'Dwyer. This chapter was written by BK Gage.

This thesis was written by BK Gage with editing provided by SA White, C Toselli, UH Neumann, AM D'souza, JD Johnson, and TJ Kieffer. Animal studies described in this thesis were approved by the University of British Columbia Animal Care Committee (Certificates # A07-0072, A08-0543 and A10-0260). Studies associated with stem cells were approved by the CIHR Stem Cell Oversight Committee (Certificate # 229333).

Table of Contents

List of Tables

List of Figures

List of Abbreviations

AA	activin A
ABCC8 (SUR1)	ATP-binding cassette, sub-family C (CFTR/MRP), member 8
aCGH	array comparative genomic hybridization
Ad	adenovirus serotype V
ALK5	TGF-β type 1 receptor kinase
APC	allophycocyanin
ARX	aristaless related homeobox
ARX ko	aristaless related homeobox knock out
BCBC	beta cell biology consortium
bFGF	basic fibroblast growth factor
BMP	bone morphogenetic protein
BRN4 (POU3F4)	POU class 3 homeobox 4
BSA	bovine serum albumin
cAMP	cyclic adenosine monophosphate
CD	cluster of differentiation
cDNA	complementary deoxyribonucleic acid
CDX2	caudal type homeobox 2
CMV	cytomegalovirus
c-MYC	v-myc avian myelocytomatosis viral oncogene homolog
CV	coefficient of variation
CXCR4	chemokine (C-X-C motif) receptor 4
CYC	cyclopamine
DAPT	N-[N-(3,5-Difluorophenacetyl)-L-alanyl]-S-phenylglycine t-butyl ester
DMEM/F12	Dulbecco's modified eagle's medium / Ham's F-12 nutrient mixture
DMSO	dimethyl sulfoxide
DNA	deoxyribonucleic acid
dNTP	deoxynucleotide triphosphate

DSRE	DsRed Express
EDTA	ethylenediaminetetraacetic acid
EGF	epidermal growth factor
eGFP	enhanced green fluorescent protein
FBS	fetal bovine serum
FGF4	fibroblast growth factor 4
FGF7	fibroblast growth factor 7
FGF10	fibroblast growth factor 10
FOXA2	forkhead box A2
FOXO1	forkhead box O1
GAPDH	glyceraldehyde-3-phosphate dehydrogenase
GATA4	GATA binding protein 4
GATA6	GATA binding protein 6
GCK	glucokinase (hexokinase 4)
GLP1	glucagon like peptide 1
GLUT2 (SLC2A2)	solute carrier family 2 (facilitated glucose transporter), member 2
hAF	human amniotic fluid
HEPES	2-[4-(2-hydroxyethyl)piperazin-1-yl]ethanesulfonic acid
hESC(s)	human embryonic stem cells
HGF	hepatocyte growth factor
HHEX	hematopoietically expressed homeobox
hIP	human insulin promoter
HLA	human leukocyte antigen
HNF4α	hepatocyte nuclear factor 4, alpha
HNF1β	hepatocyte nuclear factor 1, beta
HPAP	human placental alkaline phosphatase
HPRT	hypoxanthine-guanine phosphoribosyltransferase
HTS	high throughput screening
IBMX	3-isobutyl-1-methylxanthine
IGF-1	insulin like growth factor 1

iPSC(s)	induced pluripotent stem cells
IRX1	iroquois related homeobox 1
IRX2	iroquois related homeobox 2
ISL1	ISL LIM homeobox 1
KCl	potassium chloride
KIR6.2 (KCNJ11)	potassium inwardly-rectifying channel, subfamily J, member 11
KLF4	kruppel-like factor 4
LADA	latent autoimmune diabetes of adults
LIN28	lin-28 homolog
MAFA	v-maf Avian musculoaponeurotic fibrosarcoma oncogene homolog A
MAFB	v-maf Avian musculoaponeurotic fibrosarcoma oncogene homolog B
Mb	mega base
mESC(s)	mouse embryonic stem cells
$MgCl_2$	magnesium chloride
MNX1	motor neuron and pancreas homeobox 1
MODY	maturity onset diabetes of the young
MOI	multiplicity of infection
mRNA	messenger ribonucleic acid
NAD(P)H	nicotinamide adenine dinucleotide phosphate
NANOG	nannog homeobox
NET-4	netrin-4
NEUROD1	neuronal differentiation 1
NGN3	neurogenin 3
NKX2.1	NK2 homeobox 1
NKX2.2	NK2 homeobox 2
NKX6.1	NK6 homeobox 1
NOG	noggin
OCT4 (POU5f1)	POU class 5 homeobox 1

ORF	open reading frame
PAX4	paired box 4
PAX6	paired box 6
PBS-	phosphate buffered saline without calcium or magnesium chloride
PBX1	pre-B-cell leukemia homeobox 1
PCNA	proliferating cell nuclear antigen
PCSK1 (PC1/3)	proprotein convertase subtilisin/kexin type 1
PCSK2 (PC2)	proprotein convertase subtilisin/kexin type 2
PDX1	pancreatic and duodenal homeobox 1
PE	R-phycoerythrin
PFA	paraformaldehyde
PFU	plaque forming unit
PKC	protein kinase C
pRb	phosphorylated Retinoblastoma protein
PREP1 (PKNOX1)	PBX/knotted 1 homeobox 1
PROX1	prospero homeobox 1
PSC(s)	pluripotent stem cells
PTF1A	pancreas specific transcription factor, 1a
RA	retinoic acid
RBGI	rabbit beta-globin first intron
RPMI	Roswell park memorial institute medium
RNA	ribonucleic acid
RT-qPCR	reverse transcriptase quantitative polymerase chain reaction
SCNT	somatic cell nuclear transfer
Shh	sonic hedgehog
SOX2	sex determining region Y - box 2
SOX4	sex determining region Y - box 4
SOX7	sex determining region Y - box 7
SOX9	sex determining region Y - box 9
SOX17	sex determining region Y - box 17

SSEA1	stage specific embryonic antigen-1
SSEA3/4	stage specific embryonic antigen-3/4
STZ	streptozotocin
T	brachyury homolog (mouse)
TGF-β	transforming growth factor β
VEGF-A	vascular endothelial growth factor A
WNT	wingless-int
WT	wild type
XLAG	X-linked lissencephaly with ambiguous genitalia
ZFN	zinc finger nuclease

Acknowledgements

The journey from high school to a PhD has been a long and tortuous route. There have been countless twists and turns punctuated with challenges where failure was not an option. My path started out simple, where my academic challenges were to simply to achieve an A in my academic courses. Over time (much time), the academic challenges in my path developed exponentially to the level of making accurate and precise predictions of previously unknown human developmental pathways. It has been only in this last stage that I have come to realize that failure is not necessarily negative, but an enlightening and illuminating option that is often required to succeed. Along the way I have been tremendously supported and moulded by friends, family, and colleagues through constructive criticism, helpful suggestions and critical advice about my academic career to shape the researcher I have become today.

I first want to thank my PhD supervisor, Dr. Timothy Kieffer. In January of 2007 you gave me an opportunity to explore the exciting field of stem cells and regenerative medicine as a naïve co-op student being co-supervised by Dr. Michael Riedel. Since this time I have never looked back. Throughout my PhD you have pushed me and others in the lab to try and understand the "why" of our research questions. For this influence, and allowing me to ask "why" for nearly any question that I have been truly interested in, I will always be grateful.

I also thank my advisory committee: Dr. James Piret, Dr. James Johnson and Dr. T. Michael Underhill, for your efforts to keep my research focused and for providing advice and mentorship throughout this process. I am grateful to my sources of graduate school salary funding which included the Natural Sciences and Engineering Research Council, Michael Smith Foundation for Health Research and the University of British Columbia. I must also thank Dr. J' Nelle Young, Dr. Lien Vo, Dr. Claudia Krebs, Dr. Karen Pinder, Dr. Dawn Cooper, Dr. Geoffrey Noel, Dr. Pawel Kindler and Dr. Wayne Vogl for providing me the opportunity to teach (while learning from scratch) gross anatomy and histology, giving me the opportunity to be a TA in the UBC medical program, and for igniting my passion for teaching.

During my time in the Kieffer lab I have had the pleasure and great fortune to spend time with many lab mates both past and present. The graduate students, post docs, research

associates and technical guru's that have all directly influenced how I think and undertake research: Frank, Gary, Mike, Irene, Jasna, Cathy, Heather, Ursula, Anna, Michelle, Chiara, Yukihiro, Sarah, Rhonda, Scott, Michael, Young, Majid, Jenny, Maria, Suheda, Eva, Sandra, Jessica, and Shannon. I also thank Ali for his years of mentorship in immunofluorescence, and Rob for his similar dedication to ensuring and challenging my understanding of molecular biology. I thank Travis for instilling order in my record keeping and working so hard to keep the lab running smoothly. Without all of these people above, I would not be the type of researcher I am today.

I also must thank the many friends outside the Kieffer lab who have brought both variety and camaraderie to many an RBT. It is remarkable to me how many collaborations have been forged well outside the lab, over a beer or two.

To my parents, I really can't express my appreciation for your love and support. Both of you have shown me how to struggle through the challenges of life with a smile and never give up on a dream. To my mother, your fight with type 1 diabetes is the reason why I chose this field of study. I only hope that someday you will see the day when type 1 diabetes is a diagnosis that doesn't come with a life-time supply of needles.

Finally, I thank my wife Sarah, for supporting me unconditionally at every step of this process. I was lucky enough to meet someone just down the hall that understood grad school, diabetes, the real world and apparently me. While we may not know what the future holds, I know that it will be an exciting adventure for both of us.

To the β-cells of Susan Gage,
something lost... but not forgotten

Chapter 1: Introduction

1.1 Diabetes Mellitus

Diabetes mellitus is a metabolic disease that is broadly characterized by elevated blood glucose levels due to a relative decrease or absolute loss of the glucose-lowering hormone insulin. World-wide, it is estimated that 382 million people currently have diabetes with numbers expected to grow to 592 million by the year 2035 (6). In 2011, the Canadian Diabetes Association reported that more than 9 million Canadians live with diabetes or prediabetes, with the number of new cases growing at a rate of 20 people per hour in Canada (7). By 2013, the International Diabetes Federation estimated approximately 10% of Canadians have diabetes (6). This rise in incidence brings a mounting cost to the Canadian health care system, with costs expected to reach $16.9 billion per year by 2020 (7). These growing human and economic costs of diabetes are cumulatively associated with type 2 diabetes, which accounts for ~90 % of all diabetic cases, and type 1 diabetes, which accounts for most of the remaining 10 % of diabetic cases (8).

Diabetes is divided into general categories according to disease state and pathophysiology. The most common form, type 2 diabetes, is most often diagnosed in adulthood due to hyperglycemia associated with progressive insulin resistance and inadequate insulin secretion from pancreatic β-cells (8, 9). Over time, high demands on insulin production and release lead to β-cell exhaustion and loss of functional endocrine cells mass (9) that can transition patients from oral therapies to injectable insulin analogs. Gestational diabetes is similar to type 2 diabetes in that it is generally characterized by insulin insufficiency without a loss of β-cells although gestational diabetes is generally temporary and occurs during 2-4 % of all pregnancies (6, 8). The most severe form of diabetes is type 1 diabetes, which is generally diagnosed at a young age and occurs when there is an autoimmune mediated destruction of insulin producing pancreatic β-cells resulting in uncontrolled hyperglycemia (6, 8). This targeted loss of β-cells is mediated by autoreactive CD8 positive T-cells through incompletely understood mechanisms including a number of genetic elements that are believed to influence susceptibility (HLA and insulin genes, PTPN22, IL2 receptor α, CTLA-4 and others) and specific triggers that may stimulate disease progression (enterovirus, rotavirus and bacterial infections, milk and wheat proteins, Vitamin D and others) (10). While the cause(s) of type 1 diabetes continue to be actively

explored, the universal treatment continues to be the simple replacement of the hormone insulin by injection.

In 1923, Canadian scientists Banting and Macleod shared the Nobel Prize for the discovery of the hormone insulin based on work that was published in 1922 (11). With this discovery, and the effects of insulin to lower blood glucose levels, a life-saving treatment option was born that continues to be utilized by patients with type 1 diabetes worldwide. While the exogenous administration of insulin dramatically improves quality of life, recreating the physiological regulation of blood glucose levels with this method is virtually impossible. Patients continue to suffer from debilitating complications including cardiovascular disease, kidney disease, eye disease and nerve damage (6, 12). Moreover, even when blood glucose levels are tightly controlled with insulin injections, patients are at an increased risk of potentially fatal hypoglycemic episodes due to an inability to decrease the action of injected insulin once blood glucose levels have been lowered (13, 14). This effect has lead many researchers to focus on treatment options that would provide a cellular origin of insulin release that can mimic the natural secretion rhythms and kinetics of the pancreatic β-cell.

1.2 Human Islet Transplantation

The pancreatic endocrine structure known as the Islet of Langerhans is a collection of hormone producing cells including the α-cells, β-cells, δ-cells, ε-cells and PP-cells, which secrete the hormones glucagon, insulin, somatostatin, ghrelin and pancreatic polypeptide, respectively, into the surrounding vasculature system. The isolation of pancreatic islets from rodents was developed by Lacy and Kostianovsky with the application of early enzymatic isolation methods (15, 16). Eventually, similar methods were developed and adapted to human cadaveric islet isolation and islet transplantation. Islet transplantation, in conjunction with specific anti-rejection therapies, was shown to successfully restore physiological blood glucose control in patients with type 1 diabetes (17). The success of this trial, lead to great interest in islet transplantation as a curative approach for type 1 diabetes. Seven patients regained insulin-independence and normal blood glucose control for up to one year following a relatively simple infusion of human islet cells into the hepatic circulation. Subsequent follow-up on this group of patients and others revealed that insulin independence upon islet

transplantation was not sustainable for the majority of patients over a five year time period (18). While insulin independence was maintained in only 10% of these patients, 80% had detectable C-peptide levels indicating that islet grafts were still partially functional. The continued presence of C-peptide in islet grafts may explain why these patients experienced fewer hypoglycemic events and had improved overall blood glucose control compared to patients treated by insulin injection alone (18-21). Despite a poor rate of sustained insulin independence, the clinical benefits of islet transplantation, as well as the continuing goal of improving the durability of islet transplants has lead to a number of islet transplantation programs being set up around the world as part of over 80 clinical trials (21, 22). However, these programs continue to be constrained by a significant lack of cadaveric islet tissue available for transplant, particularly considering that most recipients require multiple, independent islet preparations to achieve initial insulin independence.

1.3 Alternative Sources of Insulin Producing Cells

Generating novel sources of functional insulin-secreting cells to augment islet transplantation approaches has been the topic of a number of many reviews and articles. In general, to be considered functional these novel cells need a single characteristic, namely the ability to release processed bioactive insulin acutely in response to physiologically relevant blood glucose concentrations. Beyond the cellular mechanics of this functional aspect of insulin release, one of the most researched questions is where to obtain or generate novel insulin producing cells. While a number of groups favour the use of xenogenic sources of islets, most notably islets of porcine origin that are currently in clinical trials (23), the majority of the search for new sources of β-cells is focused on endodermal origin cell types and various stem cell populations. Overall these studies have focused on either stimulating existing β-cells to replicate, or to generate novel populations of β-cells from other tissue sources. These have included cells from the pancreas itself (ductal, acinar, pancreatic stem cells, and α-cells), other adult tissues (liver, intestine, and bone marrow), fetal tissues (umbilical cord blood, and amniotic epithelium/fluid), and pluripotent stem cell populations (24-29). To provide a background for the work described in this thesis, a brief description of these aspects of possible sources of insulin producing cells is provided below.

1.3.1 Generating β-cells from Pancreatic Cells and Replication of β-cells

The most obvious method to generate more β-cells is mitosis of pre-existing β-cells. Since β-cells are thought to proliferate in response to physiological stressors such as pregnancy and obesity it is possible that the application of either *ex vivo* or *in vivo* stimulation of β-cell replication could yield a novel source of transplantable cells (30). This idea was exemplified most notably by Dor et al. (2004) who employed a lineage tracing strategy to track the origins of new β-cells in young mice. Using a tamoxifen-inducible Cre-recombinase transgene driven from the rat insulin 2 promoter, the authors genetically tagged insulin positive β-cells with a human placental alkaline phosphatase (HPAP) reporter. In response to a 70% pancreatectomy, HPAP labelled β-cells were not diluted in numbers suggesting that the formation of new β-cells from non-β-cell origins was minimal compared to the amounts of β-cell replication (31). These data correlate well with other work from the same group that found under conditions of 70-80% β-cell loss, the remaining β-cells undergo replication (32). It should be noted that both of these studies did not preclude the formation of new β-cells from other cell sources under conditions of extreme β-cell stress.

The pancreas is also suggested to contain *ex vivo* isolatable multipotent pancreatic precursor cells which can be obtained from adult human and mouse pancreatic tissues (33, 34). These precursor cells are reported to have the ability to expand in culture and, under appropriate *in vitro* conditions, develop into insulin-positive cells capable of ameliorating diabetes when transplanted into chemically diabetic mice (34). While the origins and utility of these precursors are not fully understood, their pancreatic developmental origin (PDX1 positive lineage) suggest that they may represent a subpopulation of pancreatic ductal cells given that at least some of these precursors are reported to originate from ductal cell fractions (34). This notion follows studies by the Boner-Weir group, which reported that both insulin positive β-cells and exocrine cells could originate from carbonic anhydrase II positive ductal cells (35). It is also possible that the pancreatic precursors lie somewhere along the gastrin and epidermal growth factor (EGF)-sensitive exocrine-ductal-endocrine conversion continuum championed by the Bouwens group (36-38). However, it should be noted that a ductal cell origin of neogenic β-cells may not occur during the postnatal period in adult mice. Complementary studies by the Sander and Ferrer groups have shown that during pancreatic duct ligation in adult mice, SOX9-positive (39) or HNF1β-positive (40) ductal cells give rise

to new ductal cells but not insulin positive lineages. This was despite the activation of NGN3 expression in the ductal compartment after ligation which suggests that adult ductal cells may be able to only partially activate a proendocrine developmental program under these conditions (39). Even when β-cells were chemically ablated by alloxan treatment followed by EGF and gastrin administration to induce β-cells neogenesis in adult mice, the ductal cell lineage did not contribute significantly to the new β-cells (40). Using a more forceful genetic approach, one report examined the potential of exocrine pancreatic cells to generate insulin positive cells upon overexpression of PDX1, NGN3, and MAFA (41). Indeed in this study by Melton's group, lineage analysis of carboxypeptidase A1 positive adult exocrine cells which induced expression of insulin and were capable of reversing diabetic hyperglycemia in mice. Taken together these studies suggest that adult exocrine tissue, embryonic ductal tissue and pancreatic precursor populations, may offer cell populations amenable to the generation of new β-cells.

Remarkably, other cells that reside within the pancreatic endocrine compartment seem to have the ability to generate new β-cells in response to stress. Specifically, the ability of pancreatic α-cells to transdifferentiate into functional β-cells has recently been noted as a potential novel mechanism to form new β-cells. Using a model of highly efficient β-cell loss (99.6% reduction), Thorel et al. found that over the 10 months following β-cell loss, some mice were able to expand their β-cell mass sufficiently to normalize their blood glucose levels. The origin of at least some of these new insulin-positive cells was reported to include once glucagon-positive cells that transdifferentiated through an insulin-glucagon co-positive state to insulin-positive cells in response to the stress of extreme β-cell loss (42). While this developmental trajectory remains speculative and does not exclude the simultaneous origin of new insulin-positive cells from ductal, exocrine or other endocrine cells, the potential plasticity of α-cells under physiological conditions is remarkable. Indeed, this work by Thorel et al. follows forced transdifferentiation studies that revealed α-cells can be reprogrammed to insulin positive cells by overexpression of the transcription factor PAX4, while new α-cells seemingly arise from neighbouring ductal compartments (43).

1.3.2 Generating β-cells from Non-Pancreatic Cells

The transdifferentiation of non-pancreatic tissues, such as liver and intestinal tissue, represents another potential alternative source of new β-cells (28). Adenoviral gene delivery forcing the expression of NEUROD1 with betacellulin or PDX1 alone stimulated the formation of insulin in liver cells and in some cases, was reported to reverse chemically-induced diabetes (44-46). The ability to generate sufficiently functional insulin producing cells from a non-pancreatic endodermal tissue was also seen when the transcription factor FOXO1 was knocked out of NGN3 positive enteroendocrine progenitor cells. Remarkably, the intestines of these mice were found to contain insulin positive cells that were able to secrete insulin in response to a variety of stimuli and could protect against chemically-induced diabetic hyperglycemia (47). In a more recent study, the same cocktail seen previously to induce insulin expression in acinar tissue (PDX1, NGN3 and MAFA) was found to generate functional insulin positive clusters near the crypts of intestinal tissue when the factors were temporarily expressed (48). As a general concept, these studies and a number of others suggest that especially in endodermal tissues, transdifferentiation between cell types and the generation of newly functional β-cells is possible. However, it remains to be seen if any of these strategies can move beyond questions of the developmental competency of cell populations toward the clinically relevant generation of transplantable β-cells.

1.3.3 Fetal Stem Cell Sources

Cell populations available from fetal tissue sources often retain developmental plasticity without some of the usage limitations associated with embryonic and pluripotent cells. Some examples include human amniotic fluid and amniotic membrane cells. These highly proliferative cells have been shown to express a variety of embryonic markers and retain clonal multi-lineage differentiation capacity (adipogenic, osteogenic, myogenic, endothelial, neuronal, pulmonary, cardiac, pancreatic and hepatic) without the formation of teratomas *in vivo* (49, 50). Indeed, in our studies and others, the overexpression of pancreatic transcription factors in human and nonhuman primate amniotic fluid cells was able to induce expression of insulin as well as a number of other pancreatic lineage markers (2, 51). While other fetal derived cell populations including bone marrow stromal cells and umbilical cord

derived cells may offer future sources of β-cells, the most promising aspects of these populations seem to be associated with their natural immunosuppressive attributes (27). Specifically, adult bone marrow derived cells have been associated with increased levels of insulin and reduced levels of diabetic hyperglycemia, which is believed to be due to a natural homing mechanism of these cells to the site of cellular injury, followed by stimulation of endogenous β-cell regeneration (52, 53). A similar mechanism could prove to be true for fetal derived tissues including amniotic fluid/membrane cells, umbilical cord cells, or bone marrow cells, although a considerable amount of research in this field is yet to be done.

1.3.4 Pluripotent Stem Cells

One of the key challenges regarding the experimental generation of β-cells from the various postulated sources is first assessing whether the cell source is capable of forming β-cells. A considerable amount of research in the field of regenerative medicine is focused on pluripotent cells that, by definition, have the capacity to form all cells of the body. This broad ability to form cells of all three embryonic germ layers has become a foundational aspect of embryonic developmental biology and has been critical to most of the work described in this thesis. Given the relevance of this topic, a brief background regarding the origins of some relevant pluripotent stem cell types is described below.

While the study of pluripotency began in the early 1950s and 1960s with embryonal carcinoma cells (54, 55), it was not until 1981 that the first karyotypically normal mouse embryonic stem cells (mESCs) were isolated from the inner cell mass of cultured blastocysts (56, 57). Seventeen years after the isolation of mESCs, the derivation of human embryonic stem cells (hESCs) was first reported (58). Together, the generation of mESCs and hESCs has provided a benchmark definition of the properties that are required to define a cell as a pluripotent stem cell (PSC) and more importantly the experimental conditions that must be met to define a cell as pluripotent. The expression of key transcription factors such as OCT4, NANOG, and SOX2 as well as surface markers such as TRA-1-60, TRA-1-81, and SSEA3/4 in humans (SSEA1 in mice) is associated with the pluripotent phenotype (59, 60). Since the definition of pluripotency is functional in nature, assays to test this capacity both *in vitro* and *in vivo* have been developed to assess the ability to form cells from each of the three embryonic germ layers. These assays include embryoid body differentiation *in vitro* and

teratoma formation *in vivo* (61) and form the foundation of establishing a cell population as being pluripotent.

The development of PSCs took a dramatic step forward in 2006 with the report of induced pluripotent stem cells (iPSCs). In this work, combinatorial screening revealed that retrovirus mediated expression of OCT4, SOX2, c-MYC and KLF4 was sufficient to reprogram mouse fibroblasts into cells resembling mESCs (62). This approach was quickly extended to the reprogramming of human fibroblasts (63) and independently validated in another screen identifying OCT4, SOX2, NANOG, and LIN28 as being capable of reprogramming human somatic cells to iPSCs (64). Further studies have recapitulated this reprogramming process with even fewer factors delivered using a variety of technologies including adenoviruses, plasmids, transposons, mRNAs, proteins and even solely with small molecules (65-67). Assuming that efficient differentiation protocols exist, iPSCs derived from these methods make it theoretically possible to generate a cellular therapy for a specific disease state from PSC-derived cells that are immunologically specific to an individual patient (68). Whether such an immunological patient match provides any advantages for autoimmune diseases, such as type 1 diabetes, remains to be determined. Nevertheless, their utility for studying disease mechanisms and treatments is clearly evident.

Interestingly, the type of cell used to generate the iPSC line seems to have an effect on the resulting final product, most notably when mature specialized cell types are used as a starting material for iPSC generation. Reprogramming mature human cell types has been observed in a number of systems including both mouse and human adult β-cells (69, 70). While the reprogramming process was able to induce pluripotency, the conversion was incomplete in some aspects and the resulting iPSCs seemed to retain some legacy of their origin. Upon differentiation back to β-cells, iPSCs derived from insulin positive cells expressed higher amounts of insulin than did iPSCs derived from non-insulin positive pancreatic cells (69). This predisposition toward the somatic cell type of origin was attributed to the similar genomic DNA methylation patterns observed in human β-cells and β-cell derived iPSCs, which were not fully converted to undifferentiated PSC patterns during the reprogramming process (69).

One of the more recent advances in human PSC generation is the application of somatic cell nuclear transfer (SCNT). In this process, an unfertilized oocyte has its nucleus

removed and replaced with the nucleus of a differentiated diploid somatic cell. Upon microinjection into the oocyte and parthogenetic activation, the maternal contents of the cell elicit epigenetic changes in the somatic nucleus resulting in a diploid zygote free from the fertilization process. The SCNT method has allowed the cloning of domestic livestock such as the famed sheep "Dolly" (71). After ten years of additional research, the first nonhuman primate derived ESCs were produced, albeit at very low efficiencies (72). This process was finally extended to fetal and infant human donor cells by Tachibana et al. who were able to achieve SCNT with human recipient oocytes and subsequently generate hESC lines from the developing blastocytsts (73). Recently, this work was applied to adult donor cells as hESC lines were generated from 35 and 75 year old male dermal fibroblasts suggesting that this technique may not be restricted by the age of the donor tissue (74). Additionally one study reported the generation of hESCs derived from an adult female patient with type 1 diabetes using SCNT which retained the ability to generate PDX-1 and insulin positive cells upon *in vitro* differentiation (75). These studies represent a key milestone in efforts to develop patient specific PSCs as SCNT may offer more complete reprogramming of somatic cells without significant epigenetic legacy marks compared to iPSCs. If so, SCNT could allow efficient, patient-specific PSC generation with the reproducible differentiation capacity required for regenerative medicine applications.

Regardless of which PSC population is chosen to be used in the formation of pancreatic cells, the differentiation process has two primary goals. These are: 1) to generate functional insulin secreting cells capable of restoring euglycemia from a diabetic state; and 2) to provide a model system for exploring the processes underlying the development of glucagon, somatostatin, pancreatic polypeptide, ghrelin and insulin positive cell types in healthy and diseased humans. While both goals seek to understand and exploit natural human development processes, the limited availability of human fetal tissue and the inability to apply advanced genetic tools to such tissue continues to present hurdles. Consequently, the majority of our understanding of pancreatic development is based on data collected from model systems such as mice, frogs, and zebrafish. Zebrafish are appropriate for rapid combinatorial genetic studies and offer the advantage of a rapid life cycle in an animal that contains a minimal pancreatic endocrine islet structure (76, 77). While comparatively slower to reproduce and mature, mouse models still offer a considerable number of genetic tools,

while also enabling whole body physiological analysis through which the consequences of altered pancreatic development can be evaluated. Together these models have provided a basic framework of pancreatic development (Figure 1.1) which continues to be modified as new genes involved in pancreas development and maintenance are identified from animal models and confirmed in a wide variety of human based approaches including tissue taken from human fetal samples and from patients with monogenic forms of diabetes (*e.g.* maturity onset diabetes of the young (MODY), and neonatal diabetes). Once identified in human systems, these genes often require previously described model organisms to better understand the complex roles the genes play in mammalian pancreatic development. Ultimately this iterative process refines our pancreatic developmental model, which serves as a roadmap for many fields of study.

1.4 Pancreatic Development

Efforts to induce PSC differentiation into pancreatic endocrine cells typically attempt to recapitulate the current understanding of the normal pancreatic developmental cascade (Figure 1.1). Pancreatic induction protocols are generally derived from empirical testing of various signalling molecules and culture conditions identified in developmental model systems such as frogs, fish and mice. Stage specific differentiation conditions are optimized for each pancreatic development step that is required to convert undifferentiated PSCs to either pancreatic progenitors or hormone positive cells.

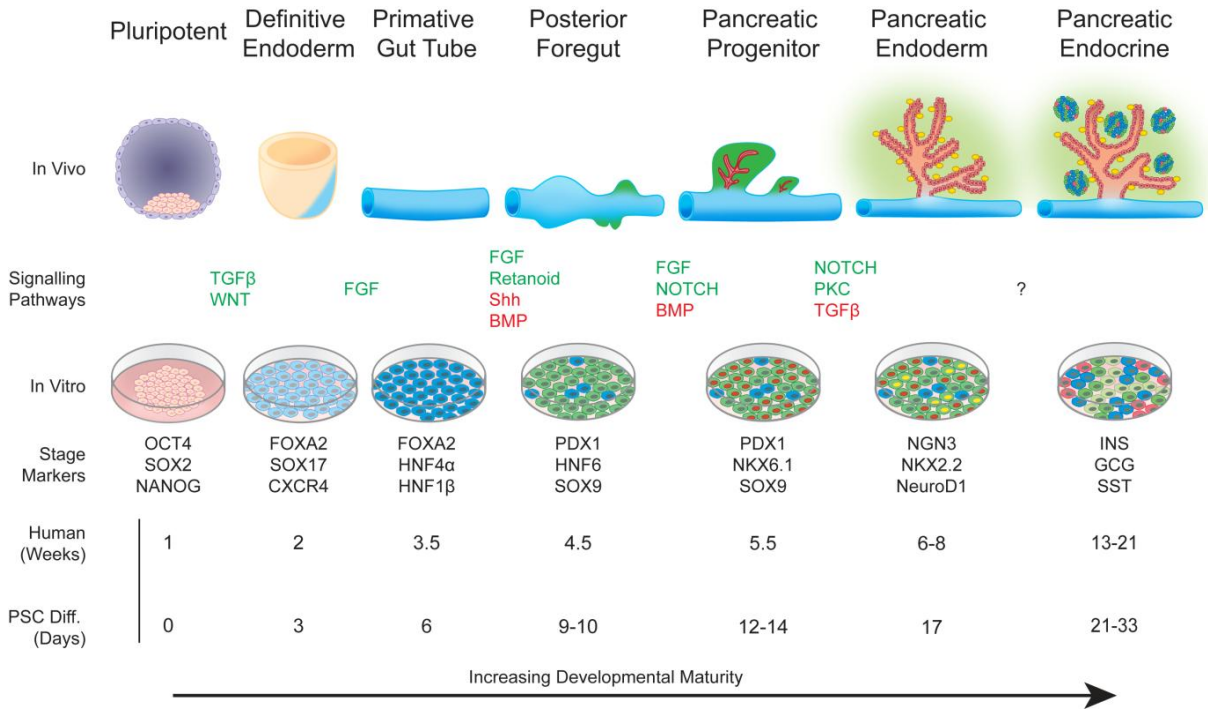

Figure 1.1. Comparative pancreatic development *in vitro* and *in vivo*

Normal pancreatic development occurs through a complex series of morphogenic events that convert pluripotent cells into all potential cell types of the body. An approximate time line for PSC differentiation (days) and human (weeks) development is provided. Initially pluripotent inner cell mass cells and their equivalent OCT4 positive hESCs (shown in pink) transition through a primitive streak intermediary stage to form cells committed to the endoderm lineage through TGF-β and WNT signalling pathways. Definitive endodermal cells (light blue) develop into endoderm derived foregut cells (dark blue), which retain the ability to form any endoderm organ, in an FGF signalling dependent process. Specification of the PDX1 positive dorsal and ventral pancreatic buds (shown in green) from the foregut tube occurs posterior to the developing stomach via high levels of FGF and retanoid signalling and inhibition of sonic hedgehog (Shh) and bone morphogenic protein (BMP) signals. Continued FGF and retanoid signalling specifies the NKX6.1/PDX1 co-positive pancreatic epithelial tree (red tree/nuclei within green bud/cells) within the expanding pancreatic buds while the ventral bud rotates to fuse with the dorsal bud. NGN3 positive pancreatic endocrine precursor cells (shown as yellow buds/nuclei) form from pancreatic epithelial tree cells in a NOTCH signalling dependent process enhanced by PKC activation and TGF-β inhibition. Over a considerable time frame and through processes that are incompletely understood these endocrine precursor cells further mature through a number of fate specification stages (not described) into hormone positive cells which coalesce into endocrine clusters (shown as clusters of red, green, and blue cells) within the surrounding pancreatic mesenchyme (light green). Signalling pathways are either activated (green text) or inhibited (red text) to drive development progression to the next stage. Key markers expressed at different developmental checkpoints are shown below the cells in culture. Figure adapted from (1).

Pancreatic development begins with gastrulation and the specification of embryonic germ layers into definitive endoderm. This process requires signalling from TGF-β family members, such as Nodal (78). TGF-β signalling induces the formation of SOX17, FOXA2 co-positive definitive endoderm cells. These cells are capable of further developing into all endodermal-derived tissues including pharynx, thyroid, lung, stomach, liver, pancreas, and

intestine (79-81). The resulting sheet of endodermal cells invaginates into a tube in response to soluble factors including FGF4, which is released from the neighbouring mesectodermal tissue (82). This tube of endoderm cells is next patterned along its length, where different portions of the tube become permissive to the development of organ buds (83). In mice, the earliest PDX1 positive pancreas competent cells are derived from the transition zone between anterior SOX2 positive stomach progenitors and posterior CDX2 positive intestinal progenitors (84). Induction of PDX1 expression occurs in response to retinoic acid (RA), BMP and Shh signalling cascades (85-88) and produces a cell population capable of generating the entire pancreatic organ in mice and humans (89, 90). Similarly, available human developmental data suggests that these PDX1 positive cells subsequently gain expression of NKX6.1, identifying them as restricted pancreatic endodermal progenitors capable of differentiation to endocrine, exocrine and ductal lineages (91). In human and mouse development, it is this population which seems to form a complex tubular epithelial system which is regionalized based on location along the lengthening ductal tube into GATA4 positive "tip" progenitors, which form PTF1A positive exocrine cells, and GATA4 negative "trunk" progenitors, which can form both ductal and endocrine cells (91-93). Commitment of PDX1/NKX6.1 co-positive, GATA4 negative "trunk" progenitors to the endocrine lineage is associated with transient expression of NGN3 to initiate endocrine fate specification (91, 94-98). During this transcription factor dependent cascade, within the pancreatic bud, some cells from the branched epithelial tree form early endocrine progenitor cells. These cells continue to develop and eventually end up embedded in the surrounding pancreatic mesenchyme through incompletely understood mechanisms where they mature into functional endocrine cells (99, 100) (Figure 1.1).

1.4.1 Definitive Endoderm, Foregut, and Pancreatic Endodermal Progenitors from PSCs *in vitro*

The induced differentiation of PSCs into pancreatic cells generally follows known developmental stages as described above, but on an accelerated time line (Figure 1.1). While the formation of endocrine cells in humans takes approximately 7 weeks of development (98), early endocrine cells are first formed in differentiating hESCs by 2 weeks of culture (101). This considerably shortened culture timeline of PSCs is possible *in vitro* because

mesodermal and ectodermal tissue development is not required and the morphogens naturally produced by these tissues are simply added exogenously as required. To begin *in vitro* differentiation, PSCs are seeded in cell culture plates. Once the cells have grown to a predetermined optimal density, which primes them to exit the replicative cell cycle (4, 102), the first inductive signals are provided via daily media changes that continue throughout the culture timeline. Key marker genes and proteins are routinely monitored to ensure stage specific differentiation and to identify cell homogeneity throughout the process. Primarily in response to Activin A (a TGF-β family member) in low or no serum conditions, the pluripotency program is repressed and the formation of cells of the endoderm germ layer is stimulated (103-106). These signals induce the PSCs to move through an intermediate mesoderm/endoderm step that is developmentally similar to the primitive streak. Cells in this transient state can be identified via expression of the transcription factor Brachyury (T) by 12-24 hours after Activin A induction (103). Expression of FOXA2 and SOX17 follows approximately 48 hours later, and together with the absence of extraembryonic primitive endoderm markers such as SOX7, demarks the formation of true definitive endoderm cells (103, 105, 107). The formation of this cell population was a key milestone in the pursuit of developing β-cells and other endodermal-derived tissues from PSCs. Remarkably, endodermal progenitors can also be isolated and expanded in culture producing a purified population free from pluripotent cells that maintains its ability to differentiate in a endoderm lineage restricted manner (108). Whether generated transiently or from expanded cultures, highly pure definitive endoderm cell populations are key to the success of later differentiation steps if a homogenous final cellular product is desired. Given the broad developmental potential of definitive endoderm progenitors, these cell populations are now being used to study the generation and continued differentiation of many tissue types including lung (109), liver (110-113) and intestine (114), as well as organs of the anterior foregut (115, 116).

Following the generation of relatively pure definitive endoderm cells, the next challenge is to further pattern the sheet of cells to mimic the foregut stage of development. This is achieved with the addition of FGF signalling agonists, namely FGF7 or FGF10, concomitant with prompt removal of the growth factors used to trigger previous differentiation stages. Expression of HNF4α and HNF1β mark the transition into foregut

cells, which occurs over the next 72 hours in culture (day 5-7 total) (101, 117-119). This population of cells can form gall bladder, hepatic, intestinal, and pancreatic cells, but requires further specification of the pancreatic lineage and repression of unwanted developmental programs. Retinoic acid plays a central role in induction of pancreas formation from the foregut and is key in stimulating PDX1 expression in differentiating hESCs (101, 120, 121). At the same time, repression of hepatic and intestinal cell fates by inhibition of BMP and Shh signalling is critical for proper specific pancreatic induction from hESCs (112, 114, 115, 118, 121-124). Together, this mix of signalling cascades stimulates the formation of relatively homogenous PDX1 positive cell populations, which approach 95% purity in some reports, over the course of 3-5 days (120, 125). These PDX1 positive cells represent a key developmental step where the PSCs are partially restricted in cell fate but still retain the ability to form off target tissues including the extra-hepatic biliary duct in humans depending on PDX1 expression levels (91).

Final maturation to PDX1/NKX6.1 co-positive pancreatic endodermal progenitors, occurs over the next 72 hours. These progenitors arise before the spatial regionalization associated with GATA4 expression to distinguish "tip" and "trunk" progenitors and are similar to progenitors that predominate in the pancreatic epithelium at 8-9 weeks of human fetal development (91, 97). The maturation of PDX1 positive cells to PDX1/NKX6.1 co-positive cells has been shown to occur in the absence of exogenous stimuli (117) but can be enhanced by a mixture of BMP and ALK5 inhibition and PKC activation (125, 126). The highest reported efficiency and homogeneity of PDX1/NKX6.1 co-positive progenitors is up to 86% PDX1/NKX6.1 co-positivity in 70% of differentiation runs (125). When transplanted into immunocompromised mouse models, these cells give rise to ductal cells and endocrine cells including functional insulin positive cells, while PDX1/NKX6.1 co-negative expressing cells appear to give rise to predominantly glucagon-positive α-cells (117, 125-128). The *in vitro* generation of a pancreatic progenitor pool from hESCs is an important checkpoint that has been achieved by many research groups and represents the second key milestone toward producing functional β-cells of sufficient quality and in quantities appropriate for future transplantation studies.

1.4.2 Maturation of Pancreatic Progenitors to Endocrine Cells *in vitro*

While the production of pancreatic endodermal progenitors has been relatively successful, the continued development of these cells in culture into fully functional endocrine cells remains poorly understood. To this end two developmental routes are being explored. Both begin with the *in vitro* differentiation of PDX1/NKX6.1 co-positive progenitors over a 14-17 day culture period as describe above (Section 1.4.1). Subsequently, these progenitors are either transplanted into immunocompromised mice to undergo relatively uncontrolled development *in vivo* toward functional endocrine cells (Section 1.4.3), or alternatively the progenitors are cultured *in vitro* under more regulated conditions in an effort to elicit functional maturation of the cells (see below, Section 1.4.2) (Figure 1.2).

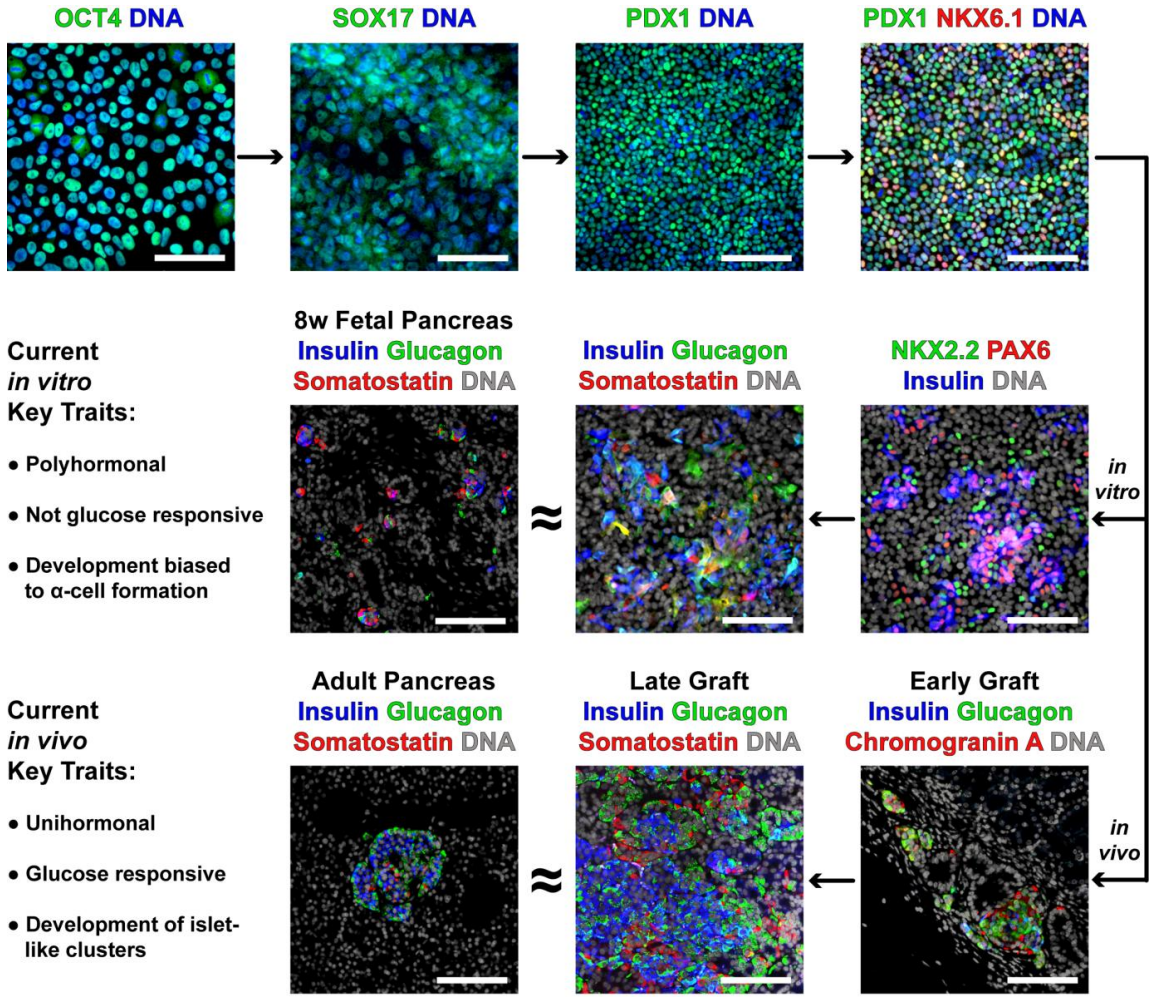

Figure 1.2. Current *in vitro* and *in vivo* hESC differentiation mimicking human pancreatic development

Representative immunohistochemical images are shown for various stages of *in vitro* generation of pancreatic progenitor cells and subsequent *in vitro* formation of endocrine cells and *in vivo* maturation to functional

endocrine grafts. Pancreatic differentiation of hESCs converts OCT4 positive pluripotent cells into SOX17 positive definitive endoderm cells. These cells further develop into PDX1 positive foregut endoderm cells that mature into pancreatic endodermal progenitors co-expressing NKX6.1 and PDX1. This population of cells is the basis for *in vitro* development and *in vivo* maturation where maturation of progenitors is achieved by transplantation into immunocompromised recipients. Transplanted hESC derived cells mature from immature polyhormonal endocrine populations expressing insulin, glucagon, and the pan-endocrine marker chromogranin A, into functional islet like clusters resembling adult pancreatic islets and comprised of unihormonal cells. The colours for each marker are as indicated above each image. All scale bars are 100 μm. Figure adapted from (1).

The cumulative developmental literature on pancreatic endocrine induction, fate specification, and functional maturation suggests that temporally and spatially regulated transcription factor expression is critical to efficient stimulation of β-cell formation. In particular, sequential expression of the endocrine restriction marker NGN3, followed by a number of fate specifying factors (NKX2.2, PAX4, ARX, PAX6, and others), is thought to be key for specification of pancreatic endodermal progenitors (100). After fate specification, endocrine cells begin to express maturation factors and eventually hormones, with MAFA driven insulin production in the β-cell being perhaps the most well-studied example (100, 129). During hESC differentiation, the induction of the endocrine cascade from restricted pancreatic progenitors remains largely stochastic for many of the early differentiation protocols (101). This suggests that the process could be cell autonomous, or more likely that the cultures themselves produce the signalling molecules required to activate endocrine development within the culture system.

In an effort to accelerate this endocrine induction process and improve its efficiency, a wide range of signalling molecules have been used, including but not limited to nicotinamide, exendin-4, IGF-1, HGF, Noggin, bFGF, BMP4, VEGF, WNT and various inhibitors of BMP, Shh, TGF-β, and Notch signalling pathways (101, 117-119, 123, 125-128, 130-132). Some of these factors have a rational basis for testing as agents driving endocrine maturation. As one example, exendin-4 is a mimetic of the natural gut-derived hormone glucagon-like peptide 1 (GLP-1), which stimulates β-cell proliferation, decreases β-cell apoptosis and renders β-cells glucose competent (133). In addition to rational factors, recently even seemingly innocuous factors have been found to have dramatic effects on differentiating hESCs. The broadly used organic solvent dimethyl sulfoxide (DMSO) decreased cell proliferation to a similar extent as high density cell culture conditions, dramatically enhancing differentiation to definitive endoderm, PDX1 positive cells, and C-peptide positive cells in more than 25 hESC and iPSC lines (102). Even the buffering

component HEPES was found to have significant inhibitory effects on endocrine maturation from pancreatic endodermal progenitors, with HEPES stimulating intestinal commitment (elevated CDX2 expression) at the expense of the pancreatic lineage (decreased NKX6.1, NGN3, NEUROD1, PDX1, and PTF1A expression) (125).

Beyond these unexpected results, modulation of TGF-β, WNT, BMP and PKC signalling have also resulted in considerable improvements in efficiency of conversion of pancreatic progenitors to an endocrine fate. Inhibition of endogenous WNT signalling from foregut stage hESC cultures impaired the eventual expression of insulin and when optimally agonized by addition of WNT3a, a 15-fold increase in insulin expression was observed (118). During the generation of pancreatic progenitors, TGF-β agonists were found to have a positive effect on hESC differentiation by increasing the number of PDX1 positive cells (134). Remarkably tight temporal regulation of this signalling pathway was required for further maturation toward endocrine cells, as continued administration of TGF-β agonists repressed insulin expression (134). Indeed, TGF-β inhibition with ALK5 inhibitor II caused a dose-dependent increase in NGN3 positive cells from progenitor cultures (127). This effect continued down the cascade, promoting increased expression of NKX2.2, NEUROD1 and eventually insulin and glucagon without appreciably decreasing PDX1 expression (127). Similarly, PKC activation has been identified as a potentially key pathway required to maintain PDX1 expression in pancreatic progenitors as reported PKC inhibition by bisindolylmaleimide I, Gö 6983 and Gö 6976 blocked PDX1 induction in hESCs (135). Indeed, when the PKC activator TPB was added to ALK5 inhibition and continued BMP inhibition by Noggin, this three factor mixture in the absence of HEPES buffering stimulated increased expression of NGN3, NEUROD1, and NKX6.1 without loss of PDX1 expression in pancreatic progenitors or induction of off target differentiation which would be characterized by expression of albumin (liver) or CDX2 (intestine) (125). Recently one report suggested that BMP signalling is key to maintaining a proliferative PDX1 positive progenitor pool, and that BMP antagonism is subsequently required to induce further pancreatic endocrine maturation (123). Taken together, this diverse set of signalling modulation experiments suggests that in developing hESCs, WNT signalling followed by TGF-β and PKC agonism in the absence of BMP signals is key to generate PDX1 positive cells, while subsequent endocrine induction requires TGF-β and BMP antagonism.

The formation of functional pancreatic progenitor endocrine cells from hESCs has been convincingly demonstrated *in vivo* (117, 125, 126, 136). While *in vivo* differentiation suggests that *in vitro* derived pancreatic progenitors should have the capacity to produce functional endocrine cells, presently the majority of pancreatic endocrine cells produced *in vitro* by various groups remain immature in function and typically express multiple hormones including insulin, glucagon, and somatostatin, with an eventual bias toward a glucagon positive lineage (4, 101, 118, 127, 130, 137, 138). Of particular note, one of the highest *in vitro* endocrine differentiation efficiencies reported to date yielded up to 75% endocrine cells (synaptophysin positive) (127). While these cells were initially polyhormonal (insulin and glucagon positive), during extended culture or transplantation they developed into functional unihormonal endocrine cells expressing only glucagon. High expression of the key α-cell transcription factor ARX, along with low expression of PAX4, PDX1 and NKX6.1, may have caused this biased maturation towards α-cells (127). So far, we have yet to create a reproducible protocol for the generation of unihormonal insulin positive cells *in vitro* which are not naturally predestined to form α-cells. By better understanding the factor(s) which positively regulate hESC-derived α-cell formation, it may be possible to block this process allowing efficient generation of hESC-derived β-cells.

One of the key objectives of *in vitro* differentiation of hESCs is the development of functional insulin secreting cells. With this goal in mind, D'amour et al. (2006) examined the capacity of their differentiated endocrine cultures to responsively release insulin/C-peptide into the culture media. In this study, differentiated hESCs clusters contained approximately one third the amount of C-peptide per μg DNA found in human islets, with a high proportion of proinsulin remaining unprocessed. hESC clusters released C-peptide (2-7 fold over basal) in response to depolarizing stimuli such as KCl, K_{ATP} channel blockade by tolbutamide, increased cAMP levels by IBMX addition, and nutrient supplementation by methyl-pyruvate α-ketoisocaproic acid, L-leucine and L-glutamine (101). Importantly, these clusters were unable to reproducibly release C-peptide in response to glucose, with many experiments recording stable or even decreased C-peptide release in response to increased extracellular glucose concentrations. While some groups have shown modest insulin secretion (~2 fold) from differentiated mESCs in response to elevated glucose levels (139), the majority of reports suggest that this key attribute is lacking under current *in vitro* culture systems which

employ human cells. These immature hESC-derived endocrine cells share some characteristics with neonatal β-cells which have significantly elevated insulin release in low glucose conditions and blunted release in high glucose conditions (140). This poor glucose responsiveness in neonatal β-cells has been attributed to a deficit in mitochondrial energy shuttling associated with poor glucose stimulated NAD(P)H generation (140, 141). One notable exception to the unresponsive nature of *in vitro* PSC-derived insulin-positive cells is the differentiated progeny of *in vitro* purified definitive endoderm progenitors (108). The differentiated cells in this study, despite being differentiated with protocols that typically generate polyhormonal cells lacking robust glucose-responsiveness with other ESC lines, were found to express C-peptide without glucagon or somatostatin and released C-peptide in response to elevated glucose levels similarly to adult human islets (108). Given that the endodermal progenitors used were lineage restricted, could rapidly self-renew yet were non-tumorigenic, and could be effectively differentiated into glucose-responsive insulin secreting cells, the authors revealed an alternative differentiation method that pauses the ESCs at the definitive endoderm stage to improve directed differentiation purity and potential safety of the final cell product. While this study stands out in terms of *in vitro* derived functional cell generation for reasons which are not completely clear, the generally limited responsiveness of most hESCs differentiated exclusively *in vitro* has led many groups to examine the development of pancreatic endodermal progenitors *in vivo* as an alternate strategy to yield functional endocrine cells with more reasonable efficiency.

1.4.3 Maturation of Pancreatic Progenitors to Endocrine Cells *in vivo*

Given that *in vitro* differentiation of pancreatic progenitors into endocrine cells tends to produce immature polyhormonal cells with poor glucose responsiveness, research efforts have turned to *in vivo* maturation strategies to elicit functional maturation of progenitor cells. This strategy is based on the success of functional maturation of human fetal pancreatic tissue upon transplantation in mice (142, 143) and on the notion that *in vivo* maturation might enable exploitation of the full complexity of cellular interactions that drive normal pancreas development. Since our knowledge of pancreatic endocrine cell development, particularly the signals governing late endocrine maturation processes, remains incomplete, rational, literature-driven *in vitro* maturation is likely to remain challenging in the short term.

However, if *in vivo* cell maturation is possible, it may provide key insights into the required signals that govern this process, which are presumably deficient in the current *in vitro* culture systems. Moreover, in considering an eventual cell therapy product, the shorter timeline associated with differentiation just to pancreatic progenitors is attractive, assuming adequate performance and safety following completion of maturation *in vivo*.

As previously reviewed, *in vivo* maturation protocols tend to begin from PDX1/NKX6.1 co-positive pancreatic endodermal progenitors generated through *in vitro* processes (Figure 1.1 and 1.2). These progenitor cells, if differentiated as an adherent monolayer cell culture, must be detached and prepared for transplantation in the form of a suspension of cell clusters (117, 125, 128) or alternatively differentiated entirely in suspension prior to transplantation (119, 144) (Figure 1.3). The composition and purity reported for these clusters varies amongst different groups, but they tend to be comprised predominantly of PDX1/NKX6.1 co-positive progenitors with lower numbers of pre-committed pancreatic endocrine cells (125). Following harvest, progenitor cells are typically transplanted under the kidney capsule (Figure 1.3) (117, 125, 127) or as part of a gel-foam disk transplanted into the epididymal fat pad (117, 119, 128) of immunocompromised rodents. Initial engraftment of the progenitor mixture occurs over the next few weeks as blood vessels from the transplant recipient grow toward the transplanted tissue, likely in a VEGF-A dependent process similar to islet engraftment and vascularisation in mice (145-148). The subsequent development of hormone positive cells within the engrafted hESC origin tissue is initially rapid and results in the production of polyhormonal cells around 1 month post transplantation (125) (Figure 1.2). Over the next two to three months, the immature polyhormonal cell population decreases in number and more mature cell types expressing a single major islet hormone predominate in the transplant tissue (Figure 1.2). This transition is also marked by the reorganization of endocrine cells within the grafts into endocrine clusters resembling islets, and a significant increase in secretion of C-peptide from the graft (117, 125). With extended *in vivo* maturation, glucose and/or meal responsive C-peptide release continues to increase in grafts, along with nuclear NKX6.1 and MAFA expression in insulin positive cells (117, 125). NKX6.1 has been shown to be both necessary and sufficient to maintain and specify the β-cell cell phenotype primarily due to repression of α-cell biasing factors such as ARX and PAX6 (149, 150). MAFA expression, which is

known to mark maturation of insulin producing cells into a glucose responsive state (129) is also associated with the point at which the hESC derived grafts were able to restore normoglycemia in diabetic transplant recipients suggesting that a key functional transition had occurred within the graft (125). Marking a key milestone in the field, this *in vivo* maturation process to yield glucose-responsive, insulin producing cells has been independently shown to occur in normoglycemic (117) and diabetic (125) environments. However, the possibility that *in vivo* cell maturation in the host environment may be variable due to differing exposure to a variety of factors such as hormones and drugs, remains a potential limitation of this approach.

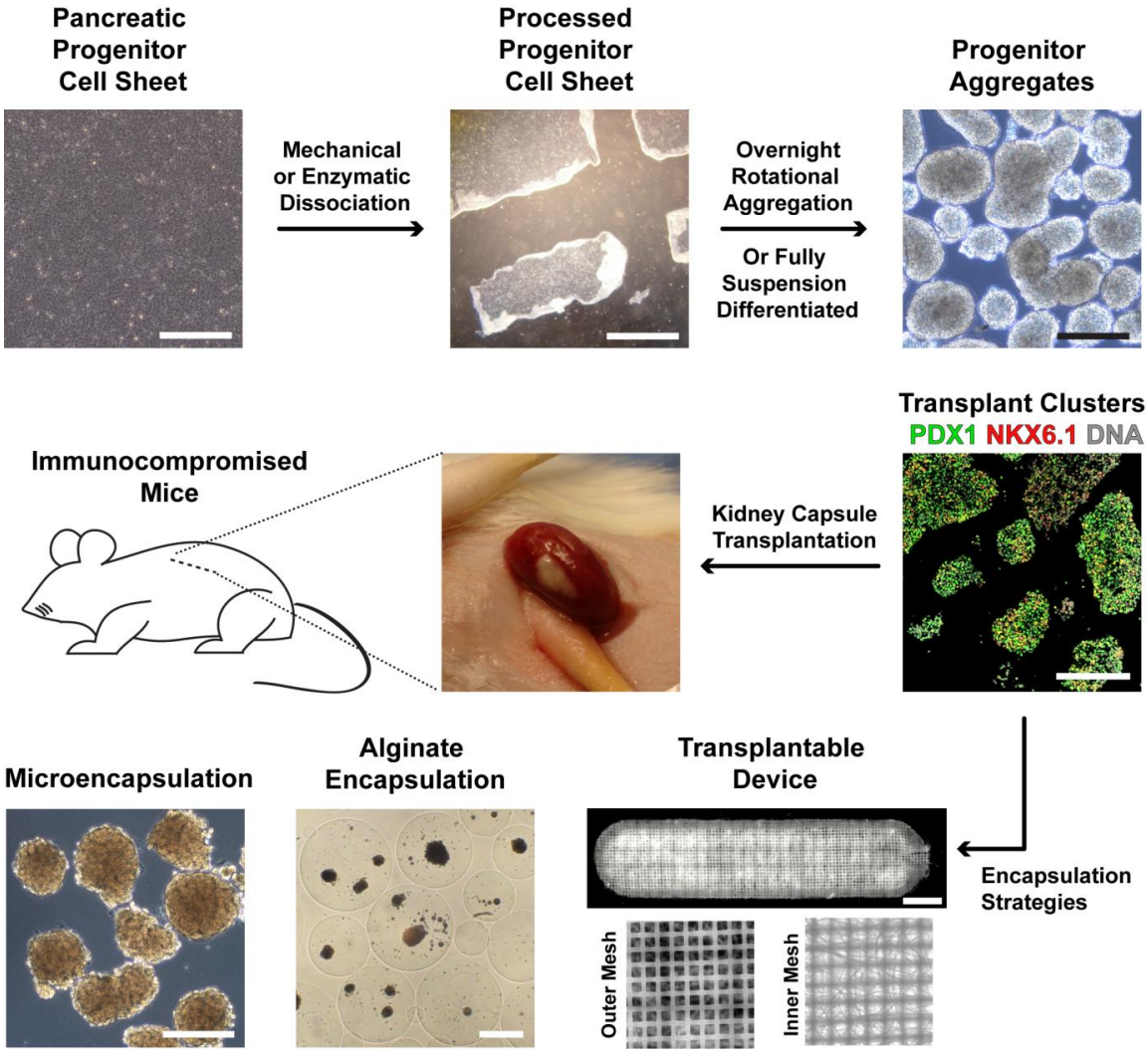

Figure 1.3. Transplantation of pancreatic progenitors and encapsulation strategies

in vitro derived monolayer cultures of pancreatic progenitors are processed into cell clusters through mechanical and enzymatic dissociation processes. After overnight dynamic rotational aggregation (or from clusters

differentiated in suspension) the pancreatic progenitor clusters still expressing PDX1 (green) and NKX6.1 (red) which localizes to the nucleus (DAPI, white). These clusters are commonly transplanted *in vivo* under the kidney capsule of immunocompromised mice to allow graft maturation. Alternatively these progenitor clusters may be encapsulated into a transplantable device (TheraCyte device shown from TheraCyte Inc.), alginate beads, or surface coated to allow immunoprotection of the graft. All scale bars are 200 μm with the exception of the Transplantable device scale bar which is 5 mm.

The ability of *in vivo* maturation strategies to functionally control blood glucose in diabetic murine models using hESC-derived cells (117, 125) has led to intriguing questions about how to mimic the functional maturation of insulin positive cells in culture and what cell population forms the final insulin positive cell compartment in glucose-responsive grafts. Kelly et al. elegantly examined this question using a cell separation and transplantation strategy (128). The authors followed an established *in vitro* differentiation protocol to produce a heterogeneous pancreatic cell population that was the basis for a flow-cytometry based assay of 217 commercially available antibodies aimed at distinguishing endocrine cells from progenitors. Ultimately CD142 was found to label a population of predominantly hormone negative, NKX6.1 positive endodermal progenitors, while CD200 and CD318 preferentially labelled hormone positive cells. The authors separated CD142 positive endodermal progenitor fractions (82% progenitors) and CD318 positive hormone positive fractions (84% endocrine) by immunomagnetic cell separation methods and transplanted the cells into immunocompromised mice. Nine weeks after transplantation, CD318 enriched endocrine cells had developed mostly into glucagon positive cells while 13 week old transplants of CD142 enriched pancreatic endodermal progenitors contained large numbers of cells expressing insulin, glucagon or somatostatin, arranged in islet like structures and surrounded by cells expressing markers of exocrine and ductal pancreatic cells. Taken together this work suggests that the CD142 positive, NKX6.1 positive, hormone negative population is the common progenitor for ductal, exocrine, and endocrine pancreatic cells including insulin, somatostatin and glucagon lineages. In contrast, the *in vitro* generated hormone positive cells expressing CD318 and CD200 seemed to be predestined to form glucagon positive cells (128). Interestingly the most functional grafts were generated from mixed cell populations which contained both the hormone negative and positive populations (128), the reasons for which are unclear. Our group compared maturation of hESC derived pancreatic progenitors that contained high (~80%) or low (~25%) fractions of NKX6.1 positive cell populations (126). Upon transplantation and *in vivo* maturation of these cells,

the NKX6.1-high grafts were found to have robust C-peptide release in response to physiological stimuli including meals, arginine, and glucose, which was not observed from the NKX6.1-low grafts. After five months of development both NKX6.1-high and -low grafts generated pancreatic endocrine cells at high efficiencies but the NKX6.1-high grafts contained increased numbers of insulin and somatostatin positive cells while the NKX6.1-low grafts contained predominantly glucagon positive cells (126). Both of these studies support previous *in vitro* extended culture and transplantation studies in which glucagon positive cells at the end of *in vitro* and *in vivo* differentiation protocols were found to arise from the glucagon/insulin co-positive cells seen in the earlier *in vitro* differentiation stages (127, 138). Analysis of human fetal pancreas samples also supports the notion that polyhormonal endocrine cells are present during development and may give rise to mature, single hormone producing cells (94, 97). Thus the *in vivo* maturation of hESC-derived precursor cells presents a useful model for exploring the developmental capacity of cells initially produced *in vitro*. Moreover, *in vivo* maturation studies may help to further define the optimal cell population to produce functional hESC-derived pancreatic endocrine cells.

1.5 Thesis Investigation

The ability of cadaveric islet transplantation to functionally restore physiological blood glucose control in patients with type 1 diabetes suggests that a cellular therapy is possible for this disease. One limitation that must be overcome to allow widespread adoption of this therapy is the limited availability of donor islets. Pluripotent and some multipotent stem cells have capacity to generate novel sources of β-cells, although the processes that govern the transition of stem cells to mature functional endocrine cells remain poorly understood and incomplete. *In vitro* derived pancreatic endodermal progenitors generated from hESCs have the capacity for *in vivo* development to functional pancreatic endocrine cells including β-cells. Currently, *in vitro* development using these same pancreatic progenitors is able to form endocrine cells, although these cells are typically polyhormonal and not fully functional. The difference between these *in vitro*- and *in vivo*-derived endocrine cells may help define the processes that control pancreatic endocrine cell fate selection and the processes that control functional maturation. Unfortunately, the *in vivo* maturation process allows only rare glimpses into the endocrine developmental environment.

To provide increased experimental control, and allow for the application of a number of tools and techniques that are not generally possible *in vivo*, we have focused our studies primarily on *in vitro* models of stem cell development. Within these model systems, we hypothesise that human stem cell development towards a pancreatic endocrine phenotype can be guided by a definable set of transcription factors that when appropriately expressed, and in the presence of appropriate environmental cues, will lead to the targeted differentiation of specific pancreatic endocrine cells.

To address this hypothesis, we began our work in Chapter 2 with human amniotic fluid cells, a readily available fetal-origin stem cell population that had previously been shown to have endodermal developmental potential. In these cells, we examined the ability of established pancreas-associated transcription factors to drive the formation of insulin positive cells. To do this, we generated a novel fluorescent reporter system, performed a combinatorial high content screen, followed up on the optimal mixture of transcription factors and performed *in vivo* functional assessments. We next moved to hESCs, given their established differentiation capacity and use as a model of human development. Our work with hESCs began in Chapter 3 with the examination of a newly isolated hESC sub-line known as CA1S. We explored the utility of CA1S cells in a number of aspects of high throughput screening as well as their capacity for pancreatic endocrine differentiation. Using these CA1S cells, in Chapter 4 we explored the simple cell culture variable of initial cell seeding density and the effects on development to definitive endoderm, pancreatic progenitor, and pancreatic endocrine cell populations. Aiming to shift the formation of hESC-derived pancreatic endocrine cells from immature polyhormonal states to more mature unihormonal ones, we next examined the effect of modulating expression of the transcription factors PAX4 and ARX in Chapters 5 and 6. This work required the development of a number of adenoviral gene expression tools as well as targeted genomic deletion techniques which allowed us to reveal the roles of these two transcription factors in the specification of hESC-derived pancreatic endocrine cells in comparison to adult and fetal pancreatic tissue samples. Collectively, these studies emphasise the role of transcription factors in the formation of stem cell derived pancreatic endocrine cells and suggest that these fully *in vitro* culture systems are powerful tools for the investigation of human development and the factors which control the formation of pancreatic β-cells.

Chapter 2: Expression of Insulin in Response to Transcription Factor Overexpression in Human Amniotic Fluid Cells

2.1 Background

During gestation, the disk-shaped human embryo undergoes many developmental changes to form the mature fetus. Throughout much of this process, the fetus is supported by extraembryonic tissues that provide for the physical and metabolic requirements of development (151). As part of this supportive system, the amniotic membrane surrounds the fetus proper and through the contained amniotic fluid, provides limited mobility and protection. The amniotic membrane itself also maintains the composition of the amniotic fluid including dissolved salts, nutritious components, and growth factors which modulate the semi-allogeneic immune response against fetal tissues (151). The amniotic membrane is comprised of multiple tissue layers which are covered by a surface layer of amniotic epithelial cells that directly contact the amniotic fluid (151). During gestation, cells from the fetal surface, fetal digestive tract, and amniotic membrane become dislodged and end up in suspension in the amniotic fluid compartment (152, 153). These cells provide the basis for genetic testing associated with amniocentesis sampling during the second trimester (152, 154). This heterogenous mixture of cells has also been reported to contain populations of mesenchymal stem cells capable of osteogenic and adipogenic differentiation (49, 155). Furthermore, clonal cells isolated from human amniotic fluid samples have been shown to have the ability to differentiate towards each of the three major germ layers, creating such cell types as neurons, hepatocytes, and bone (50). Interestingly, hAF-derived cells are considered to be largely non-tumourogenic and locally immunosupressive, suggesting that multipotent cells within this population may represent an ideal source of cells to be converted to insulin-producing cells (49, 151, 154).

In order to coax the generation of insulin producing cells, stimulating signals are required to guide development. These can come from either exogenous sources such as growth factors similar to *in vitro* differentiation of hESCs as described in Section 1.4.2 or as gene expression systems as applied in the direct reprogramming of somatic cells *in vivo* following forced overexpression of pancreatic endocrine cell transcription factors (44, 45, 156, 157). For the purpose of our work we define cellular reprogramming as the process by

which a cell can be converted from one type to another by expression of one or more exogenous genes. Here we assessed the ability to reprogram hAF cells *in vitro* towards a β-cell phenotype through overexpression of up to six different transcription factors involved in the development or maintenance of the mature β-cell phenotype (100). We developed a novel fluorescent reporter system to allow for continuous image-based assessment of differentiation and coupled this with an unbiased high-content screen to determine the optimal transcription factor combination for insulin promoter activation. Reprogrammed hAF cells were then characterized both *in vitro* and *in vivo* for their potential to adopt a β-cell phenotype.

2.2 Methods

Isolation and Culture of Human Amniotic Fluid Cells

Through a supply agreement with Memorial Health Services (Long beach, CA, USA), amniotic fluid samples (2-5 ml) were obtained from donors undergoing amniocentesis in the second trimester of pregnancy for standard obstetrical reasons. The study was approved by the Institutional Review board of Long Beach Memorial Medical Center and written informed consent was obtained from each donor. hAF cells were cultured as a heterogeneous population of adherent cells in AmnioMAX-II complete medium (Invitrogen, Burlington, ON, Canada) maintained at 37°C and 5% CO_2 in all experiments unless otherwise described. hAF cells were maintained between 20 and 80% confluent by enzymatic subculture every 2-3 days using 0.05% Trypsin/EDTA (Invitrogen) up to passage 26.

Generation of a hAF Cell Reporter Line

Early passage (4-6) hAF cells were grown to 60% confluence and infected with pTiger-CMV-eGFP feline immunodeficiency virus lentivirus (generously provided by Dr. J. Piret from the University of British Columbia) at increasing multiplicity of infection (MOI) from 3 to 10. Infection occurred over 24 hours in serum-free minimal essential medium (Invitrogen) at 37°C and 5% CO_2. Three days post infection, eGFP fluorescence and cellular morphology was visualized by epifluorescence on an Axiovert 200 inverted microscope (Carl Zeiss Canada; Toronto, ON, Canada) connected to a Retiga 2000R CCD camera (Qimaging; Burnaby, BC, Canada) controlled using Open*lab* 5.0 imaging software (Improvision;

Waltham, MA, USA). Using an optimal infection MOI of 5, heterogeneous hAF cells were infected with a pTiger-hIP-DSRED lentiviral reporter vector developed by Dr. Y. Fujita from a kind gift from Dr. G. Nolan to contain a fragment of the human insulin promoter (hIP; -881 to +54 relative to the transcriptional start site) controlling expression of the red-fluorescent protein DsRed Express (DSRED). These reporter hAF cells were subsequently passaged, frozen, and thawed as required for the experiments outlined below.

Adenoviral-Mediated Transcription Factor Overexpression

All adenoviral expression vectors were independently purified as high titer (1 - 3 x 10^{10} PFU/ml) stocks by ViraQuest, Inc. (North Liberty, IA, USA). In all cases expression of eGFP and transcription factors (human PDX1, human NEUROD1, human NGN3, mouse ISL1, mouse PAX6, mouse MAFA) was driven from the CMV early E1 promoter. Adenoviruses expressing PDX1, NEUROD1, ISL1, PAX6, and MAFA were generated by Drs. Y. Fujita and R. Baker by cloning appropriate cDNA sequences into a shuttle vector which was then loaded into the pADENO-X (Clontech) viral production plasmid for use in transfection of HEK293 packaging cells to produce complete virions. Ad-NGN3 and Ad-eGFP were kind gifts from Dr. M. German and Dr. P. Robbins, respectively. Reporter hAF cells were cultured until they reached 65 – 75% confluency at which point a single adenoviral infection was carried out at 37°C in AIIC medium at an MOI of 10 for each viral construct delivered as a cocktail of individual constructs. Twenty-four hours post infection, culture medium was removed and replaced with fresh AIIC supplemented with nicotinamide (Sigma-Aldrich, Oakville, ON, Canada) at a final concentration of 10 mM. Following infection, hAF cells were cultured without passaging at 30°C with medium changes every 2 – 3 days with fresh AIIC + 10 mM nicotinamide. Qualitative analysis of DSRED expression was monitored by epifluorescence (Zeiss).

Flow Cytometry DSRED and eGFP Expression

Quantification of DSRED and eGFP expression was accomplished by flow cytometric analysis using an LSRII instrument (BD Biosciences, San Diego, CA, USA). hAF cells were released using 0.05% Trypsin/EDTA (Invitrogen), pelleted and resuspended in PBS + 2% FBS (Invitrogen). Examining the live single-cell population as determined by

forward and side scatter parameters, DSRED-positive or eGFP-positive cells were identified compared to undifferentiated or no virus controls, respectively. Subsequent data analysis was carried out using FlowJo software (TreeStar, Ashland, OR, USA).

High-Content Imaging and Cellomics Analysis

Reporter hAF cells were seeded at a density of 8000 cells per well in 150 µl AIIC media into clear-bottom 96-well polystyrene microplates (PerkinElmer; cat. no. 6005182, Woodbridge, ON, Canada). Following overnight culture, cells (~60% confluent) were infected for 24 hours in the AmnioMAX-II complete media at an MOI of 10 for each vector (see Appendix A for 96-well plate layouts) by transferring 10 µl of virus containing solution by multichannel pipette from a premixed master plate of adenoviral combinations prepared less than 16 hours before use, into the 96-well plate containing reporter hAF cells. At appropriate time points hAF cells were stained with Hoechst 33342 dye (Invitrogen) at a final concentration of 2 ng/µl in 100 µl of AIIC for 30 minutes at 37°C and 5% CO_2. Images were captured using a Cellomics ArrayScan V^{TI} instrument (Thermo Fisher Scientific; Pittsburgh, PA, USA). Images were analyzed using the associated Cellomics software and the "Target-Activation" module, which allows nucleus-oriented object identification and subsequent DSRED intensity assessment of surrounding cellular cytoplasm. Cell-by-cell fluorescence intensity data were averaged per well to provide a mean cellular DSRED intensity per treatment. Biological triplicate assays were used for statistical analysis by student T-test versus no virus control wells, and significant hits were confirmed by manual examination of representative images.

RT-PCR and RT-qPCR Analysis of Gene Expression

At selected time points, hAF cell RNA was isolated using the RNeasy kit (Qiagen; Mississauga, ON, Canada) and converted to cDNA using the iScript cDNA synthesis kit (BioRad; Hercules, CA, USA) after DNase treatment (Invitrogen) following all manufacturers protocols. Quantitative expression analysis was carried out using a StepOnePlus instrument (Applied Biosystems, Foster City, CA, USA) using Maxima Hot Start Taq DNA polymerase (Fermentas, Burlington, ON, Canada), EvaGreen (Biotium; Hayward, CA, USA), and the following reaction conditions: 25 µl reaction volume with 2.5

mM $MgCl_2$, 0.1 mM dNTPs, 0.2 µM each primer, 1x EvaGreen; 40 cycles, denaturation at 95°C for 15 seconds, annealing at 57°C for 30 seconds, extension at 72°C for 30 seconds. Expression analysis was carried out following the ΔΔCt method normalized to the housekeeping gene β-actin and compared to cDNA prepared from isolated human islet RNA. All assays were performed in technical and biological triplicate. RT-qPCR used Platinum Taq (Invitrogen) under standard reaction conditions described above and using primers described in Table 2.1.

Table 2.1 Sequences of primers used in semiquantitative and quantitative RT-PCR in chapter 2

Gene Name	Gene Accession	Product Size (bp)	Primer Sequence Forward / Reverse 5'→3'	Reference
Insulin	NM_000207.2	245	AGCCTTTGTGAACCAACACC GCTGGTAGAGGGAGCAGATG	(158)
Glucagon	NM_002054.4	275	CATTCACAGGGCACATTCAC CGGCCAAGTTCTTCAACAAT	(158)
Somatostatin	NM_001048.3	126	AGCTGCTGTCTGAACCCAAC CCATAGCCGGGTTTGAGTTA	(158)
PDX1	NM_000209	178	CGTCCAGCTGCCTTTCCCAT CCGTGAGATGTACTTGTTGAATAGGA	(2)
PAX4	NM_006193	169	AGCAGAGGCACTGGAGAAAGAGTT CAGCTGCATTTCCCACTTGAGCTT	(2)
NKX6.1	NM_006168	186	GCCCGCCCTGGAGGGACGCA ACGAATAGGCCAAACGAGCCC	(2)
NKX2.2	NM_002509	221	CTTCTACGACAGCGACAACCCG CCTTGGAGAAAAGCACTCGCCGCTTT	(2)
HNF1β	NM_000458	197	TGACTCAGCTGCAGAACTCACACA GTTGTTGCGCACGAAGTAAGTGGT	(2)
KIR6.2	NM_000525	183	ACTACTCCAAGTTTGGCAACACCG ACAGGGAATCTGGAGAGATGCTGA	(2)
ABCC8 (SUR1)	NM_000352	142	ACCACAGCACATGGCTTCATTTCC ATGTACAGGTGCAGATGGTGGGAT	(2)
PCSK2 (PC2)	NM_002594	162	AAGATGGCTTTGCAGCAGGAAGGA AGCCACATTCAAATCAAGGCCAGG	(2)
GAPDH	NM_002046.5	541	TTAGCCCCCCTGGCCAAGG CTTACTCCTTGGAGGCCATG	(2)
β-actin	NM_001101	377	GGCATGGGTCAGAAGGATT AGGGCATACCCCTCGTAGAT	(2)

Immunocytochemistry

Undifferentiated or induced hAF cells were grown on glass coverslips and fixed in 4% paraformaldehyde (wt/vol.) for one hour at room temperature. Cells were permeabilized for 15 minutes with 0.2% Triton X-100 (Sigma) in PBS, blocked (Dako), and incubated overnight at 4 °C with primary antibody. The primary antibodies used are described in Table 2.2. Cells were subsequently incubated with appropriate secondary antibodies (Alexa Fluor

488 or 594-conjugated goat anti-guinea-pig or anti-rabbit or anti-rat IgG or IgM; Invitrogen) and imaged as described above (Zeiss).

Table 2.2 Antibodies used in Immunocytochemistry in chapter 2

Protein Name	Host Species	Supplier / Catalogue number	Staining Method	Dilution	Antigen Retrieval
SSEA3	Rat (IgM)	R&D Systems MAB 1434	4% PFA fixed monolayer and Flow Cytometry	1:250	None
Insulin	Guinea Pig	Millipore 4011-01F	4% PFA fixed monolayer	1:1000	None
DsRed (RFP)	Rabbit	Millipore AB3216	4% PFA fixed monolayer	1:100	None
GLUT2	Rabbit	Millipore AB3216	4% PFA fixed monolayer	1:200	None
GCK	Rabbit	Sigma HPA007034	4% PFA fixed monolayer	1:200	None
PC2	Rabbit	Millipore AB1262	4% PFA fixed monolayer	1:100	None

Animals

Male Rag1^{tm1Mom}/J mice (stock 2216), which lack functional T and B-cells (159) rendering them immunocompromised and providing a good model for xenogenic transplantation, were obtained from the Jackson Laboratories (Bar Harbor, ME, USA) at 8-10 weeks of age. Mice were maintained on a 12 hour light/dark cycle and had *ad libitum* access to a standard irradiated diet (PicoLab 20; Cat. no. 5058l PMI International; St. Louis, MO, USA). Blood glucose and body weight were monitored 2-3 times weekly following a 4-hour morning fast. Blood glucose was measured via the saphenous vein using a handheld glucometer (Lifescan; Burnaby, BC, Canada). Diabetes (blood glucose >18 mM on at least two consecutive days) was induced following a single intraperitoneal injection of 150 mg/kg streptozotocin (STZ; prepared in sterile citrate buffer pH 4.5, Sigma).

Transplant of hAF Cells

Mice were anaesthetized with inhalable isofluorane and received transplants beneath the surface of the left kidney capsule of ~ 1.9 million hAF cells that had been cultured for 14 days in the presence or absence of transcription factor overexpression. Following transplantation all mice were treated with oral enrofloxacin (Bayer Animal Health; Shawnee Mission, KS, USA) for one week (50 mg/500 mL in drinking water). At 5 days post-

transplant a 30-day, slow-release insulin pellet (LinBit; Linshin Canada; Toronto, ON, Canada) was implanted subcutaneously to maintain normoglycemia. Insulin pellets were removed 36 days post-transplant and animals were sacrificed 42 days post-transplant.

2.3 Results

Characterization of Human Amniotic Fluid Cells

To examine the utility of hAF cells in the context of recapitulating a β-cell phenotype, cells were cultured as a heterogeneous adherent cell population (Figure 2.1A), which was subsequently characterized for markes of pluripotency and lineage restriction. Robust expression of the membrane-bound pluripotency marker SSEA3 was observed in hAF cells in their naïve, undifferentiated state (Figure 2.1B). Analysis of the population by flow cytometry revealed that 16.2 ± 6.6% of the original hAF cells were SSEA3-positive, compared to 84.9 ± 12.5% in a prototypical culture of the pluripotent H1 hESCs (Figure 2.1C and D). Furthermore this population of hAF cells was found to express multiple markers of pluripotency (eg. SSEA3, SSEA4, CD9) to some degree, indicating that multipotent cells may exist in this hAF cell population. Analysis of additional markers revealed that like hESCs, most hAF cells express the adhesion and signalling integrins CD29, CD49e and CD49b and the multipotent progenitor marker CD90 (2). Other pluri/multipotency markers such as Tra-1-60, Tra-1-81, CD133, CD117 (c-kit), and CD106 were nearly or completely absent from the hAF cell population used in this study as was the endodermal marker CD184 (CXCR4) (2).

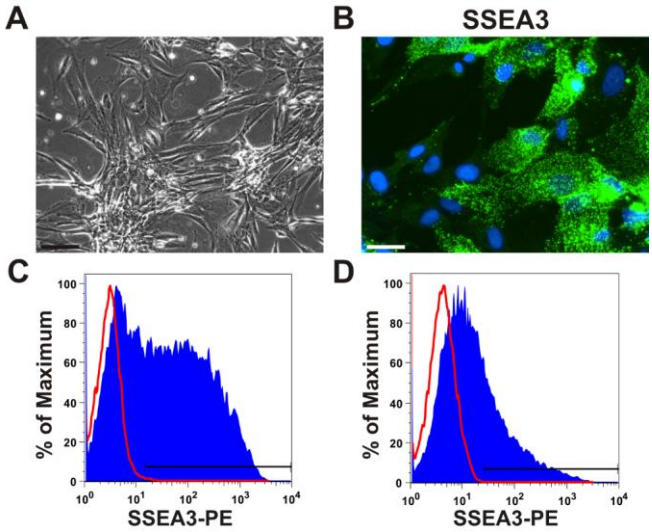

Figure 2.1. Characterization of human amniotic fluid cells for SSEA3 expression.

(A) Representative brightfield image of undifferentiated hAF cells. Scale bar is 100 µm. (B) Representative SSEA3 immunofluorescence (green) in undifferentiated hAF cells. Nuclei are blue (hoechst). Scale bar is 50 µm. (C and D) Representative flow cytometry analysis of SSEA3 expression in (C) undifferentiated H1 hESCs and (D) undifferentiated hAF cells. Red line indicates unstained population (isotype antibody treated) compared to the SSEA3-stained cell sample (blue fill).

Establishment of a Fluorescent Reporter hAF Cell Line

To facilitate identification of successfully reprogrammed hAF cells, we developed a feline immunodeficiency virus-based lentiviral fluorescent reporter in which DSRED expression is driven by a 935 bp fragment of the human insulin promoter (Figure 2.2A). Infection of the mouse β-cell line Min6 with this reporter construct resulted in robust DSRED expression (Figure 2.2B), indicating that sufficient DSRED can be produced for simple visual identification of cells with an active insulin promoter. We first infected naïve hAF cells with a control lentiviral vector in which enhanced green fluorescent protein (eGFP) expression is driven by a CMV promoter, at increasing MOIs. While the number of cells expressing eGFP increased in proportion to the MOI, higher MOIs (≥ 10) resulted in significant alterations in cellular morphology (Figure 2.2C). Using an MOI of 5, hAF cells were infected with the hIP-DSRED lentivirus, which produced a viable reporter line for future experiments. Infection of the hAF cells with this vector did not disrupt expression of the pluripotency marker SSEA3 (Figure 2.2F), nor did it result in the production of DSRED (Figure 2.2D), confirming that the insulin promoter fragment is not active within the naïve hAF cell population. DSRED expression was observed following hAF cell adenoviral transduction (Figure 2.2E) as described below.

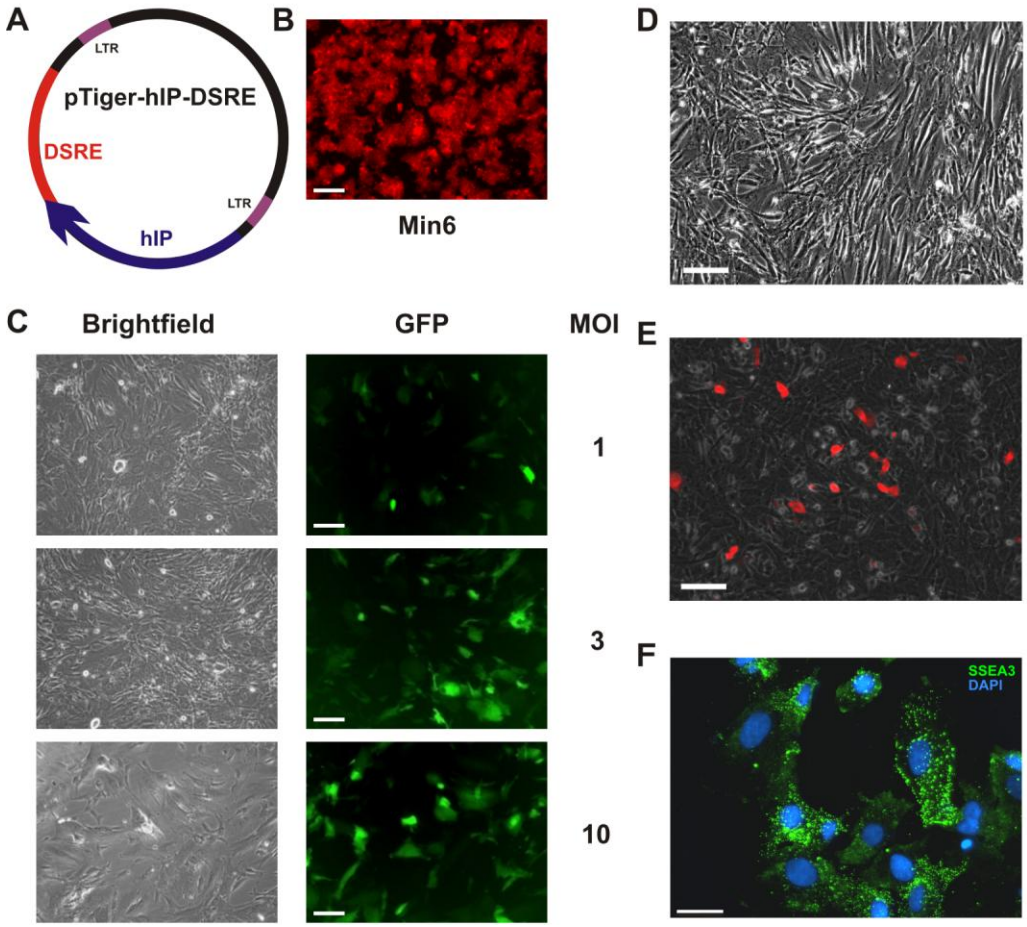

Figure 2.2. Generation of a fluorescent reporter hAF cell population.

(A) Schematic of the lentiviral reporter construct designed to allow for the fluorescence-based detection of insulin gene expression. (B) Representative fluorescent image of mouse insulinoma cells (Min6) infected with the pTiger-hIP-DSRED (DSRE) lentivirus. (C) Representative brightfield (left panel) and corresponding fluorescent (right panel) images of hAF cells infected with increasing MOI of a CMV-eGFP containing lentivirus. (D and E) Representative brightfield and fluorescent overlay images of (D) undifferentiated and (E) differentiated hAF reporter cells indicating the activation of the insulin promoter fragment in differentiated AF cells. (F) SSEA3 immunostaining in undifferentiated hAF reporter cells. Scale bars for B-E is 200 µm, panel F is 50 µm.

High-Content Screening for Transcription Factors Capable of Differentiating hAF Cells.

Initial examinations of the efficiency of Ad-eGFP delivery to hAF reporter cells revealed an expected dose dependant increase in the number and brightness of eGFP positive hAF cells. Infection with Ad-eGFP at an MOI of 1, 10 and 60 resulted in 1.1 ± 0.1, 13.6 ± 0.2, 83.7 ± 2.4 percent eGFP positive cells, respectively as assessed by flow cytometry four days after adenoviral transduction (Figure 2.3).

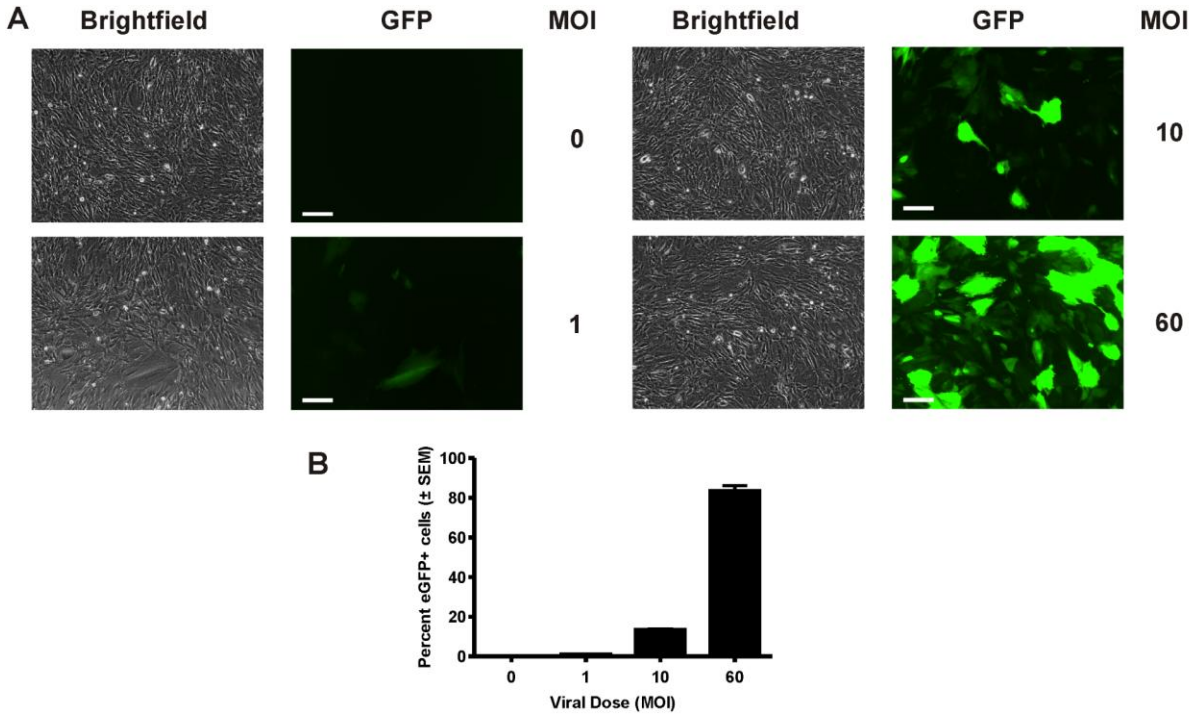

Figure 2.3. Adenoviral infection efficiency of hAF cells.

(A) Representative bright field (left panel) and corresponding fluorescent (right panel) images of hAF cells infected with increasing MOI of Ad-eGFP imaged four days post infection. Scale bar is 50 μm. Fluorescent images were uniformly contrast enhanced after capture to better represent low intensity eGFP positive cells. (B) Quantification by flow cytometry of live hAF cells in comparison to identically cultured uninfected hAF cells.

A panel of six transcription factors was selected based on previous data supporting their critical role in the development of the endocrine pancreas and islet β-cells (100). These were PDX1, NEUROD1, NGN3, ISL1, PAX6, and MAFA under expression control of a CMV promoter and delivered as individual adenoviral vectors. Using an MOI of 10 for each virus, a high-content screen was performed in triplicate where every one of the possible 64 combinations of these six transcription factors were tested in a 96-well plate format (See Appendix A for plate layout) for their ability to efficiently activate the human insulin promoter fragment and thus produce DSRED, as an indication of cellular reprogramming.

Cells were infected for 24 hours and subsequently cultured in the presence of 10 mM nicotinamide to promote cell survival and at 30°C to reduce proliferation. Following 14 days of culture, each well was imaged using a Cellomics ArrayScan V^{TI} high-content fluorescent imager. Images were acquired in three channels corresponding to blue (nuclei), green, (autofluorescence), and red (DSRED) fluorescence. Individual cells were first automatically

identified following labeling of nuclei with Hoechst as a basis for nucleocentric cellular intensity measurements. A region of cytoplasm surrounding each identified nucleus was then assessed for fluorescent signal in the green and red channels, with DSRED-positive cells exhibiting high red, and low green fluorescence. This cellular data was averaged over the number of cells in the well to give a mean intensity value for the well.

In the absence of transcription factor overexpression, rare DSRED-positive cells were identified, indicating that a small subset of the original cell population is capable of spontaneous activation of the insulin promoter fragment under these culture conditions (Figure 2.4A). To facilitate interpretation of the screening data, the level of red intensity in these wells was arbitrarily set at a value of 1 (Figure 2.4). The results from this unbiased screen reveal that the relative intensity of DSRED expression increases with increasing numbers of transcription factors applied. For example, addition of all six viruses resulted in an 8.05 ± 0.52 fold increase in DSRED expression as compared to cells not receiving virus (Figure 2.4). In some cases, overexpression of fewer than all six viruses (eg. PDX1, ISL1, PAX6, and MAFA) resulted in a similar relative increase in DSRED expression (7.25 ± 1.18 fold). To confirm the primary screen, select combinations of transcription factors, including PDX1, ISL1, PAX6, and MAFA, as well as NEUROD1, NGN3, ISL1, PAX6, and MAFA and the six-virus combination were tested in larger cultures. Despite similar results in the primary screen amongst these three sets of transcription factors, the six-virus combination was superior in producing DSRED-positive hAF cells in larger cultures. Therefore, the remainder of the experiments focused on the optimized overexpression of all six transcription factors.

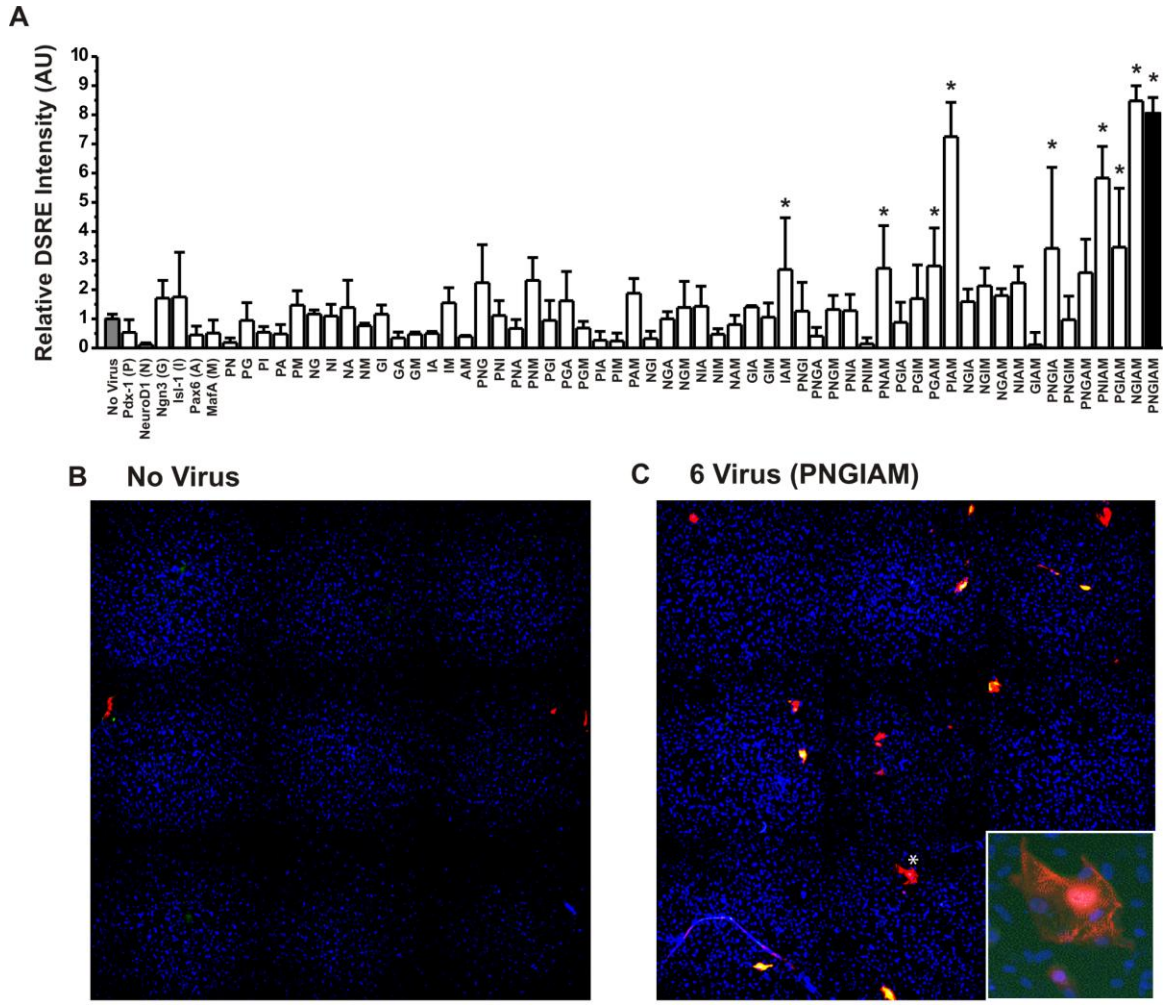

Figure 2.4. High throughput analysis of insulin promoter reporter activation in hAF cells following adenoviral-mediated transcription factor overexpression.

(A) Relative DSRED (DSRE) intensity was measured following 14 days of culture in the presence or absence of adenovirus-delivered transcription factor over-expression. Data are expressed as relative fluorescence intensity over hAF cells cultured in the absence of transcription factor over expression. Error bars represent the standard error from the mean of three independent screens. Each transcription factor is represented by a single letter code. P = PDX1; N = NEUROD1; G = NGN3; I = ISL1; A = PAX6; M = MAFA. **P*<0.05 versus No Virus. (B and C) Representative fluorescent images of differentiated hAF cells cultured in the presence of (B) no virus or (C) the combination of all six viruses. DSRED expression is shown in red with nuclei marked with Hoechst in blue. * Indicates region depicted in the enlarged inset of C.

Overexpression of β-Cell Transcription Factors Results in a Time-Dependent Increase in Insulin Gene Expression

We next evaluated the time course of insulin promoter reporter activation using DSRED expression as a surrogate marker for endogenous insulin gene transcription. Human AF cells were either treated with the six transcription factor combination, or left uninfected. At specific times following delivery of adenoviral vectors, cells were harvested and analyzed

for DSRED expression by flow cytometry (Figure 2.5). Within the first 3 days of infection, DSRED expression was not visible by fluorescence microscopy. Therefore, hAF cells were first analyzed for DSRED expression on day 4 (Figure 2.5A and C). In cells that received no transcription factors, only 0.047 ± 0.001% expressed DSRED at day 4 and reached a maximum of 0.145 ± 0.001% by day 28. Conversely, over the same period, the percentage of DSRED-expressing hAF cells that had been infected with the six virus cocktail increased from 0.447 ± 0.001% on day 4 to its maximum value of 10.646 ± 0.006% on day 28 (N = 3 for each time point; Figure 2.5).

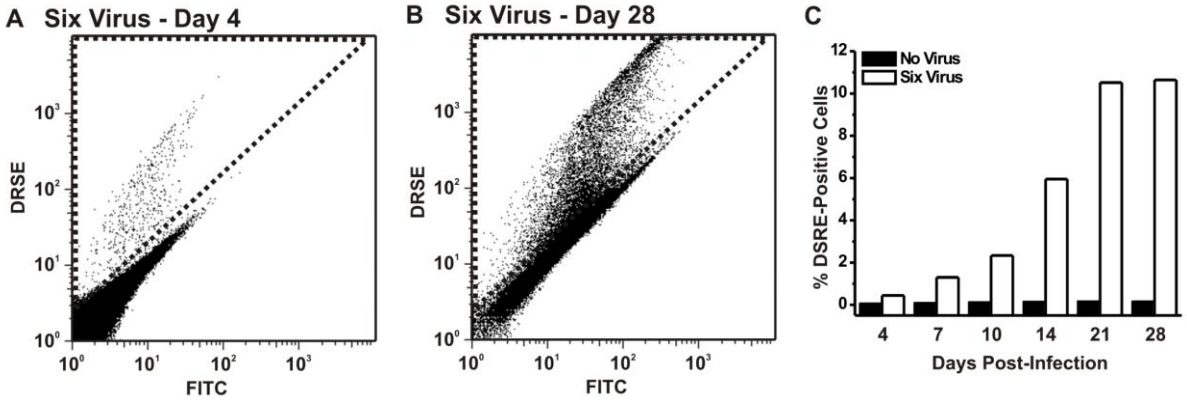

Figure 2.5. hAF cells show a time-dependent increase in DSRED expression after transcription factor delivery.

(A and B) Representative FACS analysis of DSRED (DSRE) expression in hAF cells (within polygon gate defined by black dotted line) over-expressing the six virus combination at (A) 4 days and (B) 28 days post-infection. (C) Pooled data from three independent differentiation trials for hAF cells treated with no virus (black bars) or the six virus combination (white bars) at various time points post-infection. Data are expressed as the percentage of DSRED (DSRE)-expressing cells. Error bars indicate standard error from the mean.

To correlate DSRED expression to endogenous insulin gene expression, we quantified insulin mRNA levels at multiple time points following transcription factor overexpression. Transduced hAF cells show a time-dependent increase in insulin gene expression, reaching a maximum level of 7.5 $x10^{-5}$ times that of human islets at 21 days post-infection (Figure 2.6A). Glucagon gene expression also exhibited a time-dependent increase in expression, reaching 1 $x10^{-3}$ versus human islets at day 10 post-infection (Figure 2.6B). To ensure that adenoviral delivery resulted in sustained transgene delivery, we also quantified expression of PDX1 at the same time points post-infection. As shown in Figure

2.6C, PDX1 expression was maximal at 4 days post-infection (26-fold over human islets), with levels decreasing but detectable levels observed over the course of the experiment.

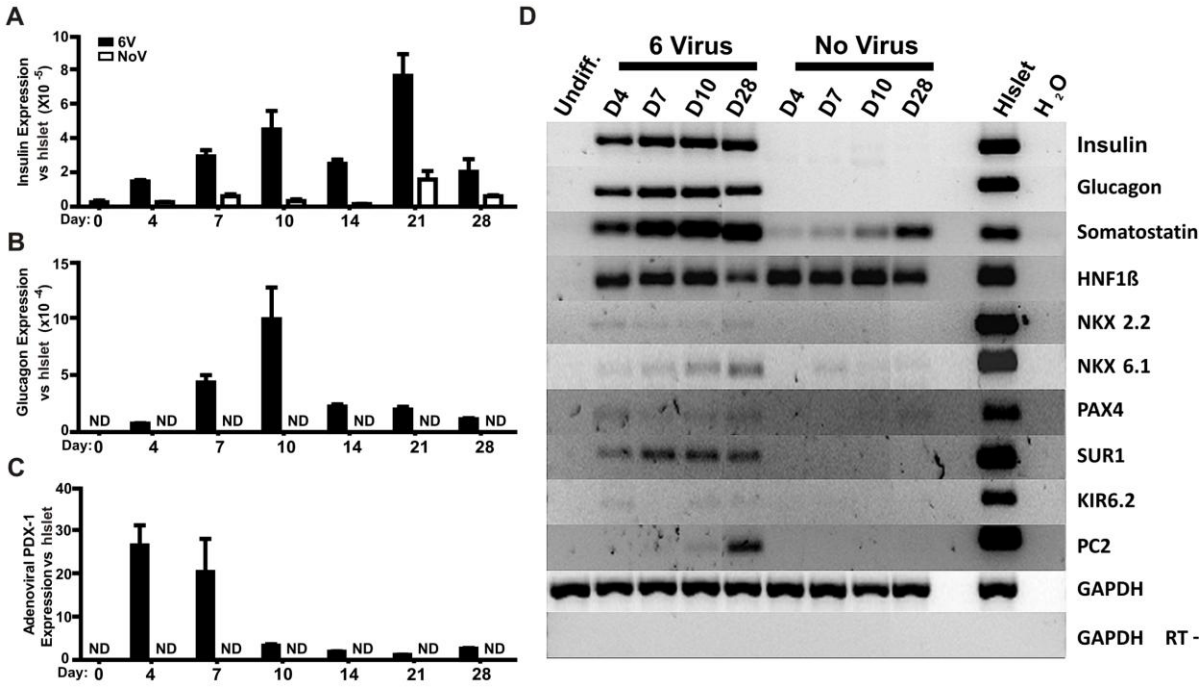

Figure 2.6. Transcription factor overexpression results in a time-dependent increase in insulin and glucagon message as well as other transcription factors and key β-cell components.

(A) Quantification of insulin gene expression in hAF cells treated with no virus (white bars) or the six virus combination (black bars) at various time points during the differentiation. (B) Quantification of glucagon gene expression in hAF cells treated with no virus (white bars) or the six virus combination (black bars). (C) Quantification of PDX1 gene expression in hAF cells treated with no virus (white bars) or the six virus combination (black bars). Data are expressed as mean relative expression level compared to adult human islets. Error bars represent standard error from the mean. ND, not detected. (D) End point RT-PCR was performed on hAF cells treated with no virus or the six virus combination at various time points during the culture period. Undifferentiated hAF cells were included as a negative control, while cDNA from adult human islets was included as a positive control.

Characterization of Induced hAF Cells

Undifferentiated hAF cells did not express markers of islet endocrine cells, nor of more mature β-cells. In the absence of transcription factor induction, insulin and glucagon levels were lower than in hAF cells treated with the transcription factor cocktail (Figure 2.6D). Interestingly, some markers of endocrine cells do appear in these non-induced *in vitro* cultured hAF cells. For example, somatostatin gene expression is absent from naïve hAF cells, but is expressed in a time-dependent manner in the presence of nicotinamide. In addition, HNF-1β gene expression can be detected during the 28-day culture in the absence

of transcription factor over-expression. Conversely, overexpression of the six virus transcription factor cocktail activates insulin gene expression along with glucagon and a number of additional markers of mature islet endocrine cells (Figure 2.6D). These include transcription factors normally expressed during β-cell maturation such as NKX6.1 and NKX2.2, as well as genes encoding functional proteins involved in excitation/secretion coupling (KIR6.2 and SUR1) and insulin processing (PC2).

As indicated above, insulin was expressed at only a fraction of that observed in adult human islets. In agreement with these data, we identified only rare hAF cells with robust insulin immunoreactivity following transcription factor induction (Figure 2.7). As expected based on the infection efficiency of the reporter virus as shown in Figure 2.2, insulin immunoreactivity was detected in cells that expressed DSRED (Figure 2.7B, top panel) as well as in some cells that did not (Figure 2.7B, bottom panel). Similarly, rare cells were identified as expressing the glucose transporter GLUT2 as well as the glucose sensing enzyme glucokinase, and the insulin processing enzyme PC2 (Figure 2.7C). Conversely, naïve AF cells did not exhibit immunoreactivity for these proteins.

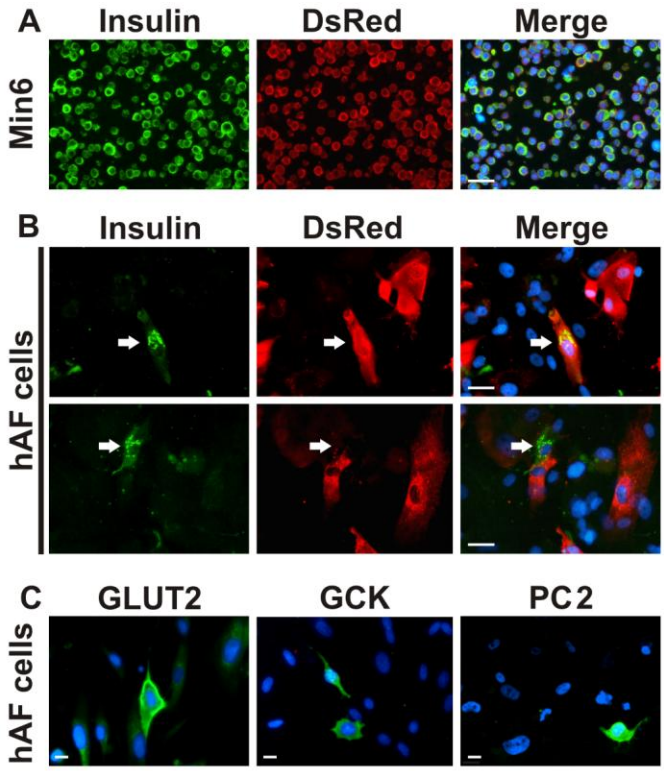

Figure 2.7. Identification of insulin-expressing hAF cells.

(A) Representative immunostaining of pTiger-hIP-DSRED-infected Min6 cells for insulin (green) and DSRED (red) showing extensive colocalization of these two proteins (merge). (B) Representative immunostaining of hAF cells infected with the pTiger-hIP-DSRED reporter lentivirus and induced with six transcription factors for 17 days of culture showing insulin protein in cells that do express the fluorescent reporter (white arrow in upper panels) and cells that do not express the fluorescent reporter (white arrow in lower panels). (C) Representative immunostaining of six transcription factor induced hAF cells cultured for 21 days showing immunoreactivity for glucose transporter 2 (GLUT2), glucokinase (GCK), and prohormone convertase 2 (PC2). Nuclei are marked with DAPI (blue). Scale bar is 50 μm for all images.

Induced hAF Cells are not able to Reverse Streptozotocin-Induced Diabetes

It has been recently demonstrated that pancreatic precursor cells can differentiate into more mature β-cells in an *in vivo* setting following transplantation (117, 125). To assess the ability of our partially reprogrammed hAF cells to further differentiate or mature *in vivo*, cells treated with either nicotinamide alone or nicotinamide and the six virus transcription factor combination were transplanted under the kidney capsule of diabetic Rag1^{tm1Mom}/J mice. Five days after transplant, recipients of either cell type did not show evidence of body weight gain (Figure 2.8A) or reduced hyperglycemia (Figure 2.8B). Sustained-release insulin pellets were implanted subcutaneously to restore normoglycemia, thus allowing the hAF cells additional time to acquire a functional β-cell phenotype. Thirty days later, insulin

pellets were removed to assess the ability of the graft to contribute to normoglycemia. All mice immediately returned to a hyperglycemic state (Figure 2.8B), indicating a failure of the hAF cell graft to regulate blood glucose levels within the allowed maturation timeline.

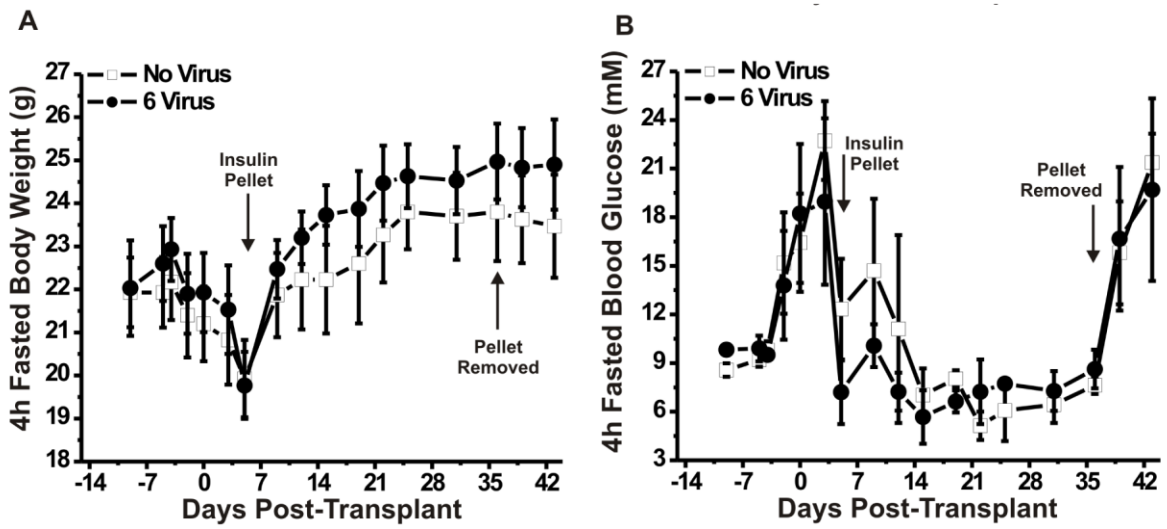

Figure 2.8. Insulin-producing hAF cells are unable to correct streptozotocin-induced hyperglycemia.

(A) Body weight following a 4 hour morning fast in animals receiving hAF cells treated with no virus (□) or the six virus combination (●). Animals were treated with 150 mg/kg streptozotocin 5 days prior to transplant. Slow release insulin pellets were implanted subcutaneously at day 5 post-transplant as indicated on the graph. (B) Blood glucose levels following a 4 hour morning fast. Insulin pellet implantation and removal is indicated. All data are expressed as the mean ± SEM. N = 3 animals per group.

Isolation of Clonal Cell Populations Potentially more Amenable to Reprogramming

Due to the heterogeneous nature of the hAF cell population used in this study, we aimed to identify expandable cell types that could yield a more efficient starting material for the generation of new β-cells. To address this, hAF cells containing the fluorescent reporter construct were cloned by limiting dilution. Of the nearly two hundred clones isolated, 48 were sufficiently expandable to be split into duplicate plates for viral induction and outgrowth, respectively. Of these, 11 were able to effectively activate the insulin promoter fragment following transcription factor induction. During expansion, six clones retained sufficient proliferative potential for larger reprogramming trials. Ultimately, two clones yielded high percentages of DSRED-positive cells following viral induction (Figure 2.9), however these clones too lost proliferative potential upon further expansion. Therefore, it is

unclear at this time if a suitably expandable hAF cell population exists that can be efficiently reprogrammed towards a β-cell phenotype.

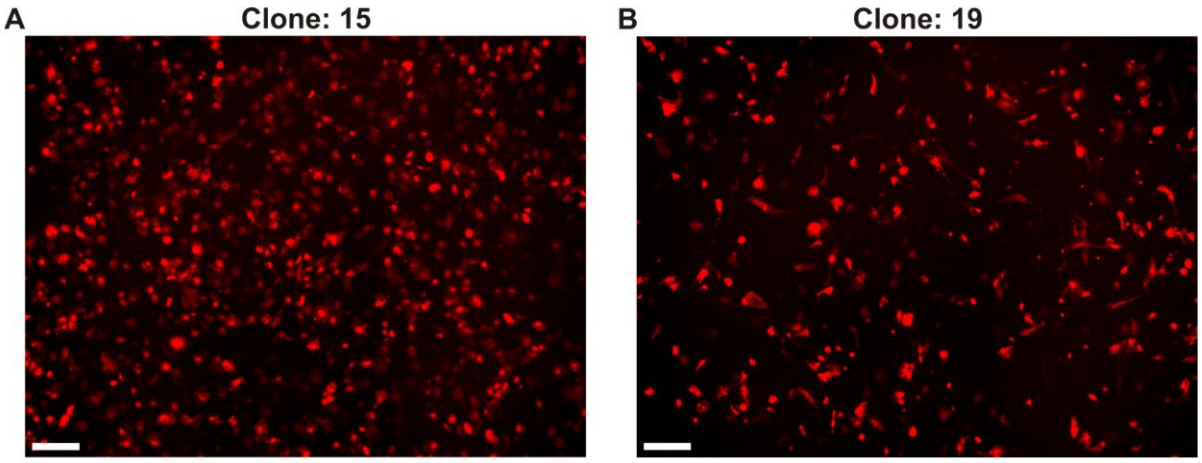

Figure 2.9. Clonal hAF cell populations activate the insulin promoter reporter following adenoviral-mediated transcription factor induction

Representative epifluorescence images of DSRED expression (red) in initially expandable (A) clone 15 and (B) clone 19. Imaged areas are of over-confluent differentiated and infected cultures. Scale bar = 500 μm.

2.4 Discussion

Human amniotic fluid has been shown to contain cells capable of differentiation towards a number of cell lineages (50), however pancreatic endocrine cell differentiation from these easily obtainable cells had yet to be demonstrated at the time of study. In two previously published studies, human amnion epithelial cells were isolated through complex mechanical and enzymatic methods from the luminal surface of the amniotic membrane with the goal of producing surrogate β-cells (160, 161). In both studies, extended culture in the presence of nicotinamide induced insulin transcription and transplantation of these processed amniotic epithelial cells into diabetic rodents resulted in rapid and sustained reversal of their hyperglycemia and weight loss. While these studies suggest a physiological recovery of hyperglycemia, concerns about spontaneous recovery from streptozotocin (STZ)-induced diabetes similar to that seen in young STZ-treated rats (162) and a lack of rigorous *in vitro* or *in vivo* characterization of these cells make interpretation challenging. As Hou et al. in 2008 reported a plasma human specific C-peptide concentration in immunocompotent transplanted BL6 mice of 0.30 ng/ml versus 0.27 ng/ml in sham operated and normal controls, it is hard to

correlate the recovery from diabetes observed by the authors without the cell transplants generating the established circulating levels of 1-2 ng/ml needed to recover STZ-induced diabetes using a hESC derived transplant (125). Given that the transplanted mice did recover, a mechanism outside of amniotic epithelial cell generated insulin seems likely. It is possible that the transplanted cells may have migrated away from the graft and somehow stimulated endogenous β-cell regeneration. This process has been suggested for bone marrow derived stromal cells, which when transplanted in diabetic mice naturally homed to the pancreas where they were associated with increased levels of insulin and reduced hyperglycemia (52, 53). Specifically whether or not diabetes reversal in the case of amniotic epithelial cells was due to the transplanted amnion epithelial cells or enhanced endogenous pancreatic regeneration capacity remains an outstanding question.

Focusing on the *in vitro* differentiation capacity of hAF cells with the goal of better understanding the potential of human amniotic fluid-derived cells in the development of surrogate β-cells, we applied an unbiased combinatorial high-content approach of overexpressing up to six transcription factors known to be critical for the development or maintenance of a β-cell phenotype (100). To efficiently monitor cellular reprogramming, we developed a lentivirus delivered fluorescent reporter system where DSRED expression is controlled by activation of a fragment of the human insulin promoter. Stable integration of this reporter construct in hAF cells allowed for image-based, high-content, live-cell screening of the reprogramming process. Using this unbiased approach, we identified that overexpression of all six transcription factors used in this study resulted in the greatest activation of the insulin promoter reporter. It should be noted that this cell based screen was missing a high does control virus group to validate that the activation of the reporter construct was not simply in response to non specific viral effects. While this is unlikely to be the case with low viral doses, as multiple single, double and triple factor combinations did not elicit a response, this control cannot be inferred for the six factor combination.

Growing evidence has shown the potential for the use of cellular reprogramming in regenerative medicine. Ber and colleagues reported that transient expression of rat PDX1 in liver cells resulted in the activation of the endogenous mouse PDX1 gene, leading to the ectopic expression of insulin within the liver of treated animals (44). Ectopic expression of the mouse PDX1 gene in human mesenchymal stem cells likewise was reported to induce the

activation of the endogenous human PDX1 gene, leading to the production and secretion of insulin from this cell population (163). In addition, Zhou and colleagues demonstrated that expression of PDX1, NGN3 and MAFA from adenoviral vectors in pancreatic exocrine tissue stimulated the formation of extra-islet insulin-positive cells, showing that direct reprogramming of pancreatic exocrine tissue to endocrine cells is achievable *in vivo* (156). This same mixture of factors was recently shown to induce insulin positive cell clusters from human and mouse intestinal cells (48). In our high-content screen, this particular combination of three pancreatic transcription factors did not result in significant activation of the insulin promoter fragment. In fact, our results show that the only three-virus combination to result in significantly greater activation of the insulin promoter reporter as compared to no virus was the combination of ISL1, PAX6, and MAFA. This combination of transcription factors was however significantly less efficient in activating the reporter than the combination of all six factors. The difference between our results and those of the Melton and Stanger groups likely reflects differences in the starting cell population. Specifically, pancreatic exocrine tissue and intestinal tissue is developmentally closer to islet endocrine tissue than cells derived from amniotic fluid. Therefore, reprogramming of this hAF cell population towards a β-cell phenotype requires more extensive input than is required to reprogram pancreatic exocrine tissue or perhaps other somatic tissues with close developmental ties to pancreatic endocrine cells.

In our model system, transcription factor expression resulted in the activation of the insulin promoter reporter construct. Of the transcription factors used in our study, PDX1, NEUROD1, ISL1, PAX6 and MAFA are capable of directly binding and activating the insulin promoter (164-168) without necessarily resulting a *bona fide* reprogramming of the cell. Similarly, the transcription factors ISL1 and PAX6 are known to be involved in activation of the glucagon promoter (168, 169) and presumably are responsible for our observed expression of the proglucagon gene. Interestingly, we show that addition of the six-virus cocktail leads to the expression of additional transcription factors also involved in the development or maintenance of the β-cell phenotype including NKX2.2, NKX6.1, and HNF1β. Furthermore, some components of the glucose sensing and insulin processing pathways appeared to be present, with mRNA for both subunits of the ATP-sensitive potassium channel and PC2 being detected in this hAF cell population only following

transcription factor overexpression. Further support for cellular reprogramming is the observation that insulin and glucagon gene expression peaked at 21 days and 10 days after infection, respectively. This is in contrast to the much earlier peak expression of PDX1. The lag time between expression of the adenoviral-delivered transcription factors and the induction of insulin and glucagon gene expression suggests that a cascade of events must occur in the cell prior to activation of the given promoters.

Our data are also very similar to a recent study in non-human primate AF cells which were readily transduced by adenovirus constructs overexpressing transcription factors (PDX1, NGN3 and MAFA) with the goal of inducing pancreatic endocrine development (51). This study found that MAFA alone was able to induce insulin gene expression but a combination of all three transcription factors was more effective at inducing the expression of other pancreatic genes including NEUROD1, ISL1, NKX2.2, PCSK2 and glucagon (51). This combination of exogenous PDX1, NGN3 and MAFA, with or without the endogenous NEUROD1 and ISL1 expression were both found to not significantly improve DSRED expression in our screen. While the reason for this is unknown, variables including the cell populations (human versus primate), viral dose (MOI of 10 versus 100), monitoring method (DSRED versus endogenous insulin) or culture conditions (low temperature with nicotinamide versus 37°C with nicotinamide, EGF, and B27 supplement) may have had significant effects. It is also possible that the remaining factor PAX6 may play a dominant role in the induction of insulin in our system. Further support of this notion comes from the fact that out of the 9 conditions which showed significant DSRED induction, all 9 included PAX6 (Figure 2.4). Given that PAX6 is a known regulator of pancreatic endocrine development and is implicated in controlled expression of the hormone convertase enzymes PC1/3 and PC2, it is possible that this transcription factor is a key direct or indirect regulator of the insulin promoter reporter construct used in our system (168, 170-172).

Our results indicate that despite the activation of the insulin promoter, the level of insulin gene expression is extremely low in this particular mixed cell population. Unlike partially differentiated hESCs that show the ability to further mature *in vivo* (117, 125), it appears that the heterogeneous hAF cell population cultured under the conditions described above in this study does not possess this quality. Transplantation of hAF cells at 14 days post-infection, when insulin gene expression is maximal in *in vitro* cultures did not decrease

hyperglycemia in our chemically induced diabetic model, nor did these cells mature *in vivo* sufficiently over the next 30 days to regulate blood glucose levels. This particular transplant experiment was performed with a heterogeneous population of hAF cells to maximize the presence of any sub-population capable of reverting the diabetic phenotype. While purification of DSRED-expressing reprogrammed hAF cells may have yielded a more robust cell population for transplant therapy, the sheer number of cells required to achieve significant levels of insulin production are likely limiting even in this scenario.

Attempts to produce hAF cell clones that can more efficiently respond to our reprogramming protocol were initially promising, as multiple cell types were isolated from the original fluorescent reporter cell line that were able to respond to the transcription factor cocktail with efficiencies of DSRED expression vastly exceeding that of the original heterogeneous cell population. However, unfortunately these clones exhibited reduced *in vitro* expansion potential. Nevertheless, a further characterization of these cells may yield important information as to the type of cell that is amenable to β-cell reprogramming. Given that hAF cells have been demonstrated to be largely non-tumourogenic, isolation of particular cell populations within AF cell preparations may yet result in a useable source of tissue for cell-based therapeutics.

The development of a fluorescence-based integrating reporter system using the FIV lentivirus allowed for repeated live-cell, non-cytotoxic assessment of reprogramming in the same cells by simple visual inspection with a fluorescent microscope. Coupling the expression of DSRED to a human insulin promoter fragment allowed us to observe the time course of insulin promoter activation as well as to easily quantify the efficiency of reprogramming. In addition, monitoring of live cells at multiple time points allowed us to perform high-content screening to discover conditions that improved the reprogramming efficiency. This simple tracking method can theoretically be applied to monitoring any stimuli which may influence the induction of insulin expression in hAF cells such as culture characteristics (oxygen availability, nutrient composition, growth matrix composition, etc.), developmental signalling cascades (TGF-β, BMP, Shh, WNT, among many others). The use of such a fluorescent monitoring system during the differentiation of other more plastic starting cell populations such as hESCs may aid in the discovery of conditions that promote the formation of *bona-fide* β-cells.

Chapter 3: Development and Application of CA1S hESCs

3.1 Background

hESCs are derived from the inner cell mass of blastocysts, can be maintained for prolonged periods in culture and can give rise to cells from all 3 germ layers (58, 173). In addition to providing an essentially unlimited stem cell supply for basic research, hESCs may be used for generating cells and tissues for therapeutic applications, screening drug and gene effects, toxicology studies, and the production of other biomaterials. A major limitation to progress in achieving these goals is the poor survival and low cloning efficiencies of hESCs (<1%) when they are mechanically or enzymatically dissociated to produce a single-cell suspension (174-176). Susceptibility to physical damage and rapid activation of apoptotic pathways, due to loss of cell-cell and cell-matrix attachments, are believed responsible for the considerable losses of hESCs exposed to these treatments (177-179). Several groups have described methods to obtain adapted hESCs that exhibit more tolerance to single-cell dissociation without overtly compromising pluripotency (175, 180-182). However, the widespread adoption of these cells has been discouraged by the observations that these methods can promote the outgrowth of karyotypically abnormal cells (183) or by more subtle features of neoplastic progression (184). If outweighed by advantages, the adapted nature of some hESC and iPSC lines should not preclude their use in HTS applications. This utility has been acknowledged with karyotypically abnormal human embryonal carcinoma cells (185-188). Similarly adapted or incompletely reprogrammed iPSC lines are being developed as practical HTS tools, especially when their disease modeling characteristics are needed. In an effort to avoid the use of adapted hESC lines but achieve efficient screening protocols, some groups have treated single-cell hESCs to an inhibitor of Rho kinases (Y-27632), resulting in a markedly increased cloning efficiency (176). This use of Y-27632 has eased hESC screening despite the understanding that it has multiple other cellular effects that arguably compromise its usefulness (189, 190). Most hESC lines nonetheless continue to be routinely maintained using arduous mechanical dissociation to generate multicellular aggregates for culture expansion and screening (177-179, 191, 192).

In an effort to circumvent these technical constraints associated with the application of hESCs, Dr. N. Caron working in the lab of Dr. J. Piret subjected a hESC line (CA1) (59)

from the lab of Dr. A. Nagy to a single cell passaging adaptation procedure to obtain a subline (CA1S). These CA1S cells were are relatively insensitive to enzymatic dissociation and can be maintained for months in this state. CA1S cells express standard markers of pluripotent hESCs, produce typical well-differentiated multi-lineage teratomas *in vivo,* and importantly, retain the ability to differentiate *in vitro* through a multi-stage pancreatic differentiation. As a proof of principle of their utility for high throughput screening (HTS) studies, we demonstrated their ability to be seeded and differentiated uniformly in 96-well plates, generate definitive endoderm upon WNT3A and Activin A induction in an HTS assay format and respond to a simple concentration based growth factor screen of definitive endoderm induction.

3.2 Methods

Culture and characterization of hESCs

The previously published CA1 hESC line (59) was provided by Dr. A. Nagy (Mount Sinai Hospital Toronto, ON, Canada) and approval for its use obtained from the Canadian Stem Cell Oversight Committee and the UBC ethics board. CA1, CA1S and H1 cells were maintained between 20 and 95 % confluence in 1:30 diluted growth factor reduced Matrigel-coated (BD Biosciences) plates as previously described (174, 193) in mTeSR1 complete media (194, 195) (STEMCELL Technologies, Vancouver, BC, Canada) with daily media changes.

To test for pluripotency via teratoma formation assay, CA1S cells were cultured for 10 consecutive passages using the CA1S enzymatic dissociation protocol and aliquots of 1-2 x 10^6 cells were resuspended in Matrigel and injected subcutaneously into 3 month-old NOD/SCID mice maintained in micro-isolators with sterile food and water under pathogen-free conditions (196). Subsequent teratomas were fixed, paraffin-embedded, sectioned for histological analysis. Identification of graft composition and differentiated cell types was confirmed by an experienced pathologist.

To assess the possibility of chromosomal alterations in CA1S cells, metaphase spreads were prepared and G-banded as previously described (174). 25 metaphases were counted and 8 analyzed in detail. To check for small genomic alterations array-comparative genomic hybridization (aCGH) analysis was performed on a sample of passage 85 CA1S

hESCs at the WiCell Research Institute (Maddison, WI, USA) using a NimbleGen 4x72K array (HG18 WG CGH v2 x4) and confirmed using the higher resolution 12x135K array (HG18 WG CGH v3.1 HX12). Data analysis was performed using NimblScan™ software (CGH Fusion RBS v1.0) by members of WiCell. Quality assurance criteria included: 1) opposite gender reference DNA ratio change in X and Y chromosomes; 2) presence of Xpter and Xq21.3 pseudoautosomal imbalance; and 3) presence of known reference DNA copy number changes.

Immunochemistry of OCT4 in hESCs was performed as previously described (196, 197). Briefly, cells were plated on Matrigel-coated Lab-Tek Permanox slides (Nalge Nunc, Rochester, NY, USA) and maintained in an undifferentiated state until the desired confluence was reached. CHO-K1 cells were used as negative staining controls. Cells were fixed with 4% PFA, permeabilized with 0.1% Triton in PBS and then stained with 10 µg/ml monoclonal anti-human/mouse-OCT3/4 rat IgG (R&D Systems, Minneapolis, MN, USA) and 10 µg/ml Goat $F(ab')_2$ PE-Cy5 anti-rat IgG (Cedarlane, Burlington, ON, Canada) and stained with DAPI (Invitrogen). Cells were examined using an epifluorescence inverted microscope (Motic, Hong Kong, Hong Kong) and photomicrographs obtained using a Nikon D100 digital camera (Mississauga, ON, Canada).

To assess expression of PSC associated surface antigens, cells were dissociated into a single cell suspension, transferred to a PBS/FBS (10%) solution and then stained with primary and secondary antibodies at 4ºC for 20 min. Negative controls were either CA1 cells differentiated for 3 weeks in FBS or undifferentiated cells stained with the relevant secondary antibody only (196). Cells were stained with 5 µg/ml propidium iodide (Sigma) and washed before analysis with a FACSCalibur (BD Biosciences) and Flowjo software (Tree Star). The percentage of positively stained viable cells was determined using gates excluding 99.5% of the negative control and propidium iodide positive cells. Concentrations for antibodies used were: 5 µg/ml rat anti-human/mouse-SSEA3 (R&D Systems), 5 µg/ml mouse anti-TRA-1-60 (Abcam, Cambridge, MA, USA), 20 µg/ml Alexa 647 goat anti-Rat IgM (Invitrogen) and 20 µg/ml goat Alexa 488 anti-mouse IgM (Invitrogen).

qPCR determination of growth rate and plating efficiency

Plating efficiency (yield of adherent cells after 24 hours) and cell growth rates were calculated using qPCR over a regular passaging cycle (5 days for CA1S and 6 days for CA1). Average doubling times were estimated with an exponential model assuming no appreciable cell death between days 1 and 5. Plating efficiencies were obtained as the ratio between the number of cells present 24 hours after plating a defined number of cells into the culture dish using quantitation of genomic DNA. Adherent cells were lysed and genomic DNA was isolated using a GenElute™ Mammalian Genomic DNA Miniprep Kit (Sigma-Aldrich). A fixed fraction of DNA (0.5%) was used for qPCR using a 7500 Fast Real-Time PCR system (Applied Biosystems) and EXPRESS SYBR® GreenER™ (Invitrogen) and the primers ASPolGF 5-gaggtgttgacggaaaggag-3 and ASPolGR 5-cagaagagaatcccggctaag-3, 45 cycles, Tm 60°C. Duplicate samples were assayed based on a standard curve of known CA1 hESC numbers.

Definitive endoderm and pancreatic progenitor differentiation and assessment

CA1S cells were seeded on Matrigel coated plates in mTeSR1 medium to be 95% confluent the next day. Differentiation toward definitive endoderm and subsequent pancreatic precursor stages was induced by exposing the cells to daily media changes as previously described (117, 128). Briefly, on day 1, 95% confluent CA1S cell cultures were fed RPMI 1640 medium (Invitrogen) containing 25 ng/ml WNT3A (R&D Systems) and 100 ng/ml Activin A (R&D Systems), then incubated for 2 more days in RPMI 1640 with Activin A and 0.2% v/v defined FBS (HyClone Laboratories, South Logan, UT, USA). Cultures with >80% CXCR4 positive cell populations on day 4 were fed for 2 more days with RPMI 1640 + 2% FBS and 50 ng/ml FGF7 (PeproTech, Inc., Rocky Hill, NJ, USA). Following 3 days in DMEM/F12 (Invitrogen) containing 2 μM all-trans Retinoic Acid (Sigma-Aldrich), 250 nM Cyclopamine (Calbiochem, La Jolla, CA, USA), 100 ng/ml Noggin (PeproTech) and 1% v/v B-27 supplement (Invitrogen), cultures were maintained in DMEM/F12 containing 1% B-27 (Invitrogen). Evidence of CA1S-derived pancreatic endocrine cells was examined by radioimmunoassay of 24-hour static secretion media samples to measure the C-peptide levels (HCP-20K, Millipore, Billerica, MA, USA). Insulin, glucagon, and PDX1 transcript expression was assessed by RT-qPCR as previously described (2) (see methods of Chapter 2

and Table 3.1). Immunocytochemistry of paraformaldehyde-fixed cell cultures was performed as previously described (97, 198) using agarose embedded cell pellets. The primary antibodies used can be found in Table 3.2. After washing, cells were incubated with Alexa 488, 555, or 647-conjugated secondary antibodies (Invitrogen, 1:1000) and counterstaining with DAPI before imaging with an ImageXpress$^{MICRO\ TM}$ microscope and associated software (Molecular Devices Corporation, Sunnyvale, CA, USA).

Table 3.1 Sequences of primers used in RT-qPCR in chapter 3

Gene Name	Gene Accession	Product Size (bp)	Primer Sequence Forward / Reverse 5'→3'	Reference
Insulin	NM_000207.2	245	AGCCTTTGTGAACCAACACC GCTGGTAGAGGGAGCAGATG	(158)
Glucagon	NM_002054.4	275	CATTCACAGGGCACATTCAC CGGCCAAGTTCTTCAACAAT	(158)
PDX1	NM_000209	178	CGTCCAGCTGCCTTTCCCAT CCGTGAGATGTACTTGTTGAATAGGA	(2)
β-actin	NM_001101	377	GGCATGGGTCAGAAGGATT AGGGCATACCCCTCGTAGAT	(2)

Table 3.2 Antibodies used in immunocytochemistry in chapter 3

Protein Name	Host Species	Supplier / Catalogue number	Staining Method	Dilution	Antigen Retrieval
Insulin	Guinea Pig	Millipore 4011-01F	Slide	1:1000	HIER
Glucagon	Rabbit	Thermo Scientific PA1 - 37768	Slide	1:100	HIER
PDX1	Rabbit	Dr. J. Habener Gift	Slide	1:1000	HIER
NKX6.1	Rabbit	Dr. A. Rezania Gift	Slide	1:1000	HIER

HIER (heat induced epitope retrieval): 15 minutes at 95 °C in 10 mM citrate buffer with 0.05 % tween-20 pH 6.0.

Slide: PFA fixed, paraffin section of agarose embedded cell pellet or pancreatic tissue

High throughput analysis of definitive endoderm induction

CA1 and CA1S cells were dissociated, and seeded onto 1:30 diluted Matrigel coated 96-well plates such that CA1S cells were 90-95% confluent 16 hours later. Cells were differentiated to definitive endoderm as described previously with enumeration on day 1 and 4 by nucleocentric object identification (Molecular Devices) using 2 µg/ml Hoechst 33342 nuclear dye (Invitrogen). On day 4, CA1 and CA1S cells were also examined for CXCR4

expression by high-throughput flow cytometry using an LSRII with a high throughput sampler (BD Biosciences). Live-cell CXCR4 staining was carried out in a 96-well format. Cells were detached with Accutase, triturated to single-cells, washed twice in PBS/FBS (2%) and resuspended in 50 µl 1:100 diluted anti–CXCR4-PE or relevant isotype control antibodies (R&D Systems). After 1 hour at room temperature and two washes, cells were analyzed. Data analysis was carried out using FlowJo Software (Tree Star) with CXCR4 positive cells being defined as emitting a level of fluorescence exceeding that of 99.5% of the isotype control-stained cells.

3.3 Results

Isolation of a subline of CA1 hESCs adapted for single cell propagation

Early passage pluripotent CA1 hESCs were dissociated into 3-20 cell aggregates by limited exposure to TrypLE and by the addition of FBS before a single cell suspension was obtained. A high cell seeding density in mitomycin C-treated embryonic fibroblast conditioned culture medium effectively maintained pluripotency (199) during the adaptation process. Initially, the cells had a low plating efficiency of less than 5%, but by the 3rd passage, confluency was reached more rapidly. Starting with passage 4, the cells were exposed to TrypLE for a longer period to produce a single cell suspension with small aggregates of 2 to 6 cells accounting for only ~30% of the cells (3). At this stage the cells again transiently demonstrated a low efficiency of re-attachment that improved until passage 10 and beyond with cells that had typical hESC morphology and adherence. These cells were then assigned the subline name of CA1S.

CA1S cells retain multiple features of pluripotent hESCs

To determine whether CA1S cells retain classical features of hESCs, undifferentiated CA1S cells were monitored for expression of SSEA-3 at monthly intervals between passages 8 and 65 after adaptation. At all times, a high proportion of the cells were SSEA-3, Tra-1-60, OCT4 and alkaline phosphatase positive (Figure 3.1). While expression of SSEA3 and TRA-1-60 was also maintained over 26 days of culture in mTeSR1 medium prepared without bFGF, which suggests a loss of bFGF dependence, CA1S cells were capable of generating typical teratomas that contained the expected mixture of well-differentiated tissues including

representatives from all 3 germ layers after 2 months post transplantation in NOD/SCID mice (Figure 3.1F and G) (3).

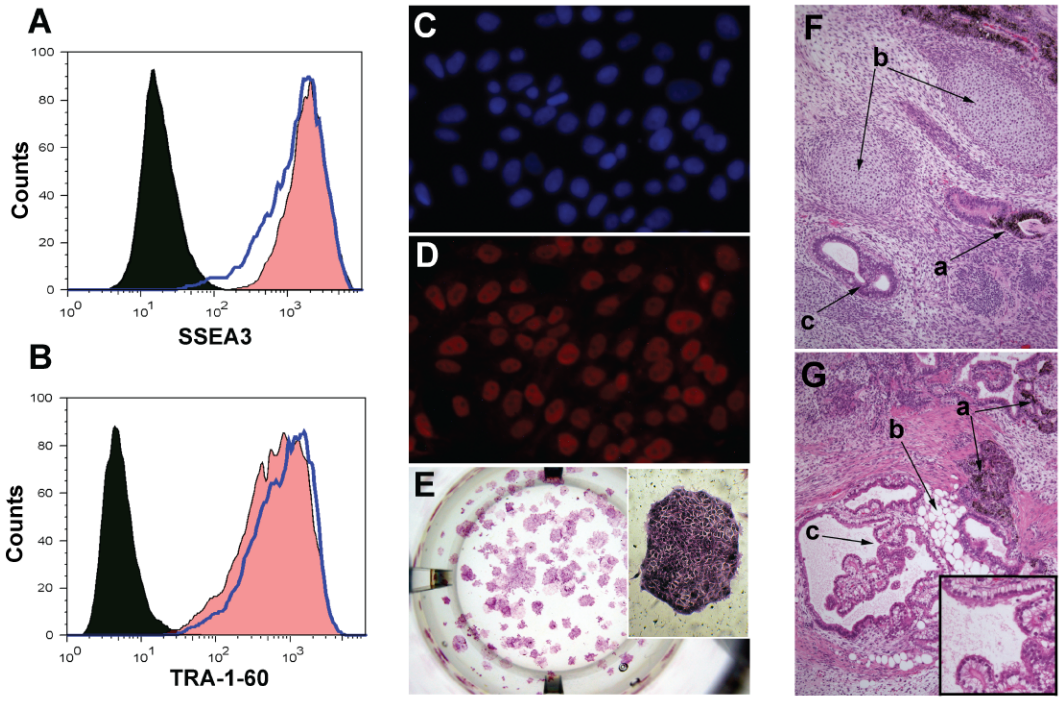

Figure 3.1. CA1S cells retain pluripotency markers and *in vivo* differentiation capacity.

CA1S flow cytometric profiles for SSEA-3 (A) and anti-TRA-1-60 (B) compared to stained CA1S cells induced to differentiate by exposure to FBS. In both cases, results for CA1S cells proliferating in MEF-CM (thick blue), in mTeSR1 (shaded pink) and after FBS treatment for 3 weeks (black filled) are shown. Undifferentiated CA1S cells (P25) maintained in mTeSR1 and stained for DAPI (C) or OCT4 (D). Alkaline phosphatase positive colonies generated from CA1S cells assayed at P30 (E). Inset: alkaline phosphatase positive colony shown at a greater magnification. CA1S cells form well differentiated teratomas that contain cells from all 3 germ layers after 6.5 weeks of maturation (F and G). Haematoxylin-Eosin-stained sections reveal (F) retinal pigmented epithelium (a, ectodermal); cartilage (b, mesodermal); respiratory-like epithelium (c, endoderm). (G) Retinal pigmented epithelium (a, ectodermal); adipose tissue (b, mesodermal); villous structures with gut-like endoderm overlying delicate fibro-vascular cores (c, endoderm). Inset: higher magnification of region indicated in 'c'. These data were contributed by Dr. Nicolas Caron (3).

CA1S cells demonstrate a higher cloning efficiency

CA1S cells were next evaluated for alkaline phosphatase-positive (AP+) colony-forming efficiency of single-cell suspensions. The mean value obtained for CA1S cells was 24 ± 4%, i.e., 57-fold higher than the parental CA1 cells (0.4 ± 0.1%, Figure 3.2A). When CA1S cells were similarly assayed with the Rho kinase inhibitor Y-27632, the frequency doubled (to 47 ± 3%), indicating that their survival could be further increased by exposure to this inhibitor. Comparing doubling time and plating efficiency of CA1S and CA1

maintenance cultures showed no difference in doubling time (Figure 3.2B), but a 4.4 fold increase in plating efficiency (Figure 3.2C). The compound effect of an increased survival at each passaging time point translated into significant increases in culture yields of undifferentiated CA1S cells in both short (Figure 3.2D) and long term (Figure 3.2E) cultures. Given the unchanged growth rates this increased cell output is due exclusively to the increased CA1S cell survival and not to an alteration of their proliferation control, a finding that contrasts with the hyperproliferative growth patterns previously associated with transformed hESC populations (184).

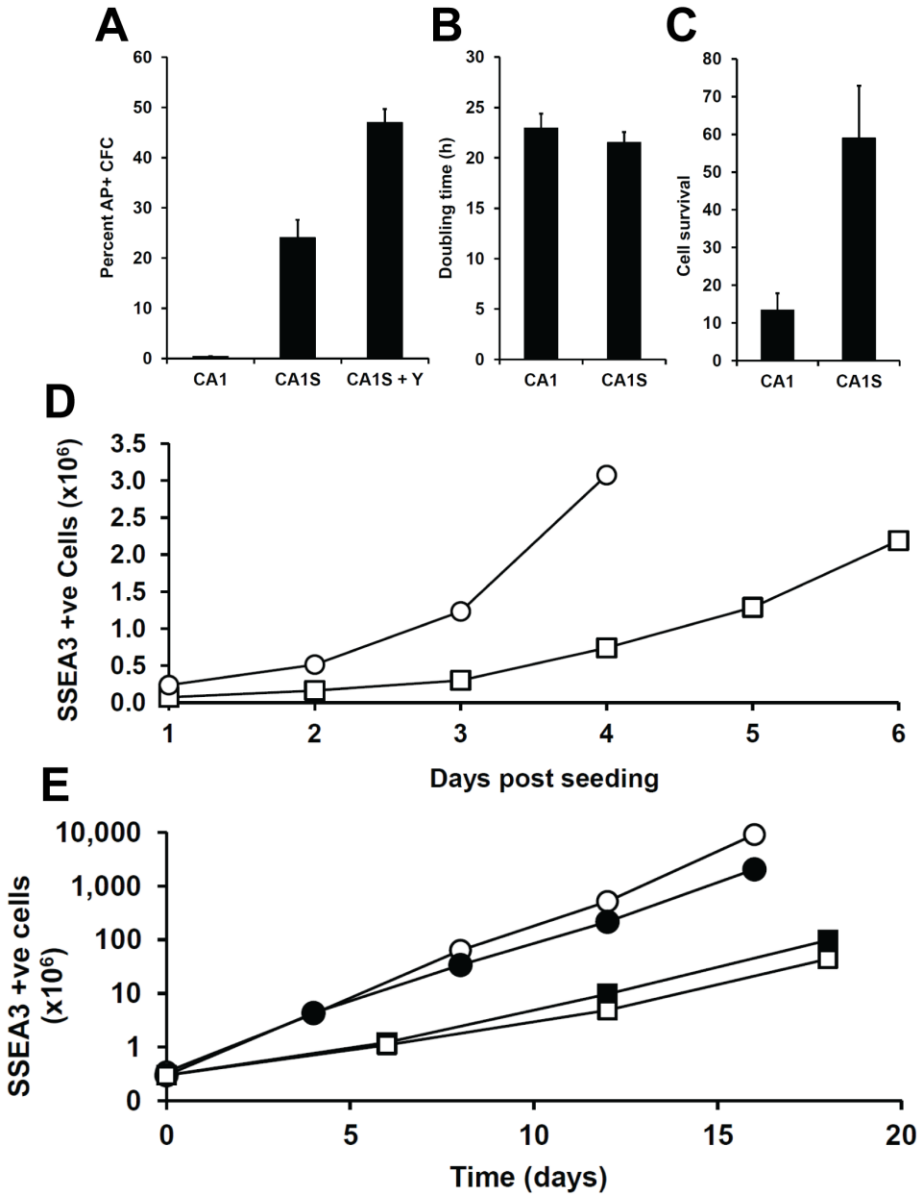

Figure 3.2. CA1S cells yield more cells due to increased cell survival following enzymatic dissociation.

(A) Frequency of AP^+-colonies in CA1, CA1S and CA1S+Y cells (10 µM Y-27632, $p<0.001$ for all comparisons). (B) Average doubling time for CA1 and CA1S cells based on genomic DNA content. (C) Comparison of average cell yield (24 hours) after enzymatic dissociation (CA1S) and mechanical dissociation. Data are presented as the mean + SEM of at least 4 independent experiments (A-C). (D) Growth kinetics over a single passage of SSEA3 + CA1 and CA1S cells. (E) Extended growth kinetics over a period of two weeks for SSEA3+ cells (Legend for D and E, CA1 ■ CM, □ mTeSR and CA1S ● CM, ○ mTeSR). These data were contributed by Dr. Nicolas Caron (3).

CA1S cells are genetically altered

To investigate the possibility that the novel properties of CA1S cells might be due to a genetic alteration, we had them analyzed both by standard cytogenetics and by high

resolution array comparative genomic hybridization (array CGH). Giemsa-banded metaphases prepared from long-term cultured passage 85 cells showed a normal 46, XY karyotype with no observed abnormalities in all 25 metaphases examined. Subsequent high resolution array CGH analysis did reveal a 3.8 Mb genomic duplication on chromosome 20 (20q11.21 - q11.22; 29,306,528 - 32,688,095; Figure 3.3). This region represents a well known hotspot of mutations in culture adapted hESCs that includes several genes associated with the regulation of pluripotency, decreased apoptosis, cell cycle progression and differentiation (e.g. *DNMT3B*, *BCL2L1*, *ID1*, *PDRG1*, and *TPX2*, Figure 3.3D) (188, 200-203).

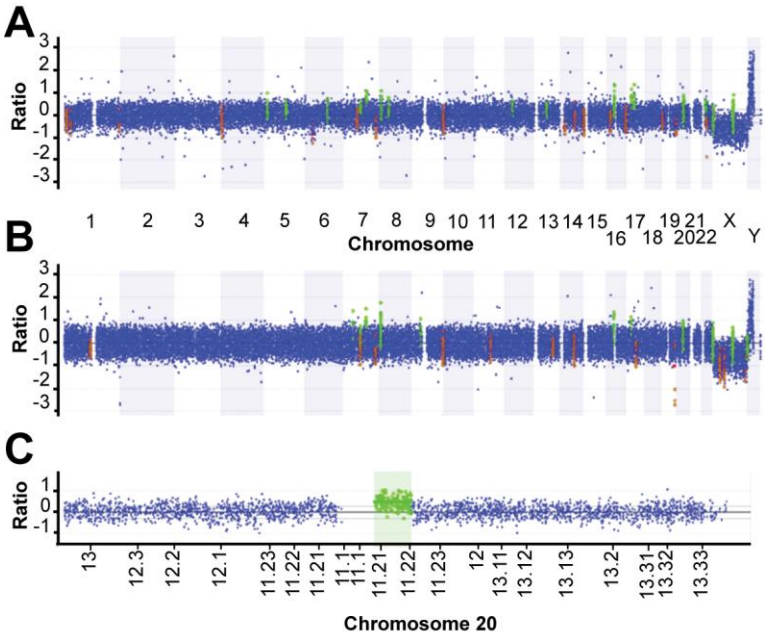

Figure 3.3. Genomic alterations in CA1S cells

CA1S cells were analyzed by array CGH to examine the genomic gains and losses relative to a control female hESC line (WA09). Results obtained by the WiCell Research Institute using the 72K array (A) and 135K array (B) reveal that the vast majority of the CA1S genome is unchanged (blue dots) with some gains (green) and losses (red) observed. A notable 3.8 Mb gain was observed on chromosome 20q11 (C) in addition to known human copy number variants, centromere associated false-positive calls, or aberrations also observed in the parental CA1 cells. The affected region of chromosome 20 is associated with a number of genes (D) linked with pluripotency, apoptosis, and differentiation of cell types (bold and underlined).

CA1S cells retain *in vitro* pancreatic differentiation capacity

With the *in vivo* teratoma assay suggesting that CA1S cells were capable of pluripotent development, but genomic alterations detected within the cell population, we moved on to test the *in vitro* differentiation capacity of CA1S cells to see if these alterations modified the utility of the cell line. To do this we exposed undifferentiated CA1S cells to an elaborate sequential series of developmental cues following an established pancreatic differentiation protocol (117) (Figure 3.4A). Immunohistochemical characterization of the 19-day cultured cell types confirmed that the CA1S cells are capable of functional response to the numerous *in vitro* differentiation signals allowing development from hESCs to pancreatic progenitors and subsequent endocrine cells. These cells produced insulin and glucagon, as well as the key pancreatic progenitor transcription factors PDX1 and NKX6.1 in a temporally regulated manner as shown by RT-qPCR and immunocytochemistry (Figures 3.4B-G). Release of C-peptide into culture medium was also found to increase over the course of extended culture (Figure 3.4H).

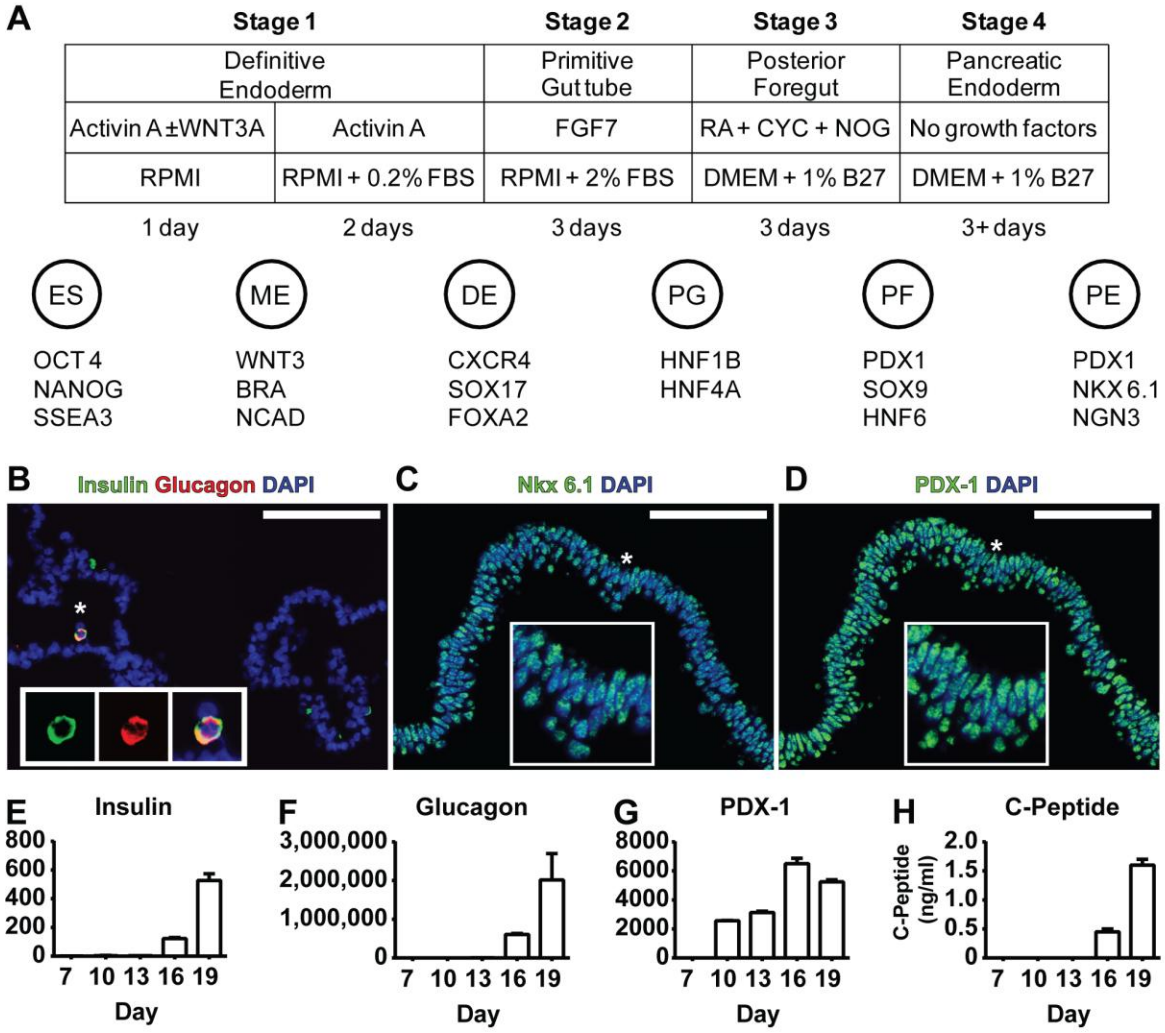

Figure 3.4. CA1S hESCs are capable of pancreatic differentiation

(A) Previously published pancreatic endocrine precursor differentiation method (117, 128). (B) CA1S cells differentiated to the end of stage 4 express pancreatic endocrine hormones insulin (green) and glucagon (red) at low frequency. DAPI (blue). Inset: enlarged image panel of an insulin and glucagon co-positive cell. (C and D) CA1S cells differentiated to the end of stage 3 express nuclear NKX6.1 and PDX1 (both green). Inset: enlarged region indicated by asterisk in C and D. (E, F, and G) CA1S cells express insulin, glucagon, and PDX-1 in a temporally regulated manner as measured by RT-qPCR. Fold expression is compared to day 7 values and each sample is normalized to β-actin. (H) CA1S cells express and release increasing amounts of C-peptide into culture media over differentiation. Error bars in panels E-H represent mean ± SEM of technical replicates. Scale bar for all images is 100 μm.

CA1S cells are amenable to high throughput screening

With classical hESCs poorly suited to many aspects of HTS (poor cell survival, poor culture uniformity in microwell plates and poor differentiation homogeneity) we were interested to see if the culture adapted CA1S cells could display improved performance in HTS assays. We first tested how linear CA1S cell seeding was in 96-well plates over a

number of seeding densities. Similar to previous findings, CA1S cells were found to seed well at low density and showed a good linear correlation (R^2 = 0.94) between CA1S inoculum and the number of cells counted 16-hours after seeding (Figure 3.5A).

We were next interested in testing the uniformity of differentiation in CA1S cells. To do this we examined the simple system of definitive endoderm development from the undifferentiated state. Given that CA1S cells were shown to undergo pancreatic differentiation (Figure 3.4), we generated day 4 definitive endoderm cells in bulk and performed a high throughput flow cytometry optimization assay testing staining conditions in this miniaturized volume format. Examination of a number of antibody staining doses ranging from 0.005 µl to 1 µl of anti-CXCR4-PE antibody revealed a classical antibody titration curve where 0.5 µl / 96-well was found to have near maximal staining with a maintained negative staining left shoulder and good signal compared to a 2 x concentration of isotype control antibody (Figure 3.5B).

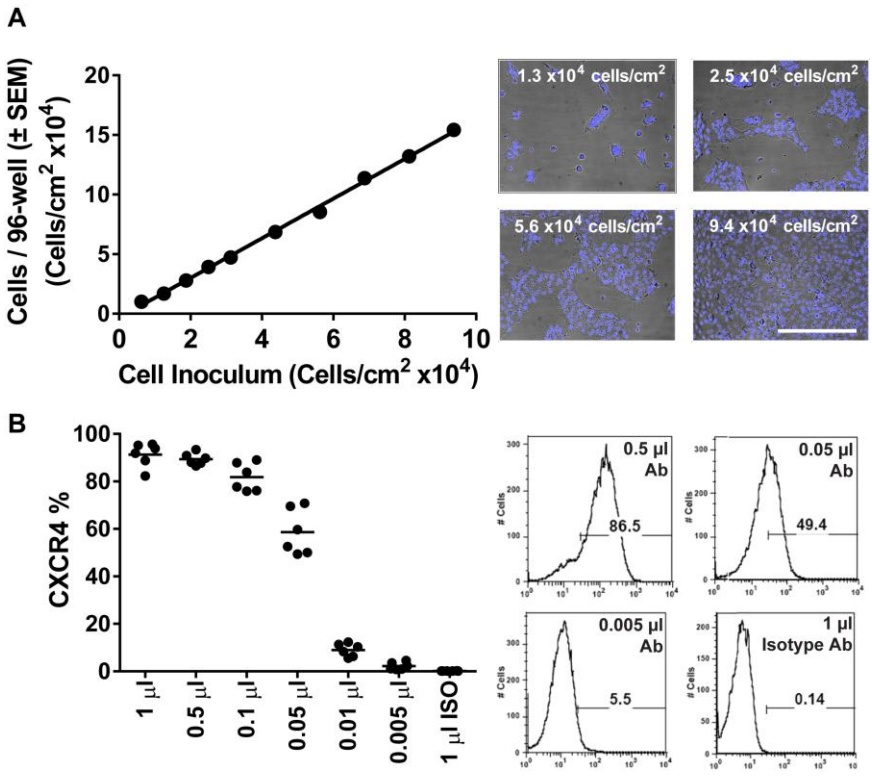

Figure 3.5. CA1S cell seeding in 96-well plates and optimization of high throughput CXCR4 flow cytometry

(A) CA1S cells were reduced to single cells for seeding at a number of densities in 96-well plates. 16-hours later cells were stained with Hoechst (blue overlaid on phase contrast) to allow automated cell counting. Linear

relationship between inoculum and outgrowth was observed under all tested densities (R^2 = 0.94). Scale bar is 200 μm. (B) High throughput 96-well staining of CXCR4. 4 day differentiated definitive endoderm CA1S cells (Kroon 2008 protocol) were dispersed and evenly dispensed into V-bottomed 96-well plates. Following washes, variable volumes of anti-CXCR4 antibody or isotype control antibody (ISO) were added to the cells for 1 hour at room temperature incubation in the dark. Subsequently washed cells were assessed on a flow cytometer with high throughput sampling attachment for CXCR4 staining and later quantified using FlowJo software. Mean (horizontal line) and six individual replicates are shown. Representative histograms of different staining conditions are shown right of the plot with the percentage of positive cells depicted above the gate.

We next compared the seeding, growth, and differentiation homogeneity of CA1 and CA1S cells. To do this we prepared near single cell suspensions of both parental CA1 and CA1S cells and then assessed the number of cells per well at the start (day 1) and end of definitive endoderm induction (day 4). The CA1S cells showed a low well-to-well variation in cell number per well at day 1 (coefficient of variation (CV) = 3.9%) and day 4 (CV = 4.1%), in contrast to the low cell viability and high well-to-well variation exhibited by the CA1 cultures at day 1 (CV = 54%) and day 4 (CV = 98%, Figure 3.6A and B). Upon differentiation to definitive endoderm, CA1S cells show an increased percentage of cells expressing the definitive endoderm marker CXCR4 (82.7 ± 0.6 % CXCR4 positive cells) and a more uniform distribution (CV = 5.7%), whereas CA1 cells showed a decreased CXCR4 expression (59.6 ± 1.4 % CXCR4 positive cells) and a greater variability (CV = 18.3%, Figure 3.6C and D).

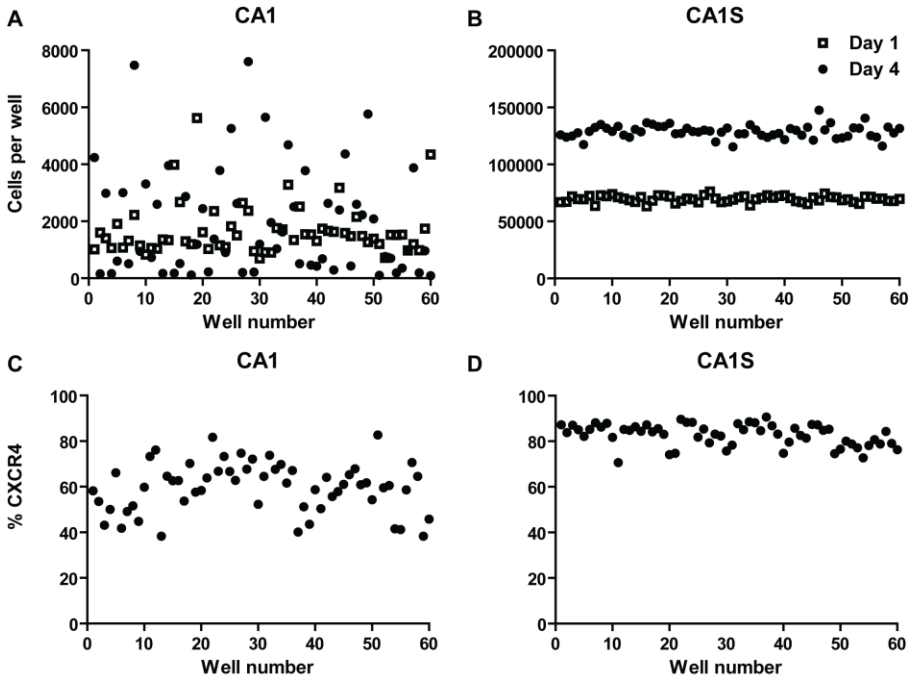

Figure 3.6. CA1S cells show low well-to-well variation compared to CA1 hESCs

CA1S and CA1 cells were seeded into 96-well plates and induced to differentiate into definitive endoderm (Day 1: 0 % FBS, 25 ng/ml WNT3A, 100 ng/ml Activin A. Day 2-4: 0.2 % FBS, 100 ng/ml Activin A) for four days. (A) CA1 cells had high well-to-well variation and low cell viability from day 1 to day 4. (B) CA1S cells had low well-to-well variation from day 1 to day 4. (C) CA1 cells had high well-to-well variation in CXCR4 expression. (D) CA1S cells differentiate uniformly and express CXCR4 at high efficiency.

We next investigated the influence of signalling factors believed to be involved in stimulation of definitive endoderm during early embryonic development. To do this, we seeded CA1S cells in 96-well plates and applied various concentrations of WNT3A (0-250 ng/ml) and Activin A (0-1000 ng/ml) alone and combination. Using high-throughput flow cytometry of CXCR4 as an index of differentiation, we observed a dramatic dependence of CXCR4 expression on Activin A concentration with little if any dependence on WNT3A (Figure 3.7A). Notably, maximal yields of CXCR4 positive cells were observed at Activin A concentrations of 100 ng/ml and above, independent of the initial WNT3A concentration. To test whether the resulting endoderm cells were capable of pancreatic differentiation, we continued differentiation to late pancreatic progenitors. In these extended cultures, we found similar levels of C-peptide in the culture media (data not shown) and the frequencies of cells containing insulin and glucagon were independent of the original WNT3A concentrations (Figure 3.7B). To examine whether these data were directly applicable to other hESC lines we compared CA1S and H1 hESCs during definitive endoderm differentiation at 100 ng/ml

Activin A and either 0, 25, or 250 ng/ml WNT3A for day 1. CA1S cells showed the expected WNT3A independent expression of CXCR4 by day 4 of culture while H1 cells revealed a modest but significant increase in response to WNT3A administration suggesting some level of line-to-line variation in minor signalling pathways but the core Activin A signalling was capable of stimulating definitive endoderm in H1 cells (Figure 3.7C).

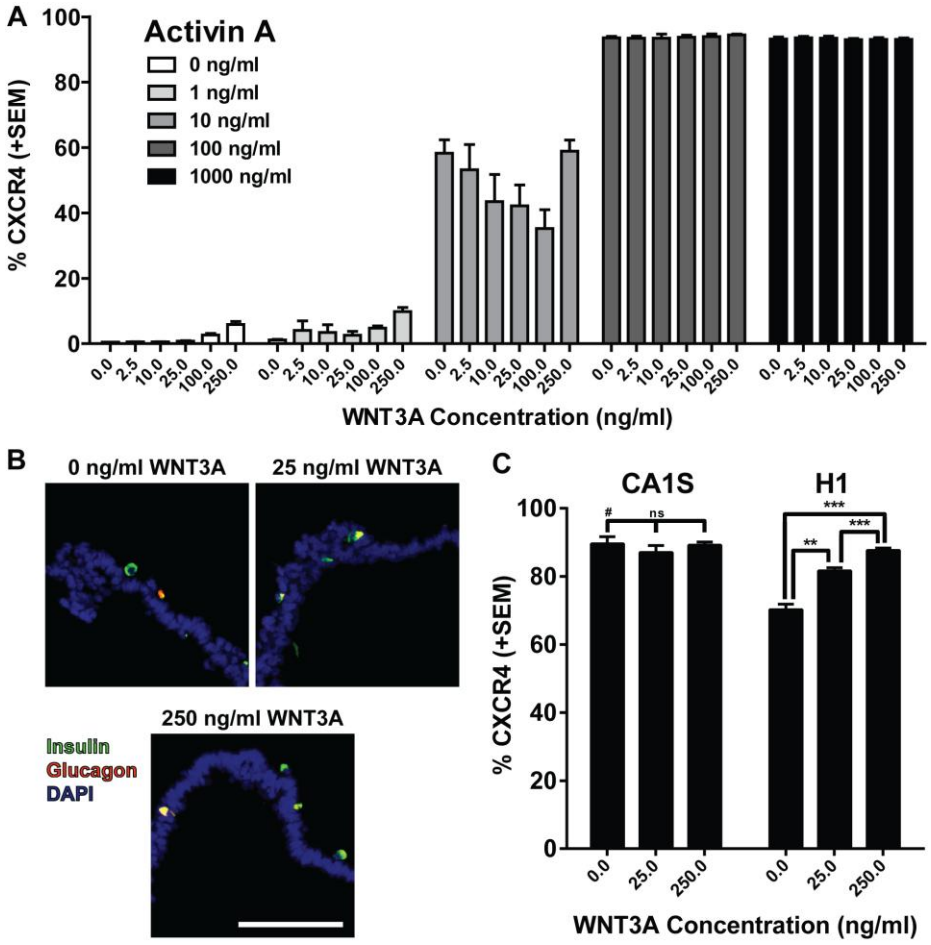

Figure 3.7. Utility of CA1S cells for HTS-type assessment of growth factor requirements for inducing definitive endoderm

(A) CA1S cells seeded into 96-well plates and incubated with varying concentrations of Activin A and WNT3A were differentiated toward definitive endoderm and analyzed for CXCR4 expression by high-throughput flow cytometry. (B) Continued development of CA1S hESCs to pancreatic progenitor stages in cells receiving 100 ng/ml Activin A and varying WNT3A doses revealed expression of pancreatic hormones (insulin green, glucagon red, DAPI blue) is not dependent on an initial WNT3A stimulus. Scale bar is 100 μm. (C) CA1S and H1 hESCs seeded into 12-well plates were differentiated to definitive endoderm in 100 ng/ml Activin A and varying WNT3A doses with differentiation efficiency monitored by CXCR4 expression. **, and *** denote $P<0.005$ and 0.0005 for the delineated comparison. #, $P<0.05$ compared to H1 (0 and 25 but not 250 ng/ml WNT3A). ns is not significantly different.

3.4 Discussion

The low survival and precocious differentiation of classical hESCs when completely dissociated to single cell suspension makes them challenging for high-throughput applications. Furthermore, when classic hESCs are incompletely dissociated the inoculum variability of aggregates, makes them poorly suited to high-throughput, low culture volume applications, resulting in high well-to-well variability. A minimum initial population of 6 x 10^9 viable cells has been reported to be required to screen a library of 10^6 compounds (204). To generate this number of hESCs by aggregate passaging would involve approximately 1,000 10-cm diameter dishes. Given this technical limitation, optimization of hESC culture and differentiation has been largely limited to screening fewer variables and where relatively marked effects are observable based on fewer replicates.

In collaboration with the lab of Dr. James Piret, we have characterized a previously generated novel and stable subline of CA1 hESCs that can be serially passaged at high efficiency using enzymatic dissociation. Although karyotypically normal, array CGH analysis of CA1S cells revealed duplication of a 3.8 MB segment of chromosome 20 known as a hESC mutation hotspot associated with enhanced pluripotency and reduced apoptosis (184, 188, 203). While CA1S maintenance in mTeSR1 proved to be bFGF-independent careful scrutiny showed no other apparent change in pluripotency, proliferation control, differentiation rate, or differentiation capacity from the parental CA1 hESC line. The improved homogeneity and uniformity of CA1S hESCs allowed reproducible data to be obtained from small initial inocula (3) over a wide range of seeding densities. This suggests that using CA1S cells, as few as 10^8 cells generated from 6 T-175 cm^2 flasks in one week, could be used to screen 10^6 wells at 100 cells/well. Given the homogeneity displayed by CA1S cells, it can be expected that even smaller inocula could be used in 384 or 1516-well plates or microfluidic devices. While use of the Rho kinase inhibitor (176) did influence cell survival in CA1S cells (suggesting that sensitivity to the signalling pathway was not lost during culture adaptation), any screening done with this factor added would be complicated by the many effects of Rho kinases on other processes (189, 190), including growth (176). Given the marked improvements in clonogenicity over the parental CA1 line by culture adaptation, CA1S cells seem amenable to screening applications even in the absence of prosurvival drug applications.

When dissociated to single cells, hESCs can be more susceptible to differentiation as compared to multicellular aggregates that are believed to condition their local environment. Evidence to support this concept was reported by Peerani et al. who noted that the levels of GDF-3, a pluripotency-promoting factor, are increased around large colonies (199) while suboptimal culture resulted in increased SSEA3 negative hESCs (205). Since many HTS assays have suboptimal culture conditions due to technical limitations, the capacity of CA1S cells to be uniformly seeded as single cells without spontaneous differentiation removes this confounding inoculation variability from hESC populations analysis (3). In a 96-well format CA1S cells were found to respond homogenously and as expected during definitive endoderm induction despite small inoculum numbers and low initial plating density. Further application of CA1S cells to screens for compounds that induce differentiation could be envisaged using a proliferation assay combined with an apoptosis assay to identify cytotoxicity. Subsequent pathway focused screens could be applied to the differentiation induction hits to develop highly desirable small molecule based directed differentiation protocols.

In testing this capacity of screening within the context of pancreatic differentiation we found that CA1S cells have the capacity to follow elaborate *in vitro* differentiation methods all the way to pancreatic progenitors and subsequent hormone-positive cell types. Focusing on the early stages of this differentiation process we explored how CA1S cells can be used in a prototype HTS experiment to monitor dose-response effects on definitive endoderm induction. We obtained a Z-factor for this assay of 0.965, approaching the theoretically maximal value of 1.0, identifying this HTS assay using CA1S cells as nearly ideal by this metric (206). This assay revealed the ability of Activin A at high concentrations to abrogate the requirement for WNT3A in CA1S cells. Following our primary screen we assessed a narrower set of conditions (e.g. 0, 25, 250 ng/ml WNT3A) in a conventional hESC line (H1) where we confirmed the ability of the differentiation protocol to stimulate definitive endoderm induction but contrary to the CA1S data prediction we did find a small but significant effect of WNT3A on H1 differentiation. However, a tenfold increased WNT3A dose compared to previous reports (101, 117, 121, 128) was required to achieve the CXCR4 purities of CA1S cells differentiated in the absence of WNT3A. While this could suggest a deficiency within CA1S cells to respond to WNT signalling in general, these data are most

likely explained by variations in differentiation capacity of between hESC lines as has been noted by others (207).

Given the low variation and homogenous response of CA1S during early differentiation processes, they are an attractive cell line for future studies of pancreatic and other cell lineage induction. The CA1S hESCs offer a rapid initial screening platform that can then focus subsequent efforts to a limited number of variables and doses in secondary screens and comparative studies in conventional hESCs. Thus, the use of CA1S cells have the potential to greatly reduce the burden of the initial large scale screening since working with these cells is much less variable and labor-intensive than conventional hESC cultures. The CA1S or similar hESC and iPSC lines should be increasingly widely used since they facilitate efficient screening of pluripotent cell responsiveness to a wide range of factors and conditions. This should in turn make a substantial contribution to the goal of accelerating the development of new differentiated cells and related reagents as well as the knowledge of the pathways that control different stages of hESC and tissue development in general.

Chapter 4: Cell Density: a Simple Factor that Influences Pancreatic Differentiation

4.1 Background

In order to effectively utilize hESCs as a therapeutic source for islet transplantation, highly efficient differentiation of pancreatic endocrine cells must be achieved either *in vitro* or *in vivo* following known developmental cues (100, 208). Based primarily on developmental literature from murine and zebrafish model systems, considerable advances have been made in generating pancreatic endocrine cells from hESCs (209). These advances have been centered around the efficient differentiation of hESCs to definitive endoderm (103, 104), developmentally competent pancreatic progenitors (117, 125) and *in vitro*-derived fetal endocrine like cells (101, 118, 210). However, differences between human and mouse islet architecture and nutrient responsiveness (211-214) suggests that more empirical optimization may be required to successfully adapt hESC differentiation protocols to human applications (99).

To date, a number of landmark studies have explored the ability to produce functional pancreatic endocrine cells from hESCs both *in vitro* and *in vivo* (See Chapter 1.4.1-1.4.3). While *in vivo* maturation of *in vitro* derived pancreatic progenitors has been able to produce pancreatic endocrine cells capable of controlling blood glucose in mice, *in vitro* studies have been far less successful at producing functional endocrine cells. Most *in vitro* studies have used empirical testing of different culture conditions in order to determine the ideal stage-specific differentiation conditions required to convert hESCs to either progenitors or hormone-positive cells. Typically culture conditions have been designed to mimic developmental signalling pathways controlling germ layer specification, foregut formation and pancreatic regionalization (209). Many signalling molecules have been applied to coax endocrine cell development from endocrine-competent progenitors; these include exendin-4, IGF1, HGF, noggin, bFGF, BMP4, VEGF, WNT and various inhibitors of Shh, TGF-β, and NOTCH signalling pathways (101, 118, 215).

We sought to examine whether cell seeding density, the first step of any hESC differentiation protocol, might also influence the efficiency of hESC differentiation into pancreatic endocrine cells. Recently even the common media components such as glucose,

the pH buffer HEPES and the organic solvent DMSO have been found to dramatically effect pancreatic differentiation of hESCs (102, 125, 210), suggesting that previously unrecognized components of the hESC differentiation protocol may profoundly impact results. In addition, seeding density has previously been shown to be important during other *in vitro* differentiation models including adipocyte differentiation (216). To examine this factor in hESC differentiation we seeded cells at four different densities (1.3 to 5.3 x 10^4 cells/cm^2), examined cell cycle progression of undifferentiated cells and tracked the formation of definitive endoderm (CXCR4/SOX17 co-positive cells) followed by pancreatic progenitors (PDX1 positive) and ultimately pancreatic endocrine formation (insulin, glucagon, and somatostatin positive populations). While efficient definitive endoderm induction was observed above moderate densities of 2.6 x 10^4 cells/cm^2, PDX1 expression and subsequent hormone positive populations were increased in cultures seeded at 5.3 x 10^4 cells/cm^2. These high seeding density cultures followed the expected temporal expression patterns of maturing pancreatic progenitors that specify endocrine cell fates and finally adopt hormone expression.

4.2 Methods

Culture of hESCs

Undifferentiated CA1S and WA01 (H1) ESCs were cultured as described in Chapter 3.2 and as previously described (3). WA01 hESCs were passaged using Versene EDTA dissociation solution (Lonza, Walkersville, MD, USA) every 4-5 days.

Pancreatic differentiation of hESCs

Pluripotent CA1S and WA01 hESCs were seeded onto 12-well culture plates coated with 1:30 diluted growth factor reduced Matrigel at defined densities between 1.3 and 5.3 x 10^4 cells/cm^2 for CA1S cells and 2.6 to 10.6 x 10^4 cells/cm^2 for WA01 cells in 1.5 ml of mTeSR1 media per well. Cells were enumerated using a Scepter^{TM} 2.0 Automated Cell Counter using 60 μm tips (Millipore). Sixteen to twenty hours after seeding for CA1S cells, and forty-eight hours after seeding for WA01 cells, differentiation to pancreatic endocrine cells was initiated following a previously published 21-day protocol (Figure 4.1) known to produce polyhormonal pancreatic endocrine cells in culture with H1 hESCs (127) but until

now not tested in CA1S hESCs. Undifferentiated hESCs were exposed to RPMI 1640 (RPMI; cat. no. 61870, Life Technologies, Burlington, ON, Canada) containing 2% fatty acid-free bovine serum albumin (BSA; Proliant, Ankeny, IA, USA), 100 ng/ml Activin-A (AA; R&D Systems), 20 ng/ml WNT3A (R&D Systems), and 8 ng/ml bFGF (R&D Systems) for one day. On days 2 and 3 cells were given the same medium, but without WNT3A. On day 4, cultures were examined by flow cytometry for expression of CXCR4 as a marker of definitive endoderm. Cultures greater than 85% positive for CXCR4 were fed DMEM/F12 (D/F12; Life Technologies) containing 2% BSA, 50 ng/ml FGF7 (PeproTech), 0.25 μM Cyclopamine-KAAD (CYC; Calbiochem) for days 4 through 6. Media for days 7 to 10 was D/F12 supplemented with 1% v/v B-27 (Life Technologies), 50 ng/ml FGF7, 0.25 μM CYC, 0.2 μM retinoic acid (RA; Sigma-Aldrich), and 100 ng/ml Noggin (PeproTech). Stage 4 media (day 11-13) was D/F12 + 1% B-27, 100 ng/ml Noggin, 1 μM ALK5 Inhibitor (ALK5inh; Alexis Biochemicals, San Diego, CA, USA), 1 μM DAPT (Calbiochem), and 100 ng/ml Netrin-4 (NET-4; R&D Systems). Stage 5 media (day 14-21) was D/F12 + 1% B-27, and 1 μM ALK5inh. Between each differentiation stage the cells were washed twice with phosphate buffered saline without calcium or magnesium chloride (PBS-; Sigma) between media changes. On days 1, 4, 11, and 21 of the differentiation trial, cells seeded at each density were detached in triplicate by extended treatment with Accutase (STEMCELL Technologies, 5-15 minutes, 37°C, 5% CO_2), washed once in PBS- and counted as a 1:10 diluted cell suspension using the Scepter^{TM} cell counter.

On day 19 of differentiation a one-hour sequential static glucose-stimulated hormone secretion assay was performed on differentiated cells. Briefly, the medium was aspirated and the cells were washed twice with PBS-, then incubated in 1.5 ml/well RPMI (Life Technologies, cat. no. 11879) containing 2 mM D-glucose (Sigma-Aldrich) at 37°C, 5% CO_2 for two hours. Cells were incubated sequentially for 60 minutes in RPMI + 2 mM glucose followed by RPMI + 25 mM glucose then RPMI + 2 mM glucose with 30 mM potassium chloride. After each incubation period samples were collected, clarified of cell debris by centrifugation, and stored at -20°C to be assayed later. For similar assessment using radioimmunoassay, twenty-four hour static media samples were taken at the end of each stage.

Flow cytometry of definitive endoderm induction and cell cycle analysis

On the morning of day 4, differentiating cells were detached with Accutase for 8-10 minutes at 37°C in 5% CO_2 and then washed twice in PBS- supplemented with 5% FBS (Life Technologies). Cell pellets were resuspended in 300 µl of BD CytofixCytoperm (BD Biosciences, cat. no. 554722) and incubated for 20 minutes at 4°C followed by two washes in BD Perm/Wash (BD Biosciences, cat. no. 554723). Fixed and washed cells were stained with α-CXCR4-PE (R&D Systems, 1:50), and α-SOX17-APC (R&D Systems, 1:50) and/or relevant labelled isotype controls (R&D Systems) diluted in BD Perm/Wash for 1 hour at room temperature. After two additional washes in BD Perm/Wash, cells were analyzed using an LSRII cytometer (BD Biosciences) for co-positive (CXCR4 and SOX17) cells relative to double isotype controls using FlowJo Software (Tree Star).

To determine cell cycle status prior to induction of definitive endoderm, undifferentiated CA1S and WA01 hESCs seeded at varying densities were dissociated with Accutase, washed twice in PBS- supplemented with 1% BSA, and fixed in 1% PFA in PBS- for 15 minutes on ice. After two washes in PBS- plus BSA, cells were resuspended in ice cold 80% ethanol added dropwise while vortexing (speed 3 of 10) before storage at -20°C for up to one month. On the day of analysis, cells were washed twice with PBS- plus BSA and treated with 10 µg/ml RNAse A (Sigma-Aldrich) in PBS- for 15 minutes at 37°C. Following two washes in PBS plus BSA, cells were incubated with 20 µg/ml propidium iodide (Sigma-Aldrich) for 15 minutes at room temperature before analysis using a LSRII cytometer and FlowJo Software using standard gating strategies outlined in Figure 4.2.

Quantitative reverse transcriptase PCR

Quantitative reverse transcriptase PCR (RT-qPCR) was performed according to the manufacturer's recommended protocols. Briefly, RNA was isolated using an RNeasy MiniKit (Qiagen) including on-column DNAse digestion (Qiagen). cDNA was prepared from 250 ng RNA using iSCRIPT (BioRad) and 2.5 ng of cDNA was used per qPCR reaction in SsoFast EvaGreen Supermix (BioRad) on a StepOnePlus instrument (Applied Biosystems). Primers used for RT-qPCR can be found in Table 4.1. Unless otherwise stated, all RT-qPCR reactions were assayed in technical and biological triplicate with gene expression normalized first to its hypoxanthine-guanine phosphoribosyltransferase (HPRT)

internal control, then to an external reference sample used to correct for plate-to-plate variation using the ΔΔCt method (217). These external reference samples were pooled biological triplicates from different tissues including human liver, lung, pancreas (all from Life Technologies), and human islets (kindly provided by Dr. Ao and Dr. Warnock from the Irving K. Barber Human Islet Isolation Laboratory, Vancouver, BC, Canada).

Table 4.1 Sequences of primers used in RT-qPCR in chapter 4

Gene Name	Gene Accession	Product Size (bp)	Primer Sequence Forward / Reverse 5'→3'	Reference
OCT4	NM_002701.4	78	TGGGCTCGAGAAGGATGTG GCATAGTCGCTGCTTGATCG	(103)
FOXA2	NM_021784.4	89	GGGAGCGGTGAAGATGGA TCATGTTGCTCACGGAGGAGTA	(103)
Goosecoid	NM_173849.2	70	GAGGAGAAAGTGGAGGTCTGGTT CTCTGATGAGGACCGCTTCTG	(103)
PDX1	NM_000209	178	CGTCCAGCTGCCTTTCCCAT CCGTGAGATGTACTTGTTGAATAGGA	(2)
MNX1	NM_005515.3	115	TCGCTCATGCTCACCGAGA CCTTCTGTTTCTCCGCTTCCT	(4)
PTF1a	NM_178161	180	GCAGCCAGGCCCAGAAGGTC TTCTGGGGTCCTCTGGGGTCCA	(4)
NKX6.1	NM_006168	186	GCCCGCCCTGGAGGGACGCA ACGAATAGGCCAAACGAGCCC	(2)
NGN3	NM_020999	286	AGACGACGCGAAGCTCACC AAGCCAGACTGCCTGGGCT	(4)
ARX	NM_139058.2	141	CTGCTGAAACGCAAACAGAGGC CTCGGTCAAGTCCAGCCTCATG	(4)
PAX4	NM_006193	169	AGCAGAGGCACTGGAGAAAGAGTT CAGCTGCATTTCCCACTTGAGCTT	(2)
MAFA	NM_201589	195	CTTCAGCAAGGAGGAGGTCA TTGTACAGGTCCCGCTCTTT	(4)
Insulin	NM_000207.2	245	AGCCTTTGTGAACCAACACC GCTGGTAGAGGGAGCAGATG	(158)
Glucagon	NM_002054.4	275	CATTCACAGGGCACATTCAC CGGCCAAGTTCTTCAACAAT	(158)
Somatostatin	NM_001048.3	126	AGCTGCTGTCTGAACCCAAC CCATAGCCGGGTTTGAGTTA	(158)
NEUROD1	NM_002500.2	146	GCCCCAGGGTTATGAGACTAT GAGAACTGAGACACTCGTCTGT	(4)
BRN4	NM_000307.3	150	CTGCAACTGGGTGCGATCAT AGGCTGCGAGTACACGTTGA	(4)
NKX2.2	NM_002509	221	CTTCTACGACAGCAGCGACAACCCG CCTTGGAGAAAAGCACTCGCCGCTTT	(2)
Albumin	NM_000477.5	216	CCTTGGTGTTGATTGCCTT TTGCACAGCAGTCAGCCAT	(121)
NKX2.1	NM_001079668.2	164	GTACCAGGACACCATGAGGAAC CCATGTTCTTGCTCACGTCCC	(109)
Amylase	NM_000699.2	141	AATGTCAAGCTACCGTTGGCC TTCACAGACCCAGTCATTGCC	(121)
HPRT	NM_000194.2	148	TGTTGTAGGATATGCCCTTGACTAT GCGATGTCAATAGGACTCCAGA	(4)

Immunocytochemistry

Differentiated cells were immunostained either directly in culture dishes (Figures 4.1, 4.4, 4.5 and 4.6) or as sectioned cell pellets (Figures 4.8, 4.9 and 4.10). For in-well staining, cells were fixed in 4% paraformaldehyde (PFA) in PBS- overnight at 4°C, washed twice in PBS-, and permeabilized in 0.2% Triton X-100 (Sigma-Aldrich) in PBS- for 30 minutes at room temperature. After two more washes in PBS-, cells were incubated with primary antibodies (Table 4.2) overnight at 4°C. After five sequential three minute washes in PBS-, Alexa 488-, Alexa 555-, or Alexa 647-conjugated secondary antibodies (Life Technologies; 1:1000 diluted in Dako Antibody diluent) were applied for 1 hour at room temperature followed by five, 3-minute washes in PBS- containing 2 ng/ml Hoechst 33342 (Life Technologies). For sectioned cell pellets, cultures were mechanically detached by scraping without enzymes. Detached cell sheets were transferred to 4% PFA in PBS- to fix overnight at 4°C. After two washes in PBS-, fixed cells were embedded in molten (50°C) 2% agarose (Life Technologies), chilled briefly on ice and fixed again in 4% PFA in PBS- for 1 hour at room temperature. Agarose embedded cell pellets were then stored in 70% ethanol prior to paraffinization and sectioning (Wax-it Histology Services, Vancouver, BC, Canada). Subsequent immunostaining of 5 μm sections on slides was performed as previously described (97, 198) using primary antibodies described in Table 4.2 and appropriate secondary antibodies (Life Technologies). Imaging for both slides and cells in culture plates was performed using an ImageXpress Micro^{TM} automated microscope and associated software (Molecular Devices).

Table 4.2 Antibodies used in immunocytochemistry in chapter 4

Gene Name	Host Species	Supplier / Catalogue number	Staining Method	Dilution	Antigen Retrieval
CXCR4	Mouse IgG2A - PE	R&D Systems FAB170P	Fixed cell flow	1:50	None
SOX17	Goat IgG APC	R&D Systems IC1924A	Fixed cell flow	1:50	None
OCT4	Goat	R&D Systems AF1759	4% PFA fixed monolayer	1:500	None
PDX1	Guinea Pig	Abcam Ab47308	4% PFA fixed monolayer	1:250	None
pRb S780	Rabbit	Cell Signalling 9307	4% PFA fixed monolayer	1:350	None
PDX1	Guinea Pig	Abcam Ab47308	Slide	1:1000	HIER

Gene Name	Host Species	Supplier / Catalogue number	Staining Method	Dilution	Antigen Retrieval
PDX1	Rabbit	Dr. J. Habener Gift	Slide	1:1000	HIER
Insulin	Guinea Pig	Sigma I8510	Slide	1:1000	HIER
Glucagon	Rabbit	Thermo Scientific PA1-37768	Slide	1:200	HIER
Glucagon	Mouse	Sigma G2654	Slide	1:1000	HIER
Somatostatin	Mouse	BCBC AB1985	Slide	1:1000	HIER
Pancreatic Polypeptide	Goat	R&D Systems AF6297	Slide	1:200	HIER
NKX6.1	Rabbit	Dr. A. Rezania Gift	Slide	1:1000	HIER
ARX	Rabbit	Dr. P. Collombat Gift	Slide	1:500	HIER
PAX6	Rabbit	Covance PRB-278P	Slide	1:250	HIER
Cytokeratin 19	Mouse	DAKO Cytomation M0888	Slide	1:200	HIER
Chromo-granin A	Sheep	Biomol CA1128	Slide	1:200	HIER
Alpha-Amylase	Rabbit	Sigma A8273	Slide	1:500	HIER

HIER (heat induced epitope retrieval): 15 minutes at 95°C in 10 mM citrate buffer with 0.05% Tween-20 pH 6.0.

Slide: PFA fixed, paraffin section of agarose embedded cell pellet or pancreatic tissue

BCBC (Beta Cell Biology Consortium)

Animals and transplants

Eight-week old male SCID-beige mice (Taconic, strain: C.B-*Igh*-1b/GbmsTac-*Prkdc*^{scid}-*Lyst*^{bg}N7, Hudson, NY, USA) were housed under a 12-hour light/dark cycle with free access to water and standard irradiated food (Harlan Laboratories cat. no. 2918, Madison, WA, USA). Mice were anesthetized by inhalable isofluorane and received transplants of 2-2.5 million 21-day differentiated, partially dissociated CA1S cells under the left kidney capsule following an established transplant model (125, 127). Surgeries were performed by Dr. Jenny Bruin. 12 mice were transplanted with differentiated CA1S cells, 4 were retained as sham-operated controls. Animals were sacrificed at 1 month and 4 months post-transplant by cardiac puncture blood collection under isofluorane anesthesia and subsequent cervical dislocation. Cell grafts attached to the surface of the kidney were

trimmed of adhering tissue, fixed overnight in 4% PFA, and stored in 70% ethanol until tissue processing for paraffin sectioning by Wax-it histological services.

Radioimmunoassay

Radioimmunoassays were performed on cardiac puncture samples and static media samples collected at the end of each differentiation stage or during the glucose-stimulated hormone release procedure. Both C-peptide (Millipore HCP-20K) and glucagon (Millipore GL-32K) were analyzed, following the manufacturer's recommended protocols except using half volumes of all reagents and samples. Analysis was performed in technical duplicate and biological triplicate.

Statistical Analysis

Data are reported as mean ± SEM with significance set at $p \leq 0.05$ unless otherwise stated. Statistical comparisons were performed using one-way ANOVA and Bonferonni post-hoc test calculated in Prism 6.0 (GraphPad Software Inc. La Jolla, CA, USA).

4.3 Results

Definitive endoderm induction

To examine the effect of initial cell seeding density on subsequent differentiation to definitive endoderm and further to pancreatic endocrine hormone-producing cells, we applied an established culture protocol (Figure 4.1A) known to yield polyhormonal pancreatic endocrine cells (127) in H1 hESCs to the CA1S hESC line. The CA1S line was chosen due to its previously described high seeding uniformity and capacity to form pancreatic endocrine cells (3) (Chapter 3). Using this cell line we examined four seeding cell densities: 1.3×10^4 cells/cm^2, 2.6×10^4 cells/cm^2, 3.6×10^4 cells/cm^2, and 5.3×10^4 cells/cm^2, that corresponded to approximately 30%, 60%, 80%, and 100% confluence, respectively, by 16 hours after seeding (Figure 4.1B). After 4 days of differentiation the cultures seeded at 3.6×10^4 cells/cm^2 and 5.3×10^4 cells/cm^2 had similar cell densities (Figure 4.2). Induction of definitive endoderm was assessed by flow cytometry of CXCR4/SOX17 co-expression and RT-qPCR of *FOXA2* and Goosecoid. Cultures seeded at 2.6×10^4 cells/cm^2 or greater were found to contain significantly increased populations of CXCR4/SOX17 double positive cells

as well as increased *FOXA2* and Goosecoid expression compared to those seeded at 1.3 x 10^4 cells/cm^2, suggesting enhanced definitive endoderm induction in cultures seeded at high density (Figure 4.1C). To partially explain the composition of the non-definitive endodermal population we examined the expression of OCT4, a marker of maintained pluripotent cell populations, by RT-qPCR and immunocytochemistry. Increased OCT4 levels were observed in cultures seeded at 1.3 x 10^4 cells/cm^2 at the end of differentiation stage 1 compared to cultures initially seeded at higher densities (Figure 4.1D) suggesting that cultures seeded at lower density contained cells which remained arrested in the pluripotent state and failed to differentiate.

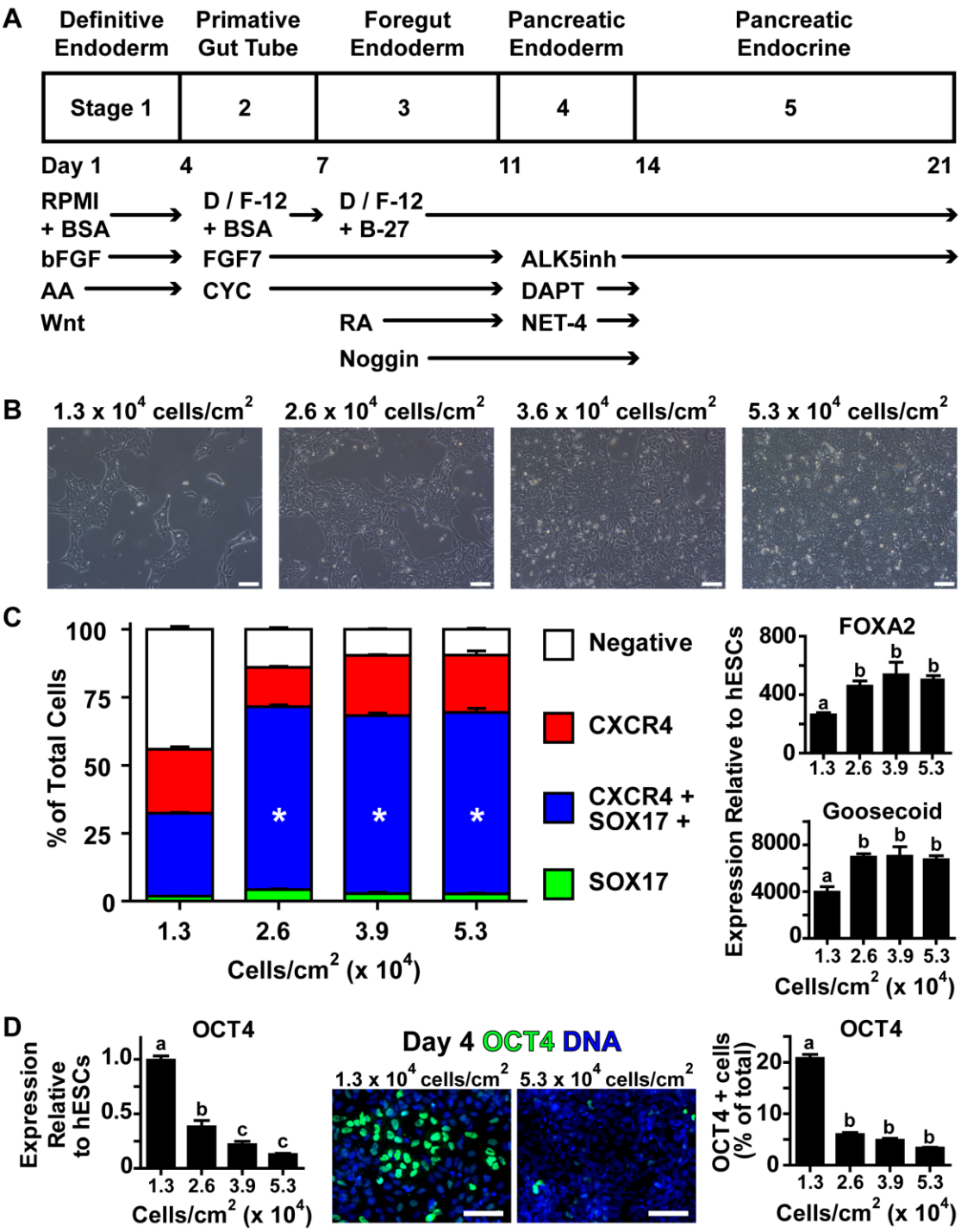

Figure 4.1. Higher cell seeding density improves definitive endoderm differentiation in CA1S cells

(A) CA1S hESCs were differentiated using a protocol designed to mimic human development in a 21 day, 5 stage process. (B) hESCs were seeded onto Matrigel-coated culture plates at the indicated density, yielding 30%-100% confluence as shown at 24 hours after seeding. (C) On day 4 of differentiation, markers of definitive endoderm induction were assessed by flow cytometry (CXCR4 and SOX17 expression) or RT-qPCR (*FOXA2* and Goosecoid, shown relative to undifferentiated hESC expression levels). (D) Expression of OCT4 (marker of pluripotent cells) was assessed by RT-qPCR and immunofluorescence as a percentage of the total number of nuclei (OCT4 is green, nuclei are blue). * represents significant difference from 1.3 x 10^4 cells/cm^2

by one-way ANOVA with Bonferonni post-hoc test. Different superscripts (a, b, c) are significantly different from each other within each graph by one-way ANOVA with Bonferonni post-hoc test. Scale bars are 100 μm.

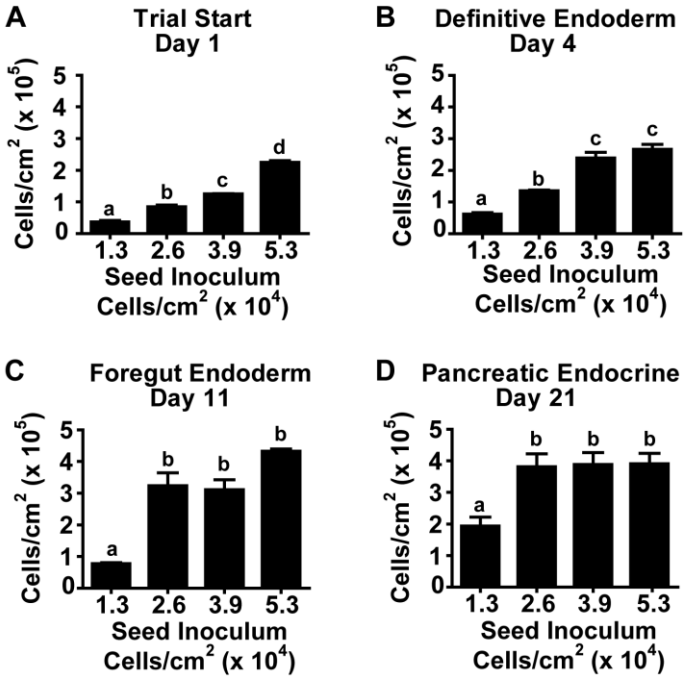

Figure 4.2. Cell density tracking over differentiation in CA1S cells

Differentiating CA1S hESCs were counted at a series of time points during culture following complete enzymatic dissociation and automated cell counting. (A) hESC cell counts 24 hours after seeding at the indicated cell inoculums at the time just prior to starting the differentiation protocol. (B) 4 day differentiated cell counts at the time of analysis for markers of definitive endoderm. (C) 11 day differentiated cell counts at the end of stage 3. (D) 21 day cell counts at the end of stage 5 at the termination of the differentiation protocol. Different superscripts (a, b, c, d) are significantly different from each other within each graph by one-way ANOVA with Bonferroni post-hoc test.

To examine whether this effect of cell density on definitive endoderm induction was specific to the CA1S hESC line, we applied a similar approach to the widely used WA01 (H1) hESC line. While WA01 cells required a higher initial cell seeding density and 48 hours of growth to achieve similar initial confluence as CA1S cells (Figure 4.3A), a higher initial cell seeding density was associated with increased numbers of CXCR4/SOX17 double positive definitive endoderm cells. Conversely, cultures of WA01 hESCs seeded at low density suffered from considerable cell losses during differentiation and the few cells which did survive were poorly specified to the endoderm germ layer (Figure 4.3B).

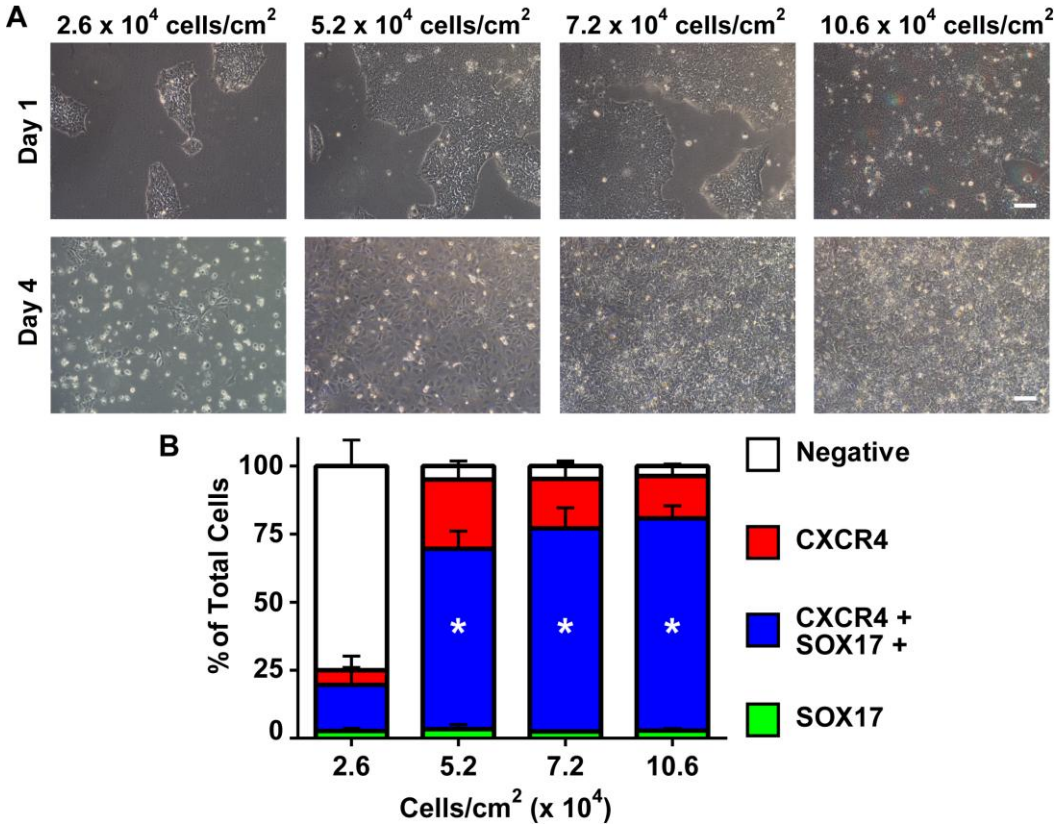

Figure 4.3. Higher cell seeding density improves definitive endoderm differentiation in WA01 cells

(A) WA01 hESCs were seeded onto Matrigel-coated plates at the indicated densities, allowed to expand for 48 hours (day 1 of protocol) and differentiated to definitive endoderm (day 4) following the protocol in Figure 4.1. (B) On day 4 of differentiation, markers of definitive endoderm induction were assessed by flow cytometry (CXCR4 and SOX17 expression as a percentage of the total single cell fraction). * Represents significant difference from 2.6 x 10^4 cells/cm^2 by one-way ANOVA with Bonferroni post-hoc test within the same population. Scale bars are 100 μm.

To better understand how cell density potentially altered definitive endoderm induction we examined the role of cell cycle in both CA1S and WA01 hESCs at the start of our differentiation protocol. CA1S and WA01 hESCs seeded at low cell density were biased toward the G2 and M phases of the cell cycle using DNA content assessment by flow cytometry (Figure 4.4A/B and Figure 4.5A/B). Similar to WA01 hESCs, CA1S cells seeded at low density cultures contained 27% cells in G0/G1 while high density cultures contained significantly more cells in G0/G1 (33%) and cultures treated with 2% DMSO to induce cell cycle arrest contained 60% cells in G0/G1 (Figure 4.4B). Given the well established role of hyperphosphorylated retinoblastoma protein (pRb) in active cell cycle progression (218) we examined CA1S and WA01 hESCs seeded at different densities for pRb (serine 780) by immunocytochemistry. Undifferentiated hESCs stained brightly for pRb S780 including a

fraction of cells that were in active mitosis as defined by DNA morphology and contained pRb S780 in the cytoplasm (Figure 4.4C and Figure 4.5C). Similar to WA01 hESCs, low density cultures of CA1S hESCs were found to contain significantly more of these cells (~25% of total cells) compared to high density cultures (~7% of total cells) and 2% DMSO treated hESCs (~3% of total cells). Together these data suggest that in high cell density cultures, similarly to DMSO treated cells, undergo a shift in cell cycle toward G0/G1 states. This shift is also associated with a decrease in cells that are undergoing active mitosis as marked by cytoplasmic pRb S780 positive cells.

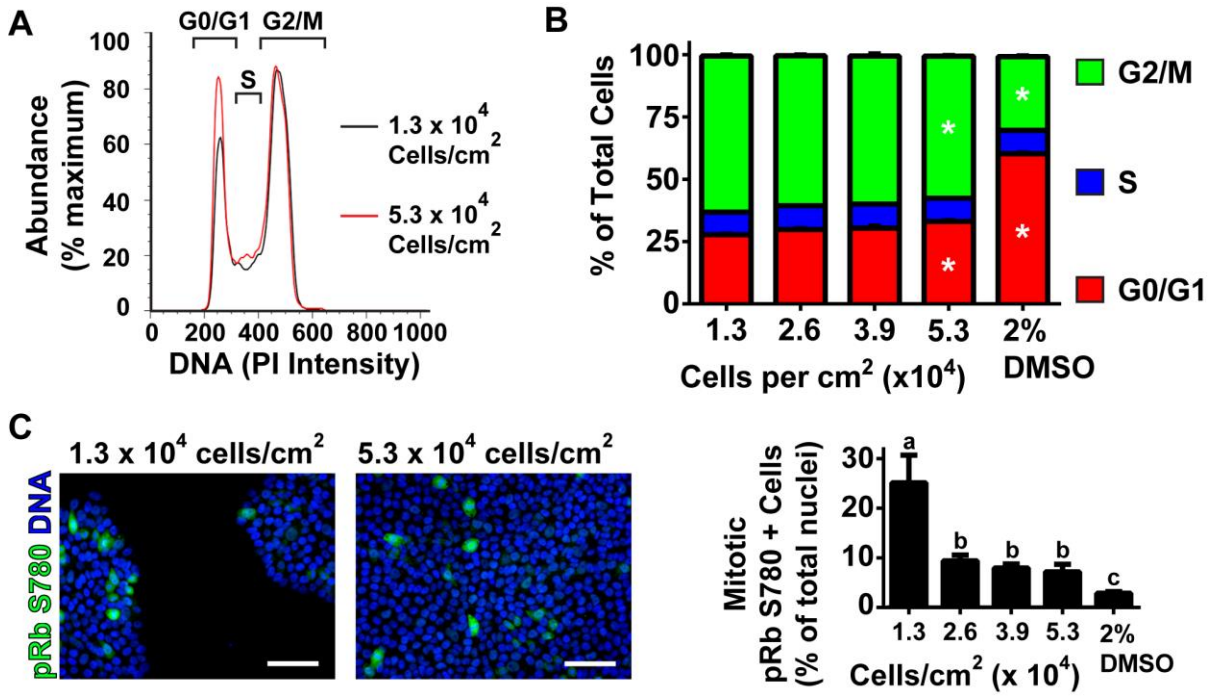

Figure 4.4. Higher cell seeding density decreases cell cycle progression in CA1S cells

(A) A representative histogram of low density (1.3 x 10^4 cells/cm^2, black line) and high density (5.3 x 10^4 cells/cm^2, red line) seeded CA1S hESCs stained for DNA content by propidium iodide to indicate cell cycle state within the depicted gates 24-hours after seeding. (B) Single cells gated for uniform DNA width were assessed in triplicate and quantified as either G0/G1, S or G2/M phases using the gates in (A) as a percentage of the total single cell population. Four cell seeding densities of CA1S cells (1.3, 2.6, 3.9 and 5.3 x 10^4 cells/cm^2) along with 5.3 x 10^4 cells/cm^2 seeded cells treated overnight with 2% DMSO to induce cell cycle arrest (2% DMSO) were quantified. * represents significant difference from 1.3 x 10^4 cells/cm^2 by one-way ANOVA with Bonferroni post-hoc test within the same cell cycle population. (C) Representative images and quantification of immunocytochemistry of pRb S780 (green, nuclei are blue). pRb S780 positive mitotic cells were quantified as a percentage of the total cell populations in five randomly selected images. Different superscripts (a, b, c) are significantly different from each other by one-way ANOVA with Bonferroni post-hoc test. Scale bars are 100 μm.

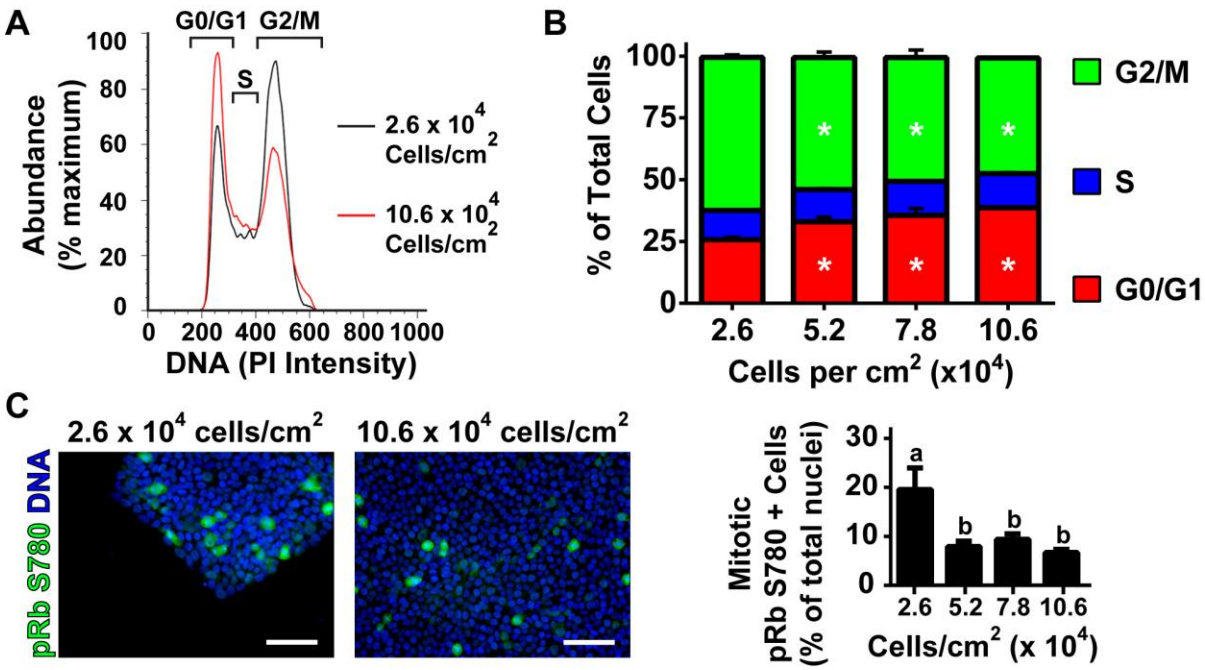

Figure 4.5. Higher cell seeding density decreases cell cycle progression in WA01 cells

(A) A representative histogram of low density (2.6 x 10^4 cells/cm^2, black line) and high density (10.6 x 10^4 cells/cm^2, red line) seeded WA01 hESCs stained for DNA content by propidium iodide to indicate cell cycle state within the depicted gates 48-hours after seeding. (B) Single cells gated for uniform DNA width were assessed in triplicate and quantified as either G0/G1, S or G2/M phases using the gates in (A) as a percentage of the total single cell population. Four cell seeding densities of WA01 cells (2.6, 5.2, 7.8 and 10.6 x 10^4 cells/cm^2) were examined for cell cycle status. (C) Representative images and quantification of immunocytochemistry of pRb S780 (green, nuclei are blue). pRb S780 positive mitotic cells were quantified as a percentage of the total cell populations in five randomly selected images. * represents significant difference from 2.6 x 10^4 cells/cm^2 by one-way ANOVA with Bonferroni post-hoc test within the same population. Different superscripts (a, b, c) are significantly different from each other by one-way ANOVA with Bonferroni post-hoc test. Scale bars are 100 µm.

Pancreatic progenitor restriction

After induction of definitive endoderm, cultures were continued to day 11; at this time point cultures seeded at 2.6 x 10^4 cells/cm^2 and above showed similar differentiated cell densities (Figure 4.2). To examine the efficiency of pancreatic progenitor formation, PDX1 expression was examined by immunocytochemistry in day 14 cultures. Quantification of total nuclear PDX1 revealed a significant increase in PDX1 positive cells approaching 50% of the total cell population in cultures seeded at 5.3 x 10^4 cells/cm^2. The lowest seeding density culture (1.3 x 10^4 cells/cm^2), which demonstrated poor definitive endoderm induction, produced almost no PDX1 positive cells while the middle density cultures (2.6 x 10^4 cells/cm^2 and 3.9 x 10^4 cells/cm^2) contained approximately 20% PDX1 positive cells (Figure 4.6A and B).

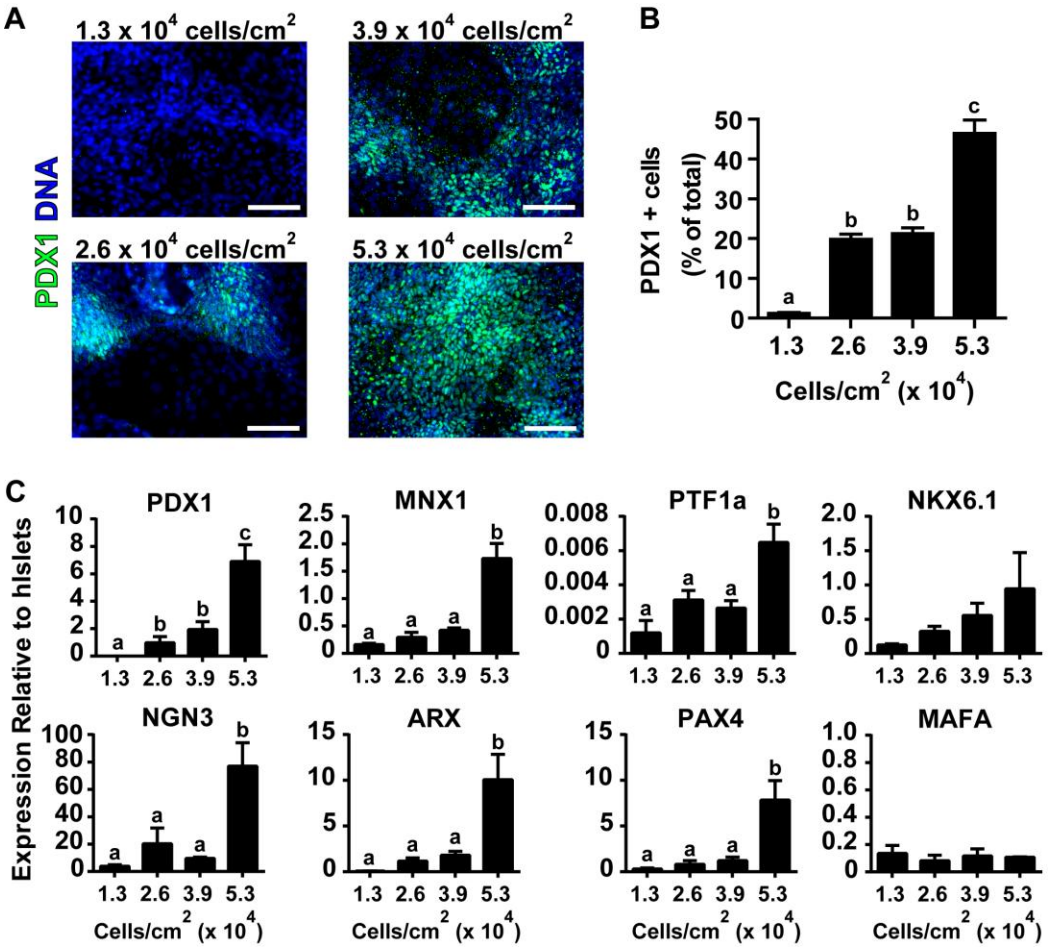

Figure 4.6. High cell seeding density increases pancreatic progenitor differentiation

(A) hESCs seeded at different densities were differentiated for 14 days and immunostained for PDX1 (green) and DNA (blue). (B) Single-cell quantification of PDX1 positive nuclei as a percentage of total nuclei. (C) RT-qPCR of 21 day differentiated cells. Expression is shown relative to isolated human islets. Different superscripts (a, b, c) are significantly different from each other within each graph by one-way ANOVA with Bonferroni post-hoc test. Scale bars are 100 μm.

Continued differentiation to day 21 revealed sustained expression of a number of pancreatic progenitor and endocrine fate specification transcription factors. *PDX1*, *MNX1*, and *PTF1A* expression was increased in cultures seeded at high density; *NKX6.1* expression also tended to be increased in high density cultures, although it did not reach statistical significance (Figure 4.6C). Similarly endocrine commitment markers *NGN3*, *ARX*, and *PAX4* were increased in cultures seeded at 5.3 x 10^4 cells/cm^2 while the maturation marker *MAFA* expression levels did not differ amongst cultures seeded at different densities (Figure 4.6C). By day 21, culture density had plateaued at nearly 4 x 10^5 cells/cm^2 for cells seeded at

2.6 x 10^4 cells/cm^2 and above (Figure 4.2), possibly owing to the limited capacity of the standard adherent culture system used.

To examine cultures for unwanted non-endocrine differentiation, RT-qPCR was undertaken on cultures differentiated for 21 days to measure expression of albumin, *NKX2.1*, and amylase (markers of liver, lung, and exocrine pancreas, respectively). While albumin expression was significantly increased in cultures seeded at 2.6 x 10^4 cells/cm^2 compared to other seeding densities, no significant alternative cell fates predominated the cultures (Figure 4.7).

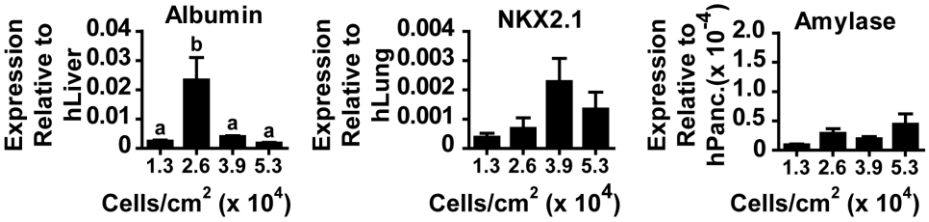

Figure 4.7. Cell seeding densities effects on off target differentiation.

RT-qPCR of 21 day differentiated cells. Expression relative to human liver (albumin), human lung (*NKX2.1*), or human pancreas (amylase). Different superscripts (a, b) are significantly different from each other within each graph by one-way ANOVA with Bonferroni post-hoc test.

Pancreatic endocrine specification

Knowing that cultures seeded at high density contained increased numbers of PDX1 positive pancreatic progenitor populations, we next examined differentiated cells for expression of pancreatic endocrine hormones using RT-qPCR. By day 21 of the differentiation protocol, cultures initially seeded at high density expressed significantly elevated levels of insulin, glucagon and somatostatin mRNA compared to cultures seeded at lower density (Figure 4.8A). We also assessed the content of glucagon and C-peptide, a marker of processed insulin, in 24-hour static media samples taken between days 11 and 21. Cultures seeded at 5.3 x 10^4 cells/cm^2 demonstrated significantly higher C-peptide and glucagon release from day 17 to 21 compared to all lower initial seeding densities (Figure 4.8B). Similarly, a sequential glucose or potassium chloride stimulation test carried out on day 19 of the differentiation protocol revealed that only the cultures seeded at 5.3 x 10^4 cells/cm^2 were able to release detectable C-peptide or glucagon in response to the stimuli tested. Importantly, the high glucose-stimulated C-peptide release and low glucose-

stimulated glucagon release kinetics typical of a native human islet were not observed under any condition, and only potassium chloride was able to stimulate significant hormone release, suggesting that the cell populations were immature (Figure 4.8B).

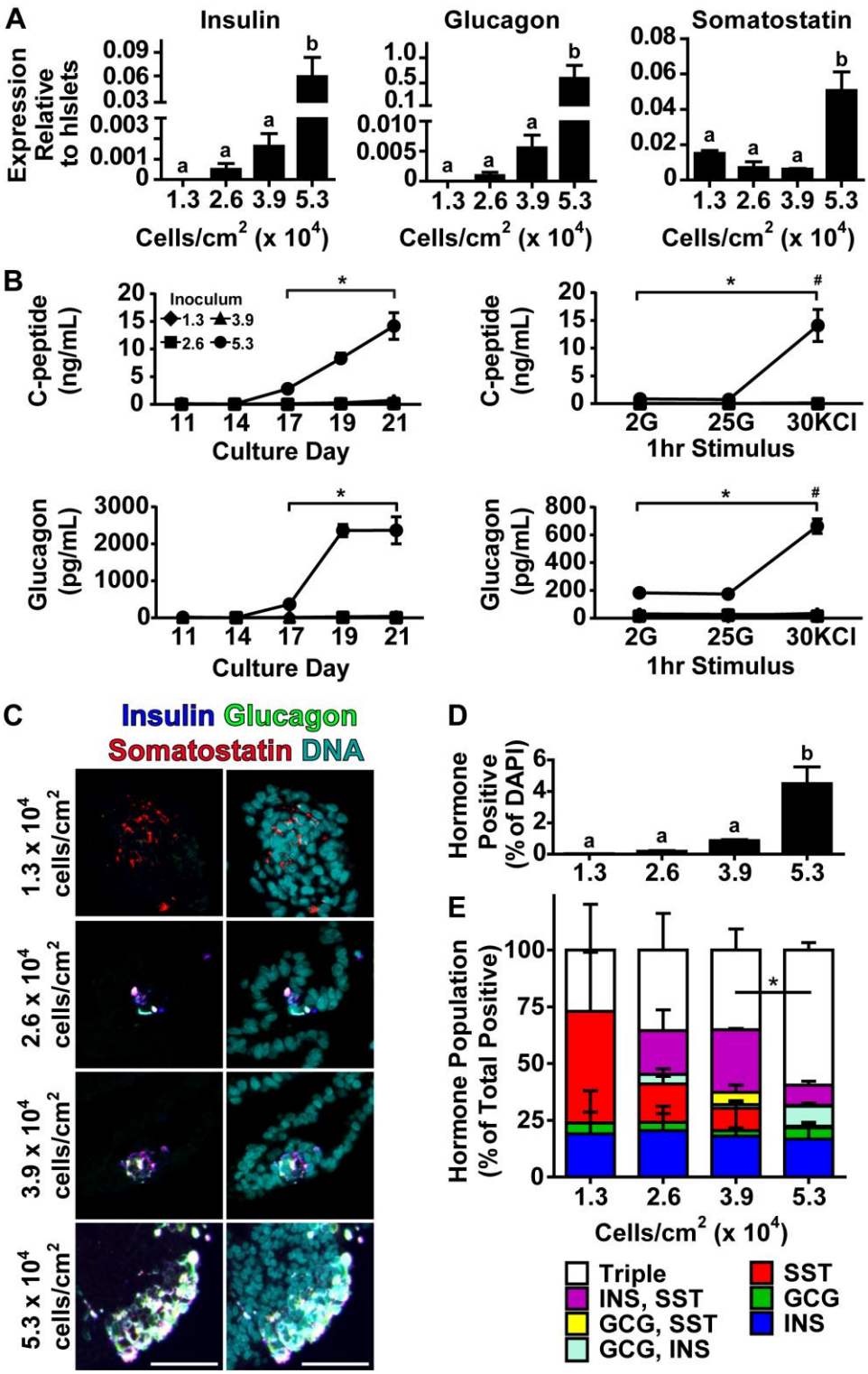

Figure 4.8. Higher cell seeding density enhances pancreatic endocrine formation

(A) Insulin, glucagon, and somatostatin expression were assessed in 21 day differentiated hESCs using RT-qPCR (shown relative to human islets). (B) C-peptide and glucagon release were assayed in static 24 hour media samples taken on the indicated culture day, or during a sequential glucose (G) and potassium chloride (KCl) stimulated hormone release assay performed on day 19 of culture. Following a 2 hour, 2 mM glucose

wash, cells were treated for 1 hour with 2 mM glucose (2G), 25 mM glucose (25G), then 30 mM KCl (30KCl). Diamonds, squares, triangles, and circles represent 1.3 x 10^4 cells/cm^2, 2.6 x 10^4 cells/cm^2, 3.9 x 10^4 cells/cm^2, and 5.3 x 10^4 cells/cm^2 initial seeding density respectively. * represents $p<0.05$ comparing 5.3 x 10^4 cells/cm^2 with other cell densities. # represents $p<0.05$ comparing KCl stimulation versus other stimuli within the 5.3 x 10^4 cells/cm^2 seeding density. (C) hESCs seeded at different densities and differentiated for 21 days were agarose-embedded and immunostained for insulin (blue), glucagon (green), somatostatin (red) and DNA (cyan). Right panel shows hormone staining and left panel shows the same hormone image with DNA. (D) Single-cell quantification of hormone population showing the number of cells positive for insulin, glucagon, or somatostatin as a percentage of the total number of nuclei. (E) Single-cell polyhormonal analysis of the hormone positive population in C as a percentage of total hormone positive population. Triple indicates cells scored positive for all three hormones. * represents $p<0.05$ comparing triple positive populations of 5.3 x 10^4 cells/cm^2 vs 3.9 x 10^4 cells/cm^2. In panels A and D, different superscripts (a, b) are significantly different from each other within each graph by one-way ANOVA with Bonferroni post-hoc test. Scale bars are 50 μm.

Since the 21 day differentiated cultures were producing pancreatic endocrine hormones, we next assessed whether the endocrine cell populations were producing single hormones suggesting maturation, or were polyhormonal, suggesting immaturity in line with what is thought to occur during human fetal development (94, 95, 97). Agarose-embedded, paraffinized sections of 21-day cultures were immunostained for insulin, glucagon, and somatostatin (Figure 4.8C). Nucleocentric (nucleus based) automated cell scoring revealed that cultures seeded at high density had increased numbers of cells that were positive for any combination of these hormones approaching 6% of the total DAPI positive cell population (Figure 4.8D). While all four seeding densities had the capacity to induce formation of unihormonal, bihormonal, or trihormonal subpopulations of cells, cultures from the highest initial seeding density produced mostly polyhormonal cells (white; insulin, glucagon, and somatostatin positive), which tended to cluster together (Figure 4.8C).

Given that high initial cell seeding density seemed to promote increased numbers of immature polyhormonal cells, we were interested in whether expression of transcription factors in these cultures followed the expected temporal patterns of human fetal gene expression during hESC differentiation. Numerous subsequent differentiation trials using high initial seeding densities recapitulated the progressive release of glucagon and C-peptide into culture media during the differentiation period (Figure 4.9A). Expression of pancreatic progenitor markers *PDX1* and *MNX1* were upregulated at day 11, while expression of endocrine fate specification factors *BRN4*, *NKX2.2*, *ARX* and *PAX4* was observed around day 14. Expression levels of maturation factors *NKX6.1* and *NEUROD1* were enhanced at day 21, coincident with insulin, glucagon and somatostatin expression (Figure 4.9B). However, *MAFA* expression was not observed, suggesting a lack of maturation in all of these cell

populations. We also examined final cell populations for expression of some of these transcription factors using immunocytochemistry. We again observed polyhormonal cells predominating the cultures with fewer unihormonal cells. Expression of PAX6 and ARX was observed in developing endocrine (insulin or glucagon positive) clusters, while abundant PDX1 staining and rare NKX6.1 staining was observed in a separate cell compartment not positive for insulin or glucagon (Figure 4.9C).

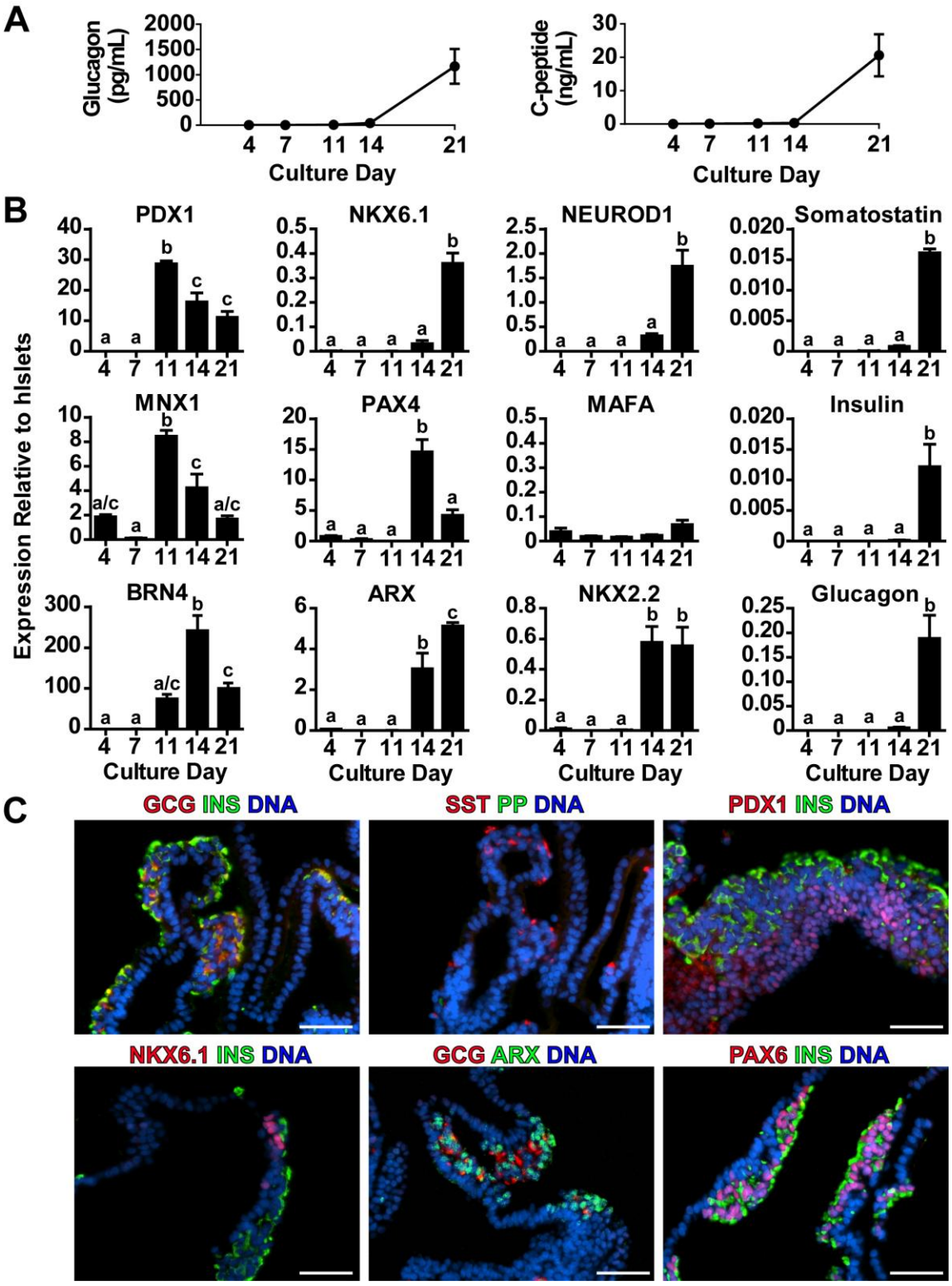

Figure 4.9. High cell seeding density cultures follow the expected endocrine developmental timeline

(A) Media samples from multiple (N =12) high hESC cell seeding density differentiations contain reproducibly high levels of C-peptide and glucagon as measured by radioimmunoassay. (B) Over the differentiation time course expression of transcription factors and islet hormones was examined by RT-qPCR relative to adult human islet expression levels. (C) 21 day differentiated hESCs were immunostained as agarose-embedded,

paraffinized sections for pancreatic hormones and key transcription factors involved in pancreatic endocrine induction and maturation. * represents $p<0.05$ comparing day 14 and 21 media content. Different superscripts (a, b, c) are significantly different from each other within each graph by one-way ANOVA with Bonferroni post-hoc test. Scale bars are 50 μm.

To evaluate whether these cells were biased to an α-cell fate, as previously described for this protocol (127), we performed maturation studies in immunocompromised mice using a kidney capsule transplantation method. 21-day differentiated CA1S cells were detached by partial enzymatic dissociation, sheared into large cell aggregates (~200 - 500 μm diameter) by manual pipetting, centrifuged into a cell pellet in PE50 tubing, and surgically transplanted under the left kidney capsule. CA1S transplants were then allowed to mature *in vivo* with one kidney graft sample taken after one month of maturation and the remaining grafts taken after three months. Immunostaining of the relatively large volumes of engrafted CA1S cells revealed a considerable heterogeneity of tissues including non-pancreatic tissue (mesodermal cartilage was observed in ~50% of grafts). Regions of ductal epithelium (CK19 positive) tissue were also observed in close association with endocrine (chromogranin A positive) tissue with few exocrine (amylase positive) cells observed. The endocrine population of cells was predominantly composed of glucagon positive cells at both 1 and 3 months post transplant with a small proportion of somatostatin positive and very rare insulin positive cells (Figure 4.10A and B). Examination of cardiac plasma samples of transplanted and sham operated mice revealed an elevation of plasma glucagon levels, which correlated with the observation of glucagon positive cells within the grafts (Figure 4.10D).

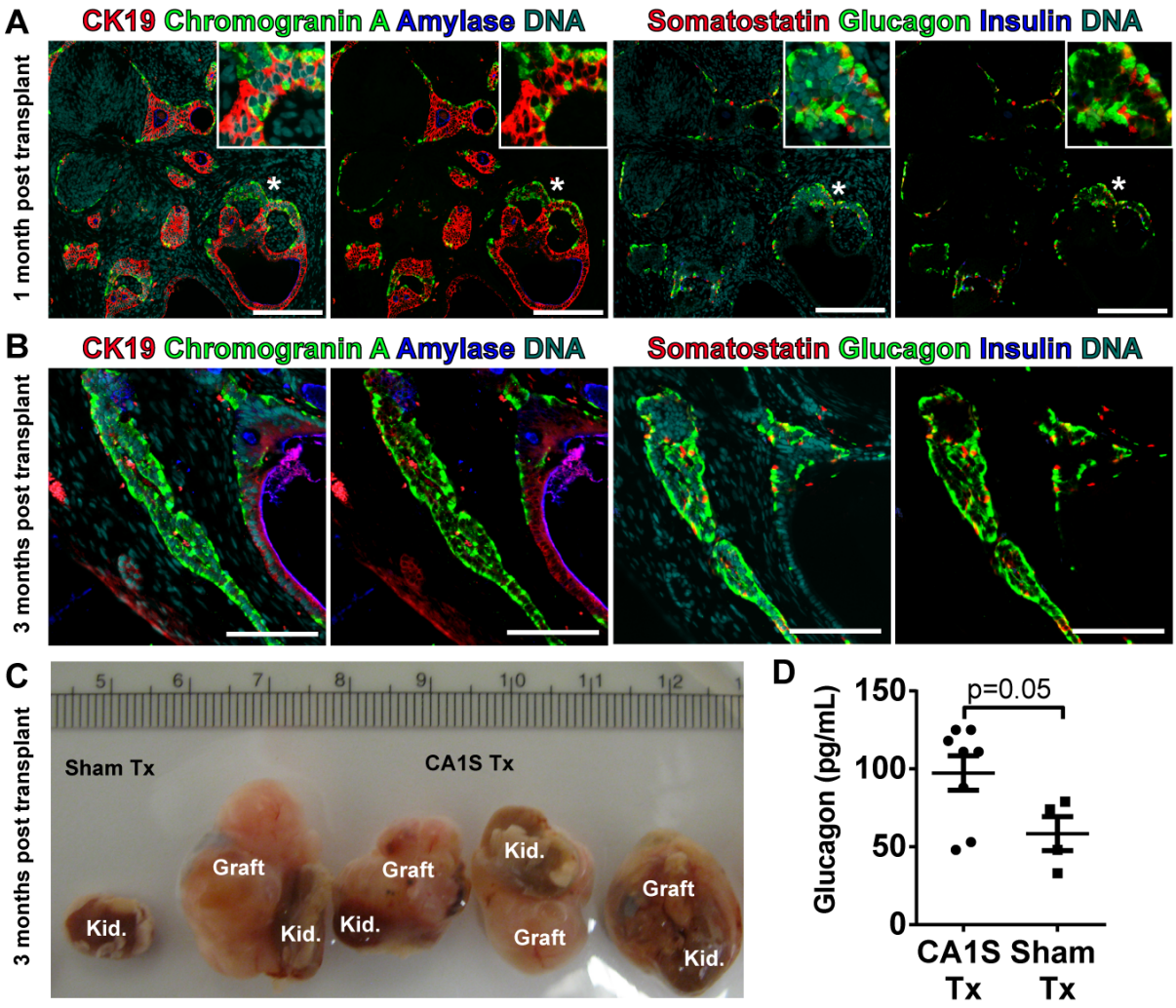

Figure 4.10. CA1S cells show biased glucagon positive cell development *in vivo*

CA1S hESC's seeded at high cell density were differentiated *in vitro* and transplanted under the left kidney capsule of SCID-beige mice. After 1 month (A) and 3 months (B) of maturation grafts were retrieved, processed and immunostained for pancreatic cell types including ductal epithelial cells (CK19, red), endocrine cells (chromogranin A, green) and exocrine cells (amylase, blue). Neighbouring sections were immunostained to determine the specification of the pancreatic endocrine cells into somatostatin (red), glucagon (green), and insulin (blue) positive cell types. Scale bar is 500µm. * denotes location of enlarged images which are shown to the right in A. (A and B) left image is the same image as the right but with DNA counterstain channel added. Scale bar is 100µm. (C) CA1S grafts after 3 months of maturation *in vivo*. Kidney, Kid.; Transplant, Graft; upper ruler is in centimeters. (D) Glucagon levels in cardiac plasma samples taken at 3 months post transplant after an overnight fast.

4.4 Discussion

In this work we examined the effect of modifying initial cell seeding density at the start of pancreatic endocrine differentiation of hESCs. We predominantly used the CA1S hESC line, which allows uniform and highly reproducible cell seeding at a number of densities without loss of pluripotency (3) (Chapter 3). Upon differentiation, we observed an

early failure to commit to definitive endoderm in cultures seeded at low density. These cultures contained a small fraction (~30%) of cells that were co-positive for CXCR4 and SOX17 compared to nearly 75% co-positive fractions in cultures seeded at higher density. Further examination of the low-density cultures revealed remaining OCT4 positive cells, which had presumably failed to differentiate under the conditions that were suitable for definitive endoderm induction in cultures seeded at higher density. This suggests that despite the availability of differentiation signals, cultures seeded at low density were apparently unable to fully convert from the pluripotent gene expression programme to one of definitive endoderm expression.

One possible reason for this failure of low density cultures to differentiate to definitive endodermal cells could be the increased number of cells in the G2/M phases of the cell cycle associated with hyperphosphorylation of retinoblastoma protein. As previous studies have noted, hESCs are amenable to differentiation during the G1 phase of cell cycle and prefer to remain undifferentiated during the G2 and M phases (219, 220). In the cultures seeded at higher density (2.6×10^4 cells/cm^2 and above) we observed a bias away from the G2/M phases of the cell cycle with decreased phosphorylation of retinoblastoma protein and a threshold effect of efficient definitive endoderm induction including expression of SOX17, CXCR4, Gooscoid, *FOXA2* and low OCT4. Taken together these data suggest a link between the cell cycle status of hESCs at the start of differentiation and the efficiency of definitive endoderm induction four days later. This idea is further supported by a key study using the FUCCI cell cycle indicator in hESCs followed by *in vitro* differentiation. Pauklin et al. (2013) found that hESCs in early G1 but not late G1, G1/S, or G2/M phases of the cell cycle were able to rapidly generate definitive endoderm. This early improvement in germlayer specification resulted in increased generation of other endoderm derivatives (liver and pancreas) including insulin positive cells (221). The mechanism which seems to control this bias in endoderm generation was suggested by Pauklin et al. to involve tightly regulated expression of cyclin D1, D2, and D3 where efficient endoderm induction is associated with low expression of D2/D3 and a specific reduction in cyclin D1 to allow the Activin A/Nodal-Smad2/3 signalling pathway to activate endoderm developmental genes. Further, the inhibition of cyclinDs-CDK4/6 by PD0332991 was sufficiently potent to make late G1 hESCs competent for endoderm differentiation effectively replacing the need for Activin A

(221). Taken together these studies reinforce the importance of cell cycle control as a determinant of the differentiation propensity of hESCs to the endoderm lineage, which is a required developmental stage during the eventual formation of pancreatic endocrine cells.

In our study as differentiation continued between days 4 and 21, the CA1S cultures, initially seeded at variable density, grew to the apparent capacity of the 12-well culture system. During this time period the process of sequential maturation from definitive endoderm (Figure 4.1) through pancreatic progenitors (Figure 4.6) to polyhormonal pancreatic endocrine cells (Figure 4.8) followed a temporal cascade of transcription factor expression (Figure 4.9) that ultimately resulted in an α-cell biased pancreatic endocrine developmental profile when transplanted *in vivo* (Figure 4.10). Based on the order of transcription factor expression, the cultures seemed to follow a trajectory of pancreatic progenitors expressing *PDX1* and *MNX1*, followed by endocrine specification with expression of *BRN4*, *ARX*, *PAX4*, *NKX6.1*, and *NEUROD1*, and eventually expression of insulin, glucagon, and somatostatin. This expression pattern follows many of the transcription factor mediated developmental pathways believed to drive formation of pancreatic endocrine cells in humans and mice (84, 99, 100, 222). Notably, *MAFA* expression and glucose stimulated insulin secretion was not observed under any of the seeding densities we tested or at any differentiation time point. Given that MAFA is believed to be critical for proper insulin secretion kinetics in mice (129, 223), and has been observed in adult human β-cells but not in immature human fetal endocrine cells (97), it is perhaps not surprising that the endocrine cells produced in this study did not exhibit mature capacity for glucose-induced insulin release. The immaturity of the endocrine cells produced in this study is in line with previously published *in vitro* differentiation results which report the formation of polyhormonal cells with biased α-cell development that release C-peptide in response to potassium chloride depolarization but are not capable of the mature glucose regulated insulin secretion observed with native islets (126, 127, 138). While this does not preclude the presence of mature β-cells within the cultures, such cells likely make up a small fraction of the total cell population at 21 days of differentiation, although they may increase in number during extended culture (127).

Previous studies have suggested that cell density may influence pancreatic development. In one report, the role of retinoic acid on pancreatic and liver progenitor

formation was examined using an enzymatic dissociation and replating strategy (120). In this work the authors observed that retinoic acid dependent PDX1 expression was increased when cells were seeded at higher densities (120). While not the primary finding, the study implicated cell density as a contributing factor enabling retinoic acid to promote PDX1 expression. The enzymatic and mechanical dissociation protocol used to control cell density is not ideal for a simplified scalable differentiation protocol and warranted further examination. Our data show that even initial seeding density can affect PDX1 expression in differentiating hESCs even without further mechanical dissociation during the differentiation protocol. This notion is also supported by the recent work of Chetty et al. (102) who found that higher initial cell seeding density increased the number of SOX17 positive definitive endoderm cells as well as subsequent PDX1 positive cell populations. Furthermore, high density seeded cultures had increased numbers of cells in the G1 phase of the cell cycle, which was associated with hypophosphorylation of the retinoblastoma protein further implicating cell cycle progression as a key aspect of hESC differentiation capacity. Our current study indicates that initial seeding density also impacts the formation of definitive endoderm, PDX1 positive pancreatic progenitors, and eventual hormone positive cells arising from hESCs. While the mechanism of action for this effect seems to be related to the cell cycle status of the initial seeded population and specifically the phosphorylation status of retinoblastoma protein as seen in this study and others (102, 219, 220), the link between extracellular cell-cell interactions and the associated pause in the G1 phase of the cell cycle is not completely clear. hESCs are known to be highly proliferative, with a particularly short G1 cell cycle, minimal check point control and decreased sensitivity to extracellular cues (224-227). Cell density likely plays a key role regulating cell-cell interactions, which prime hESCs to be receptive to instructive differentiation signals. This priming effect seems to be linked to decreased proliferation allowing key pancreatic developmental checkpoints to be efficiently achieved.

Ultimately, the goal of this work was to determine the effect of initial cell seeding density on pancreatic endocrine differentiation of hESCs. This variable, inherent to nearly all cell culture processes, was found to have marked effects at every differentiation stage examined including germ layer induction, pancreatic progenitor restriction, and endocrine specification with the notable exception of functional *in vitro* maturation. In efforts to

produce glucose responsive insulin-positive cells from hESCs, it seems likely that as signalling pathways that control hESC development are identified, their efficiency of action will be dependent on the culture conditions to which the cells are exposed. While cell density was examined in this study, other factors including temperature, oxygen tension, pH, osmolarity, and metabolite compositions are candidates that should be examined to modify the formation of pancreatic endocrine cells from hESCs. Optimization of these simple factors could increase the yield of pancreatic progenitor and endocrine cells from differentiation protocols, while improving our understanding of hESC development and advancing the possibility of a clinical scale therapeutic product for diabetes.

Chapter 5: Overexpression of PAX4 Reduces Glucagon Expression in Differentiating hESCs

5.1 Background

While hESCs have the theoretical ability to generate any cell type by definition, the protocols and methods required to generate fully functional pancreatic endocrine cells have been relatively unsuccessful using *in vitro* culture approaches alone (209). However, these fully *in vitro* protocols have been relatively efficient at achieving targeted differentiation of pancreatic progenitor populations from undifferentiated cells, and to a lesser extent the generation of polyhormonal pancreatic endocrine cells that express a variety of islet hormones in the same cell (4, 101, 118, 127, 130, 137). While these polyhormonal cells are a natural component of human development (94, 95, 97), the eventual bias of these cells, which most notably co-express glucagon and insulin, is to a glucagon positive α-cell fate (126-128, 138)(Chapter 4). Therefore, new methods that shift the polyhormonal nature of cells away from a glucagon positive lineage could significantly improve the generation of functional β-cells *in vitro*.

One of the influences in pancreatic development that determines pancreatic endocrine cell specificity is the expression of transcription factors. Many factors are known to play a key role in the generation of the pancreas as an organ (eg PDX1, PTF1A, MNX1, HNF1B, GATA6), or the endocrine sub-compartment (eg NGN3) (100, 208). Although the specification of endocrine cells to specific mature fates (eg α, β, δ, ε, and PP cells) is incompletely understood, ARX (aristaless related homeobox) and PAX4 (paired box 4) are known to mutually repress each other's transcription within pancreatic endocrine precursors, and ultimately only one or the other is predominantly expressed in mature endocrine cells. When ARX expression predominates, PAX4 is repressed and the genesis of α-cells is favoured; conversely, when PAX4 expression is high, ARX levels are reduced and the specification of β-cells and δ-cells is enhanced (43, 228, 229). Furthermore, the PAX4 knockout mouse displays an increased number of α-cells and an absence of β- and δ-cells, which suggest that PAX4 is required for both β- and δ-cell lineages (230). This role in pancreatic development may also be true in humans as both PAX4 and ARX are simultaneously expressed in the developing human fetal pancreas beginning at week 8-9 of

gestation (97, 222, 231). Furthermore, PAX4 dysfunction has been implicated in human MODY9 further supporting the hypothesis that this factor plays a role in the maintenance of the adult β-cell phenotype (232).

Based on the established role of PAX4 in pancreatic endocrine development as a positive regulator of β-cell specification, PAX4 is an attractive potential tool for increasing the proportion of β-cells derived from stem cell populations, including ESCs. Indeed, it has been shown that in both mESCs and hESCs, constitutive overexpression of PAX4 has broadly beneficial effects in terms of improved pancreatic endocrine differentiation of insulin positive cells (233, 234). Using relatively non-specific differentiation conditions these studies found that PAX4 increased the expression of insulin, a number of β-cell associated transcription factors, and insulin processing pathway components (233, 234). These improvements over control cultures were achieved despite the lack of temporal control on PAX4 expression or the more recently developed stage-specific differentiation methods such as those used in this chapter.

In order to influence the developmental fate specification of hESC derived pancreatic endocrine cells *in vitro*, we generated an adenoviral vector to allow for acute expression of human PAX4 in pancreatic progenitors during differentiation. Viral delivery of PAX4 to developing monolayers of pancreatic progenitor cells resulted in dose dependent and robust PAX4 overexpression. Ultimately increased levels of PAX4 resulted in reduced ARX and glucagon expression and led to decreased numbers of polyhormonal cells and maintenance of insulin positive cells which lost expression of glucagon.

5.2 Methods

Generation of Human PAX4 Adenovirus

A human PAX4 cDNA was generated by RT-PCR using high-fidelity Accuprime Taq polymerase (Invitrogen) and cloning primers (fwd, 5' CCACCATCTAGAGGGATCAGCAGCATGAACCAGCTTG 3'; rev, 5' CCACCAGCGGCCGCTCATTCCAAGCCATACAGTAGTGGGCAGC 3'). These primers contain heterologous *XbaI* and *NotI* sites to facilitate cloning. A 1.05 kb amplicon was produced from adult human islet cDNA, digested with XbaI and NotI, and cloned into a shuttle vector, pScore3. pScore3 is a derivative of pShuttle (Clontech), containing a rabbit

beta globin intron (RBGI, GenBank #V00878.1, nucleotides 557-1187), followed by a custom polylinker, between the CMV promoter and BGH polyadenylation sequences of pShuttle. The cloned PAX4 ORF was validated by sequencing to be the same as that used by Liew et al. (2008), and is identical to the ORF in Genbank #NM_006193, bases 207-1238. The recombinant CMV-RBGI-PAX4 transgene cassette was excised from pScore3, and subcloned into pAdeno-X (Clontech), using the homing endonucleases *I-CeuI* and *PI-SceI* (New England Biolabs). Molecular cloning of the human PAX4 vector was completed by Dr. Robert Baker. Complete virions were generated by transient transfection of HEK293 cells with CMV-RBGI-PAX4 loaded pAdeno-X plasmid followed by amplification and purification to high titer viral stocks (Ad PAX4 ;3 x 10^{10} PFU/ml) by ViraQuest Inc. Control adenoviral virions expressing eGFP from the CMV promoter were similarly generated (Ad eGFP; 4 x 10^{9} PFU/ml).

Culture of hESCs

Undifferentiated CA1S hESCs were maintained on 1:30 diluted growth factor reduced Matrigel (BD Biosciences) in mTeSR1 media (STEMCELL Technologies) as previously described in Chapter 3.2.

Pancreatic Differentiation and Adenoviral Delivery of hESCs

Subconfluent CA1S hESCs were seeded in 1:30 diluted Matrigel coated, 12-well culture plates at a previously established optimal density of 5.3 x 10^{4} cells/cm^{2} in 1.5ml of mTeSR1 in the absence of Rho Kinase inhibition (4) (Chapter 4.2). Approximately 16-hours after seeding, undifferentiated cultures were 95-100% confluent and were subjected to a pancreatic endocrine differentiation cascade as previously described for CA1S hESCs (4) (Chapter 4.2). On day 11 of culture, randomly assigned 12-wells were transduced over 24-hours with either an Ad eGFP, Ad PAX4 or no virus in the standard day 11 culture media. Viral delivery was at a MOI of 6 for the low dose or 60 for the high dose based on a cell count of 4.3 x 10^{5} cells/cm^{2}. During the protocol, 24-hour static media samples were collected, centrifuged to remove cell debris, individually aliquoted and stored at -20°C on days 11, 14, 17, 19, and 21 of culture. On day 19 of culture a sequential static glucose and

potassium chloride stimulated hormone secretion assay was performed on differentiated cells as described in Chapter 4.2.

Quantitative Reverse Transcriptase PCR (RT-qPCR)

Quantitative reverse transcriptase PCR was performed on day 21 cell samples using previously frozen cell pellets according to manufacture recommended protocols as described in Chapter 4.2. Primers were optimized for identical fast two-step cycling conditions with a Tm of 62°C. All reactions were performed in technical duplicate and biological triplicate with gene expression normalized to HPRT then to a pooled sample of adult human islet cDNA. Primer sequences can be found in Table 5.1. Human islets were kindly provided by Drs. Ao and Warnock from the Irving K. Barber Human Islet Isolation Laboratory (Vancouver, BC, Canada).

Table 5.1 Sequences of primers used in RT-qPCR in chapter 5

Gene Name	Gene Accession	Product Size (bp)	Primer Sequence Forward / Reverse 5'→3'	Reference
ARX	NM_139058.2	141	CTGCTGAAACGCAAACAGAGGC CTCGGTCAAGTCCAGCCTCATG	(4)
PAX4	NM_006193	169	AGCAGAGGCACTGGAGAAAGAGTT CAGCTGCATTTCCCACTTGAGCTT	(2)
MAFA	NM_201589	195	CTTCAGCAAGGAGGAGGTCA TTGTACAGGTCCCGCTCTTT	(4)
Insulin	NM_000207.2	245	AGCCTTTGTGAACCAACACC GCTGGTAGAGGGAGCAGATG	(158)
Glucagon	NM_002054.4	275	CATTCACAGGGCACATTCAC CGGCCAAGTTCTTCAACAAT	(158)
Somatostatin	NM_001048.3	126	AGCTGCTGTCTGAACCCAAC CCATAGCCGGGTTTGAGTTA	(158)
HPRT	NM_000194.2	148	TGTTGTAGGATATGCCCTTGACTAT GCGATGTCAATAGGACTCCAGA	(4)

Immunocytochemistry

hESCs differentiated for 21 days were detached from the 12-well culture plates as intact cell sheets fixed and processed for agarose embedded paraffin sectioning as previously described in Chapter 4.2 and (4). Immunostaining using primary and secondary antibodies described in Table 5.2, was performed as described in Chapter 4.2 and as previously described including nucleocentric single-cell hormone quantification (4, 198).

Table 5.2 Antibodies used in immunocytochemistry in chapter 5

Gene Name	Host Species	Supplier / Catalogue number	Staining Method	Dilution	Antigen Retrieval
PAX4	Goat	R&D systems AF2614	Slide	1:250	HIER
eGFP	Mouse	Clontech 632375	Slide	1:500	HIER
Synapto-physin	Rabbit	Novus NB120 - 16659	Slide	1:50	HIER
Insulin	Guinea Pig	Sigma I8510	Slide	1:1000	HIER
Glucagon	Rabbit	Cell Signalling 8233P	Slide	1:500	HIER
Somatostatin	Mouse	BCBC AB1985	Slide	1:1000	HIER
PAX4	Goat	R&D systems AF2614	Slide	1:250	HIER

HIER (heat induced epitope retrieval): 15 minutes at 95°C in 10 mM Citrate buffer with 0.05% Tween-20 pH 6.0.

Slide: PFA fixed, paraffin section of agarose embedded cell pellet or pancreatic tissue

BCBC (Beta Cell Biology Consortium)

Radioimmunoassay

Static and stimulated media samples were assessed for hormone content by radioimmunoassay following manufacture recommended protocols with volumes halved for all reagents as described in Chapter 4.2. Analysis for human C-peptide (Millipore, HCP-20K) and glucagon (Millipore, GL-32K) was performed in technical duplicate and biological triplicates.

Statistical Analysis

Unless otherwise stated data are reported as mean ± SEM. Significance was set at $p \leq 0.05$ based on the results of one-way ANOVA and Bonferonni post-hoc tests.

5.3 Results

Adenoviral Gene Delivery of PAX4 to hESCs

Based on the potential to improve endocrine fate specification of hESCs toward the β-cell lineage, we examined the effect of increased PAX4 expression during staged *in vitro* pancreatic differentiation. To do this we used a 21 day protocol designed to mimic the

changing embryonic environment that induces the development of hESCs into pancreatic endocrine cells (Figure 4.1A). We have previously shown that the expression of PAX4 and its antagonistic partner ARX begins between day 11 and 14 of this protocol (4) (Figure 4.9). Based on this timeline, and one of the presumed PAX4 targets being ARX, we performed infections of developing hESC cultures at day 11 with either control virus expressing enhanced green fluorescent protein (Ad eGFP) or PAX4 virus (Ad PAX4) at a MOI of 6 or 60 based on a day 11 cell density of 4.3×10^5 cells/cm^2. By day 12, eGFP positive cells were observed in the control group, and eGFP expression was maintained until day 21 (Figure 5.1A). At day 21, cultures treated with a MOI of 6 and 60 were 10.7% and 51.6% positive respectively for eGFP expression. These eGFP positive cells were predominantly non-endocrine cells, based on their lack of synaptophysin immunoreactivity although some cells did co-express eGFP and synaptophysin (Figure 5.1B and C). This suggests that transgene expression was more efficient at targeting pancreatic progenitor populations with a lower efficiency of maintained expression in differentiated progeny. Similar to the transduction efficiency results, overexpression of PAX4 in day 21 cultures was dose-dependent with the MOI of 6 and 60 for Ad PAX4 resulting in ~5,000, and ~19,000 fold overexpression compared to adult human islet levels, respectively. PAX4 overexpression levels were also significantly elevated compared to the 3-6 fold human islet levels seen in non-virally treated and Ad eGFP treated cultures (Figure 5.1D). Delivery of Ad PAX4 was also associated with nuclear PAX4 immunoreactivity, which was in contrast to the cytoplasmic immunoreactivity seen in rare cells of control cultures (Figure 5.1E).

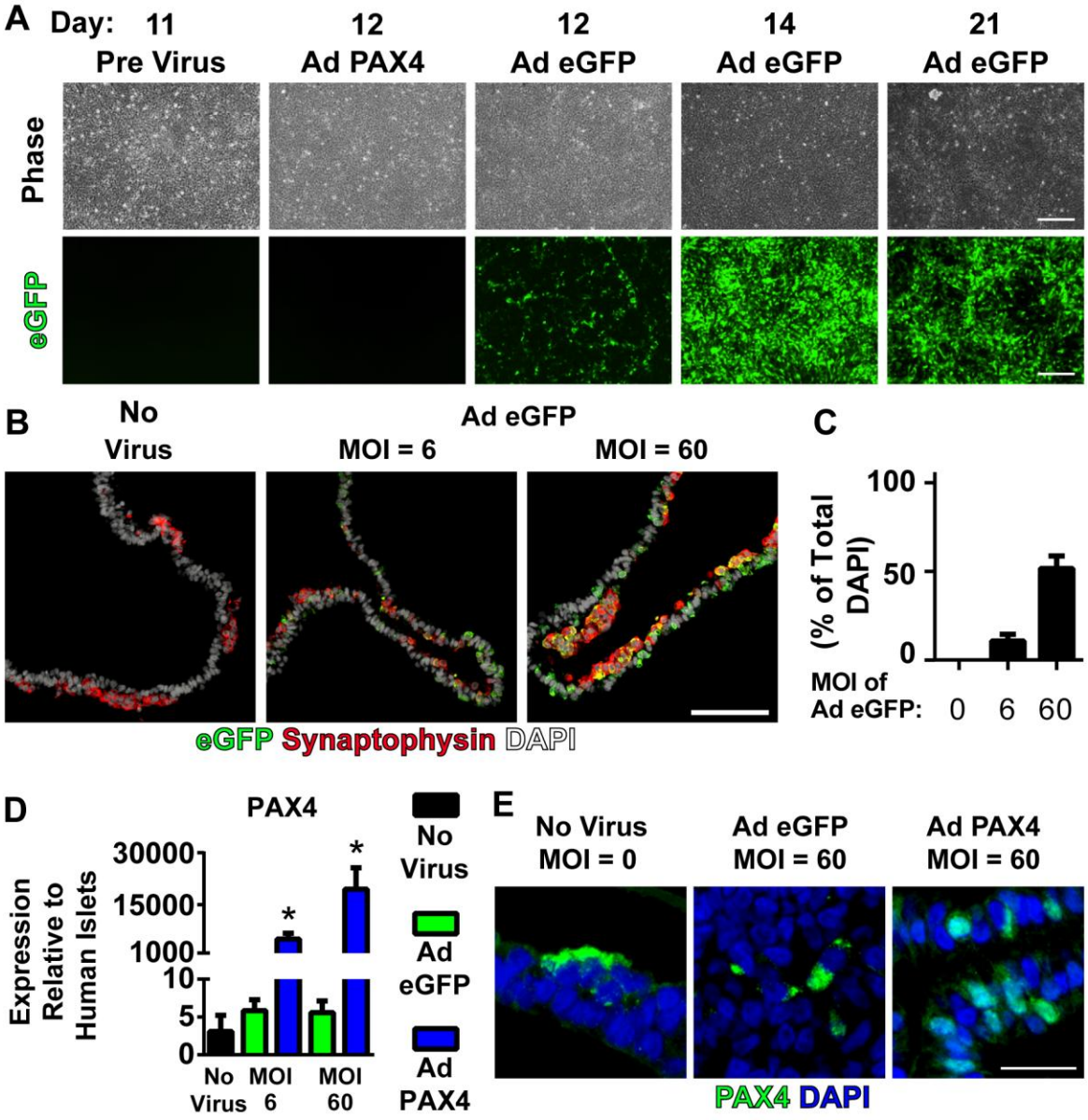

Figure 5.1. Adenoviral infection and PAX4 overexpression in hESCs

(A) Adenoviral infection of 11 day differentiated hESCs yields eGFP expression (green) by 24 hours post viral delivery which persists through the culture period. (B) 21-day differentiated pancreatic endocrine cultures were immunostained for eGFP (green) to mark expression of the adenoviral vector and synaptophysin (red) to mark the endocrine cell population as a portion of the total cells (DAPI, white). (C) Quantification of the total number of eGFP positive cells as a percentage of the total number of nuclei. (D) Infection of day 11 cells with an adenoviral human PAX4 expression construct resulted in a dose dependent increase in PAX4 transcript levels as measured by RT-qPCR of day 21 samples relative to expression in human islets. (E) PAX4 delivery was also associated with nuclear localizing immunoreactivity (PAX4, green) which was in contrast to rare cytoplasmic PAX4 immunoreactivity seen in uninfected and control infected day 21 cultures (nuclei, blue). * Indicates significant overexpression of human PAX4 compared to control virus (Ad eGFP) at the same dose ($p < 0.05$ by one-way ANOVA with Bonferroni post-hoc test). Scale bar is 200 μm in A, 100 μm in B and 25 μm in E.

PAX4 overexpression blocks glucagon expression

To examine the effect of PAX4 for the last 10 days of hESC *in vitro* differentiation, we tested the bulk cell population for expression of islet hormones and key transcription factors at day 21 of culture. Adenoviral delivery of PAX4 at both low viral dose (MOI = 6) and high viral dose (MOI = 60) significantly reduced ARX transcript levels compared to control virus (Ad eGFP) treated cultures (Figure 5.2A). This approximately 50% reduction of ARX correlates well with the ~50% transgene expression efficiencies observed in the high viral dose (Figure 5.1B and 5.2A). Furthermore, high dose Ad PAX4, but not low dose, reduced glucagon levels and modestly increased insulin levels with no significant change in somatostatin or MAFA levels (Figure 5.2A). Since the low viral dose infected relatively few cells compared to the high viral dose, and these were predominantly non-endocrine (Figure 5.1 C-D), we speculate that this biased gene delivery could explain the reduction of ARX at both doses yet reduction of glucagon only at the high dose.

To assess the hormone release capacity of PAX4 cultures, we next examined media samples taken between days 17 and 21 for glucagon and C-peptide levels. High viral dose, but not low dose, PAX4 overexpression significantly reduced glucagon release with a non-significant trend to decreased C-peptide levels (Figure 5.2B). To examine the potential for improved stimulus-coupled hormone secretion in hESCs, day 19 differentiated cells were tested by a static sequential secretion assay including low and high glucose levels and potassium chloride. Under these conditions, no significant effect was observed in terms of C-peptide or glucagon release in either glucose or potassium chloride stimulated conditions (Figure 5.2C). Notably, a trend is evident that Ad eGFP may have had a negative effect on the stimulated release of both glucagon and C-peptide although this did not reach statistical significance with the number of replicates used in this study. Taken together these data suggest that overexpression of PAX4 has dose-dependent effects on the expression of ARX and glucagon which, in high dose PAX4 conditions results in a reduction of glucagon release under static conditions.

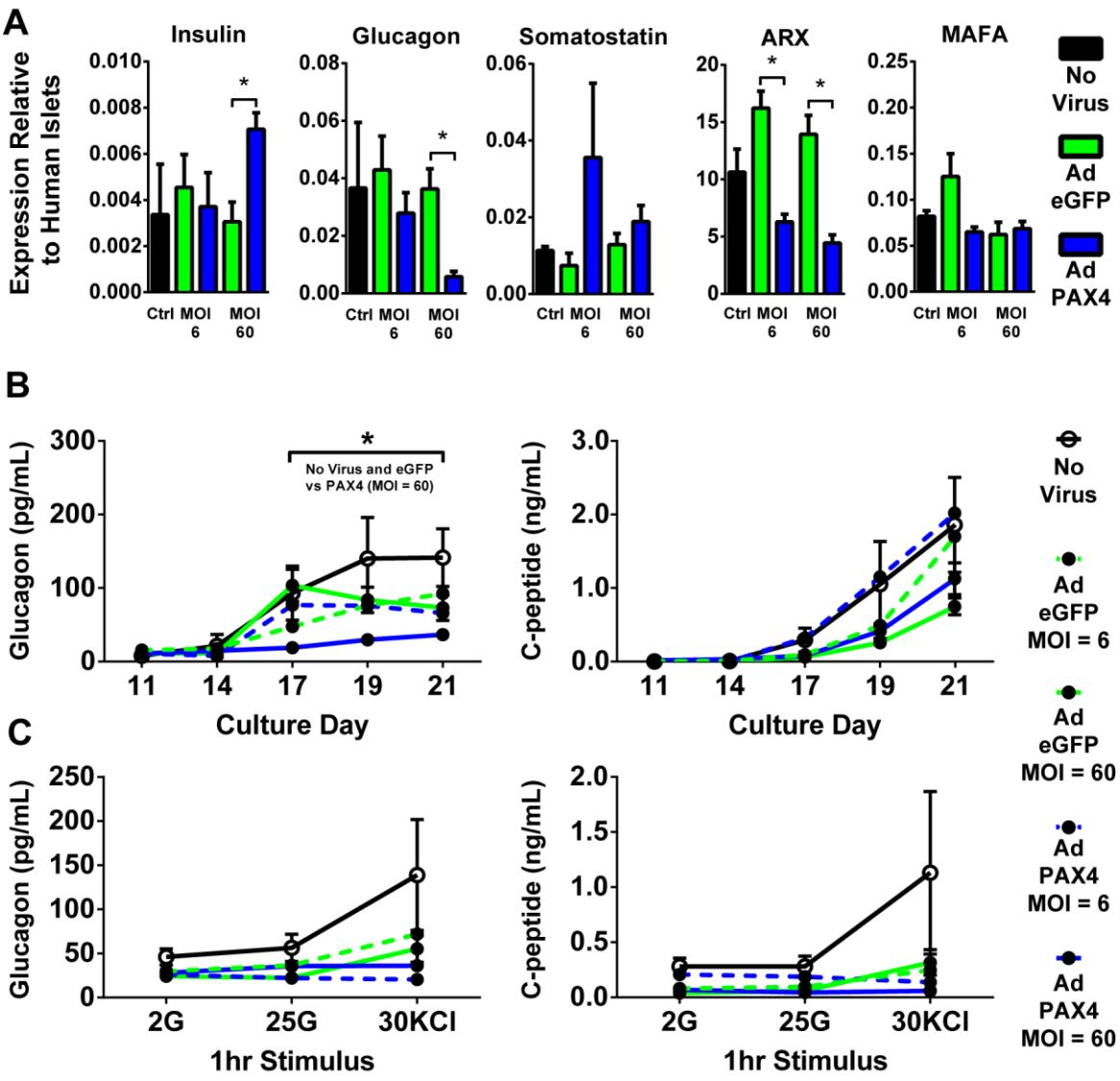

Figure 5.2. PAX4 overexpression reduces glucagon and ARX

(A) 21 day differentiated hESC cultures uninfected or infected with either Ad eGFP or Ad PAX4 at an MOI of 6 or 60 were assessed for expression of a number of targets by RT-qPCR relative to adult human islets. * Indicates significant overexpression of human PAX4 compared to control virus (Ad eGFP) at the same dose ($p < 0.05$ by one-way ANOVA with Bonferroni post-hoc test). (B) 24 hour static media samples were taken between days 11 and 21 were assayed by radioimmunoassay for glucagon and C-peptide content. (C) 19 day differentiated hESCs were tested for glucose regulated glucagon and C-peptide release in response to 1 hour incubations in low glucose (2 mM), high glucose (25 mM), and potassium chloride (30 mM).

While the bulk population data suggested a loss of glucagon expression upon PAX4 overexpression, we next tested if this effect was based on changes in the number of endocrine cells and, more specifically, in a change within subpopulations of hormone positive cells. To do this we examined the single-cell hormone expression of 21 day differentiated hESCs treated with low or high doses of Ad eGFP or Ad PAX4 as well as untreated controls.

Staining for insulin, glucagon, and somatostatin in paraffin sections of agarose-embedded cell sheets revealed that in all conditions tested approximately the same number of cells expressing any combination of hormones were present (Figure 5.3A and B). Quantification of the individual hormone expression status of each cell using unbiased image analysis software revealed that the generally polyhormonal nature of untreated and Ad eGFP treated cultures significantly shifted upon treatment with a high dose of Ad PAX4. This shift included a significant decrease in the triple positive fraction (insulin positive, glucagon positive and somatostatin positive; white bar) and a significant increase in the unihormonal insulin positive fraction (insulin-only; blue bar) comparing Ad PAX4 and Ad eGFP at an MOI of 60 (Figure 5.3C). The reason for this shift toward insulin-only cells was not due to a change in the total number of insulin-or somatostatin-positive cells but was a specific decrease in the number of glucagon-positive cells upon treatment with a high dose of PAX4 (Figure 5.3D). This maintenance of insulin and loss glucagon correlates well with the observation of maintenance of static C-peptide release and loss of static glucagon release in PAX4 treated cultures (Figure 5.2).

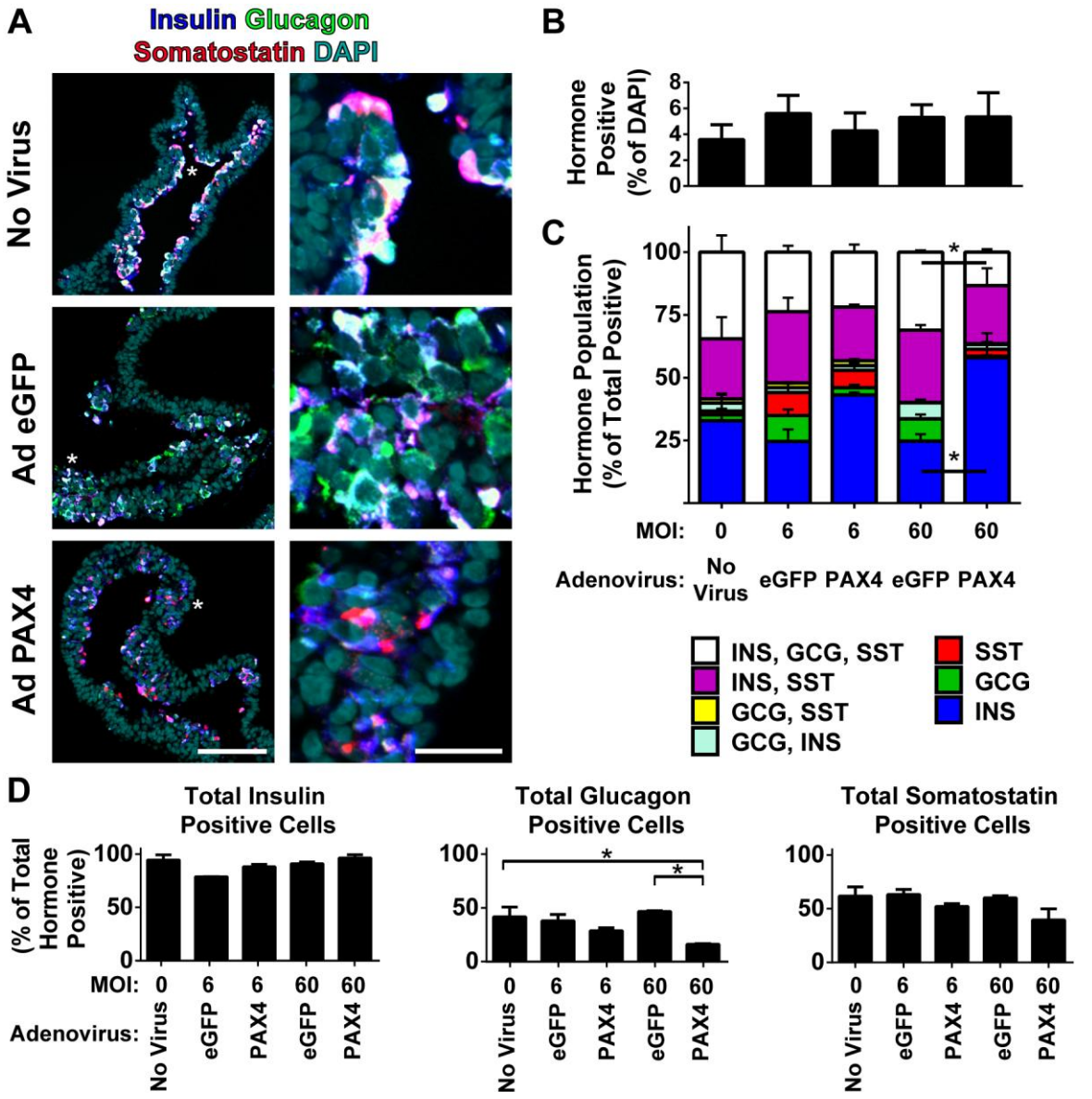

Figure 5.3. PAX4 overexpression reduces the number of glucagon positive cells

(A) Agarose-embedded sections of 21 day differentiated hESC cultures uninfected or infected with either Ad eGFP or Ad PAX4 (MOI = 60) were immunostained for insulin (blue), glucagon (green), and somatostatin (red) with a nuclear counterstain (DAPI, cyan). Right image is an enlargement of the region indicated by the white *. Right scale bar is 100 µm, left scale bar is 25 µm. (B) Single cell quantification of the number of total nuclei that are positive for any combination of insulin, glucagon, or somatostatin. (C) Single cell population profile of hormone positive cells as a percentage of the total number of hormone positive cells. * Indicates significant change in cell population between PAX4 and eGFP treated cultures given an MOI of 60 ($p < 0.05$). (D) The total number cells positive for insulin, glucagon, and somatostatin were examined regardless of polyhormonal nature. * Indicates significant change in the glucagon positive cell population between untreated and PAX4 or eGFP treated cultures at an MOI of 60 ($p < 0.05$ by one-way ANOVA with Bonferroni post-hoc test).

5.4 Discussion

The goal of this study was to develop and apply a model of acute PAX4 expression in hESCs under defined *in vitro* pancreatic endocrine differentiation conditions. To do this we built upon our previous work differentiating CA1S hESCs to pancreatic endocrine cells (3, 4) and applied a newly generated adenoviral human PAX4 expression vector that allowed temporally controlled gene delivery and maintained gene expression. This model system generated the expected nuclear localizing PAX4 immunoreactivity, and PAX4 transcript levels were overly high (~5,000 - 19,000 fold greater than in adult human islets) in both the low and high viral doses. While a decreased viral dose was able to reduce the average PAX4 expression, there was a significant reduction of infection efficiency, to an extent that the low viral dose delivered PAX4 to relatively few cells. From these data we can extrapolate that in the gene delivery method applied in this study, a relatively high PAX4 expression level was generated even on a cell-by-cell basis. Thus changing viral dose altered the number of cells which obtained PAX4 overexpression at a high level. The high expression results from our use of the CMV promoter element, similar to that of other PAX4 overexpression studies (43, 233, 234). In order to achieve more physiologically relevant levels of overexpression even when high MOI's are employed to maintain infection efficiency, alternate promoters, such as EF1α or an inducible expression system such as that used by Brun et al. (2004 and 2008), could be employed.

In our study PAX4 had no effect on the number of endocrine cells. Since the number of endocrine cells is generally controlled by expression of NGN3 (235, 236), the absence of an effect of PAX4 on endocrine cell number is consistent with reports that PAX4 expression lies directly downstream of NGN3 (237). However, PAX4 overexpression significantly influenced which endocrine cell types were formed by repressing glucagon production, leaving unihormonal insulin positive cells to predominate the endocrine fraction of the cultures. The modest effect of human PAX4 that we observed follows work done on human and rat islets, which found that adenoviral overexpression of human PAX4 was relatively ineffective compared to murine PAX4 at inducing proliferation of human and rat islet cells (238, 239). While this work by Brun et al. was focused on the pro-proliferative effect of PAX4 on islet cells, it highlights the importance of examining the effects of human transcription factors in human cell types as the murine homologues do not necessarily show

the same effects. Moreover, building upon studies by Blyszczuk et al. who overexpressed murine PAX4 in mouse ESCs, Liew et al. examined the effects of constitutive overexpression of human PAX4 in hESCs. Using the same human PAX4 sequence as used in our study, the authors found that PAX4 expression generally accelerated the endocrine differentiation time-line including the formation of a small proportion of cells that were zinc positive (based on Newport green dye uptake) and enriched for C-peptide (234). While the polyhormonal nature of these Newport green positive cells or the total cell population was not reported in the PAX4 overexpressing hESCs, improved responsiveness to potassium chloride depolarization was noted specifically in the PAX4 expressing cells. While our data supports a role for PAX4 in the repression of glucagon positive cells, we observed a trending reduction in potassium chloride stimulated hormone secretion (both glucagon and C-peptide) in PAX4 treated cultures, similar to control virus treated cells. Ultimately this negative effect of the viral gene delivery vector on hormone secretion precludes functional analysis of PAX4 treated cultures.

PAX4 may have further roles in the maintenance of β-cell function once a mature cell type is formed. In mice constitutively overexpressing PAX4 in PDX1-, PAX6-, and glucagon- positive lineages, young mice have neonatal hypoglycemia due to reduced numbers of glucagon producing α-cells and improved glucose tolerance during a glucose challenge due to increased β-cell mass (43). Over time, despite increased numbers of β-cells overexpressing PAX4, these mice developed hyperglycemia, decreased insulin secretion and elevated blood glucose during a glucose challenge, which suggests a failure of these older β-cells to functionally respond to elevated glucose levels (43). Therefore, while PAX4 is beneficial and critical to the genesis and specification of β-cells, sustained high expression of PAX4 is detrimental to maintenance of functional aspects of the β-cell phenotype. This notion of transcription factor expression peaking during human pancreas development and decreasing in more mature cell types has also been reported for PDX1 and contrasts the expression profile of MAFA, which has peak expression in mature β-cells (222). Additionally PAX4 has an established role of repressing the α-cell phenotype (229, 240, 241), and acts as a transcriptional repressor of both the human glucagon and insulin genes (232). This repressive activity of PAX4 suggests that in the mature β-cell low PAX4 expression is required to permit efficient insulin production while also helping to maintain β-

cell identity. A strong negative autorepression via PAX4 binding to and repressing the human PAX4 promoter may help to limit PAX4 expression levels (242). Given that we used a PAX4 expression system which results in artificially sustained overexpression, it is possible that fully functional maturation of β-cells including high insulin expression could have been actively repressed by high levels of PAX4 or the adenoviral vector itself. While our data show a small increase in insulin expression, which was unexpected given the repressive nature of PAX4, the predominant role of PAX4 is associated with pancreatic endocrine fate specification of hESCs. However, it remains to be seen if more physiological expression levels of PAX4 through a gene delivery method which has no deleterious effects on cellular secretory capacity can modulate hESC differentiation to a fully functional cell type.

In addition to effects on the β-cell lineage, PAX4 has also been shown to influence the formation of somatostatin positive δ-cells as PAX4 null mice have decreased numbers of both β and δ-cells (230). Remarkably, in mice that lack both PAX4 and ARX, δ-cell numbers are dramatically elevated, suggesting that neither factor is required for the genesis of δ-cells (243). Based on this developmental data we examined our model of PAX4 overexpression for effects on δ-cell formation. We found no changes in somatostatin transcript levels or the numbers of cells immunoreactive for somatostatin protein. These data correlate well with conditional PAX4 overexpression mice where PAX4 is constitutively expressed in cells from PDX1-, PAX6- or glucagon- positive embryonic lineages (43). Islets from these mice display biased formation of insulin positive cells with no increase in somatostatin positive cells (43). Together this suggests that while PAX4 may be a positive regulator of the development of insulin and somatostatin positive lineages, PAX4 is not required for somatostatin cell formation, and high levels of PAX4 acts as a selective driver the insulin positive lineage.

Taken within the context of other PAX4 overexpression studies, most evidence supports the roles of PAX4 as a cell fate specification and endocrine induction transcription factor with a key attribute of repressing the α-cell biasing factor ARX during both murine and human development. In mature β-cells, PAX4 may be associated more with activating proliferation in response to unknown extracellular cues seemingly at the expense of cellular function if left unchecked. While this study has focused on a defined hESC differentiation

system and the role of human PAX4 in endocrine cell fate specification, the work builds upon the growing knowledge of the multitude of roles of PAX4 during pancreatic development and maturity.

Chapter 6: Genomic Deletion of ARX in hESCs Reduces Pancreatic Polypeptide, Glucagon, and Insulin Positive Cells

6.1 Background

While PAX4 is established to positively regulate the formation of the β- and δ-cell lineage through the repression of other transcription factors, another way to improve the formation of insulin positive cells from hESCs is to remove positive regulators of other islet endocrine cells. The most numerous of the non-insulin positive pancreatic endocrine cells within human islets are glucagon positive α-cells (244). In humans, adult α-cells have been found to have a distinct expression pattern compared to other pancreatic endocrine cells including high expression of transcription factors such as Iroquois Homeobox 2 (IRX2) and Aristaless Related Homeobox (ARX) (245). In addition to the pancreas the expression of ARX is also found in other tissues including the brain, heart, skeletal muscle, testis, and intestine (229, 246-250). Humans with X-linked lissencephaly with ambiguous genitalia (XLAG, OMIM # 300215) represent some of the most severe clinical effects of the various functional null mutations in *ARX* (251). As a result of this null mutation, the population of pancreatic cells in patients with XLAG is altered such that there is an absence of glucagon and pancreatic polypeptide positive cells, while insulin, somatostatin and ghrelin positive cell numbers remained unchanged in two XLAG pancreatic samples (252). Similarly, ARX-deficient mice fail to form glucagon positive cells, but still form insulin and somatostatin positive cells (229). Conversely in mice where *ARX* was overexpressed in various pancreatic and pancreatic endocrine lineages (PDX1-, PAX6- or insulin-positive), increased numbers of glucagon and pancreatic polypeptide positive cells were observed at the expense of both the insulin and somatostatin positive lineages (228). This positive regulation of the α-cell lineage by ARX is based on an elegant model of reciprocal transcriptional repression between ARX and PAX4. Work by Collombat et al. revealed that ARX represses PAX4 through a transcriptional enhancer upstream of the *PAX4* gene, whereas PAX4 represses *ARX* transcription by binding to a 3' enhancer of the *ARX* gene (243). This model of specification of the α- versus β/δ- lineages of pancreatic endocrine cells may also be present in human fetal development as the early expression of both PAX4 and ARX are found at the same time frame of 8-9 weeks of gestation (97, 222, 231).

During this stage of human development (9-12 weeks) the expression of ARX is found in glucagon positive and polyhormonal cells (insulin/glucagon co-positive) (97). In hESC differentiation, ARX expression is seen within *in vitro* derived polyhormonal endocrine cells at approximately the equivalent stage of human development (4, 118, 127, 138). When transplanted, these immature cells are predestined to become α-cells that maintain prominent expression of ARX among other markers (127, 138). While the role of ARX in the development of hESCs is not completely clear, it seems closely associated with the early formation of pancreatic endocrine cells and more specifically the glucagon linage.

Given the α-cell biased *in vitro* development of endocrine cells generated from hESCs, and the data suggesting human α-cell specification may be governed by ARX expression similarly to that in mice, we generated hESCs deficient for ARX and examined pancreatic endocrine development. These *ARX* knockout hESCs were able to efficiently differentiate through a multi-stage protocol including the formation of definitive endoderm, foregut, pancreatic progenitors and pancreatic endocrine cells. These ARX knockout endocrine cells did not express glucagon or pancreatic polypeptide in a similar manner to human XLAG endocrine populations. ARX knockout endocrine cells also had a low expression of insulin, which resulted in large populations of unihormonal somatostatin positive cells. These somatostatin positive cells expressed low levels of PAX6 and high levels of HHEX. Upon re-expression of low levels of human *ARX* by adenoviral infection, we observed an increase in PAX6 expression, a decrease in HHEX, and an increase in the numbers of insulin positive cells from ARX knockout hESCs. These data suggest that during hESC differentiation, ARX influences the formation of glucagon and pancreatic polypeptide positive cells. Additionally, ARX also seems to play a role in the formation of insulin positive cells potentially through actions of PAX6 in this model of human embryonic development.

6.2 Methods

Generation of ARX knockout CA1S Cells by Genomic Editing with Zinc Finger Nucleases

Undifferentiated CA1S hESCs were maintained as previously described in Chapter 3.2. In order to enable genetic modification of the *ARX* locus in CA1S cells, sub-confluent

hESCs were enzymatically dissociated to 5-25 cell clusters using Accutase (STEMCELL Technologies, 7 min, 37°C,) and counted using a Scepter^{TM} 2.0 cell counter (Millipore). For electroporation of hESCs using a Neon transfection system (Invitrogen), optimal gene delivery was obtained with 2 pulses at 1050 V for 30 ms which had minimal effect on cell viability but was able to deliver reporter plasmids to approximately 40-50% of cells. Using these conditions 2.5 x 10^5 cells were mixed with 5 µl (2 µg per ZFN of the pair) of purified *in vitro* transcribed mRNA encoding a custom made CompoZr® Zinc Finger Nuclease pair targeted to the 3' end of exon 1 of the *ARX* gene (Catalogue number CKOZFN3556, Sigma). After culture for 72 hours, heterogeneous *ARX* targeted CA1S cells were subjected to single cell limiting dilution cloning with 576 wells being seeded. Sixty three clonal populations were isolated with hESC-like morphology and were subjected to a PCR based screen of the *ARX* locus ZFN cut site (forward primer 5'-TCAGTACCAGGAGGAGGGC, reverse primer 5'- GAGACAGCCCTGGCTAGATG). Based on a band shift on an 2% agarose gel, putative deletion and control clones were sequenced to reveal that ARX knockout clone 1 (C1) and clone 2 (C2) contained 23 and 41 base deletions centered around the predicted ZFN cut site (Figure 1B). Following previously described in-well immunocytochemistry methods outlined in Chapter 4.2 (4), undifferentiated wild type and ARX knockout cells were immunostained for pluripotency markers OCT4 and SSEA3 using primary antibodies listed in Table 6.2.

Pancreatic Differentiation of hESCs

Undifferentiated CA1S cells that were 90% confluent were subjected to a 26 day *in vitro* pancreatic endocrine differentiation protocol previously described in detail (210) (See Appendix B for details) and summarized in Figure 6.2A. At day 5, 11, and 17 of the culture, developing cells were assessed for expression of CXCR4 (definitive endoderm), PDX1 (foregut endoderm), and NKX6.1 (pancreatic endoderm) by flow cytometry (N = 4 independent differentiation trials) as previously described (210)(Chapter 4.2) using antibodies described in Table 6.2. At the end of each differentiation stage, media samples (24-hour) were taken for assessment of hormone content (N = 3 samples for each day of 4 trials). On day 24 of culture, a static sequential glucose and potassium chloride secretion assay was performed as previously described in Chapter 4.2 (4) which included 1 hour

incubations in 2 mM glucose, 25 mM glucose, and 30 mM potassium chloride with 2 mM glucose (N = 3 samples for each treatment of 4 trials).

Cloning and Application of Adenoviral ARX Re-expression Vector

Since the *ARX* gene has relatively high GC content (70-90%) which is empirically resistant to complete reverse transcription reactions, the human *ARX* open reading frame (ORF) was cloned from genomic DNA as individual exons that were seamlessly reassembled using Golden Gate cloning methods (253) by Dr. R. Baker. Once fully assembled, the *ARX* ORF was cloned downstream of the human EF1α promoter and its first intron such that the start codon of *ARX* replaced that of EF1α. Subsequently the 3' end of the *ARX* ORF was appended with a SV40 polyadenylation sequence and the completed plasmid once sequence verified was cloned into the pAdeno-X (Clonetech) vector using the endonucleases *I-CeuI* and *PI-SceI* (New England Biolabs). Complete virions were generated by Travis Webber following standard adenovirus production methods involving HEK293 cells to eventually produce Ad ARX vector concentrates (1×10^7 PFU/ml) used in future studies. Control Ad eGFP virions (1×10^9 PFU/ml) (CMV promoter), similar to those used in Chapter 5.2, were a kind gift from Dr. P. Robbins and were similarly amplified and used alongside Ad ARX.

Adenoviral infection of differentiating hESCs (wild type and ARX knockout) occurred on days 13 and 19 of differentiation in the standard culture media of the day over 24 hours at a MOI of 2 based on a cell count of 1×10^6 cells per well. Expression of eGFP was visualized as previously described in Chapter 5.2. Transgene delivery efficiency was assessed by flow cytometry of eGFP 72 hours after infection. Briefly, cells were dissociated to single cells with Accutase (15 minutes at 37°C, 5% CO_2), washed twice and resuspended in PBS + 2% FBS, and assayed (N = 3) using a LSRII cytometer (BD Biosciences) and FlowJo Software (Tree Star). eGFP positive cells were defined as having an intensity greater than 99.5% of a non infected cell sample.

Quantitative reverse transcriptase PCR

At days 17 and 26 of culture, cell sheets were manually detached from the plate bottom by scraping in the absence of enzymes. Cell samples were washed once in PBS, centrifuged, and the supernatant was discarded before freezing in liquid nitrogen and storage

at -80°C. These samples were used in RNA isolation, cDNA synthesis, and RT-qPCR as previously described in Chapter 4.2 (4) or in the preparation of cell lysates for total protein content analysis. Primers for RT-qPCR performed in this chapter can be found in Table 6.1. All RT-qPCR reactions were assessed in technical duplicate and 3-4 biological replicates. Gene expression was normalized to HPRT then to a reference sample of pooled adult human islet cDNA. Data were quantified by one-way ANOVA with Bonferroni post-hoc tests used to compare like genotypes over time or unlike genotypes at given time points ($P<0.05$ was considered significant).

Table 6.1 Sequences of primers used in RT-qPCR in chapter 6

Gene Name	Gene Accession	Product Size (bp)	Primer Sequence Forward / Reverse 5'→3'	Reference
HNF4a	NM_000457.4	212	TTGCCAACACAATGCCCACT GATAACTTCCTGCTTGGTGATGGTCG	
PROX1	NM_001270616.1	159	GTACGCACGTCAAGCCATCA CGTAATGTGATCTGAGCAACTTCCAG	
FOXA2	NM_021784.4	89	GGGAGCGGTGAAGATGGA TCATGTTGCTCACGGAGGAGTA	(103)
SOX9	NM_000346.3	198	CCAGAATTCCCTTTGGACATTTGTG CTGCTCCATTTAGCCAAGGTTG	
MNX1	NM_005515.3	115	TCGCTCATGCTCACCGAGA CCTTCTGTTTCTCCGCTTCCT	(4)
PDX1	NM_000209	178	CGTCCAGCTGCCTTTCCCAT CCGTGAGATGTACTTGTTGAATAGGA	(2)
NKX6.1	NM_006168	186	GCCCGCCCTGGAGGGACGCA ACGAATAGGCCAAACGAGCCC	(2)
NGN3	NM_020999	286	AGACGACGCGAAGCTCACC AAGCCAGACTGCCTGGGCT	(4)
PAX4	NM_006193	169	AGCAGAGGCACTGGAGAAAGAGTT CAGCTGCATTTCCCACTTGAGCTT	(2)
ARX	NM_139058.2	141	CTGCTGAAACGCAAACAGAGGC CTCGGTCAAGTCCAGCCTCATG	(4)
NKX2.2	NM_002509	221	CTTCTACGACAGCAGCGACAACCCG CCTTGGAGAAAAGCACTCGCCGCTTT	(2)
ISL1	NM_002202	200	GAGCAGCGGCTCTTTCAGC CCGCAACCAACACATAGGGAAATCAG	
PAX6	NM_000280	130	AACCAATTCCACAACCCACCACAC TTATTTGCCATGGTGAAGCTGGGC	
IRX2	NM_033267.4	153	CGGCTACGAGCCCAAGAAAG GCAAGTTGGTGCTGGGAGG	
HHEX	NM_002729.4	198	CATGTTCAGAAAACTGGATTTAGGAATAATGT CCTAAGAGCAGTACATAAACTATTTGTTAAGTC	
SOX4	NM_003107.2	159	CGTTCTCGTCGTCGGATCAA CAACAACATCAATAACAACAATCAACAGG	
NEUROD1	NM_002500.2	146	GCCCCAGGGTTATGAGACTAT GAGAACTGAGACACTCGTCTGT	(4)
MAFB	NM_005461.3	146	TATAAACGCGTCCAGCAGAAGC CCGGAGTTGGCGAGTTTCTC	

Gene Name	Gene Accession	Product Size (bp)	Primer Sequence Forward / Reverse 5'→3'	Reference
MAFA	NM_201589	195	CTTCAGCAAGGAGGAGGTCA TTGTACAGGTCCCGCTCTTT	(4)
PREP1 (PKNOX1)	NM_004571.3	161	GGCTACACAGACATTAAGTATAGACAGC GCTTGTCCACATCCATCGGG	
PBX	NM_002585.3	229	TTAAACTGCCACAGAATGAAGCCT AGTTGTCTGAACCTGCCCCT	
PCSK1	NM_000439	117	AAGCAAACCCAAATCTCACCTGGC TCACCATCAAGCCTGCTCCATTCT	
PCSK2	NM_002594	162	AAGATGGCTTTGCAGCAGGAAGGA AGCCACATTCAAATCAAGGCCAGG	
Insulin	NM_000207.2	245	AGCCTTTGTGAACCAACACC GCTGGTAGAGGGAGCAGATG	(158)
Glucagon	NM_002054.4	275	CATTCACAGGGCACATTCAC CGGCCAAGTTCTTCAACAAT	(158)
Somatostatin	NM_001048.3	126	AGCTGCTGTCTGAACCCAAC CCATAGCCGGGTTTGAGTTA	(158)
Pancreatic Polypeptide	NM_002722.3	180	ACCTGCGTGGCTCTGTTACT CAGCGTGTCCTCTTTGTGTC	(158)
Ghrelin	NM_016362.3	156	AACACCAGAGAGTCCAGCA CAACATCAAAGGGGGCGTT	
HPRT	NM_000194.2	148	TGTTGTAGGATATGCCCTTGACTAT GCGATGTCAATAGGACTCCAGA	(4)

Immunocytochemistry

Various pancreatic tissue samples or differentiated hESCs were immunostained as 5 μm paraffin sections as previously described (4, 198). Briefly after xylene/ethanol step gradient de-waxing and rehydration, heat induced epitope retrieval was performed (10 mM sodium citrate, pH 6.0, 0.05% Tween-20, 95°C, 15 minutes), followed by a 5 minute wash in flowing cold tap water, then 5 minutes shaking in double distilled water and 10 minutes in PBS. Subsequently slides were blocked with Dako serum-free protein block (Dako Canada Inc, Burlington, ON, Canada) for 15 minutes at room temperature, followed by primary antibodies (see Table 6.2 for dilutions) diluted in antibody diluent (Dako) overnight at 4°C. 16-24 hours later, primary antibodies were washed off by 3 successive 10 minute shaking incubations in PBS at room temperature followed by 1 hour room temperature incubation with secondary antibodies (1:1000, Alexafluor-488, -555, -647, Invitrogen). After 3 washes in PBS, slides were mounted in Vectashield hardset mounting medium containing DAPI (4', 6-diamidino-2-phenylindole) (Vector Laboratories, Burlington, ON, Canada). Images for all in-well and slide-based immunofluorescence were captured using an ImageXpress Micro™ automated microscope and associated MetaXpress software (Molecular Devices). Single cell quantification of immunoreactive positive cells was performed using MetaXpress software

and associated Multi-Wavelength-Cell-Scoring module, which allows unbiased nuclear and cytoplasmic scoring of cells using user-defined intensity thresholds in a nucleocentric manner. All quantification was performed on 3-4 biological replicates. Data are reported as mean ± standard error of the mean with significance reported as $P< 0.05$ based on one-way ANOVA with Bonferroni post-hoc analysis.

Table 6.2 Antibodies used in immunocytochemistry in chapter 6

Gene Name	Host Species	Supplier / Catalogue number	Staining Method	Dilution	Antigen Retrieval
CXCR4	Mouse IgG2A-PE	R&D Systems FAB170P	Fixed cell flow	1:50	None
PDX1	Mouse IgG1k-PE	BD Biosciences 562161	Fixed cell flow	1:50	None
NKX6.1	Mouse	DHSB F55A12	Fixed cell flow	1:50	None
OCT4	Goat	R&D Systems AF1759	4% PFA fixed monolayer	1:500	None
SSEA3	Rat IgM	R&D Systems MAB1434	4% PFA fixed monolayer	1:250	None
Insulin	Guinea Pig	Sigma I8510	4% PFA fixed monolayer	1:500	None
Glucagon	Rabbit	Cell Signalling 8233P	4% PFA fixed monolayer	1:250	None
Somatostatin	Mouse	BCBC AB1985	4% PFA fixed monolayer	1:500	None
CK19	Mouse	Dako Cytomation M0888	Slide	1:100	HIER
Chromogranin A	Sheep	Biomol International CA1128	Slide	1:200	HIER
ARX	Rabbit	Dr. P. Collombat Gift	Slide	1:500	HIER
PDX1	Guinea Pig	Abcam Ab47308	Slide	1:1000	HIER
PDX1	Rabbit	Dr. J. Habener Gift	Slide	1:1000	HIER
NKX6.1	Rabbit	Dr. A. Rezania Gift	Slide	1:500	HIER
PCNA	Mouse	BD Biosciences 610665	Slide	1:100	HIER
Insulin	Guinea Pig	Sigma I8510	Slide	1:1000	HIER
Glucagon	Rabbit	Cell Signalling 8233P	Slide	1:500	HIER
Somatostatin	Mouse	BCBC AB1985	Slide	1:1000	HIER
Somatostatin	Rabbit	Sigma HPA019472	Slide	1:1000	HIER
Ghrelin	Rabbit	BioVision 5991-100	Slide	1:200	HIER
Pancreatic	Goat	R&D Systems	Slide	1:200	HIER

Gene Name	Host Species	Supplier / Catalogue number	Staining Method	Dilution	Antigen Retrieval
Polypeptide		AF6297			
NKX2.2	Mouse	DHSB 74.5A5	Slide	1:100	HIER
PAX6	Rabbit	Covance PRB-278P	Slide	1:250	HIER
ISL1	Goat	R&D Systems AF1837	Slide	1:25	HIER
PREP1 (PKNOX1)	Rabbit	Santa Cruz SC-6245	Slide	1:500	HIER
PBX1a/1b	Rabbit	Cell Signalling 4342	Slide	1:500	HIER
PC1/3	Rabbit	Lakshmi Devi Gift	Slide	1:500	HIER
PC2	Rabbit	Affinity BioReagents PA1-058	Slide	1:500	HIER
C-peptide	Guinea Pig	Abcam Ab30477	Slide	1:100	HIER
eGFP	Mouse	Clontech 632375	Slide	1:500	HIER

HIER (heat induced epitope retrieval): 15 minutes at 95°C in 10 mM Citrate buffer with 0.05% Tween-20 pH 6.0.

Slide: PFA fixed, paraffin section of agarose embedded cell pellet or pancreatic tissue

BCBC (Beta Cell Biology Consortium)

DHSB (Developmental Studies Hybridoma Bank), University of Iowa

Radioimmunoassay and Enzyme-linked Immunoassay

Glucagon and C-peptide were assayed from static 24-hour culture media, 1-hour stimulated secretion media and total protein lysate samples according to recommended protocols, but using half volumes for all components (C-peptide; HCP-20K, glucagon; GL-32K, both Millipore). Somatostatin levels were quantified from the same sample set as above using and enzyme-linked immunoassay (EK-060-03, Phoenix Pharmaceuticals Inc., Burlingame, CA, USA). Total protein samples were prepared as a previously frozen cell pellet from approximately one half of a 12-well plate thawed in 250 µl of RIPA lysis buffer (50 mM Tris HCl pH 7.5, 150 mM NaCl, 1% NP-40, 0.5 % sodium deoxycholate, 0.1 % SDS, 1 x protease inhibitor cocktail (P8340), 50 ng/ml DNAse and RNAse) (All Sigma) followed by vortexing for 30 seconds, clarification by centrifugation and quantification of total protein content by BCA assay (Pierce Biotechnology, Rockford, IL, USA) following manufacturer recommended protocols for the microplate assay modifications.

Tissue Samples

Human fetal pancreatic tissue was provided by Dr. R. Wang according to protocols approved by the Health Sciences Research Ethics Board at the University of Western Ontario. XLAG pancreatic tissue and age-matched control pancreatic tissue was provided by Drs. M. Itoh, M. Hayashi, R. Miyata, and T. Akashi, as previously described (252, 254). Adult human pancreatic tissue and isolated islets were provided by Drs. G. Warnock and Z. Ao of the Irving K. Barber Human Islet Isolation Laboratory in Vancouver BC. *Arx* knockout and wild type E18.5 murine pancreata were provided by Dr. P. Collombat (University of Nice Sophia Antipolis, UFR Sciences, Nice, France).

Cell Transplantation and *in vivo* Maturation

Wild type and ARX knockout hESCs were differentiated to day 17 of culture as described above. To form cell clusters amenable to kidney capsule transplantation, intact cell sheets were partially enzymatically detached in Accutase (1.5-2.5 minutes, 37°C), and were then promptly aspirated and blocked with complete media containing BSA. Loosened cell sheets were then mechanically scraped off the bottom of the culture plate (6-well) using a 5 ml serologcial pipette (~20 X and Y motions) in the 2.5 ml volume followed by two passes through a P1000 tip. Detached, sheared cells were cultured (37°C, 5% CO_2) in 2.5 ml of day 17 media per well of an Ultra-low attachment plate (3471, Corning Incorporated, Corning, NY, USA) on a low speed orbital shaker (MaxQ 2000, Thermo) at 95 rpm. The morning of transplantation, cell clusters were collected, pooled within genotypes (ARX knockout vs WT), and redistributed in 6-well plates at a density of ~2 x 10^6 cells per well (one well transplanted per mouse). Clusters were transplanted under the left kidney capsule following established methods (125, 127) by Dr. Majid Mojibian and Shannon O'Dwyer. A total of 8 ARX knockout, 6 wild type, and 4 sham transplanted SCID-beige mice were subsequently monitored biweekly for changes in body weight and blood glucose. At 4, 8, 12 and 16 weeks post transplant, mice were fasted overnight and subjected to a meal challenge involving *ad libitum* feeding of standard diet for 45 minutes. Blood glucose was measured and heparinized plasma samples were collected at time 0 and 45 minutes of feeding to monitor the human C-peptide secretion from the transplanted grafts. C-peptide levels were measured by a human C-peptide ELISA (80-CPTHU-E10, Alpco Diagnostics, Salem, NH, USA). At

either 4 or 16 weeks post transplant, graft bearing kidneys were removed and fixed in 4% PFA overnight followed by dehydration for 7 days in 70% ethanol and processing as paraffin embedded tissue sections for immunohistochemical analysis.

6.3 Results

Generation and Validation of ARX knockout hESCs

The human *ARX* gene is located on the X chromosome and has five exons, which together encode a number of protein domains of the transcription factor. These domains include a series of clinically relevant poly-alanine repeats in exon 2 and 4 whose expansion is associated with multiple seizure phenotypes and Partington syndrome in humans and in mice is additionally linked to reduced α-cell specification and α-cell loss due to apoptosis (251, 255). Functional loss of the DNA binding prd-like homeodomain encoded from exons 2-4, most often due to protein truncation mutations, is associated with multiple brain malformaitons and XLAG in humans (251). To examine the role of ARX in pancreatic endocrine differentiation, we generated two independent ARX knockout hESC clones with genomic deletions in exon 1 such that all protein components from exons 2-5 would be lost (Figure 6.1A). This was done by targeted genomic editing using a zinc-finger nuclease (ZFN) pair that stimulated double stranded DNA breaks in the single copy of ARX in male (XY) CA1S hESCs. After allowing non-homologous end joining to repair the DNA damage, low frequency genomic deletion mutants were screened by a simple PCR assay with primers spanning the ZFN cut site. Of the 576 wells seeded for dilution cloning of ZFN targeted hESCs, 11% of the wells were manually identified as having an undifferentiated morphology and originating from a clonal population by daily observation of cultures. Of these clones, three were identified as containing deletions at the ARX locus on the X chromosome including clone 1 (C1) and clone 2 (C2) which contained 23 and 41 base pair deletions respectively (Figure 6.1B). The third ARX ko deletion clone contained a complex genomic inversion and was not examined further (data not shown). Mutations from clones 1 and 2 were confirmed by sequencing and found to cause frameshift mutations that resulted in a premature stop codon and an ARX protein that lacked all domains from exons 2-5. Similar to wild type hESCs, both ARX knockout hESC clones maintained expression of the pluripotency associated factors OCT4 and SSEA3 suggesting that the genomic editing and

cloning process did not compromise pluripotency of the clones (Figure 6.1C). To validate the loss of ARX protein expression in the ARX knockout clones, we applied multistage pancreatic endocrine differentiation protocol previously described by Bruin et al (Figure 6.2A) (210). At day 26 of the differentiation protocol, cell samples were stained for the pan-endocrine marker chromogranin A and ARX. Differentiated wild type cells expressed ARX in both chromogranin A positive and negative populations, similar to human fetal pancreatic tissue controls, while ARX knockout clones did not show ARX immunoreactivity (Figure 6.1D-E).

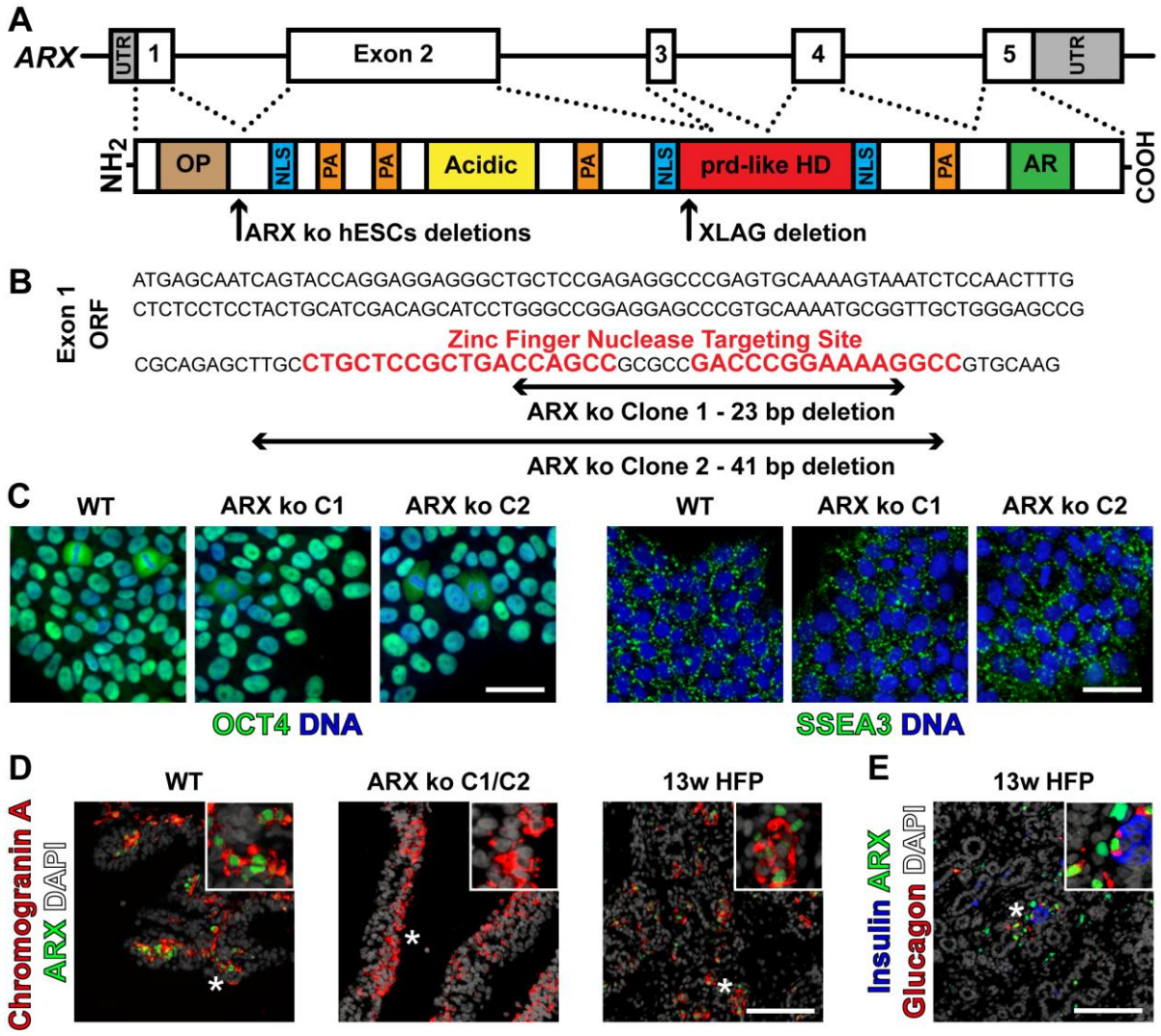

Figure 6.1. Generation of ARX knockout hESCs

(A) Schematic representation of the *ARX* gene and contained exons. Approximate protein domains and important functional regions of ARX including: octapeptide domain (OP), nuclear localization signals (NLS), poly-alanine expansion repeats (PA), Acidic domain (Acidic), prd-like homeodomain (prd-like HD), and

Aristaless domain / C-peptide (AR). Approximate location of zinc finger nuclease mediated genomic editing induced deletion mutations in ARX knockout (ARX ko) hESCs and naturally occurring mutation of the XLAG pancreatic sample used in this study are also depicted. (B) Specific nucleotide deletions within exon 1 of ARX knockout hESCs clones resulted in a frameshift mutation and premature stop codons in ARX. (C) Wild type (WT) and ARX knockout clones 1 and 2 immunostained for pluripotency associated markers OCT4 (green) or SSEA3 (green) and counterstained for DNA with Hoechst 33342. Scale bar is 50 μm. (D) Immunostaining of ARX protein in agarose-embedded sections of 26-day differentiated wild type or ARX knockout pancreatic cells as well as human fetal pancreatic tissue at 13 weeks of gestation (13w HFP); ARX (green), chromogranin A (red), and DAPI (white). (E) 13w HFP immunostained for ARX (green), insulin (blue), glucagon (red), and DAPI (white) showing natural ARX expression patterns. Inset is a ~3x enlarged portion from the region indicated by the star. Scale bar for D and E is 100 μm.

Pancreatic Differentiation of ARX knockout hESCs

Given the numerous developmental stages that must be efficiently passed in order to achieve the formation of hormone positive cells, we began the characterization of our ARX knockout clones by monitoring key checkpoints during differentiation by flow cytometry. Similar to wild type hESCs, both ARX knockout clones efficiently formed CXCR4-positive definitive endoderm cells (wild type: 94±1%, ARX knockout C1: 95±1%, ARX knockout C2: 95±2%) and PDX1-positive foregut endoderm (wild type: 91±3%, ARX knockout C1: 94±3%, ARX knockout C2: 96±1%). However, ARX knockout clones expressed a greater amount of NKX6.1-positive pancreatic progenitors compared to wild type (wild type: 49±3%, ARX knockout C1: 70±2%, ARX knockout C2: 66±4%, $p<0.05$) (Figure 6.2B). Similar to wild type cells and 13 week human fetal pancreatic tissue, ARX knockout pancreatic progenitors co-expressed PDX1 and NKX6.1, which were present throughout the differentiation timeline from day 14 to day 26 (Figure 6.3A and B). In both wild type and ARX knockout cells, a number of markers of early pancreatogenesis were decreased with culture maturation from day 17 to 26 (*HNF4a*, *PROX1*, *FOXA2*, *PDX1*). However, in contrast to wild type cells, ARX knockout cells had significantly elevated *NKX6.1* expression at day 17, suggesting a significant build up of *NKX6.1* positive progenitors (Figure 6.3C). Similar to 13 week human fetal pancreatic samples NKX6.1 positive progenitors, but not chromogranin A positive endocrine cells, were proliferative as determined by PCNA staining in both wild type and ARX knockout cell populations (Figure 6.3D). Taken together, these data suggest that ARX knockout does not hinder efficient germ layer specification, gut tube regionalization, and induction of pancreatic progenitors. The ARX knockout cells induce significantly increased numbers of NKX6.1 positive progenitors, which remain as a distinct

population of proliferative cells alongside the developing endocrine cells through to the end of the differentiation protocol.

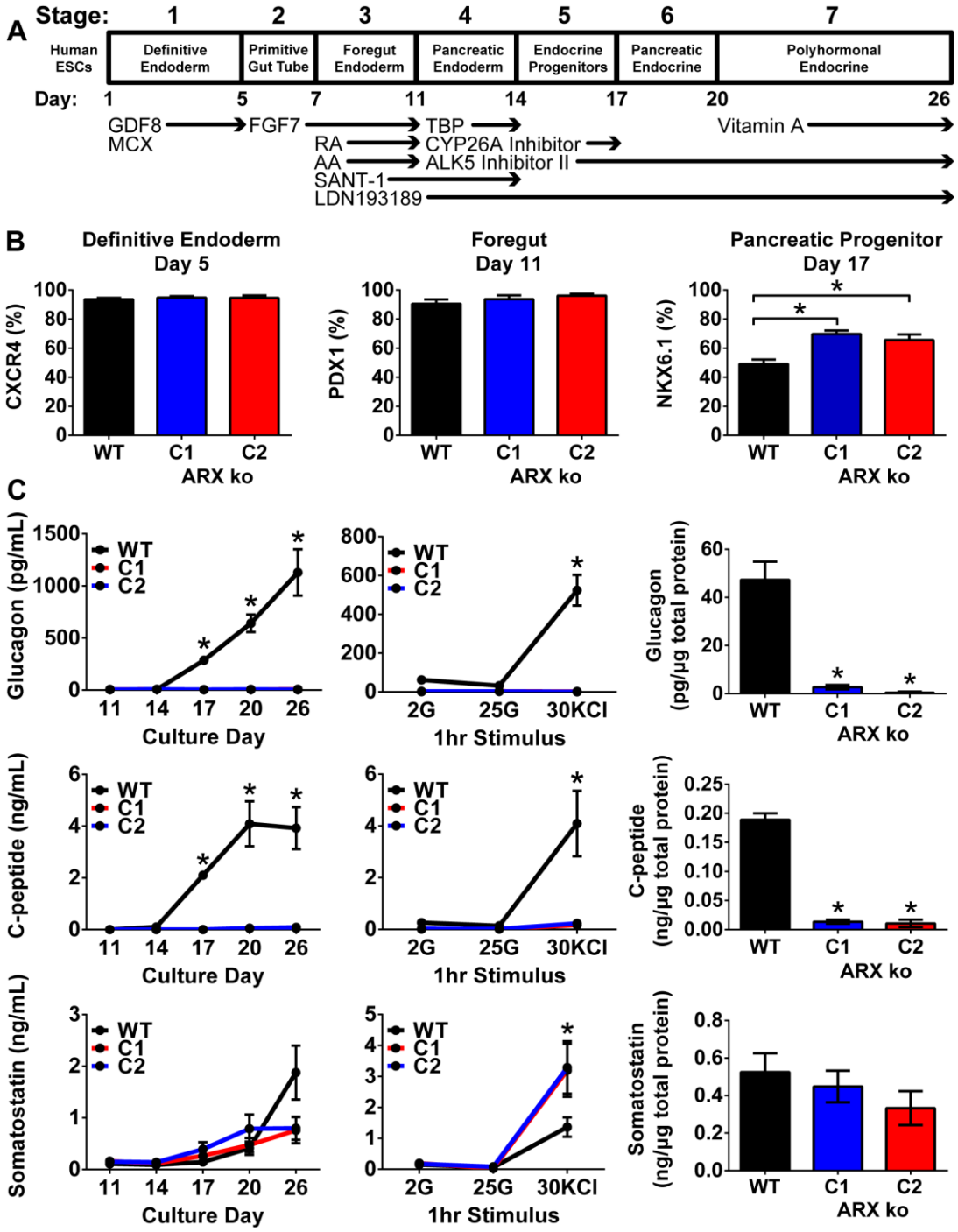

Figure 6.2. Pancreatic differentiation of ARX knockout hESCs

(A) Schematic representation of the *in vitro* pancreatic endocrine differentiation method as previously described by Bruin et al. (2014). (B) Flow cytometry of wild type (WT), ARX knockout (ARX ko) clone 1 (C1), and ARX knockout clone 2 (C2) at the end of definitive endoderm (CXCR4), foregut (PDX1), and pancreatic

progenitors (NKX6.1). (C) Media composition and cellular content analysis of differentiating wild type and ARX knockout hESCs. Glucagon, C-peptide and somatostatin were assayed from un-stimulated media samples collected from days 11 to 26 (left column); a static sequential glucose stimulated hormone release assay was performed on day 24 of culture which included 1 hour treatments of low glucose (2 mM), high glucose (25 mM), and potassium chloride (30 mM). Right column; total hormone content measurements of day 26 cell lysate samples normalized for total protein content. (N = 4 independent differentiation trials for all data sets). * indicates $p < 0.05$ wild type vs ARX knockout C1 and C2 at indicated time point or treatment based on a one-way ANOVA and Bonferroni post hoc test.

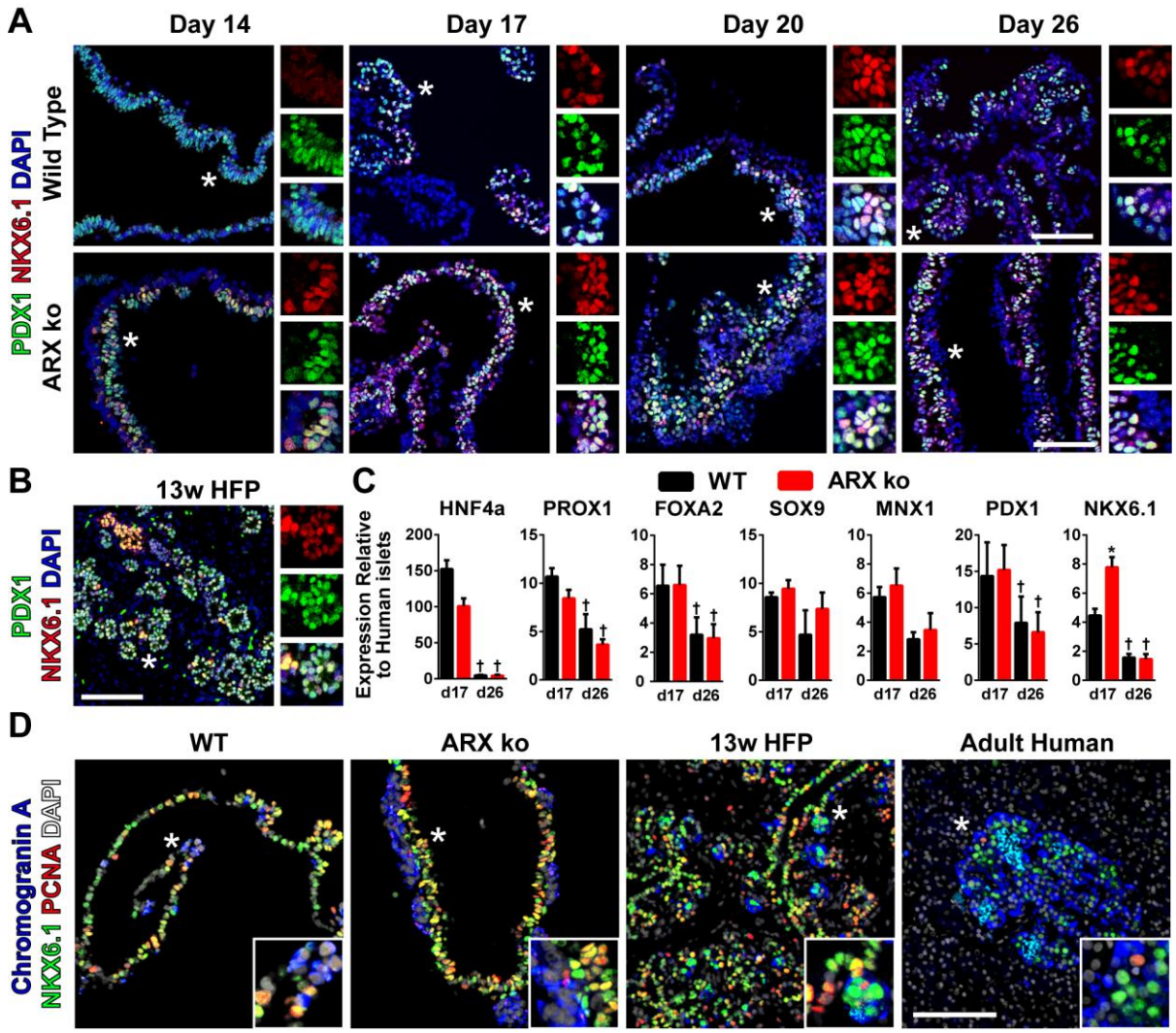

Figure 6.3. Pancreatic progenitors in ARX knockout hESCs

(A) Immunostaining of PDX1 (green) and NKX6.1 (red) in agarose-embedded wild type (WT) and ARX knockout (ARX ko) cell sheets from day 14, 17, 20, and 26 of culture. * indicates region of enlargement (right) which includes individual red and green channels and overlay with DAPI (blue) showing coexpression patterns. (B) Immunostaining of 13 week human fetal pancreatic tissue the same as A. (C) RT-qPCR of day 17 and day 26 whole population samples examining the expression of transcription factors believed to be involved in pancreatic progenitor induction. Wild type (black bars) and ARX knockout (red bars) cell samples relative to adult human islets expression levels. † indicates $p < 0.05$ within the genotype over time, * indicates $p < 0.05$ wild type vs ARX knockout at given culture day, N = 4 per group. (D) Immunostaining of NKX6.1 (green), proliferating cell nuclear antigen (PCNA, red), and chromogranin A (blue) in 26 day differentiated wild type

and ARX knockout cells, 13 week human fetal pancreatic tissue, and adult human pancreatic tissue. Inset is a ~3x enlarged portion from the region indicated by the star. Scale bar is 100 μm for all panels.

As previously described for this differentiation protocol, we expected early hormone positive cells to be formed from day 17 of culture onward (210). To account for potentially accelerated developmental timelines based on ARX knockout cultures we began tracking basal hormone release at day 11 (foregut progenitors). We also tracked the stimulated release (day 24) and total content (day 26) of glucagon, C-peptide (marker of processed insulin), and somatostatin in these cultures (Figure 6.2C). ARX knockout cells released significantly less glucagon and C-peptide over the course of culture and in response to a depolarizing potassium chloride stimulus at day 24. These findings are in line with the reduced glucagon and C-peptide content of cell lysates measured on day 26. Despite having a similar degree of basal secretion and similar levels of total somatostatin, ARX knockout cells released significantly more somatostatin upon stimulation by 30 mM KCl compared to WT. Taken together, these data suggest that the formation of glucagon and insulin positive lineages was partially disrupted in ARX knockout cells, though the somatostatin positive population to remain unchanged.

Pancreatic Endocrine Differentiation of ARX knockout cells

In order to better understand what may be occurring during the formation of pancreatic endocrine cells in the ARX knockout hESCs, we examined human pancreatic tissue samples from a 16-month old patient with XLAG (*ARX* deficiency) (252, 254) and relevant controls. Immunostaining of 16 month old control, 13 week human fetal pancreatic tissue, and adult human pancreatic tissue revealed the presence of unihormonal insulin, glucagon, somatostatin, pancreatic polypeptide and ghrelin positive cells arranged as expected as developing or fully formed islets. Close examination of XLAG pancreatic tissue revealed an absence of glucagon and pancreatic polypeptide positive cells with an approximately normal proportion of insulin, somatostatin, and ghrelin cells compared to age matched control pancreata (Figure 6.4).

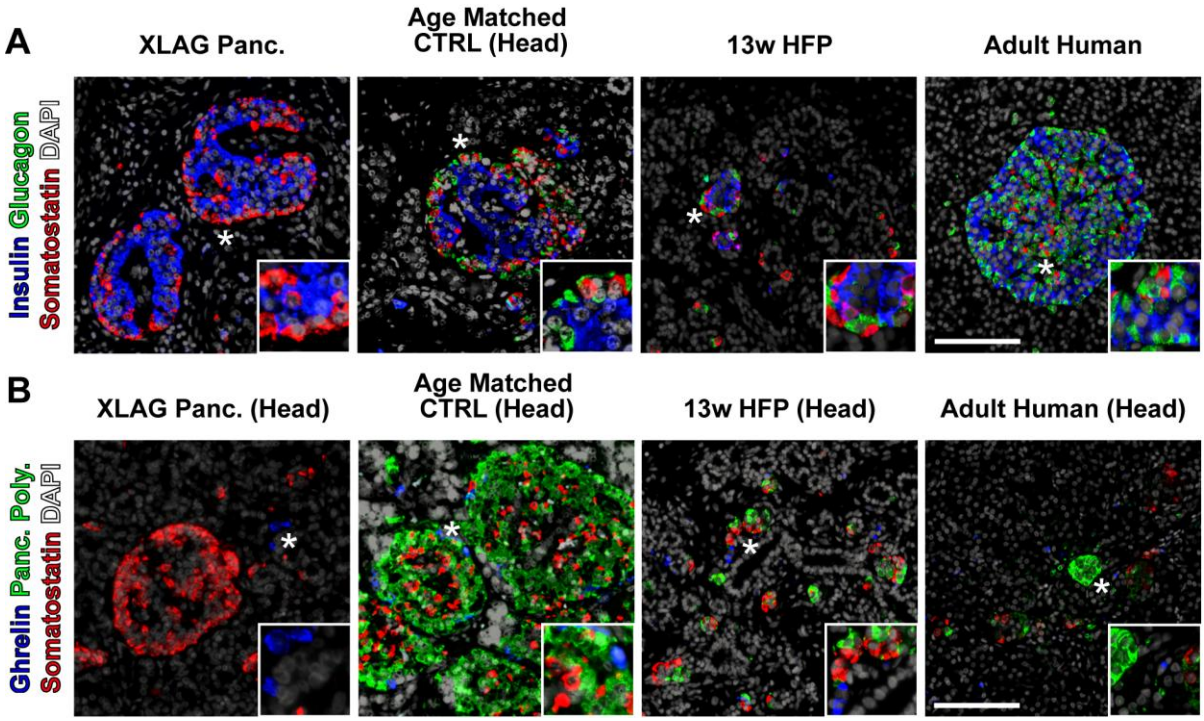

Figure 6.4. XLAG pancreatic endocrine profile

16-month old XLAG (ARX knockout) pancreatic tissue, age-matched control pancreatic tissue, 13w human fetal pancreatic tissue, and adult human pancreatic tissue were immunostained for insulin (blue), glucagon (green), somatostatin (red) and DAPI (white) in (A) and ghrelin (blue), pancreatic polypeptide (green), somatostatin (red) and DAPI (white) in (B). "Head" indicates specific sample from head region of the pancreas. Inset is a ~3x enlarged portion from the region indicated by the star. Scale bar is 100 μm for all panels.

Given that available samples of humans with *ARX* deficiency lack glucagon and pancreatic polypeptide positive cells, we next examined the endocrine subpopulations of wild type and ARX knockout cells. RT-qPCR analysis of day 17 (predominantly pancreatic progenitor cells) and day 26 (progenitors and endocrine cells) samples revealed that ARX knockout cells expressed significantly lower levels of insulin, glucagon, and pancreatic polypeptide with elevated levels of somatostatin and no significant change in ghrelin levels (Figure 6.5A). Immunostaining and single cell analysis of insulin, glucagon, and somatostatin positive cells revealed that compared to wild type cells, ARX knockout cells showed no change in the number of cells positive for any of these three hormones (Figure 6.5B and C). Closer examination of endocrine cell populations revealed that wild type cells were a mixture of polyhormonal cells, however ARX knockout clones were composed primarily of somatostatin positive cells that did not express other hormones (Figure 6.5D). Furthermore, the total number of somatostatin positive cells regardless of copositivity

appeared to be higher in ARX knockout cells compared to wild type cells (wild type: 71±4%, ARX knockout C1: 94±1% ARX knockout C2: 94±1%, $p<0.05$). The generation of unihormonal somatostatin positive cells was associated with a modest decrease in the total number of insulin-positive cell types (wild type: 78±1%, ARX knockout C1: 27±4%, ARX knockout C2: 24±2%, $p<0.05$) and a dramatic decrease in glucagon-positive cell types (wild type: 40±8%, ARX knockout C1: 4±1%, ARX knockout C2: 5±1%, $p<0.05$). ARX knockout cells did not have elevated numbers of ghrelin positive cells (with or without coexpression of somatostatin), nor did they express significant amounts of pancreatic polypeptide (Figure 6.5E-G), which was in line with our RT-qPCR results (Figure 6.5A). Staining of human XLAG samples revealed a limited amount of glucagon and pancreatic polypeptide positive cells (Figure 6.4), which was also reflected in ARX knockout endocrine cells. However, in contrast to XLAG samples, which had an abundance of insulin positive cells, ARX knockout clones had a decreased number of insulin positive cells. To understand the factors that may be driving the absence of insulin in ARX knockout cells, we next examined the expression a series of transcription factors in day 17 and day 26 differentiated wild type and ARX knockout cells by RT-qPCR and immunocytochemistry.

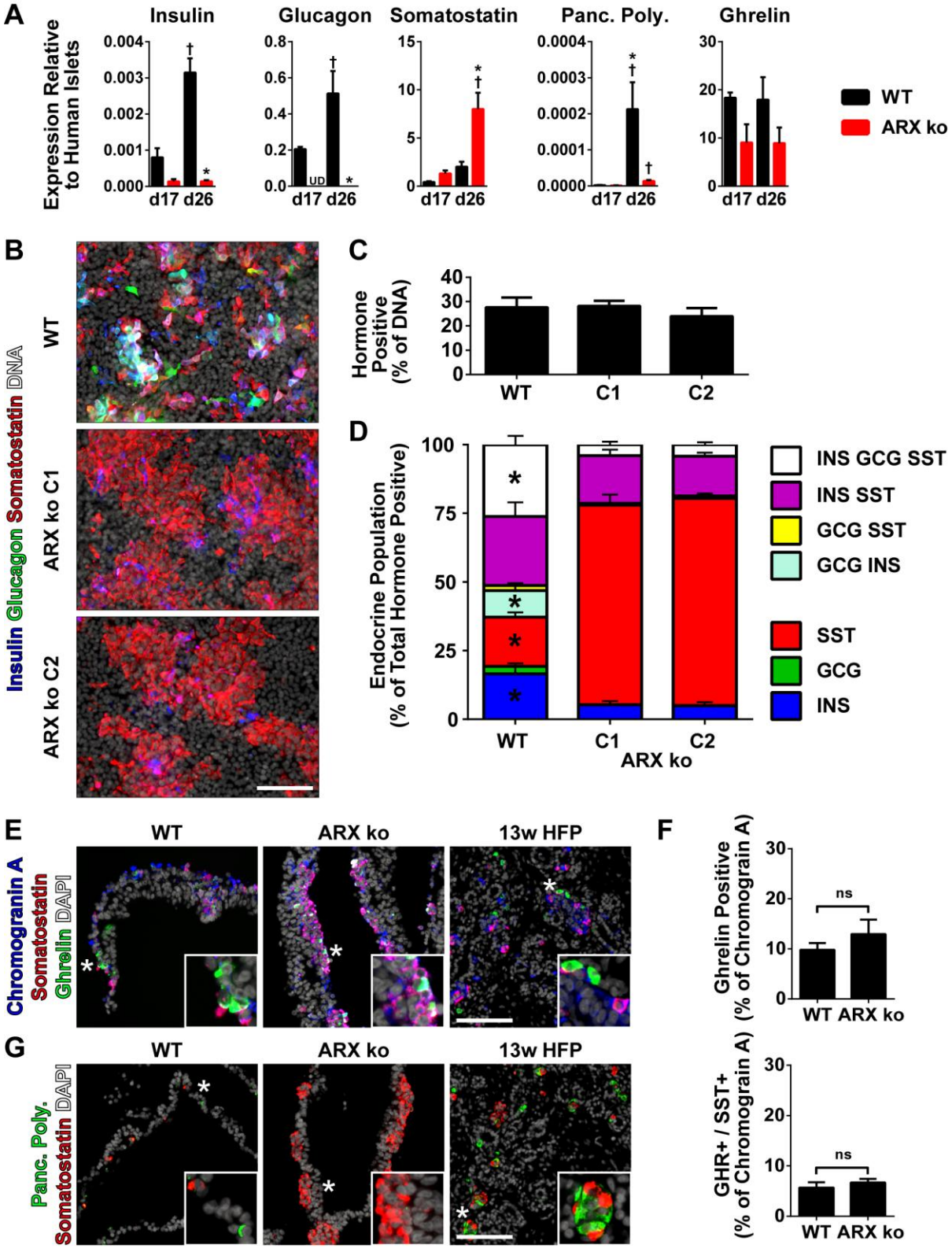

Figure 6.5. Pancreatic endocrine profile of ARX knockout hESCs

(A) RT-qPCR of day 17 and day 26 whole population samples examining the expression of the five major pancreatic hormones in wild type (WT; black bars) and ARX knockout (ARX ko; red bars) relative to adult

human islets expression levels. † indicates $p < 0.05$ within the genotype over time, * indicates $p < 0.05$ wild type vs ARX knockout at given culture day. (B) 26-day differentiated cultures were stained *in situ* for insulin (blue), glucagon (green), somatostatin (red), and nuclei (white). (C) Image based cell counting was performed to determine the number of cells positive for any of the three hormones as a percentage of the total number of nuclei. (D) Single cell pancreatic endocrine population profile as a percentage of the total number of insulin, glucagon and somatostatin positive cells. * indicates significant changes in the population between wild type and ARX knockout (both clones). (E) Immunostaining of 13w HFP and 26-day differentiated wild type and ARX knockout cells for chromogranin A (blue), somatostatin (red), ghrelin (green) and DAPI (white). (F) Single cell quantification of ghrelin positive and ghrelin/somatostatin co-positive cells as a percentage of the total hormone (chromogranin A) positive fraction. (G) Immunostaining of pancreatic polypeptide positive cells in day 26 cultures and 13w HFP with pancreatic polypeptide (green), somatostatin (red) and DAPI counterstain (white). Inset is a ~3x enlarged portion from the region indicated by the star. Scale bar is 100 μm for all panels.

Pancreatic Endocrine Fate Specification of ARX knockout cells

As previously mentioned, other than NKX6.1 levels, markers of pancreatic progenitors were not altered in ARX knockout cells at day 17 of culture. Therefore, we focused our attention on candidate transcription factors implicated in the specification of individual endocrine lineages to explain the relative absence of insulin positive cells. Expression of *NGN3* was unaltered in 26-day differentiated ARX knockout hESCs suggesting that the commitment from progenitor to the endocrine program was maintained. Downstream of NGN3, transcript levels of *PAX4* were elevated in ARX knockout cells, and this correlated with decreased levels of *ARX* transcription. Expression of *NKX2.2*, *ISL1*, and *HHEX* were elevated in ARX knockout cells, while *PAX6* and *IRX2* levels were diminished compared to wild type cells (Figure 6.6A). Other transcription factors including *SOX4*, *NEUROD1* and *MAFB* were unchanged while *MAFA* was unchanged and hardly detected in ARX knockout or wild type cell samples. Focusing on 26-day differentiated cell samples, we examined the expression patterns of a subset of these transcription factors by immunostaining in comparison to 13 week fetal and adult human pancreatic tissue. Similar to adult, fetal and wild type samples, ARX knockout somatostatin positive cells showed prominent nuclear NKX2.2 localization in addition to some hormone negative cells (Figure 6.6B). Interestingly, in contrast PAX6 immunoreactivity was low and cytoplasmic in ARX knockout cells but was predominantly high and nuclear in wild type, fetal and adult samples (Figure 6.6C). Notably in all four sample types, some cytoplasmic PAX6 immunoreactive cells were observed which co-localized with somatostatin but not insulin (Figure 6.6C inset of wild type and human fetal pancreas). PDX1 and NKX6.1 were highly expressed in the nuclei of the pancreatic progenitor population of wild type, ARX knockout, and human fetal

pancreatic tissues with the somatostatin positive cells of the ARX knockout samples expressing weak nuclear PDX1 and no nuclear NKX6.1 (Figure 6.6D and E). Both fetal and adult human samples as well as wild type and ARX knockout cells that were positive for insulin and somatostatin also expressed bright nuclear ISL1 (Figure 6.7A). Similar to human fetal pancreatic samples, the endocrine clusters of ARX knockout cells expressed a pattern of nuclear NKX2.2 and ISL1, while PAX6 immunoreactivity was weak and localized to the cytoplasm (Figure 6.7B). This pattern, observed in human fetal somatostatin positive cells at 13 weeks of gestation and during the development of ARX knockout mice (Figure 6.8), was in contrast to the triple nuclear expression pattern observed in adult human islets (Figure 6.7B). Together, these patterns of transcription factor immunoreactivity suggest a complex interplay between the temporal expression/localization of transcription factors and the specific endocrine cell types that are forming. Given the biased development of ARX knockout hESCs to the formation of somatostatin positive cells, the expression pattern of no NKX6.1, low PDX1, high NKX2.2, high ISL1, and low/cytoplasmic PAX6 seems to be associated with this process. As a similar pattern is observed in E18.5 ARX knockout mice in our hands, and in a subset of developing human endocrine cells, this pattern may represent the natural developmental trajectory of somatostatin cell specification.

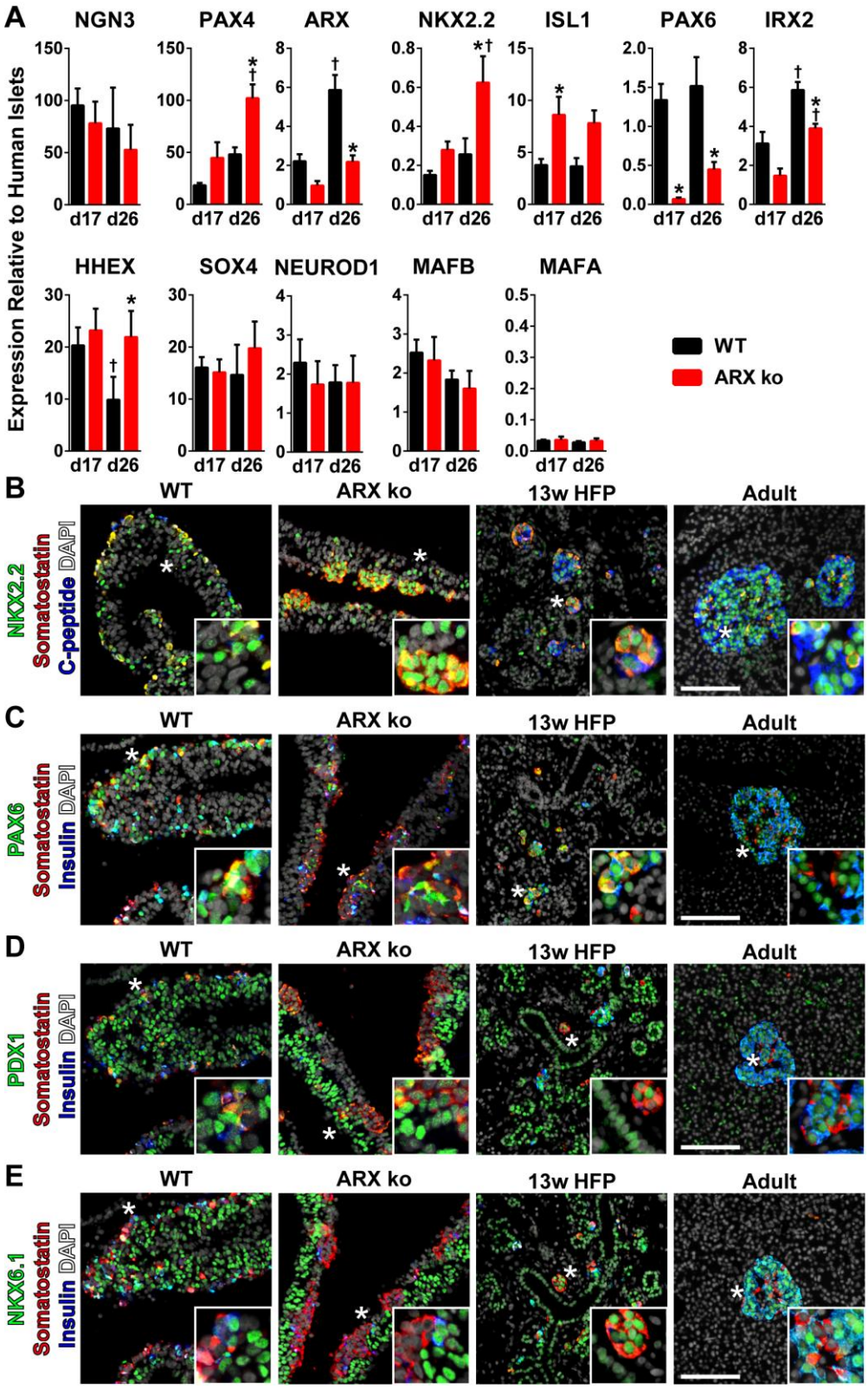

Figure 6.6. Pancreatic fate specification factors in ARX knockout hESCs

(A) RT-qPCR of day 17 and day 26 whole population samples examining the expression of transcription factors believed to be involved in pancreatic endocrine fate specification. Wild type (WT; black bars) and ARX

knockout (ARX ko; red bars) cell samples relative to adult human islets expression levels. † indicates $p < 0.05$ within the genotype over time, * indicates $p < 0.05$ wild type vs ARX knockout at given culture day, N = 4 per group. (B-E) Immunostaining of 26-day differentiated wild type and ARX knockout cells, 13 week human fetal pancreatic tissue and adult human pancreatic tissue. Inset is a ~3x enlarged portion from the region indicated by the star. Scale bar is 100 μm for all panels.

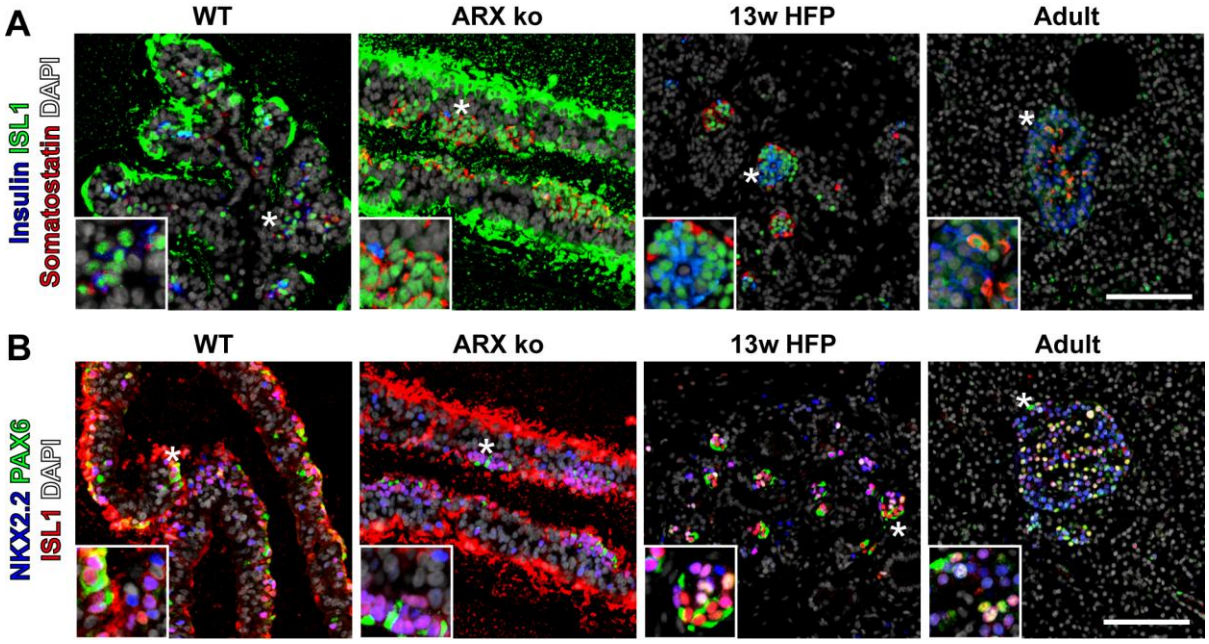

Figure 6.7. Expression of ISL1 in ARX knockout hESCs and human tissues

(A) Immunostaining of ISL1 (green), somatostatin (red), and insulin (blue) in 26 day differentiated wild type (WT) and ARX knockout cells (ARX ko), 13 week human fetal pancreatic tissue, and adult human pancreatic tissue. (B) Immunostaining of PAX6 (green), ISL1 (red), and NKX2.2 (blue) in the same sample series as above. Inset is a ~3x enlarged portion from the region indicated by the star. Scale bar is 100 μm for all panels. Extracellular immunoreactivitity of ISL1 is a staining artifact associated with the agarose which surrounds the embedded cell sheets.

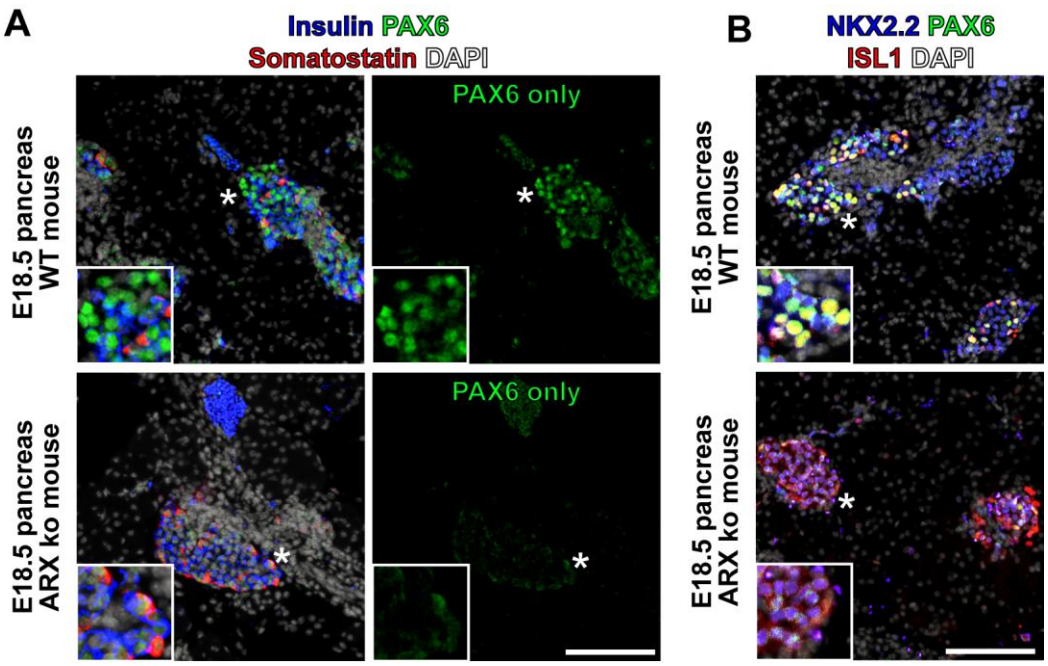

Figure 6.8. Expression of PAX6 in Arx knockout mice

(A) Immunostaining of PAX6 (green), somatostatin (red), and insulin (blue) in ARX knockout (ARX ko) and wild type (WT) E18.5 mouse pancreatic samples. Image on the right shows individual PAX6 channel showing nuclear PAX6 in wild type islet cells and lower levels of PAX6 in ARX knockout tissue. (B) Immunostaining of PAX6 (green), ISL1 (red), and NKX2.2 (blue) in the same samples as in A. Inset is a ~3x enlarged portion from the region indicated by the star. Scale bar is 100 μm for all panels.

As ARX knockout cells were capable of developing into somatostatin positive cells and were able to express and release somatostatin in response to a depolarizing stimulus such as potassium chloride (Figure 6.2C), we were interested to see if factors known to regulate somatostatin transcription were present. Previous studies examining control of the somatostatin promoter have identified a synergistic activation by PDX1, PBX1, and PREP1 to drive somatostatin transcription (256). It was previously established that PDX1 is expressed in wild type and ARX knockout cells (Figure 6.3C and 6.6D), thus we next assessed expression of PREP1 and PBX1 using RT-qPCR and immunostaining in wild type and ARX knockout cells compared to adult human pancreatic tissue. Both *PREP1* and *PBX1* were expressed 2-5 fold higher than adult human islets in wild type and ARX knockout cell samples. In day 26 cell samples, PREP1 immunoreactivity was nuclear and localized to both the pancreatic progenitor and endocrine compartments including somatostatin positive cells (Figure 6.9A). Expression of PREP1 was predominantly localized to islets including somatostatin positive cells. PBX1 localization was more robust in the progenitor

compartment but still weakly positive in somatostatin positive cell clusters of ARX knockout cells, similar to adult human expression patterns (Figure 6.9B). Together these data confirm the presence and localization of PBX1 and PREP1, and suggest their potential synergistic activation, along with PDX-1, of the somatostatin promoter.

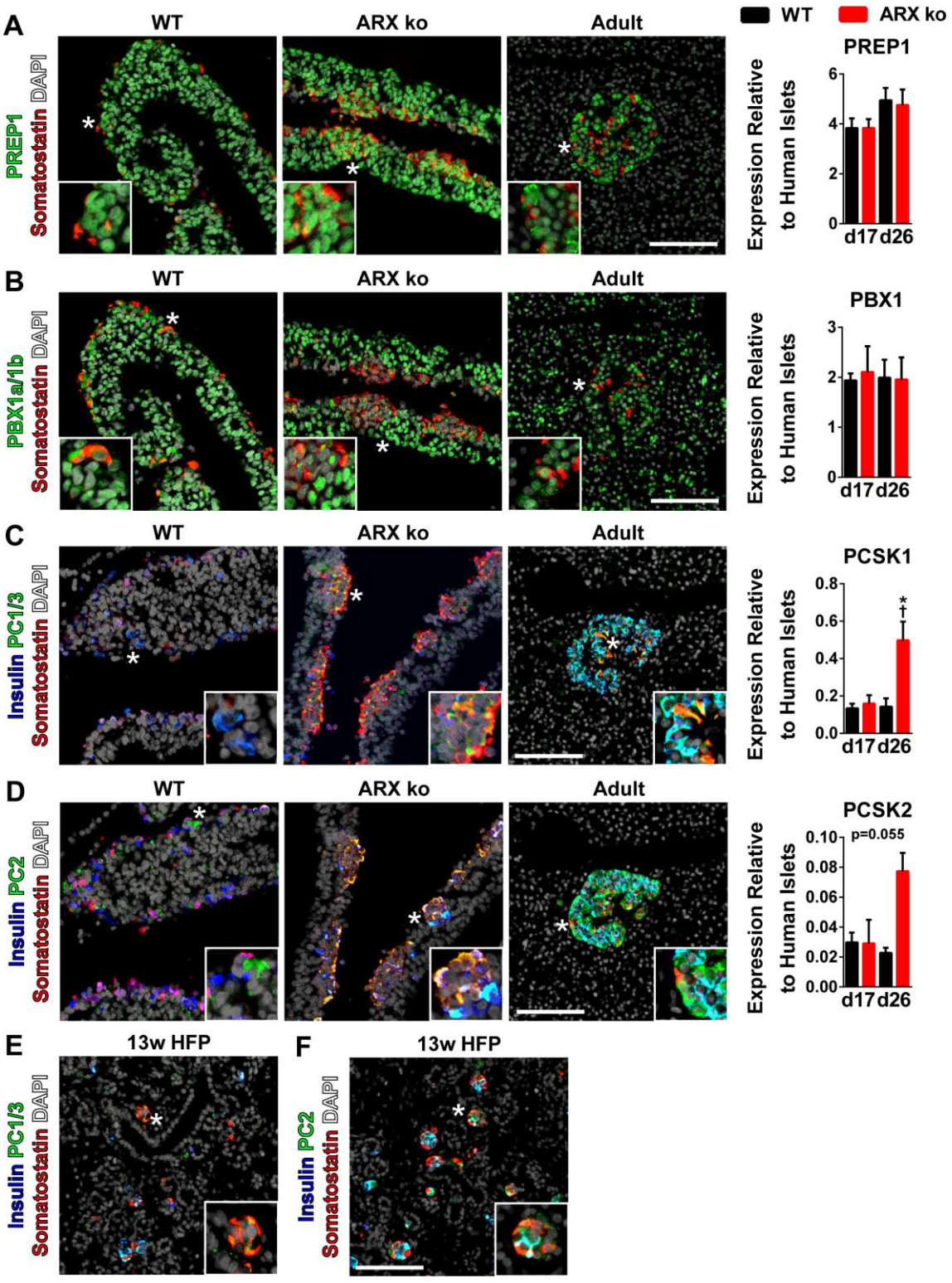

Figure 6.9. Expression of PREP1, PBX1 and processing hormones of somatostatin in ARX knockout hESCs

(A - D) Immunostaining of PREP1, PBX1a/1b, PC1/3, PC2 (all green), somatostatin (red), and insulin (blue) in 26 day differentiated wild type (WT) and ARX knockout (ARX ko) cells, and adult human pancreatic tissue.

RT-qPCR of day 17 and day 26 whole population samples examining the expression of transcription factors believed to be involved expression and processing of somatostatin. Wild type (WT; black bars) and ARX knockout (ARX ko; red bars) cell samples relative to adult human islets expression levels. † indicates $p < 0.05$ within the genotype over time, * indicates $p < 0.05$ wild type vs ARX knockout at given culture day, $N = 4$ per group. (E and F) Immunostaining of 13 week human fetal pancreatic tissue for expression of PC1/3 and PC2 (both green), somatostatin (red), and insulin (blue). DAPI is white in all images. Inset is a ~3x enlarged portion from the region indicated by the star. Scale bar is 100 μm for all panels.

The somatostatin pro-protein is processed by a number of prohormone convertases including PC1/3, PC2, furin, PACE4, and PC5 (257). In the context of the pancreatic δ-cell, the conversion of somatostatin-28 (normally found in the gut) to somatostatin-14, which is generated and released from pancreatic islets, is achieved by activity of PC1/3 and or PC2 (258-260). Based on this information we examined the expression of PC1/3 and PC2 by RT-qPCR and immunostaining. 26-day differentiated ARX knockout cells had elevated transcript levels of *PCSK1* and *PCSK2* compared to wild type cells and immunoreactivity of both proteins was found in both insulin and somatostatin positive cells. This tightly regulated expression of both processing enzymes was also seen in adult human and 13-week human fetal pancreatic tissue (Figure 6.8D-E). Given the expression levels and distribution patterns of these processing enzymes, it is possible that the ARX knockout somatostatin positive cells may be able to generate processed islet specific somatostatin-14.

Transplantation and *in vivo* Development of ARX knockout hESCs

We have observed that ARX knockout hESCs failed to generate the expected numbers of insulin positive cells during *in vitro* development (in contrast to XLAG samples), thus we postulated that one or more signalling factors were missing from our culture system which were present *in vivo*. To test this, we prepared pancreatic progenitor clusters from day 17 differentiated wild type and ARX knockout cells. Before clustering, both cell populations contained NKX6.1 positive pancreatic progenitor epithelial cells (CK19 positive), which were retained through the clustering process (Figure 6.10). This mechanical processing of the cell sheets reduced adherence to various transfer surfaces during the transplantation process under the left kidney capsule of SCID-beige immunocompromised mice. Over the course of 16 weeks of engraftment, bodyweight and 4-hour fasted blood glucose levels were similar among wild type and ARX knockout transplanted mice, and mice that did not receive a transplant (Figure 6.11A). Recovery of grafts 16 weeks post transplant revealed similar

graft size among wild type and ARX knockout transplants (Figure 6.11B). Fast-re-feed meal challenges revealed no change in glucose response or stimulated C-peptide release from either transplanted group compared to the sham operated group. Together, these data suggest that while transplantation was successful, graft maturation in both wild type and ARX knockout cells failed to generate sufficient functional endocrine masses required to impact glycemia.

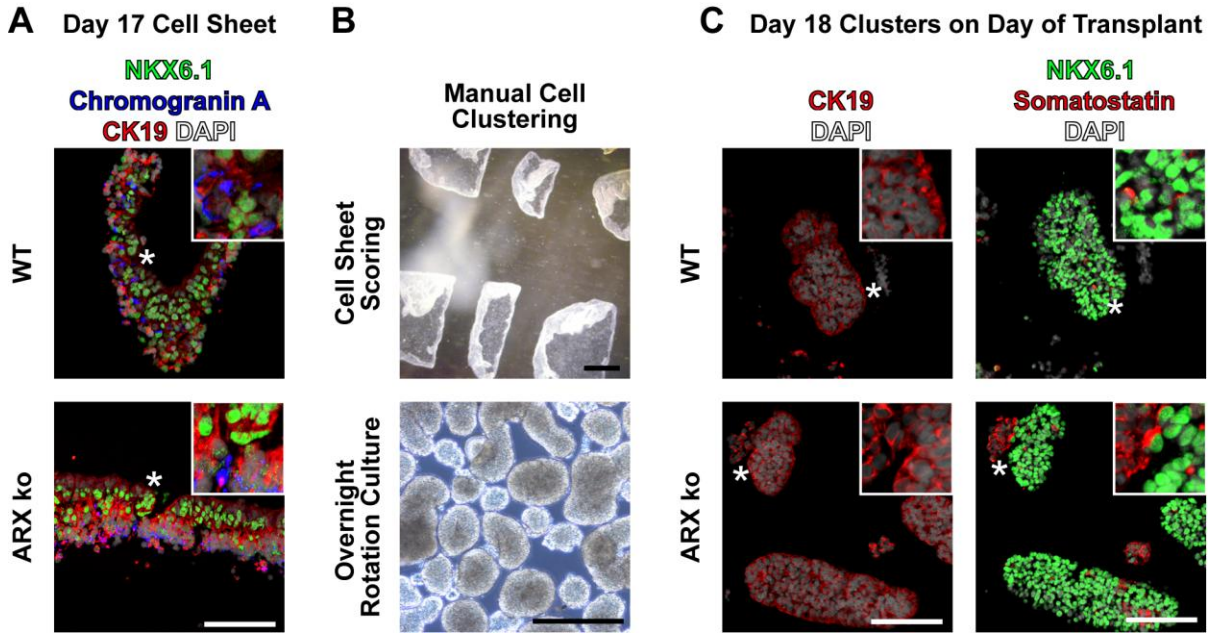

Figure 6.10. Generation of transplantable cell clusters from wild type and ARX knockout pancreatic progenitors

(A) Immunostaining of NKX6.1 (green), CK19 (red, epithelial cells) and chromogranin A (blue) in 17 day differentiated cell sheets. (B) Manual mechanical processing of homogenous cell sheets into smaller tissue sheets followed by dynamic overnight rotational culture generated relatively uniform cell clusters. (C) Wild type (WT) and ARX knockout (ARX ko) cell clusters retain expression of CK19 and NKX6.1 marking pancreatic progenitors as well as early endocrine cells (somatostatin, red). DAPI is white in immunostained images. Inset is a ~3x enlarged portion from the region indicated by the star. Scale bar is 100 μm for panels A and C, and 200 μm for B.

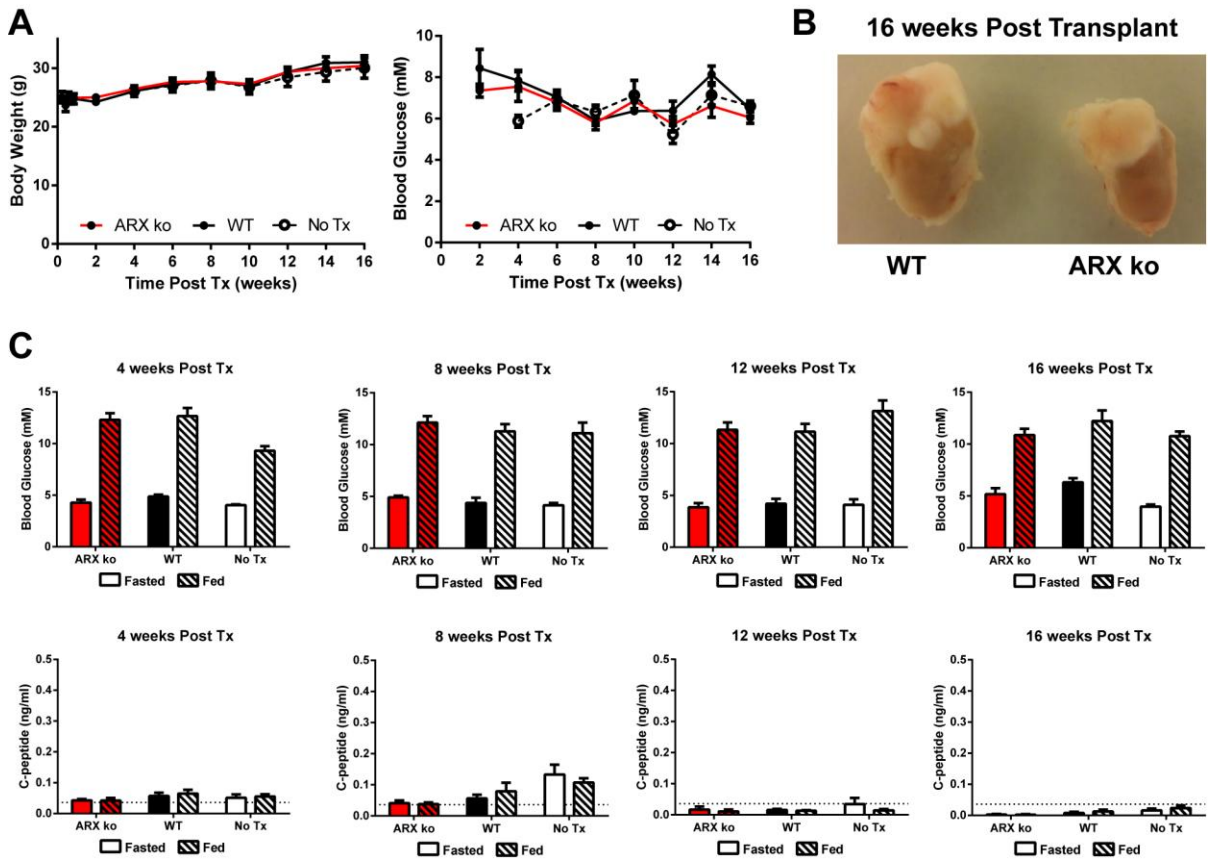

Figure 6.11. ***In vivo*** **tracking of wild type and ARX knockout transplanted mice**

(A) Body weight and saphenous vein whole blood glucose measurement tracking after transplantation in wild type (WT), ARX knockout (ARX ko), and non transplanted SCID-beige mice (8-10 week old males at time of transplant). (B) Representative excised grafts from wild type and ARX knockout cells at 16 weeks post transplant. (C) Fast-re-feed meal challenges (overnight fast, 45 minute *ad libitum* re-feed with blood glucose and C-peptide measured at 0 and 45 minutes relative to the feed) were performed at 4, 8, 12 and 16 weeks post transplant. N = 8 ARX knockout, 6 wild type, and 4 sham surgical controls. Dashed line in C-peptide data indicates reported limit of detection of the ELISA used to measure human C-peptide. Data collected with assistance from Shannon O'Dwyer.

While the endocrine development of both wild type and ARX knockout cells seemed to be incomplete given the lack of human C-peptide generated in transplanted mice, it was possible that endocrine specification may have been influenced without the formation of cells capable of altering physiological blood glucose levels. To assess this possibility, grafts were taken at 4 weeks (N = 1 per genotype) and 16 weeks post transplant (N = 7 for ARX knockout, and N = 4 for wild type) to examine potential pancreatic progenitor content and pancreatic endocrine composition. At 4 weeks post transplant, both wild type and ARX knockout grafts contained large fluid filled cysts that were surrounded by CK19 positive epithelial cells that generally did not express NKX6.1 (Figure 6.12). Neighbouring these

cystic areas were CK19, NKX6.1 co-positive pancreatic progenitors found in structures resembling early epithelial branching structures that were associated with CK19 low, NKX6.1 negative, chromogranin A positive endocrine cell clusters. In the wild type graft, these endocrine cells included glucagon, insulin, and somatostatin positive cells, where as in the ARX knockout grafts, glucagon positive cells were not observed, insulin positive cells were rare and somatostatin positive cells were abundant. These data followed the *in vitro* differentiation of wild type and ARX knockout data seen in Figure 6.5 and was further confirmed by observations in 16 week matured grafts. In these grafts, NKX6.1/CK19 positive progenitors were in abundance in comparison to the relatively sparse endocrine cells. Similar to 4 week grafts, within the endocrine population of these 16 week post transplant grafts, ARX knockout cells maintained a lack of glucagon expression but also failed to generate significant numbers of insulin positive cells. Unexpectedly, wild type cells also failed to generate significant numbers of insulin positive cells (Figure 6.13).

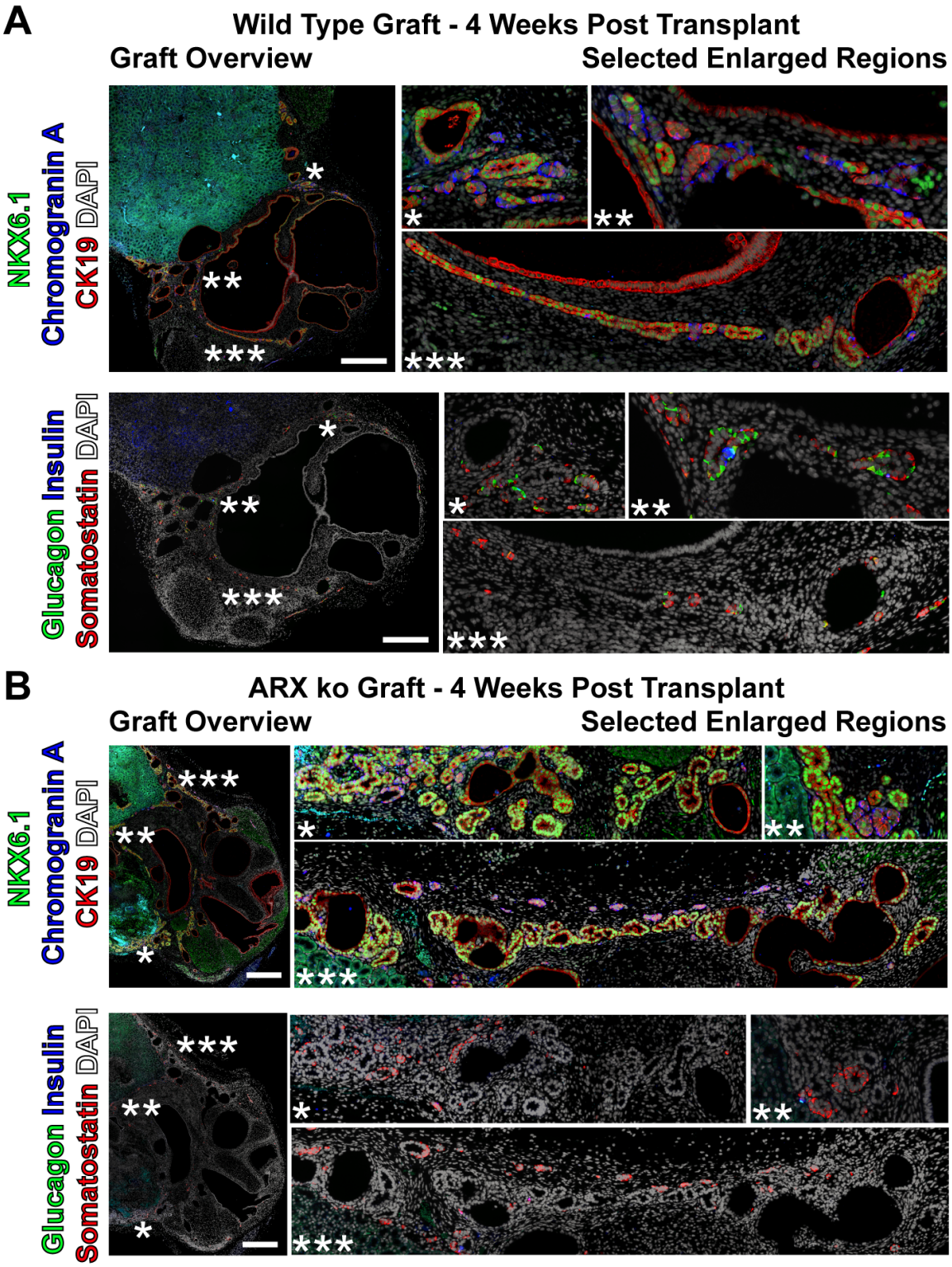

Figure 6.12. ***In vivo*** **development of wild type and ARX knockout grafts at 4-weeks post transplant**

(A) Wild type (WT) and (B) ARX knockout (ARX ko) grafts 4-weeks post transplant stained for NKX6.1 (green), CK19 (red), chromogranin A (blue), or glucagon (green), insulin (blue), and somatostatin (red). DAPI is white in all images. Selected enlarged imaged images are from regions indicated by 1-3 stars. Enlarged

images to the right of the graft overview are approximate serial sections and have been rotated for presentation purposes. Scale bar is 500 μm in the graft overview. Autofluorescent kidney tissue is observed in the upper left of each graft overview image.

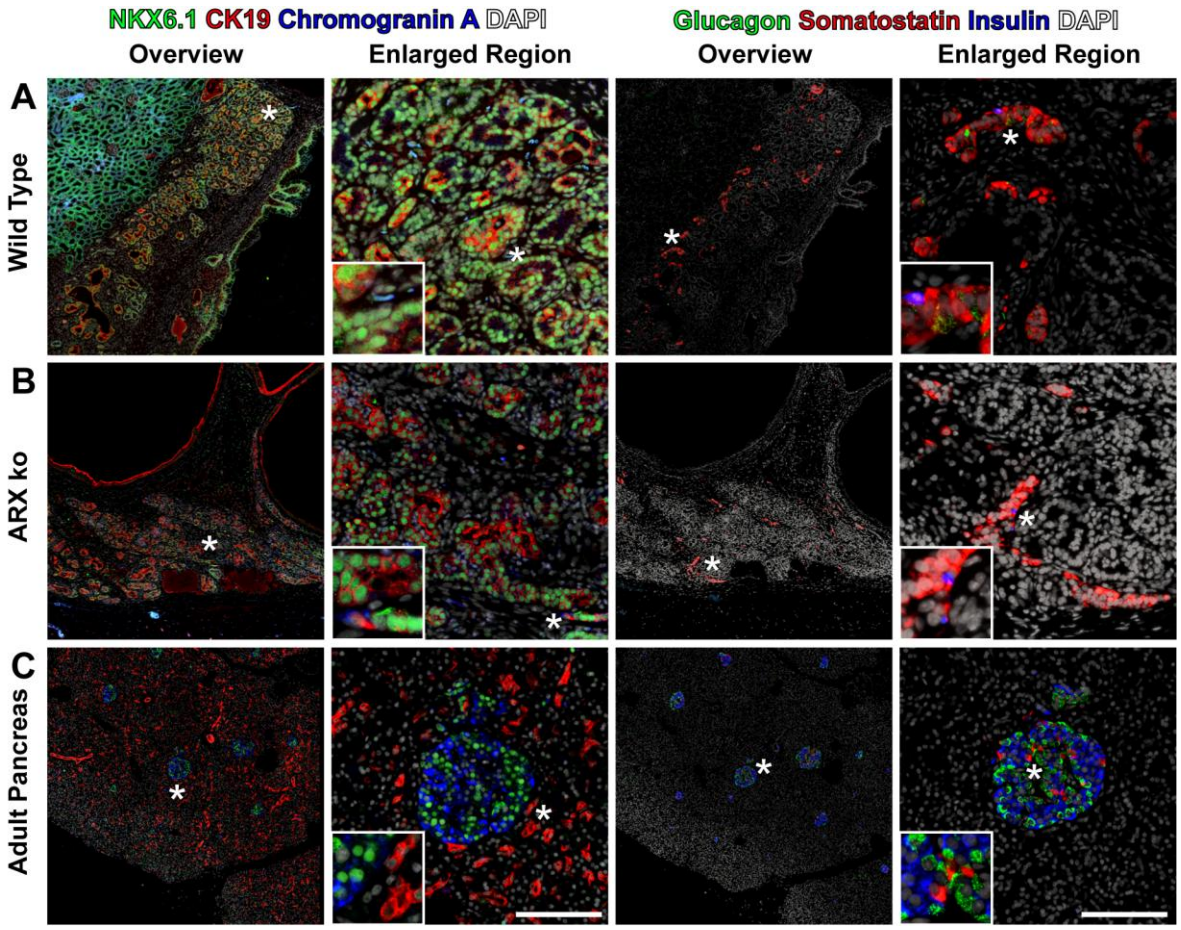

Figure 6.13. ***In vivo*** **development of wild type and ARX knockout grafts at 16-weeks post transplant**

(A) Wild type (WT) and (B) ARX knockout (ARX ko) grafts 16-weeks post transplant stained for NKX6.1 (green), CK19 (red), chromogranin A (blue), or glucagon (green), insulin (blue), and somatostatin (red). (C) Identically immunostained adult human pancreatic tissue for comparative purposes. Mature CK19 positive intercalating ductal cells are observed throughout the pancreatic exocrine tissue. DAPI is white in all images. Selected enlarged regions are from the regions indicated the star in the overview. Enlarged images to the right of the graft overview are approximate serial sections. Inset is in enlarged region a ~3x enlarged portion from the region indicated by the star. Scale bar is 100 μm in the enlarged regions. Autofluorescent kidney tissue is observed in the upper left of the wild type graft and large cystic structures are observed in the upper left of the ARX knockout graft.

Re-expression of ARX Restores Insulin Expression in ARX knockout cells

Given that differentiated ARX knockout hESCs show a failure to generate glucagon positive cells and a minimal ability to generate insulin positive cells both *in vitro* and *in vivo*, we were interested to see what aspects of this phenotype could be rescued by re-expression of *ARX* at specific developmental time points. To do this, we generated an adenoviral vector

which allowed expression of the human *ARX* open reading frame under the control of the relatively low expression EF1α promoter (Ad ARX). Aiming to have as close to physiological ARX re-expression levels as possible, we utilized a low multiplicity of infection (MOI of 2) during infection of early pancreatic progenitors and early pancreatic endocrine cells at day 13 and 19 of culture respectively (Figure 6.14A). Despite the low MOI, gene delivery at 72 hours post infection approached 40% of the cell population from both infection times and was maintained until the end of the differentiation protocol (Figure 6.15). Re-expression of ARX was similar in ARX knockout cells treated at both time points with immunoreactivity observed predominantly in hormone negative cell populations (Figure 6.14B). Quantification of Ad ARX re-expression levels by RT-qPCR in 26 day differentiated samples revealed similar expression levels (~50-150 fold adult human islets) in both wild type and ARX knockout cell populations (Figure 6.14C). Tracking of static glucagon and C-peptide release into the culture media between days 13 and 26 revealed the expected differences between wild type and ARX knockout cells in the absence of vector delivery. Compared to ARX knockout cells treated with control virus (Ad eGFP) at the same dose, delivery of Ad ARX on day 13 of culture but not day 19 of culture was associated with release of C-peptide but not glucagon into the culture media (Figure 6.14D). This specific effect of ARX re-expression in terms of both developmental timing and genetic background led us to examine the effect of Ad ARX on the individual endocrine subpopulations. Among all ten treatments examined, no effect on the total number of hormone positive (any combination of insulin, glucagon, and/or somatostatin) cells was observed (Figure 6.14E). Similarly, no effect of Ad ARX treatment was observed in wild type cells in terms of endocrine subpopulations. ARX knockout cells treated with Ad ARX at day 13 but not day 19 showed a specific decrease in unihormonal somatostatin positive cells and an increase in somatostatin cells co-expressing insulin compared to untreated and Ad GFP treated cultures (Figure 6.14E and F). This population shift was the result of a net increase in the total number of insulin positive cells with no change in either the glucagon or somatostatin positive fractions (Figure 6.16). While these data implicate ARX as a factor that can influence the generation of insulin positive cells, they do not suggest how this may occur. Given the altered expression patterns we observed in ARX knockout cells, we were keenly interested in the effects of ARX re-expression on these factors.

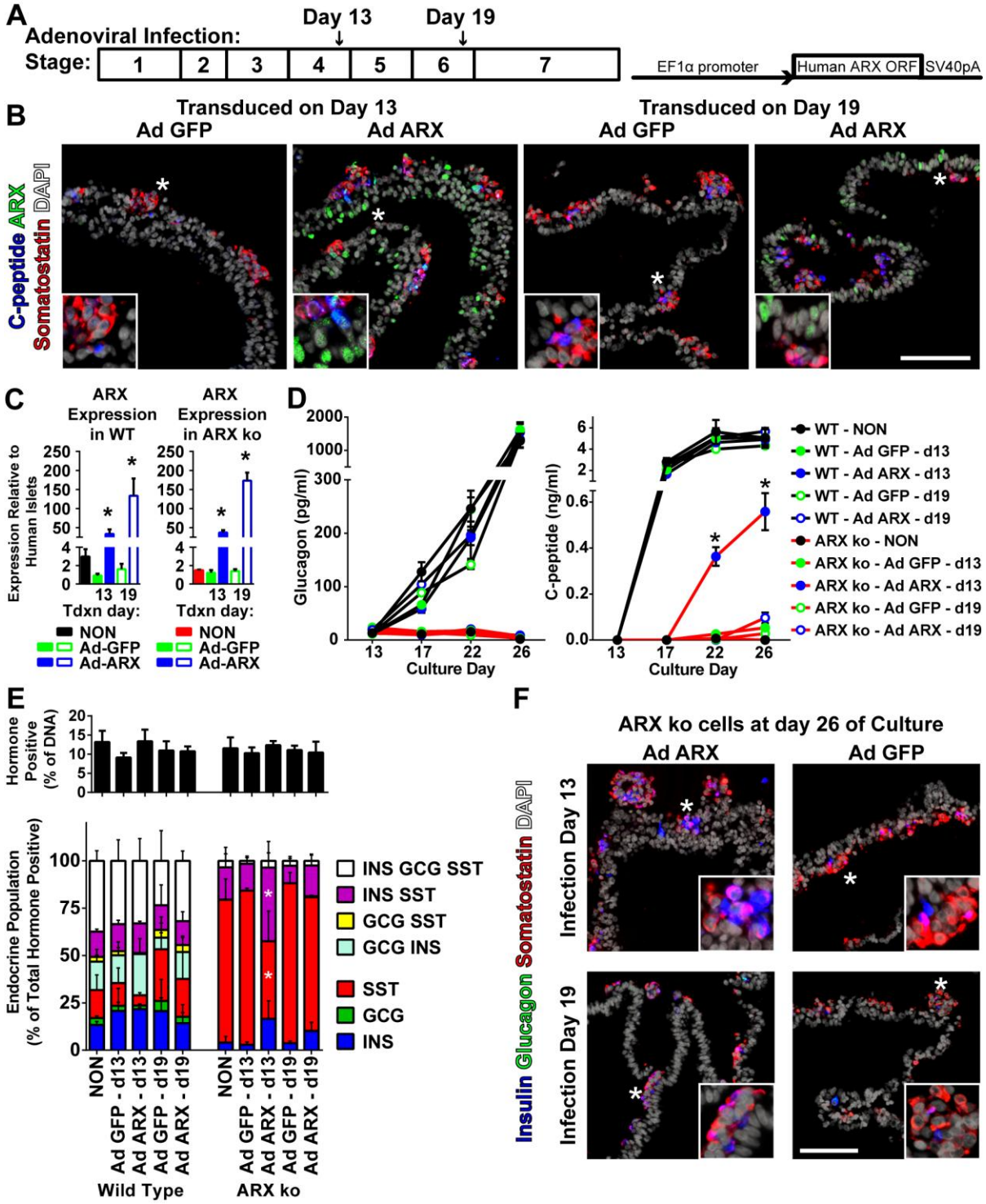

Figure 6.14. Adenoviral ARX re-expression in developing ARX knockout hESCs

(A) Schematic diagrams of adenoviral infection timeline during pancreatic differentiation stages and the adenoviral construct used to express human ARX under the constitutive EF1α promoter. (B) Immunostaining of ARX (green), somatostatin (red), and C-peptide (blue) in ARX knockout (ARX ko) cells differentiated to day 26 after transduction at day 13 or 19 with Ad GFP or Ad ARX. (C) RT-qPCR of day 26 whole population

samples examining the expression of ARX in wild type (WT) (left graph) and ARX knockout (right graph) cells treated with Ad GFP (green bars) or Ad ARX (blue bars) at an MOI of 2 on day 13 (filled bars) or 19 (open bars). * indicates $p < 0.05$ Ad GFP vs Ad ARX from a given transduction (Tdxn) day. (D) Glucagon and C-peptide levels from 24-hour static media samples taken between days 13 and 26 comparing Ad ARX treatment in wild type cells (black lines) and ARX knockout cells (red lines). Treatments are indicated by symbol colour in the figure. * indicates $p < 0.05$ Ad ARX on day 13 versus all other populations on day 22 and 26. (E - F) Immunostaining and single cell hormone analysis of Ad GFP and Ad ARX treated wild type and ARX knockout day 26 cultures for insulin (blue), glucagon (green), and somatostatin (red). (E) Total number of hormone positive cells (any combination of insulin, glucagon and or somatostatin) represented as a percentage of the total number of nuclei. Endocrine population breakdown of wild type and ARX knockout cultures. * indicates $p < 0.05$ Ad ARX delivered on day 13 versus no virus (NON) and Ad GFP delivered on day 13 in ARX knockout cells. N = 3 per group. Inset is a ~3x enlarged portion from the region indicated by the star. Scale bar is 100 μm for all panels.

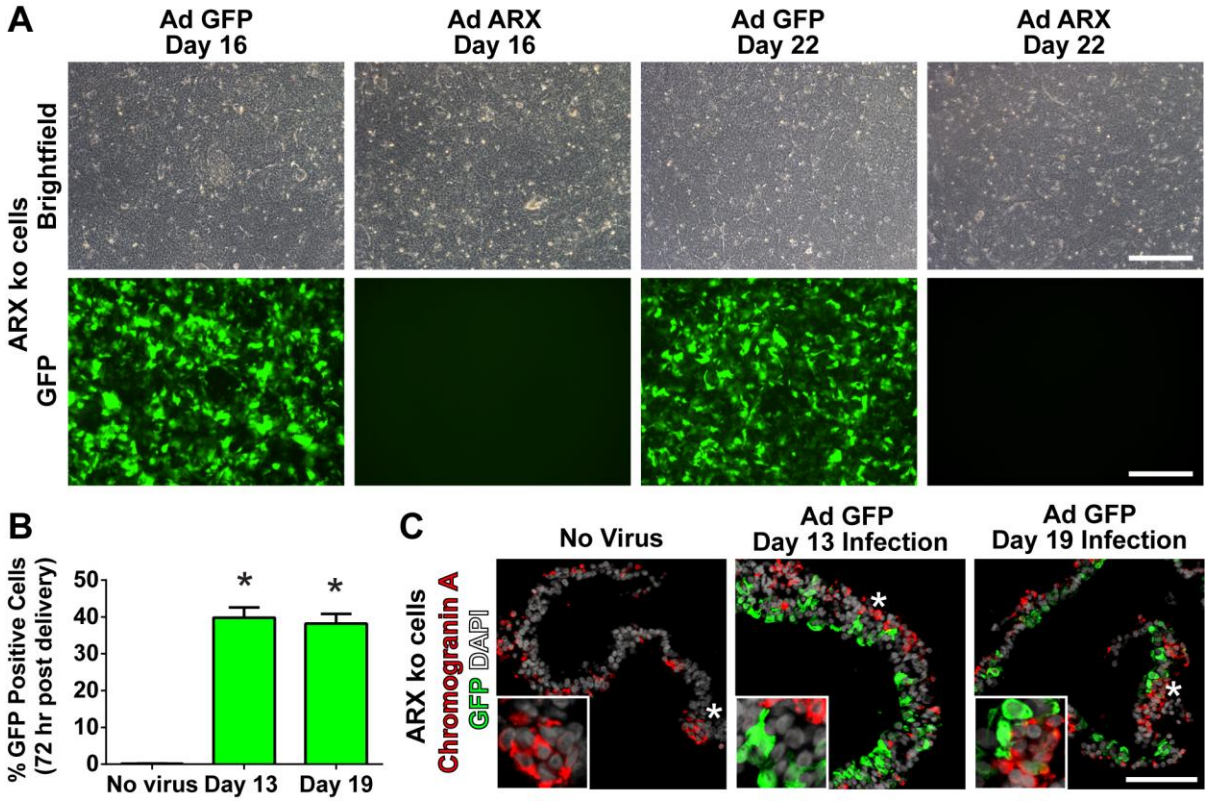

Figure 6.15. Adenoviral infection efficiency in ARX knockout hESCs

(A) Brightfield and green channel (GFP) images of differentiating ARX knockout (ARX ko) cell cultures 72 hours post adenoviral infection at a MOI of 2. (B) GFP infection efficiency quantified by flow cytometry 72 hours after viral delivery as a percentage of the total population. (C) Transgene expression (GFP) in 26-day differentiated ARX knockout hESCs based on immunostatining of GFP (green) and chromogranin A (red). Nuclei are counterstained with DAPI (white). Inset in C is a ~3x enlarged portion from the region indicated by the star. Scale bar is 200 μm for panel A and 100 μm for C.

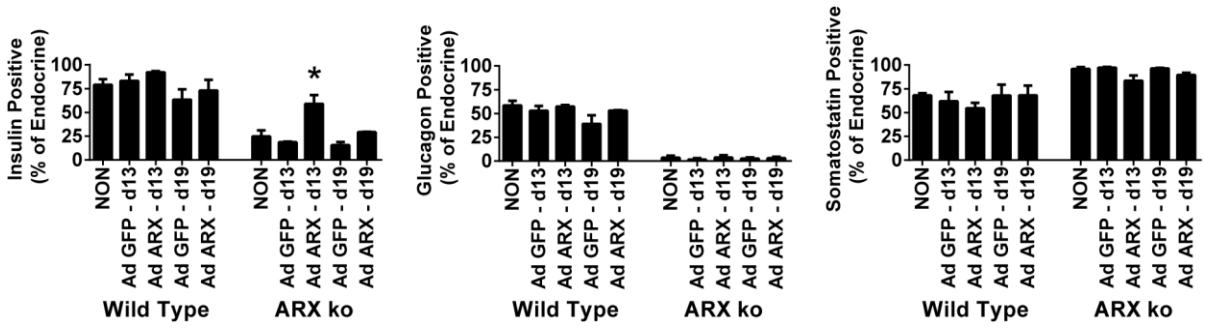

Figure 6.16. Total hormone fractions in Ad ARX treated cultures

Quantification of the total numbers of cells positive for each of the three hormones (insulin, glucagon, and somatostatin) regardless of copositivity graphed as a percentage of the total number cells positive of any of the three hormones. Based on the data from Figure 6.14. * indicates $p < 0.05$ Ad ARX delivered on day 13 versus all other ARX knockout (ARX ko) cell samples. N = 3 per group.

Re-expression of *ARX* in ARX knockout cells showed an expected pattern of increased expression of insulin and very small amounts of glucagon in a similar manner to the media sample data above with no significant effect on somatostatin levels (Figure 6.17A). Delivery of Ad ARX was also associated with an increase in PAX6, decrease in HHEX, and a trending decrease in PAX4 in ARX knockout cells at day 26 of culture. This increase in PAX6 was also seen at the protein level in ARX knockout cells where nuclear PAX6 immunoreactivity was observed in cells treated with the ARX expression construct. Taken together, these data suggest that by returning ARX expression to differentiating ARX knockout progenitor cells around day 13 of culture, the expression of other transcription factors including PAX6 and HHEX was reversed and was associated with an approximate doubling of the number of insulin positive cells in the final cultures.

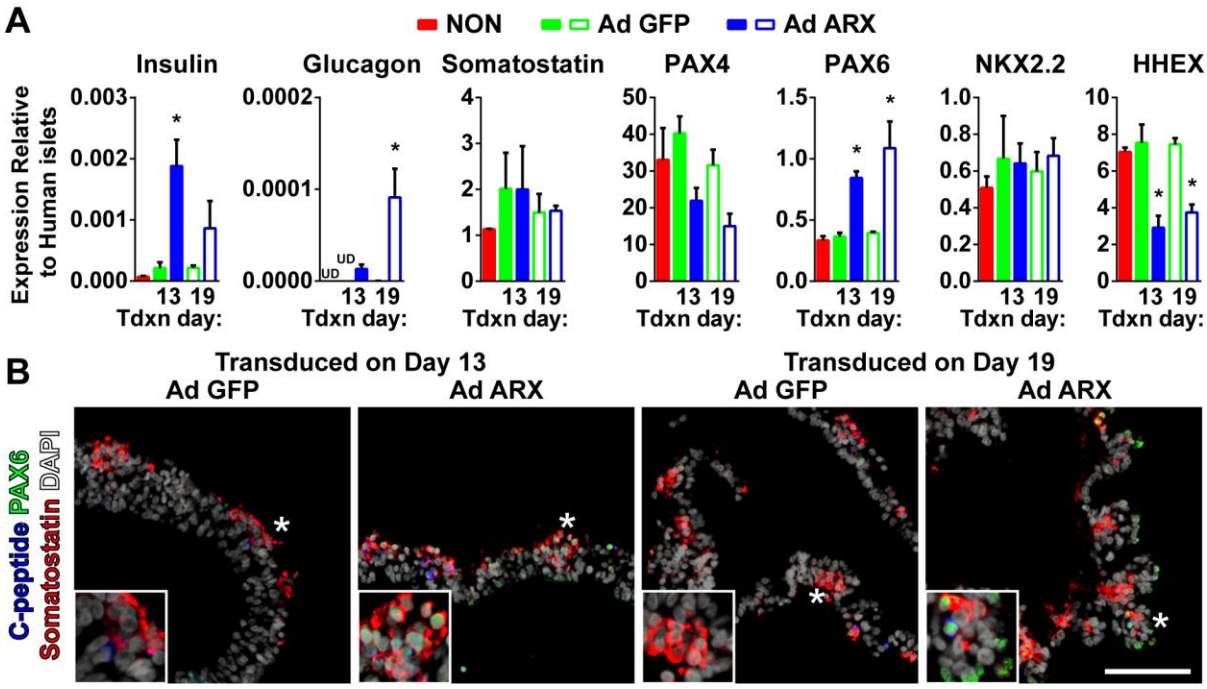

Figure 6.17. Fate specification factors in Ad ARX treated ARX knockout cells

(A) RT-qPCR of day 26 whole population samples examining the expression of three hormones and key transcription factors in ARX knockout cells treated with Ad GFP (green bars) or Ad ARX (blue bars) at an MOI of 2 on day 13 (filled bars) or 19 (open bars). * indicates $p < 0.05$ Ad GFP vs Ad ARX from a given transduction (Tdxn) day. N = 3 per group. (B) Immunostaining of PAX6 (green), somatostatin (red), and C-peptide (blue) in ARX knockout cells differentiated to day 26 after transduction at day 13 or 19 with Ad GFP or Ad ARX. Inset is a ~3x enlarged portion from the region indicated by the star. Scale bar is 100 μm for all panels.

6.4 Discussion

The goal of this study was to examine the role of *ARX* in the context of *in vitro* pancreatic endocrine development of hESCs. To do this, we stimulated genetic deletions in the *ARX* locus and isolated clonal cell populations of hESCs with null alleles due to small targeted deletions. Application of an established pancreatic differentiation protocol that mimics a number of key early developmental stages revealed that ARX knockout hESCs were quite similar to wild type hESCs in terms of pluripotency marker expression, definitive endoderm and foregut endoderm development. This general similarity between the genotypes further supports the targeted nature of the *ARX* deletion as the many other genes required for response to the differentiation cues between days 1 and 11 were apparently not altered in ARX knockout hESCs. Additionally, the similarity in developmental marker expression between wild type and ARX knockout cells in these early stages suggests that during hESC differentiation, ARX plays little developmental role during endodermal

development up to the formation of PDX1 positive foregut progenitors. Notably, since day 17 differentiated ARX knockout cells were found to have higher expression of *NKX6.1* by RT-qPCR and a higher proportion of NKX6.1 positive cells by flow cytometry, there may be a role of ARX in the conversion of PDX1 positive foregut cells to PDX1/NKX6.1 co-positive pancreatic progenitors (e.g. repression of NKX6.1 by ARX). Alternatively, it is also possible that this progenitor population simply accumulates due to a delay in endocrine induction. However, these aspects have yet to be examined.

The majority of our studies involving ARX knockout cells have been focused on the formation of hormone positive cells. Since we found that humans with ARX mutations lack glucagon and pancreatic polypeptide positive cells but retain insulin, somatostatin, and ghrelin populations, this was the expected result for our genetically altered hESCs. In line with these observations, ARX knockout hESCs generated very few glucagon and pancreatic polypeptide cells but unexpectedly showed reduced numbers of insulin positive cells leaving a large population of unihormonal somatostatin positive cells. This lack of glucagon and insulin was also seen in ARX knockout progenitors transplanted *in vivo*. To better understand the decrease in insulin in ARX knockout cells, we examined the expression of a number of transcription factors to potentially rule out candidate transcription factors which could contribute to the hormonal phenotype.

Since we had previously examined the effects of PAX4 in hESCs, where we found that high PAX4 levels were correlated with insulin positive cells, we first suspected an insufficiency in PAX4 in our ARX knockout hESCs. PAX4 has been shown to be required in the formation of both β- and δ-cells (240) and is a strong positive regulator of the β-cell lineage when overexpressed during pancreatic development (43). In double mutant *Arx/Pax4* mice, δ- and PP-cell hyperplasia is observed along with greater than 90% reduced α- and β-cell numbers (243). Additionally, overexpression of PAX4 in ESC cultures has been shown to positively regulate the formation of insulin positive cells (5, 233, 234) including their specification from polyhormonal cells (5)(Chapter 5). In our cultures, functional deletion of *ARX* was associated with a 2-fold increase in *PAX4* levels compared to wild type, and a 100-fold increase compared to adult human islet levels, both of which efficiently generated insulin positive cells. Upon re-expression of ARX by adenovirus, *PAX4* expression was attenuated in hESC, which supports the reciprocal regulatory activity between ARX and

PAX4 that has been previously observed in mice (243). Because these low levels of PAX4 were sufficient to be associated with expression of insulin in Ad ARX treated ARX knockout cells, we conclude that PAX4 levels should have been sufficiently elevated in untreated ARX knockout cells to generate insulin positive cells. Given the absence of insulin positive cells, other transcription factors implicated in pancreatic endocrine specification were examined subsequently.

The transcription factor NKX2.2 is a known regulator of pancreatic endocrine cells and was a candidate for why ARX knockout hESCs show reduced amounts of insulin. Mice with a null mutation in *Nkx2.2* show a reduction in β-, α- and PP-cells, an increase in ghrelin positive ε-cells and no change in δ-cell numbers (261, 262). Furthermore, mice lacking both *Nkx2.2* and *Arx* have an expansion of ghrelin positive cells that co-express somatostatin (263). In our cultures of differentiated ARX knockout hESCs, we observed elevated levels of *NKX2.2* compared to wild type cells. Similarly to wild type hESC, human fetal and human adult samples, NKX2.2 was localized predominantly to hormone positive cells including somatostatin positive cells. Additionally, we observed no increase in ghrelin transcript levels, total ghrelin positive cell number, or ghrelin / somatostatin co-positive cell number in ARX knockout cultures. In patients with XLAG (*ARX* deficiency), Itoh et al. reported nuclear immunoreactivity of NKX2.2 suggesting that expression of this factor was not dependant on functional ARX expression (252). Taken together these data suggest that in ARX knockout models including hESCs, NKX2.2 levels are an unlikely primary cause of the reduction of insulin positive cells in hESC-derived ARX knockout endocrine cells.

Compared to differentiated wild type hESCs, the greatest reduction in gene expression studied in ARX knockout cells was of PAX6. In mice with functional loss of *Pax6*, a decrease in the expression of insulin, glucagon, and somatostatin was observed suggesting that this factor is critical for the expression of these hormones or the genesis of the cell types (168, 171). PAX6 is well established to bind directly and activate the insulin, glucagon, and somatostatin promoters, but notably insulin and somatostatin regulatory elements contain one binding site for PAX6 while the glucagon contains two (168, 170, 264-267). This difference in number of binding sites may account for the more complete loss of glucagon in PAX6 deficient mice compared to insulin and somatostatin lineages, as previously suggested (268). Furthermore, PAX6 deficient mice contain significant numbers

of committed endocrine cells (ISL1-positive and BRN4-positive) that fail to express any hormone suggesting that the role of PAX6 may well be in final hormone expression in cells which have specified their endocrine cell fate based on other factors (268). This idea is also supported by the fact that PAX6 seems to regulate other aspects of endocrine cell maturation including the transcription factors MAFB, cMAF, and NEUROD1 and the prohormone processing enzymes PC1/3 and PC2 (170, 269). In our studies, we found that similarly to E18.5 *Arx* knockout pancreatic islets, ARX knockout cells had decreased *PAX6* levels (>3 fold vs wild type) throughout differentiation, which was in sharp contrast to the high levels seen in wild type cells that were found to correlate with bright nuclear localizing PAX6 expression patterns similar to fetal and adult human samples. When ARX was re-expressed to ~50 fold adult levels in ARX knockout cells we observed that *PAX6* levels rose significantly, showed nuclear immunoreactivity and correlated well with the return of insulin expression to the ARX knockout cultures. While we did see a small (0.0001 fold adult levels) increase in glucagon transcript levels, we did not observe an increase in the number of glucagon positive cells with ARX re-expression. It is possible that limiting amounts of PAX6 were insufficient to occupy and activate sufficient amounts of glucagon expression to be seen as protein at our level of detection. Moreover, these data suggest that the recovery of PAX6 upon re-expression of ARX in ARX knockout cells identifies PAX6 as a potentially rate limiting transcriptional activator in terms of insulin expression in developing hESCs.

Beyond the well known transcription factors described above, it is also possible that any of the many established or unknown factors could mediate the activities of ARX either directly or indirectly. For instance, BRN4 has been shown to be an α-cell enriched transcription factor but surprisingly is dispensable in terms of α-cell development and function with little effect on other factors such as PAX6 and NKX2.2 (268). In human α-cells, one of the most specific transcription factors along with ARX is IRX2 (270). In mice, both IRX1 and IRX2 are expressed downstream of NGN3 and expressed in glucagon but not insulin or somatostatin positive cells (271). In zebrafish IRX3 has been shown to be critical to the expression of insulin and glucagon (272). In our differentiated ARX knockout hESCs, IRX2 was down regulated at day 17 of culture in a similar pattern to PAX6. Together, the IRX gene family represents a number of potential candidates being effectors of ARX that impact the formation of pancreatic endocrine cells. Ultimately at this time, we cannot

exclude these transcription factors, or as yet unidentified factors, as key control elements in direct actions on insulin and glucagon expression in ARX knockout endocrine cells or through the actions of other players such as PAX6.

Regardless of how the unihormonal somatostatin positive cells formed from ARX knockout hESCs, one key outstanding question is that of functional δ-cell maturation. While the formation of mature functional β or δ-cells has yet to be achieved during complete *in vitro* differentiation of hESCs (1), the cells generated in this study do have some markers of early maturation. ARX knockout somatostatin cells express PDX1, PBX1 and PREP1, which are known regulators of somatostatin expression (256). These cells also express the prohormone convertases PC1/3 and PC2, which are required for maturation of the hormone to its biologically active products (258, 259). ARX knockout unihormonal somatostatin-positive cells express all five of these factors along with NKX2.2 and ISL1, all of which are found in adult pancreatic δ-cells. ARX knockout cells also show increased expression of HHEX which has been previously observed in hESC-derived unihormonal somatostatin positive cells after functional *in vivo* maturation of pancreatic progenitor populations (126). These data, along with the significantly elevated somatostatin release from ARX knockout cultures at day 24 of culture in response to a depolarizing potassium chloride stimulus, suggest that the endocrine cells may have some functional capacity - although this requires a considerable amount of future studies. These studies would likely require purification of somatostatin positive cells and assessment of cells by live cell calcium imaging or patch-clamp experiments with exposure of cells to δ-cell specific activation conditions involving glucose (activates mouse δ-cells at 3 mM and 11 mM but not 0.5 mM), tolbutamide (activates mouse δ-cells at 40-100 μM), and/or diazoxide (inactivates δ-cells at 100 μM) (273, 274). Though beyond the scope of our studies, an understanding of hESC derived δ-cell function could significantly improve our knowledge of this key endocrine cell population which, through its release of somatostatin, represents a prominent control mechanism of both glucagon and insulin secretion *in vivo* and *in vitro* (275-277).

In summary, our studies have generated and examined a novel hESC population that lacks functional ARX expression. Similar to humans with ARX deficiency, we observed a loss of glucagon and pancreatic polypeptide positive cells in ARX deficient hESCs. However, in contrast to XLAG pancreata, our hESC derived endocrine cells had reduced

insulin positive cell numbers leaving unihormonal somatostatin positive cells. The expression pattern of these somatostatin positive cells closely matched fetal and adult somatostatin positive cells and was associated with elevated expression of PAX4, NKX2.2, ISL1, HHEX, PCSK1, and PCSK2 and reduced levels of PAX6 and IRX2 compared to wild type hESCs. Remarkably, restoration of ARX expression through administration of an adenoviral vector to ARX knockout pancreatic progenitor cells resulted in reduction in HHEX expression and recovery of PAX6 and insulin expression. Taken together, these data suggest that during hESC differentiation, ARX is required for the formation of specific pancreatic endocrine cell fates including α- and PP-cells. This role also seems to extend to the specification of insulin positive β-cells where PAX4, PAX6, and maybe IRX2 may be involved. While these studies do not address the formation of fully functional endocrine cell development from hESCs, they do highlight the importance of understanding the roles that transcription factors including ARX play during this process.

Chapter 7: Conclusions, Future Directions, and Key Challenges

7.1 Overall Conclusions

As the number of patients with diabetes continues to grow, the economic burden associated with their medical care grows as well. While the application of insulin as a therapeutic for diabetes has saved countless lives, the dramatic quality of life improvements associated with islet transplantation are remarkable even when insulin injections are required to supplement suboptimal transplants. Islet transplant procedures have paved the way for a cellular therapy for diabetes and currently building a therapeutic infrastructure and increasing the clinical need for large numbers of transplantable β-cells. Some important questions facing the field of regenerative medicine as it pertains to diabetes are: what cell type to use to generate more β-cells, what processes govern the formation of new β-cells from these cells, and how do we make stem cell transplants as safe as current human cadaveric islet transplants or even insulin injections?

In this thesis, we have built our experiments around the ideological goal of generating functional insulin producing cells from stem cells using predominantly *in vitro* systems. This goal proved lofty and was not completely attainable within the bounds of this thesis. However, it provided an important backdrop for the developmental insights that were observed in the preceding chapters. Given the considerable developmental data that suggests key roles for transcription factor expression in controlling pancreatic endocrine development, our work has focused on the role of transcription factors in hESC differentiation. Together these data are expected to influence future studies aimed at generating stem cell-derived endocrine cells capable of glucose regulated insulin secretion through a better understanding of how transcription factors influence the formation and specification of stem cell-derived endocrine cells.

Our work began in stem cells isolated from human amniotic fluid. We chose this stem cell population based on their relative ease of procurement, reported multi-lineage differentiation capacity and the absence of teratoma formation upon transplantation (50). In our hands the heterogeneous hAF cell population we worked with showed expression of a number of pluripotency associated markers as well as some markers not seen in hESCs (2) (Chapter 2). This marker expression pattern suggested that a multipotent population was

present but was unlikely to encompass the entire population. Furthermore, since the hAF cells that we examined were not sorted or selected (other than by culture adherence), we presumed that this unbiased mixture of cells held the cumulative differentiation capacity of the individual cell types and thus an increased chance of generating insulin-positive cells *in vitro*. Using these cells as a starting population we generated hAF reporter cells where activation of a human insulin promoter fragment was associated with the expression of a red fluorescent protein. This system provided a cell based screening platform to which we applied a combinatorial series of transcription factor overexpression constructs. Through single cell analysis, we observed that the insulin promoter reporter was preferentially activated by overexpression of a mixture of six transcription factors associated with pancreatic development. This cocktail of factors was also found to activate the endogenous insulin gene as well as a number of β-cell markers at the transcript and protein levels that were similar to a recent study in primate AF cells overexpressing PDX1, NGN3 and MAFA (51). While the primate AF cells were not tested functionally, transduced hAF cells in our studies were unable to ameliorate diabetic hyperglycemia in an *in vivo* model. This work suggested that AF cells have the ability to form pancreatic lineage cells but these cells may lack sufficient function to be broadly applicable as a cellular therapy. Having said this, it is still possible that AF cells could be useful as a cellular therapy similarly to other naturally immunosuppressive fetal derived cell populations like bone marrow stromal cells and umbilical cord blood cells (27). Specifically bone marrow-derived stromal cells have been associated with increased levels of insulin and reduced levels of diabetic hyperglycemia, which was believed to be due to a natural homing mechanism to the site of pancreatic injury followed by stimulation of endogenous β-cell regeneration (52, 53).

Due to this lack of function during transplantation of hAF cells, and their generally low insulin expression levels, we refocused our efforts onto established PSC populations where the capacity to generate insulin positive cells was more studied. Knowing that many experimental approaches would require careful control of cell density and extended enzymatic culture in the absence of embryonic feeder systems, we evaluated a then novel hESC subline derived from the parental CA1 hESCs. These CA1S cells were amenable to a simplified, feeder-free enzymatic propagation and single cell dissociation without the induction of apoptosis that is generally seen in other hESC lines (3) (Chapter 3). Despite

having a chromosomal gain, which has been associated with simplified enzymatic hESC passaging and resistance to apoptosis and precocious differentiation in other hESC populations (184, 188, 203), CA1S cells were found to retain good pancreatic differentiation capacity and were thus are an attractive model system to explore factors that influence pancreatic endocrine development *in vitro*.

One of the simple variables we suspected to be influential in hESC differentiation was cell density. While cell density is a variable part of almost all cell culture systems, early tests suggested that some densities were amenable to efficient differentiation and others were not. Previous work indicated that cell density had an impact on the formation of pancreatic progenitor cells, although these studies used re-plating methods that directly impacted cell-to-cell contact and would be challenging to apply to other culture systems (120). Our studies harnessed the natural propensity of CA1S cells for very uniform and reproducible cell seeding as a starting point for pancreatic differentiation using a multistage *in vitro* differentiation protocol known to generate pancreatic endocrine cells in H1 hESCs. In this developmental model, we observed that a threshold level of initial cell seeding density was required for efficient germ layer specification. We also saw that the highest of the tested densities resulted in improved pancreatic progenitor and pancreatic endocrine cell formation through a series of established temporally regulated transcription factor expression patterns. The effect of altered cell seeding density was also found to notably influence cell cycle status in the undifferentiated hESCs, which was in line with other timely related studies (102). This influence of cell cycle has been shown to influence differentiation propensity of hESCs by a number of studies (219, 220) including the formation of endoderm-derived pancreatic endocrine cells (221). While the effect of improved endocrine development seen by our work was not unexpected, the role of such a simple manipulation (seeding density) on the multistage pancreatic differentiation process serves as a reminder of the large number of seemingly small changes that contribute to the overall efficiency of forming endocrine cells form hESCs. Other simple factors such as oxygen tension, which through activation of HIF1α has been linked to activation of notch signalling and induction of the NGN3 dependent endocrine cascade (278), as well as the role of cell cycle progression at this NGN3 positive developmental stage (279) may serve to considerably influence the efficiency of hESC-derived endocrine cell formation.

With a number of hESC differentiation protocols, including our own, generating immature polyhormonal cells *in vitro*, we were interested in influencing the endocrine specification processes that generates these cells. To do this we chose two complementary transcription factor targets aimed at redirecting polyhormonal (α-cell biased) cells to insulin positive fates. First, we chose to acutely overexpress PAX4 based on previous hESC and mouse studies that suggested PAX4 could positively regulate the formation of insulin positive cells during development (43, 233, 234). In a similar manner to previous studies, we found that high levels of PAX4 overexpression resulted in a net increase in the number of unihormonal insulin positive cells (Chapter 5). The mechanism for this effect was associated with a repression of ARX and its developmental target glucagon, which influenced the polyhormonal hESC-derived endocrine cells to express only insulin. While PAX4 has been elegantly shown to repress ARX in murine development (243), our studies were the first to examine the relationship between PAX4 and ARX in an hESC developmental model.

Given the interplay between PAX4 and ARX, we next looked carefully at the role of ARX in pancreatic hESC differentiation. To do this we generated hESC lines that lacked functional ARX expression and subjected them to an advanced *in vitro* differentiation protocol. Throughout these studies we examined in parallel *ARX* deficient tissues (XLAG humans and *Arx* knockout mice) and the relevant human fetal pancreatic tissues for comparison. Similar to *ARX* deficient humans, ARX knockout hESCs generated an abundance of somatostatin positive cells and dramatically reduced numbers of glucagon positive cells, but interestingly also showed a partial reduction in insulin positive cells. While this phenotype confirmed that the dominant role of ARX in human pancreatic endocrine development is to positively influence the formation of the glucagon (α-cell) lineage, the decreased numbers of insulin positive cells was unexpected. The expression and development of somatostatin positive cells was found to mirror human fetal pancreatic data, which suggested that the δ-cell differentiation pathway was unaffected by the loss of ARX and may have even been enhanced to some degree. In an effort to explain the reduction in insulin in ARX knockout hESCs, we examined the expression of a number of candidate transcription factors associated with pancreatic development. Associated with the formation of many somatostatin cells and few insulin cells we found high expression of PAX4, NKX2.2, ISL1 and HHEX and a reduction of PAX6 and IRX2. When ARX was re-

expressed by adenovirus at a low level in pancreatic progenitor populations this expression pattern was at least partially reversed including a recovery of insulin and PAX6 expression and a reduction in the levels of PAX4 and HHEX. PAX6 immunoreactivity was nuclear and associated with a significant rescue of insulin positive cells. While these data simply correlate PAX6 with insulin expression, this link follows available murine literature and the established roles of PAX6 as both a direct and indirect activator of insulin expression (168, 171, 280). While studies to artificially rescue PAX6 in the absence of ARX re-expression are needed to exclude the possibility of other ARX target genes being responsible for the partial recovery of insulin expression, this result highlights the need for a more complete understanding of how hESC derived endocrine cells are specified as the current literature was unable to predict the effect of genomic ARX knockout on hESC-derived insulin cell numbers.

7.2 Future Directions

The studies outlined in this thesis related to hESCs have been focused on the development of the CA1S line, application of pancreatic endocrine differentiation, and effects of augmented PAX4 and ARX expression. While this work has revealed a role for these two key transcription factors in the formation and specification of hESC-derived pancreatic endocrine cells, a number of avenues of investigation remain to be explored. Broadly, these investigations include mechanistic interactions between PAX4 and ARX with other transcription factors and how this cascade leads to functional glucose responsive cell types.

In the systems outlined in this thesis, the use of ARX knockout hESCs provides a useful base technology to examine the role of other transcription factors in endocrine specification and their effects in functional maturation. While the loss of ARX in CA1S cells had little effect in early developmental stages, or the ability to form endocrine cells, the endocrine cells that were formed seemed to follow a default developmental program. This program generated unihormonal somatostatin cells with expression patterns that matched human fetal development patterns but through poorly understood mechanisms. For example, somatostatin positive δ-cells express NKX2.2, ISL1, PDX1, PREP1, PBX1, and PAX6 (Chapter 6) but factors that positively regulate this cell type during development are

generally unknown (243). Limited *in vivo* matured hESC graft data (126) and recent studies from the Kaestner lab suggests that HHEX is a novel necessary regulator of δ-cell development and function (281). We have found that ARX knockout cells have elevated levels of HHEX and have elevated levels of unihormonal somatostatin positive cells. In response to ARX re-expression in ARX knockout cells, HHEX levels are reduced and insulin expression is elevated. While these data are merely correlative, they suggest that HHEX may be involved in the distinction between insulin and somatostatin positive lineages. To test whether HHEX is required for somatostatin cell formation from hESCs, the HHEX gene could be knocked down by RNA-interference methods or more conclusively could be knocked out by genomic editing methods similar to those used to delete ARX. Doing so in ARX knockout cells would generate ARX/HHEX double knockout cells that we hypothesise would be unable to generate somatostatin positive cells. This simple model of combinatorial genetic ablation, followed by *in vitro* pancreatic development, would be effective for a candidate gene approach.

To determine potentially unidentified drivers of somatostatin cell fates an unbiased discovery based approach could be applied. Current differentiation of ARX knockout cultures for 26-days *in vitro* generates mixed cultures containing ~30% endocrine cells and ~60% pancreatic progenitors with the remaining cells of unknown identity. While this heterogeneous population was beneficial to the simultaneous assessments of progenitors and endocrine cells using immunocytochemistry as seen in Chapter 6, it presents an obstacle which may confound discovery based transcriptome analysis. In order to accurately probe the expression by microarray or RNAseq methods of the progenitor populations and the endocrine cells they generate, the cell populations must be separately analyzed. Recently a series of antibodies from different studies may provide the ability to separate progenitor and endocrine populations. Pancreatic progenitors can be labelled and sorted with CD142, which will positively mark hESC-derived PDX1/NKX6.1 co-positive, hormone-negative cells, as opposed to CD200/CD318 that marks hormone-positive cells (128). A similar useful series of antibodies designed to isolate adult islet endocrine cell types includes an antibody panel reported to bind to all pancreatic endocrine cells (245, 282) and has been used previously to isolate hESC-derived pancreatic endocrine cells (HPi3) (118). By comparing purified pancreatic progenitors and endocrine cells from wild type and ARX knockout cells, a

comprehensive map of the transcripts altered by the loss of ARX can be generated in both pre-endocrine cells and those committed to the endocrine linage. This four point data set (2 genotypes of cells with 2 developmental stage populations) would be expected to provide evidence for novel candidate gene approaches as described above. Additionally there would be the possibility of identifying general cellular pathways by Gene Ontology analysis which could decipher how these genes may influence endocrine development.

While understanding the positive regulators of δ-cell development provides an interesting academic pursuit, clinically the formation of insulin-positive cells is of more general interest. Notably, ARX knockout cells are capable and amenable to activation of insulin expression as exemplified by the recovery of insulin upon re-expression of ARX in ARX knockout cells. Our work suggests that PAX6 may be associated with the return of insulin expression in this system but it is also possible that PAX6 is merely correlated with, but not directly or indirectly responsible for the induction of insulin. These different modes of action could be distinguished by complementary overexpression and loss of function experiments involving PAX6 in the absence of ARX and quantifying insulin levels. If PAX6 is in fact a bystander in the process, then an unbiased approach would be needed to determine the effectors that control re-expression of insulin in the system. One strategy that could be employed would be to follow the transcriptome analysis methods suggested above using only ARX knockout samples treated with or without the Ad ARX re-expression vector, again sorted into respective endocrine and progenitor cell populations. This data set would be expected to identify a mixture of ARX targets that could be compared to published data sets of adult human α-cell and β/δ-cell transcriptomes generated using the same antibody purification methods. This comparison would allow for specific identification of ARX targets expressed in the β-cell lineage which could be direct or indirect regulators of insulin expression and targets for future studies using candidate gene approaches.

7.3 Key Challenges in the Field of PSC derived Pancreatic Endocrine Cell Generation

Beyond the specific research questions outlined and addressed in Chapters 3-6 of this thesis, the field of regenerative medicine as it pertains to diabetes has a number of outstanding challenges. These challenges can be summarized by the need to differentiate PSCs in a reproducible manner, in sufficient quantities for transplantation in an

immuoprotective environment. These three clinically associated challenges are in addition to the somewhat more academic goal of developing fully functional insulin expressing cells via *in vitro* differentiation and the application of PSC culture as a model of human development. These four areas of active study are discussed below.

7.3.1 Reproducibility of PSC Differentiation and Assessment

If hESCs, or more broadly PSCs, are going to become a realistic source material for generating cellular therapies for diabetes, the reproducibility of differentiation and development must be addressed. In the undifferentiated state, hESC lines are generally considered quite uniform in terms of their expression of pluripotency markers (59). Unfortunately this uniformity does not seem to extend to the differentiation potential of hESCs. One report suggested that even among similarly derived hESC lines, more than 100 fold differences in lineage specification efficiency exist (207), perhaps because of inherent DNA methylation patterns that predispose different hESC and iPSC lines towards certain lineages (283). This inherent variability between lines has contributed to the inability of investigators to repeat published protocols with different cell lines and obtain the same results. For example, some hESC lines are better able to generate pancreatic endocrine cells with the protocol developed by D'Amour et al. than others (101, 121, 207). In our studies described in Chapter 3 using the D'Amour protocol was effective at generating pancreatic progenitors and pancreatic endocrine cells without modification in CA1S cells. The positive results that our group obtained do not necessarily match reports by others. As a direct test of the pancreatic differentiation propensity of different hESC lines, Mfopou et al. applied the differentiation conditions optimized by D'Amour et al. for the CyT203 hESC line (101) to five in house generated hESC lines (VUB01, VUB02, VUB07, VUB14 and VUB17). In the VUB lines, the D'Amour protocol effectively generated definitive endoderm, gut tube, and foregut cells but eventually produced hepatocytes instead of pancreatic endocrine cells (121). Ultimately cell line specific alterations in the differentiation protocol, namely adjustment of the timing and dosage of BMP and FGF signalling modulators, were required to restore pancreatic endocrine differentiation capacity to the VUB lines. These modifications were similar to those applied by other groups (118). Line-to-line variation was also described by the ViaCyte Inc. group (formerly Novocell, Inc.), which reported varying progenitor

differentiation efficiencies amongst the CyT49, CyT203, and MEL1 hESC lines (128). Administration of DMSO to hESC lines resistant to pancreatic lineages has recently been reported to significantly improve differentiation efficiency in more than 25 hESC and iPSC lines (102). This effect of DMSO is likely mediated by cell cycle arrest in view of other studies demonstrating a requirement for transition from the G2/M cell cycle phases to G1/Go in order for hESCs to be capable of targeted differentiation (4, 219-221) and can be mimicked by high cell seeding density as seen in Chapter 4 (4). Taken together these data suggest that while a single protocol is unlikely to be effective at inducing differentiation of multiple hESC lines, most lines are likely to be capable of efficient pancreatic development given the appropriate signals. However, it may be more effective to identify hESC (or PSC) lines which have inherently reproducible differentiation for wide spread use than to develop multiple individually optimized protocols for each PSC line.

In addition to resolving the preferred PSC starting material(s) and the reproducibility of differentiation protocols, the methods and tools used to characterize and quantify nutrient responsive hormone release from resulting cells should be harmonized to enable direct comparison amongst research groups. Previous efforts to repeat observations have revealed such things as the confounding effects of insulin uptake in differentiated mESCs (284-286) and variation in hESC pancreatic differentiation propensity (121, 207). Rigorous cell characterization is also important since the standards for surrogate β-cells are very high, including the paramount importance of glucose regulated insulin secretion (287). Within the field of pancreatic islet research, methods for assessing insulin release are well established, including normalizing secreted insulin amounts to total DNA or insulin content of the cell sample. These practices have not been uniformly applied to the task of testing PSC derived pancreatic endocrine populations. Many *in vitro* studies simply report relative fold secretion of insulin (often as C-peptide) under static high glucose conditions versus low glucose conditions with different cell samples. This makes it hard to compare results between studies and unfortunately this approach fails to account for the number of endocrine cells in each sample, the pre culture conditions (often higher glucose differentiation medias) and the kinetics of secretion. Absolute hormone secretion in response to standardized glucose concentrations ideally in a kinetic secretion system with comparison to isolated islets would be preferable. By similarly assessing the function of differentiated PSCs, labs would be able

to better compare methods and resultant cell populations, which will ultimately facilitate further improvements of PSC differentiation protocols towards developing robustly functional β-cells *in vitro*.

7.3.2 Scaling Up PSC Differentiation

Assuming that reproducible hESC differentiation can be achieved, the next major hurdle will be the production of clinically relevant quantities of pancreatic progenitors or functional endocrine cells in an economically feasible manner (288). One key aspect of this scale up is determining what population of pancreatic endocrine cells will provide the most effective and safe treatment of diabetes. The functional capacity of β-cells seems to be significantly improved when islet cells, including α-cells, are clustered together with β-cells (289, 290). This may reflect the highly conserved natural arrangement of endocrine cells within islets and established paracrine signals between these cells (275, 291-293). However, King et al. compared the ability of enriched β-cells and re-aggregated islet cells to recover glycemic control in diabetic mice (294). The authors concluded that non-β-cell endocrine cells are not essential for transplantation success suggesting that a pure a β-cell product may be as effective as mixed islet cells, should protocols be successfully developed to produce pure β-cells. Given the success in making relatively pure α-cells (Rezania et al. 2011), it should be possible to make highly enriched β-cells. While estimates vary, it is possible that 1 billion hESC derived β-cells could be required to treat a single patient with diabetes (295). In order to achieve this scale of production, considerable expansion of hESCs will be required. This is likely a reasonable goal given that hESCs are highly proliferative, doubling every 20 hours (296) to allow an up to 6 fold expansion in just 4-7 days in the undifferentiated state in stirred bioreactor systems (297). Once expanded, cultures can be differentiated towards pancreatic progenitor and or endocrine cells following the loosely established conversion ratio of 1:1 (undifferentiated hESC:differentiated progeny) (101).

Recently the ViaCyte group reported a scalable production strategy for pancreatic progenitors (119) which was subsequently reproduced and enhanced by researchers at Pfizer (144). A large bank of frozen vials of undifferentiated hESCs is maintained whereby a sample can be thawed, expanded over two weeks of adherent culture, and formed into suspension cell aggregates by dynamic rotation of dissociated undifferentiated cells. In the

ViaCyte report these aggregates were then differentiated into pancreatic progenitors in a rotating suspension format, and transplanted in the epididymal fat pad of immunocompromised mice for final maturation. Graft maturation occurred over the next few months and ultimately resulted in glucose stimulated C-peptide release at approximately 11-15 weeks post transplant. Maturation continued until 4-5 months post transplant, when graft tissue could maintain normal glycemic control in animals in which mouse pancreatic β-cells had been destroyed by injection of streptozotocin after graft maturation. In addition to the scalability of the rotational culture adaptation, the *in vitro* temporal expression patterns and the *in vivo* matured endocrine compartment were remarkably similar to previous reports, which were based on a minimally scalable two-dimensional adherent system (117). While this bodes well for increased production of pancreatic progenitors using this potentially scalable differentiation method, some challenges remain. While the suspension differentiation methods significantly reduced the formation of non-endodermal origin tissues, approximately half of the grafts were considered cystic and thus were incompletely pancreatic endocrine cells (119). The cultures did not uniformly express key pancreatic transcription factors and ~2% of the cells were unidentified, thereby carrying the risk of unknown developmental potential (119). Presuming that all uniformity and safety concerns are addressed, the generation of these therapeutic cells is going to be costly. Indeed relative to cadaveric and xenogenic islet sources, there has been some debate as to whether a therapeutic product of this nature is ultimately economically viable (288, 298).

One of the key aspects of clinical scale production which will continue to require further research and is likely to have a significant impact on the cost of the final product is the conversion of current differentiation protocols to ones relying on small molecules with fully defined composition rather than protein growth factors derived from animal products. As an example of such efforts, Borowiak et al. used high-throughput small molecule screening to form ESC derived cell types along the pancreatic developmental cascade. Using a fluorescent reporter mESC line in which expression of SOX17 was tracked by red fluorescent DSRED expression, ~4000 compounds were screened to reveal that IDE1 and IDE2 significantly enhanced definitive endoderm induction from undifferentiated human and mouse ESCs (299). These two compounds could replace Activin A, the recombinant protein widely used to activate TGF-β signalling via canonical phosphorylation of Smad2 (299).

Further down the differentiation cascade, another screen was employed to identify small molecules capable of improving induction of PDX1 positive pancreatic progenitor cells. Using an antibody based high-content screen with dissociated and replated foregut progenitor cells treated with one of ~5000 compounds or DMSO, (-)-indolactam V (ILV) was found to increase numbers of PDX1 positive cells (300). When co-administered with FGF10, it also improved production of pancreatic progenitors capable of *in vivo* maturation to functional insulin positive cells. Based on the inability of retinoic acid to synergize with ILV and the similar effects of protein kinase C activators with respect to PDX1 positive cell stimulation, ILV is believed to activate protein kinase C by direct binding, although this has yet to be proven explicitly (300). Taken together the high efficiency formation of pancreatic progenitors under clinically amenable, defined, and scalable culture conditions seems feasible. While work is still required to merge these independent research efforts, the demand for transplantable tissue remains high and progress in the field is expected to be swift.

7.3.3 Immunological Control and Encapsulation

With the efficient and scalable production of functional pancreatic progenitors getting closer to a reality, cellular therapy for diabetes nevertheless presents an immunological problem. Human PSC derived grafts will face not only alloimmune attack but also the specific autoimmune mediated attack of insulin-positive cells associated with the pathogenesis of type 1 diabetes. With just a few efficiently differentiating hESCs lines established, cells derived from an equally minimal number of human leukocyte antigen (HLA) types are expected to be available for immunological matching to patients. HLA matching is an important variable influencing the success of human islet transplantation (301), so the matching of hESC derived pancreatic progenitors to recipient HLA types may dampen alloimmune graft rejection, as was observed in the early islet transplant experience (302). While PSC-derived sources offer the potential to deliver larger amounts of pancreatic endocrine tissue, it remains to be seen whether such transplants will be able to sustain long-term insulin independence in recipients.

Upon transplantation both PSC derived grafts and cadaveric islet grafts will be faced with an activated recipient immune system. One way to prevent graft loss associated with

host immune attack, without using immunosuppressant drugs, is by using a physical barrier to isolate the graft from the circulating immune system. This idea has taken form in a series of immunoisolation devices, which range from thin cellular coatings to microencapsulation with thick cell cluster/islet coatings, or macroencapsulation with engineered transplantable devices, as previously well reviewed (303-305). These approaches are being actively developed and may be amenable to protecting PSC based cell therapies (Figure 1.3).

Alginate microencapsulation forms a coating around islets or hESC derived clusters, which protects the cells from direct contact with host immune cells. This separation is presumed to be essential to preventing cytotoxic death of the transplanted cells, but due to the porous nature of the alginate gel, the graft can still secrete insulin in response to rising interstitial glucose concentrations (303). Depending on the chemical nature of the gel, this method may also protect the graft from antibody mediated attack, but this defence typically comes at the cost of increased hypoxia related necrosis (306). Despite these considerable challenges, simple extrusion alginate encapsulation is remarkably effective in some mouse models, even with minimal surface modifications to restrict cytokine entry (307). In immunodeficient mice, alginate-encapsulated human islet cells delivered to the intraperitoneal cavity functioned better than implants under the kidney capsule (308). A pilot study was conducted in a patient with type 1 diabetes who received a peritoneal implant of the same encapsulated islet cells while on immunosuppression. While the transplant was without metabolic effect, likely due to the marginal transplant mass, functional cells within intact microcapsules were recovered 3 months post transplant (308). Clinical trials utilizing alginate encapsulated porcine islets have begun with Living Cell Technologies reporting long-term graft survival, albeit in a single patient with type 1 diabetes (23). One key limitation of the alginate encapsulation system is that standard methods are minimally scalable due to processing capacities of current extrusion technologies (309). While scalable emulsification methods can effectively encapsulate β-cell lines at efficiencies adequate to reverse diabetes in mouse models (309, 310), these methods have not yet been applied to larger animal models or at clinical scales.

Macroencapsulation methods offer an alternate approach to immunoisolation of a transplanted graft with ease of retrevial representing a key advantage over microencapsulation methods. The TheraCyte™ device offers one example of this approach,

whereby cells are loaded into the multilayered cell impermeable thin pouch via an access port. The loaded device may then be surgically implanted in a variety of places within the body, most simply subcutaneously. After vascularisation of the exterior surface by the host, the graft gains function ideally enabling effective blood glucose control without direct physical contact between the graft and host, thus providing an immunological barrier to protect the graft from the host immune system. One caveat of such an approach for diabetes therapy is that mature islets have a high demand for oxygen and thus are traditionally challenging to maintain in a macroencapsulation device in the absence of substantial vascularisation or oxygen supplementation (311). Indeed mature islets do not do particularly well within the TheraCyte™ unless the devices are preimplanted to allow some vascularisation of the outer membranes before cells are loaded (312). Notably, by directly oxygenating alginate encapsulated human islet preparations within an multilayer transplantable device, functional glucose responsive insulin secretion was maintained up to 10 months after implantation in one patient with long standing type 1 diabetes (313). Remarkably this functional islet mass was protected from attack by the recipients immune system despite the absence of any immunosuppresive agents supporting the functionality of such a macroencapsulation device (313). More immature cells may have advantages surviving in a macroencapsulation device. For example, human fetal pancreas tissue appears better able to survive the transiently hypoxic transplantation environment (312, 314). Likewise, despite one report of inconsistent development of hESC derived progenitor cells within this type of macroencapsulation device (315), our group recently showed that functional maturation of hESC derived pancreatic progenitor populations is possible and efficient within the TheraCyte™ device including the ability to reverse diabetic hyperglycemia in mice (126, 136). Thus pancreatic precursor cells derived from hESCs may be more like fetal cells and more resilient to the hypoxic transplantation environment. If similar results are not obtained when more mature islet endocrine cells are developed from PSCs, progenitor cells may have a distinct advantage for macroencapsulation.

While a considerable amount of effort continues to be focused on the generation of a scalable transplantation product, some aspects of this strategy remain concerning. The continuing concern with transplanting hESC derived cells is the notion that they might overgrow, enabling uncontrolled release of secreted products such as insulin, or that they

might form teratomas. This risk is presumably greater with transplant of progenitor cells than it would be with fully differentiated cells. Indeed, transplantation of progenitors has been associated with varying levels of teratoma or overgrowth formation, due to incomplete differentiation of cultures such that pluripotent or possibly multipotent cell types capable of ectodermal and mesodermal lineages remain at the time of transplantation (117, 125, 128). The formation of teratomas and overgrowths seems considerably reduced following enrichment of the transplanted cell population with endodermal progenitors (108) or CD142 positive cells (128), high uniformity scaled-up progenitor differentiation (119), and transplantation of an *in vitro* matured endocrine population (127). These data suggest that further adjustments to the differentiation, selection, and/or transplantation protocols may reduce or eliminate the capacity for graft overgrowth and teratoma formation. Indeed our group has shown that simple modification of established differentiation protocols followed by macroencapsulation was able to nearly eliminate all off target germ layer development to one device of 74 compared to 18 out of 40 devices with our previous protocol (136). The physical constraints provided by transplantable macroencapsulation devices also serve an important risk reduction role in containing the graft. Thus delivery of cells within a defined, growth limiting, and ultimately retrievable physical space provides considerable protection to the transplant recipient. If the device proves to be a completely effective immunoisolation system, the absence or at least minimization of immunosuppression requirements could provide an additional advantage as any escaping graft cells would presumably be quickly targeted by the host immune system given their foreign nature. Taken together this suggests that a number of strategies may alleviate the concerns of tumour formation. When uniformly differentiated cells are combined with a sturdy graft encapsulation method allowing immunocompetent recipients, the safety profile of hESC derived progenitor transplants may even rival current islet transplantation methods where immunosuppression poses significant risks.

7.3.4 *In vitro* Maturation and Models of Development

As noted, *in vitro* hormone positive cells generated by many current protocols seem to be developmentally biased to become glucagon secreting cells, while *in vivo* maturation of the same progenitors can yield the full complement of mature endocrine cells albeit in a very

uncontrolled and poorly defined manner. This suggests that our current understanding of *in vitro* pancreatic differentiation is deficient in critical stimuli which are required for the complete maturation observed *in vivo*. If we can correct this deficiency, we will be better able to produce a well-defined human pancreatic endocrine cell population that can be used as a platform for drug discovery and as a transplantation source that has reduced risk for formation of off-target cell types. Such a well-defined product free from contaminating non-endocrine cell types will have the advantage of functioning to control blood glucose levels in patients immediately following transplant and may have an improved safety profile over current progenitor populations that might respond unpredictably during their maturation in the uncontrolled transplantation environment of human patients. While previous studies have suggested that only β-cells are critical for successful reversal of diabetes, and that non β-cell islet endocrine cells are not required to ameliorate hyperglycemia during transplantation in mice (294), it remains to be seen whether this is true in hESC derived endocrine cell transplants, as pure β-cell grafts have yet to be generated under any maturation or purification process reported to date. Similarly, whether the normal islet architecture seen in both endogenous human islets and *in vivo* matured hESC-derived grafts (117, 125) is required for optimal graft function in terms of glycemic control is unknown. This issue may be particularly relevant to encapsulation technologies which may disrupt the normal islet architecture. To address these questions, the production of uniform functional endocrine cells from hESCs *in vitro* remains a key challenge in the field, and at the same time positions hESC derived pancreatic progenitor maturation as an interesting model with which to study human pancreas development.

Transcription factors play a key role in pancreatic development (100) and recently researchers are turning to genetic modification of hESCs to allow targeted study of transcription factor activated pathways and networks in a effort to understand and control pancreatic endocrine development from PSCs. Based on this concept, mouse and human ESC lines bearing forced overexpression of single or multiple transcription factors, including *SOX17*, *FOXA2*, *NGN3*, *NKX2.2*, *NKX6.1*, *NEUROD1*, *PAX4* and *PDX1* (105, 233, 234, 316-325), have been generated. The majority of these studies have expressed transgenes by random integration of plasmids or lentivirus. Such strategies suffer from transgene silencing and loss of expression, which does not seem to be the case when targeted homologous

recombination approaches using safe harbour loci are employed (326-328). Despite these limitations and the difficulties involved with modifying ESCs a considerable number of developmental insights have been gained by transcription factor overexpression studies. In almost all cases examined the forced expression of (combinations of) these transcription factors stimulated transcription of endogenous genes, most notably insulin, glucagon, and somatostatin over the course of *in vitro* differentiation. However, studies with the transcription factor PDX1 highlight a key caveat of these types of studies. Constitutive overexpression of PDX1 in hESCs increased pancreatic endocrine and exocrine induction in an embryoid body model, although robust insulin expression was distinctly absent *in vitro* (317). Given that PDX1 expression is believed to be biphasic in nature over mouse embryonic development from E13.5 and out to adulthood (84), further examinations of PDX1 expression in hESCs attempted to recreate this expression pattern. Using a tamoxifen-inducible PDX1 expressing hESC line, Bernardo et al. (2009) found that a specific expression pattern of one 5-day pulse after definitive endoderm followed by a 5-day delayed pulse most efficiently induced insulin expression while minimizing expression of exocrine (amylase) and liver (AFP and albumin) lineages. This work suggests that increased understanding of pancreatic development and the dynamics of transcription factor expression may yet inform key improvements in hESC differentiation protocols.

The idea of modeling human development in hESCs was recently applied to understanding the effects of mutations in the glucokinase gene (*GCK*), which are associated with MODY2. In an elegant study by Hua et al. (2013), skin biopsies were acquired from two patients with MODY2. Patient specific iPSCs were generated from each biopsy, and were pluripotent while retaining the heterozygous deletion in *GCK*. Upon *in vitro* differentiation and *in vivo* maturation, GCK mutant grafts developed to contain insulin producing cells which displayed an impaired functional response to elevated glucose levels similar to that commonly observed in individuals with MODY2. The authors then used homologous recombination to repair the genetic lesion in *GCK* in the undifferentiated iPSCs, and found that this restored normal glucose responsiveness to insulin producing cells upon *in vitro* and *in vivo* maturation (329). This work suggests that PSC differentiation can be used to recapitulate and understand the effects of human genetic phenotypes. Such approaches could ultimately allow for generation of patient-specific cellular therapies to restore

functionally normal cells in patients bearing genetic mutations in a particular cell type and for developing new drugs.

The strategy of retesting knowledge generated from mouse developmental and rare human models in hESCs has been relatively fruitful. However, discovery based methods using hESC lines that allow live cell lineage tracing and prospective isolation are also enabling the identification of new factors that influence the development of human diabetes. One popular recent tool has been hESC cell lines which allow tracking of endogenous human insulin promoter activation in its native loci through expression of cytoplasmic eGFP (118, 138, 330). By using homologous recombination, this approach circumvents the problems associated with variable integration and expression of transgenes and the epigenetic silencing which has been observed with lentiviral and retroviral transgenesis (326, 331, 332). The ability to illuminate and isolate the cell type of interest has allowed direct whole transcriptome analysis, as well as visualization of single-cell cytosolic calcium mobilization and single-whole-cell K_{ATP}, Ca_V, Na^+ and K_V currents in hESC derived insulin/eGFP positive cells (138). As this kind of live cell labeling strategy expands to multiple colours and even to subcellularly localized reporters, the ability to specifically examine the characteristics of rare populations such as NKX6.1, PDX1, MAFA, and insulin quadruple positive, ARX, glucagon, somatostatin triple negative cells will become possible. If it is possible to understand how a single cell functionally develops then we may be able to translate this knowledge to reproducibly guide the generation of glucose responsive cells *in vitro.*

7.3.5 Concluding Thoughts

Human pancreatic development is a complex process that is regulated by an intricate network of transcription factors and signalling pathways, along with other unknown factors that have yet to be discovered. Currently, differentiation protocols have been extensively studied and have become relatively successful at creating large populations of pancreatic progenitors. However, the diabetes field is still in its infancy working on the developmental cascades that turn human pancreatic progenitor cells into fully functional, unihormonal, endocrine cells. We have learned that the expression levels and timing of transcription factor signalling is crucial for guiding a human PSC into a pancreatic progenitor cell. Similarly, we extrapolate that the specification of mature endocrine cells is highly influenced by

transcription factor expression and, as suggested in this thesis, modulating transcription factor expression can provide a means of forming a more pure population of a single cell type. However, current attempts at modulating transcription factor signalling past the pancreatic progenitor stage have failed to yield reproducible, fully functional *in vitro* derived insulin releasing cells.

The maturation of endocrine cells is being researched in parallel with using cellular therapies for diabetes. By applying the genetic tools now available for real-time lineage reporting and lineage-tracing to pancreatic development modelled in hESCs, we can further understand and investigate the factors guiding the fate of human endocrine cell development. As Sir Frederick G. Banting said during his Nobel Prize acceptance speech in 1925 for the discovery of insulin, "Insulin is not a cure for diabetes; it is a treatment." With a deeper understanding of the elements that control the formation of a large number of functional hESC-derived pancreatic endocrine cells, a fully functional cellular therapy for diabetes is possible and represents a way of reducing the complications associated with diabetes mellitus.

References

1. Gage BK, Wideman RD, & Kieffer TJ (2014) Generating Pancreatic Endocrine Cells from Pluripotent Stem Cells. *Islets of Langerhans, 2. ed.*, ed Islam MS (Springer Netherlands), pp 1-37.
2. Gage BK, *et al.* (2010) Cellular reprogramming of human amniotic fluid cells to express insulin. *Differentiation* 80(2-3):130-139.
3. Caron NJ, *et al.* (2013) A human embryonic stem cell line adapted for high throughput screening. *Biotechnol Bioeng* 110(10):2706-2716.
4. Gage BK, Webber TD, & Kieffer TJ (2013) Initial cell seeding density influences pancreatic endocrine development during in vitro differentiation of human embryonic stem cells. *PLoS ONE* 8(12):e82076.
5. Gage BK, Baker RK, & Kieffer TJ (2014) Overexpression of PAX4 reduces glucagon expression in differentiating hESCs. *Islets* 6:e29236.
6. International Diabetes Federation (2013) IDF Diabetes Atlas. Accessed: March 27, 2014. http://www.idf.org/diabetesatlas
7. Canadian Diabetes Association (2011) The Harsh Reality - Diabetes is a global Pandemic. Accessed: June 6, 2011. http://www.diabetes.ca/diabetes-and-you/living/harsh-reality/
8. Canadian Diabetes Association (2014) Types of Diabetes. Accessed: May 16, 2014. http://www.diabetes.ca/about-diabetes/what-is-diabetes
9. Prentki M & Nolan CJ (2006) Islet beta cell failure in type 2 diabetes. *J Clin Invest* 116(7):1802-1812.
10. van Belle TL, Coppieters KT, & von Herrath MG (2011) Type 1 diabetes: etiology, immunology, and therapeutic strategies. *Physiol Rev* 91(1):79-118.
11. Banting FG, Best CH, Collip JB, Campbell WR, & Fletcher AA (1922) Pancreatic Extracts in the Treatment of Diabetes Mellitus. *Can Med Assoc J* 12(3):141-146.
12. Melendez-Ramirez LY, Richards RJ, & Cefalu WT (2010) Complications of type 1 diabetes. *Endocrinol Metab Clin North Am* 39(3):625-640.
13. The Diabetes Control and Complications Trial Research Group D (1993) The effect of intensive treatment of diabetes on the development and progression of long-term complications in insulin-dependent diabetes mellitus. The Diabetes Control and Complications Trial Research Group. *N Engl J Med* 329(14):977-986.
14. Fowler MJ (2011) The Diabetes Treatment Trap: Hypoglycemia. *Clinical Diabetes* 29(1):36-39.
15. Ballinger WF & Lacy PE (1972) Transplantation of intact pancreatic islets in rats. *Surgery* 72(2):175-186.
16. Lacy PE & Kostianovsky M (1967) Method for the isolation of intact islets of Langerhans from the rat pancreas. *Diabetes* 16(1):35-39.
17. Shapiro AM, *et al.* (2000) Islet transplantation in seven patients with type 1 diabetes mellitus using a glucocorticoid-free immunosuppressive regimen. *N Engl J Med* 343(4):230-238.
18. Ryan EA, *et al.* (2005) Five-year follow-up after clinical islet transplantation. *Diabetes* 54(7):2060-2069.
19. Merani S & Shapiro AM (2006) Current status of pancreatic islet transplantation. *Clinical science* 110(6):611-625.

20. Shapiro AM (2011) Strategies toward single-donor islets of Langerhans transplantation. *Current opinion in organ transplantation* 16(6):627-631.
21. McCall M & Shapiro AM (2012) Update on islet transplantation. *Cold Spring Harbor perspectives in medicine* 2(7):a007823.
22. Shapiro AM, *et al.* (2006) International trial of the Edmonton protocol for islet transplantation. *N Engl J Med* 355(13):1318-1330.
23. Elliott RB, *et al.* (2007) Live encapsulated porcine islets from a type 1 diabetic patient 9.5 yr after xenotransplantation. *Xenotransplantation* 14(2):157-161.
24. Pagliuca FW & Melton DA (2013) How to make a functional beta-cell. *Development* 140(12):2472-2483.
25. Furth ME & Atala A (2009) Stem cell sources to treat diabetes. *J Cell Biochem* 106(4):507-511.
26. Montanya E (2004) Islet- and stem-cell-based tissue engineering in diabetes. *Curr Opin Biotechnol* 15(5):435-440.
27. Aguayo-Mazzucato C & Bonner-Weir S (2010) Stem cell therapy for type 1 diabetes mellitus. *Nature reviews. Endocrinology* 6(3):139-148.
28. Bonner-Weir S & Weir GC (2005) New sources of pancreatic beta-cells. *Nat Biotechnol* 23(7):857-861.
29. Lysy PA, Weir GC, & Bonner-Weir S (2013) Making beta cells from adult cells within the pancreas. *Curr Diab Rep* 13(5):695-703.
30. Bonner-Weir S (2000) Perspective: Postnatal pancreatic beta cell growth. *Endocrinology* 141(6):1926-1929.
31. Dor Y, Brown J, Martinez OI, & Melton DA (2004) Adult pancreatic beta-cells are formed by self-duplication rather than stem-cell differentiation. *Nature* 429(6987):41-46.
32. Nir T, Melton DA, & Dor Y (2007) Recovery from diabetes in mice by beta cell regeneration. *J Clin Invest* 117(9):2553-2561.
33. Seaberg RM, *et al.* (2004) Clonal identification of multipotent precursors from adult mouse pancreas that generate neural and pancreatic lineages. *Nat Biotechnol* 22(9):1115-1124.
34. Smukler SR, *et al.* (2011) The adult mouse and human pancreas contain rare multipotent stem cells that express insulin. *Cell Stem Cell* 8(3):281-293.
35. Inada A, *et al.* (2008) Carbonic anhydrase II-positive pancreatic cells are progenitors for both endocrine and exocrine pancreas after birth. *Proc Natl Acad Sci U S A* 105(50):19915-19919.
36. Baeyens L, *et al.* (2005) In vitro generation of insulin-producing beta cells from adult exocrine pancreatic cells. *Diabetologia* 48(1):49-57.
37. Lardon J, Huyens N, Rooman I, & Bouwens L (2004) Exocrine cell transdifferentiation in dexamethasone-treated rat pancreas. *Virchows Archiv : an international journal of pathology* 444(1):61-65.
38. Rooman I, Lardon J, Flamez D, Schuit F, & Bouwens L (2001) Mitogenic effect of gastrin and expression of gastrin receptors in duct-like cells of rat pancreas. *Gastroenterology* 121(4):940-949.
39. Kopp JL, *et al.* (2011) Sox9+ ductal cells are multipotent progenitors throughout development but do not produce new endocrine cells in the normal or injured adult pancreas. *Development* 138(4):653-665.

40. Solar M, *et al.* (2009) Pancreatic exocrine duct cells give rise to insulin-producing beta cells during embryogenesis but not after birth. *Dev Cell* 17(6):849-860.
41. Zhou Q, Brown J, Kanarek A, Rajagopal J, & Melton DA (2008) In vivo reprogramming of adult pancreatic exocrine cells to beta-cells. *Nature* 455(7213):627-632.
42. Thorel F, *et al.* (2010) Conversion of adult pancreatic alpha-cells to beta-cells after extreme beta-cell loss. *Nature* 464(7292):1149-1154.
43. Collombat P, *et al.* (2009) The ectopic expression of Pax4 in the mouse pancreas converts progenitor cells into alpha and subsequently beta cells. *Cell* 138(3):449-462.
44. Ber I, *et al.* (2003) Functional, persistent, and extended liver to pancreas transdifferentiation. *J Biol Chem* 278(34):31950-31957.
45. Kojima H, *et al.* (2003) NeuroD-betacellulin gene therapy induces islet neogenesis in the liver and reverses diabetes in mice. *Nat Med* 9(5):596-603.
46. Ferber S, *et al.* (2000) Pancreatic and duodenal homeobox gene 1 induces expression of insulin genes in liver and ameliorates streptozotocin-induced hyperglycemia. *Nat Med* 6(5):568-572.
47. Talchai C, Xuan S, Kitamura T, DePinho RA, & Accili D (2012) Generation of functional insulin-producing cells in the gut by Foxo1 ablation. *Nat Genet* 44(4):406-412, S401.
48. Chen YJ, *et al.* (2014) De Novo Formation of Insulin-Producing "Neo-beta Cell Islets" from Intestinal Crypts. *Cell reports* 6(6):1046-1058.
49. Murphy SV & Atala A (2013) Amniotic fluid and placental membranes: unexpected sources of highly multipotent cells. *Semin Reprod Med* 31(1):62-68.
50. De Coppi P, *et al.* (2007) Isolation of amniotic stem cell lines with potential for therapy. *Nat Biotechnol* 25(1):100-106.
51. Zhou Y, *et al.* (2013) Genetic modification of primate amniotic fluid-derived stem cells produces pancreatic progenitor cells in vitro. *Cells, tissues, organs* 197(4):269-282.
52. Hess D, *et al.* (2003) Bone marrow-derived stem cells initiate pancreatic regeneration. *Nat Biotechnol* 21(7):763-770.
53. Lee RH, *et al.* (2006) Multipotent stromal cells from human marrow home to and promote repair of pancreatic islets and renal glomeruli in diabetic NOD/scid mice. *Proc Natl Acad Sci U S A* 103(46):17438-17443.
54. Stevens LC & Little CC (1954) Spontaneous Testicular Teratomas in an Inbred Strain of Mice. *Proc Natl Acad Sci U S A* 40(11):1080-1087.
55. Kleinsmith LJ & Pierce GB, Jr. (1964) Multipotentiality of Single Embryonal Carcinoma Cells. *Cancer Res* 24:1544-1551.
56. Evans MJ & Kaufman MH (1981) Establishment in culture of pluripotential cells from mouse embryos. *Nature* 292(5819):154-156.
57. Martin GR (1981) Isolation of a pluripotent cell line from early mouse embryos cultured in medium conditioned by teratocarcinoma stem cells. *Proc Natl Acad Sci U S A* 78(12):7634-7638.
58. Thomson JA, *et al.* (1998) Embryonic stem cell lines derived from human blastocysts. *Science* 282(5391):1145-1147.
59. International Stem Cell I, *et al.* (2007) Characterization of human embryonic stem cell lines by the International Stem Cell Initiative. *Nat Biotechnol* 25(7):803-816.

60. Smith KP, Luong MX, & Stein GS (2009) Pluripotency: toward a gold standard for human ES and iPS cells. *J Cell Physiol* 220(1):21-29.
61. Ungrin M, O'Connor M, Eaves C, & Zandstra PW (2007) Phenotypic analysis of human embryonic stem cells. *Curr Protoc Stem Cell Biol* Chapter 1:Unit 1B 3.
62. Takahashi K & Yamanaka S (2006) Induction of pluripotent stem cells from mouse embryonic and adult fibroblast cultures by defined factors. *Cell* 126(4):663-676.
63. Takahashi K, *et al.* (2007) Induction of pluripotent stem cells from adult human fibroblasts by defined factors. *Cell* 131(5):861-872.
64. Yu J, *et al.* (2007) Induced pluripotent stem cell lines derived from human somatic cells. *Science* 318(5858):1917-1920.
65. Gonzalez F, Boue S, & Izpisua Belmonte JC (2011) Methods for making induced pluripotent stem cells: reprogramming a la carte. *Nat Rev Genet* 12(4):231-242.
66. Hou P, *et al.* (2013) Pluripotent stem cells induced from mouse somatic cells by small-molecule compounds. *Science* 341(6146):651-654.
67. Robinton DA & Daley GQ (2012) The promise of induced pluripotent stem cells in research and therapy. *Nature* 481(7381):295-305.
68. Maehr R (2011) iPS cells in type 1 diabetes research and treatment. *Clin Pharmacol Ther* 89(5):750-753.
69. Bar-Nur O, Russ HA, Efrat S, & Benvenisty N (2011) Epigenetic memory and preferential lineage-specific differentiation in induced pluripotent stem cells derived from human pancreatic islet beta cells. *Cell Stem Cell* 9(1):17-23.
70. Stadtfeld M, Brennand K, & Hochedlinger K (2008) Reprogramming of pancreatic beta cells into induced pluripotent stem cells. *Curr Biol* 18(12):890-894.
71. Wilmut I, Schnieke AE, McWhir J, Kind AJ, & Campbell KH (1997) Viable offspring derived from fetal and adult mammalian cells. *Nature* 385(6619):810-813.
72. Byrne JA, *et al.* (2007) Producing primate embryonic stem cells by somatic cell nuclear transfer. *Nature* 450(7169):497-502.
73. Tachibana M, *et al.* (2013) Human embryonic stem cells derived by somatic cell nuclear transfer. *Cell* 153(6):1228-1238.
74. Chung YG, *et al.* (2014) Human Somatic Cell Nuclear Transfer Using Adult Cells. *Cell Stem Cell*.
75. Yamada M, *et al.* (2014) Human oocytes reprogram adult somatic nuclei of a type 1 diabetic to diploid pluripotent stem cells. *Nature*.
76. Tiso N, Moro E, & Argenton F (2009) Zebrafish pancreas development. *Mol Cell Endocrinol* 312(1-2):24-30.
77. Kinkel MD & Prince VE (2009) On the diabetic menu: zebrafish as a model for pancreas development and function. *Bioessays* 31(2):139-152.
78. Brennan J, *et al.* (2001) Nodal signalling in the epiblast patterns the early mouse embryo. *Nature* 411(6840):965-969.
79. Kanai-Azuma M, *et al.* (2002) Depletion of definitive gut endoderm in Sox17-null mutant mice. *Development* 129(10):2367-2379.
80. Ang SL & Rossant J (1994) HNF-3 beta is essential for node and notochord formation in mouse development. *Cell* 78(4):561-574.
81. Weinstein DC, *et al.* (1994) The winged-helix transcription factor HNF-3 beta is required for notochord development in the mouse embryo. *Cell* 78(4):575-588.

82. Wells JM & Melton DA (2000) Early mouse endoderm is patterned by soluble factors from adjacent germ layers. *Development* 127(8):1563-1572.
83. Wells JM & Melton DA (1999) Vertebrate endoderm development. *Annu Rev Cell Dev Biol* 15:393-410.
84. Jorgensen MC, *et al.* (2007) An illustrated review of early pancreas development in the mouse. *Endocr Rev* 28(6):685-705.
85. Stafford D & Prince VE (2002) Retinoic acid signaling is required for a critical early step in zebrafish pancreatic development. *Curr Biol* 12(14):1215-1220.
86. Tiso N, Filippi A, Pauls S, Bortolussi M, & Argenton F (2002) BMP signalling regulates anteroposterior endoderm patterning in zebrafish. *Mech Dev* 118(1-2):29-37.
87. Hebrok M, Kim SK, & Melton DA (1998) Notochord repression of endodermal Sonic hedgehog permits pancreas development. *Genes Dev* 12(11):1705-1713.
88. Chen Y, *et al.* (2004) Retinoic acid signaling is essential for pancreas development and promotes endocrine at the expense of exocrine cell differentiation in Xenopus. *Dev Biol* 271(1):144-160.
89. Jonsson J, Carlsson L, Edlund T, & Edlund H (1994) Insulin-promoter-factor 1 is required for pancreas development in mice. *Nature* 371(6498):606-609.
90. Stoffers DA, Zinkin NT, Stanojevic V, Clarke WL, & Habener JF (1997) Pancreatic agenesis attributable to a single nucleotide deletion in the human IPF1 gene coding sequence. *Nat Genet* 15(1):106-110.
91. Jennings RE, *et al.* (2013) Development of the human pancreas from foregut to endocrine commitment. *Diabetes* 62(10):3514-3522.
92. Decker K, Goldman DC, Grasch CL, & Sussel L (2006) Gata6 is an important regulator of mouse pancreas development. *Dev Biol* 298(2):415-429.
93. Ketola I, *et al.* (2004) Transcription factor GATA-6 is expressed in the endocrine and GATA-4 in the exocrine pancreas. *Mol Cell Endocrinol* 226(1-2):51-57.
94. Polak M, Bouchareb-Banaei L, Scharfmann R, & Czernichow P (2000) Early pattern of differentiation in the human pancreas. *Diabetes* 49(2):225-232.
95. Jeon J, Correa-Medina M, Ricordi C, Edlund H, & Diez JA (2009) Endocrine cell clustering during human pancreas development. *J Histochem Cytochem* 57(9):811-824.
96. Slack JM (1995) Developmental biology of the pancreas. *Development* 121(6):1569-1580.
97. Riedel MJ, *et al.* (2012) Immunohistochemical characterisation of cells co-producing insulin and glucagon in the developing human pancreas. *Diabetologia* 55(2):372-381.
98. Piper K, *et al.* (2004) Beta cell differentiation during early human pancreas development. *J Endocrinol* 181(1):11-23.
99. Pan FC & Wright C (2011) Pancreas organogenesis: from bud to plexus to gland. *Dev Dyn* 240(3):530-565.
100. Oliver-Krasinski JM & Stoffers DA (2008) On the origin of the beta cell. *Genes Dev* 22(15):1998-2021.
101. D'Amour KA, *et al.* (2006) Production of pancreatic hormone-expressing endocrine cells from human embryonic stem cells. *Nat Biotechnol* 24(11):1392-1401.
102. Chetty S, *et al.* (2013) A simple tool to improve pluripotent stem cell differentiation. *Nat Methods* 10(6):553-556.

103. D'Amour KA, *et al.* (2005) Efficient differentiation of human embryonic stem cells to definitive endoderm. *Nat Biotechnol* 23(12):1534-1541.
104. Kubo A, *et al.* (2004) Development of definitive endoderm from embryonic stem cells in culture. *Development* 131(7):1651-1662.
105. Seguin CA, Draper JS, Nagy A, & Rossant J (2008) Establishment of endoderm progenitors by SOX transcription factor expression in human embryonic stem cells. *Cell Stem Cell* 3(2):182-195.
106. Brown S, *et al.* (2011) Activin/Nodal signaling controls divergent transcriptional networks in human embryonic stem cells and in endoderm progenitors. *Stem Cells* 29(8):1176-1185.
107. Yasunaga M, *et al.* (2005) Induction and monitoring of definitive and visceral endoderm differentiation of mouse ES cells. *Nat Biotechnol* 23(12):1542-1550.
108. Cheng X, *et al.* (2012) Self-renewing endodermal progenitor lines generated from human pluripotent stem cells. *Cell Stem Cell* 10(4):371-384.
109. Mou H, *et al.* (2012) Generation of multipotent lung and airway progenitors from mouse ESCs and patient-specific cystic fibrosis iPSCs. *Cell Stem Cell* 10(4):385-397.
110. Basma H, *et al.* (2009) Differentiation and transplantation of human embryonic stem cell-derived hepatocytes. *Gastroenterology* 136(3):990-999.
111. Touboul T, *et al.* (2010) Generation of functional hepatocytes from human embryonic stem cells under chemically defined conditions that recapitulate liver development. *Hepatology* 51(5):1754-1765.
112. Gouon-Evans V, *et al.* (2006) BMP-4 is required for hepatic specification of mouse embryonic stem cell-derived definitive endoderm. *Nat Biotechnol* 24(11):1402-1411.
113. Hannan NR, Segeritz CP, Touboul T, & Vallier L (2013) Production of hepatocyte-like cells from human pluripotent stem cells. *Nat Protoc* 8(2):430-437.
114. Spence JR, *et al.* (2011) Directed differentiation of human pluripotent stem cells into intestinal tissue in vitro. *Nature* 470(7332):105-109.
115. Green MD, *et al.* (2011) Generation of anterior foregut endoderm from human embryonic and induced pluripotent stem cells. *Nat Biotechnol* 29(3):267-272.
116. Kearns NA, *et al.* (2013) Generation of organized anterior foregut epithelia from pluripotent stem cells using small molecules. *Stem Cell Res* 11(3):1003-1012.
117. Kroon E, *et al.* (2008) Pancreatic endoderm derived from human embryonic stem cells generates glucose-responsive insulin-secreting cells in vivo. *Nat Biotechnol* 26(4):443-452.
118. Nostro MC, *et al.* (2011) Stage-specific signaling through TGFbeta family members and WNT regulates patterning and pancreatic specification of human pluripotent stem cells. *Development* 138(5):861-871.
119. Schulz TC, *et al.* (2012) A scalable system for production of functional pancreatic progenitors from human embryonic stem cells. *PLoS ONE* 7(5):e37004.
120. Cai J, *et al.* (2010) Generation of homogeneous PDX1(+) pancreatic progenitors from human ES cell-derived endoderm cells. *Journal of molecular cell biology* 2(1):50-60.
121. Mfopou JK, Chen B, Mateizel I, Sermon K, & Bouwens L (2010) Noggin, retinoids, and fibroblast growth factor regulate hepatic or pancreatic fate of human embryonic stem cells. *Gastroenterology* 138(7):2233-2245, 2245 e2231-2214.

122. Mfopou JK, De Groote V, Xu X, Heimberg H, & Bouwens L (2007) Sonic hedgehog and other soluble factors from differentiating embryoid bodies inhibit pancreas development. *Stem Cells* 25(5):1156-1165.
123. Sui L, Geens M, Sermon K, Bouwens L, & Mfopou JK (2013) Role of BMP signaling in pancreatic progenitor differentiation from human embryonic stem cells. *Stem Cell Rev* 9(5):569-577.
124. Cho CH, *et al.* (2012) Inhibition of activin/nodal signalling is necessary for pancreatic differentiation of human pluripotent stem cells. *Diabetologia* 55(12):3284-3295.
125. Rezania A, *et al.* (2012) Maturation of human embryonic stem cell-derived pancreatic progenitors into functional islets capable of treating pre-existing diabetes in mice. *Diabetes* 61(8):2016-2029.
126. Rezania A, *et al.* (2013) Enrichment of human embryonic stem cell-derived NKX6.1-expressing pancreatic progenitor cells accelerates the maturation of insulin-secreting cells in vivo. *Stem Cells* 31(11):2432-2442.
127. Rezania A, *et al.* (2011) Production of functional glucagon-secreting alpha-cells from human embryonic stem cells. *Diabetes* 60(1):239-247.
128. Kelly OG, *et al.* (2011) Cell-surface markers for the isolation of pancreatic cell types derived from human embryonic stem cells. *Nat Biotechnol* 29(8):750-756.
129. Zhang C, *et al.* (2005) MafA is a key regulator of glucose-stimulated insulin secretion. *Mol Cell Biol* 25(12):4969-4976.
130. Jiang J, *et al.* (2007) Generation of insulin-producing islet-like clusters from human embryonic stem cells. *Stem Cells* 25(8):1940-1953.
131. Jiang W, *et al.* (2007) In vitro derivation of functional insulin-producing cells from human embryonic stem cells. *Cell Res* 17(4):333-344.
132. Xu X, Browning VL, & Odorico JS (2011) Activin, BMP and FGF pathways cooperate to promote endoderm and pancreatic lineage cell differentiation from human embryonic stem cells. *Mech Dev* 128(7-10):412-427.
133. Wideman RD & Kieffer TJ (2009) Mining incretin hormone pathways for novel therapies. *Trends Endocrinol Metab* 20(6):280-286.
134. Guo T, Landsman L, Li N, & Hebrok M (2013) Factors expressed by murine embryonic pancreatic mesenchyme enhance generation of insulin-producing cells from hESCs. *Diabetes* 62(5):1581-1592.
135. Chen M, *et al.* (2009) Small-molecule selectively recognizes human telomeric G-quadruplex DNA and regulates its conformational switch. *Biophys J* 97(7):2014-2023.
136. Bruin JE, *et al.* (2013) Maturation and function of human embryonic stem cell-derived pancreatic progenitors in macroencapsulation devices following transplant into mice. *Diabetologia* 56(9):1987-1998.
137. Segev H, Fishman B, Ziskind A, Shulman M, & Itskovitz-Eldor J (2004) Differentiation of human embryonic stem cells into insulin-producing clusters. *Stem Cells* 22(3):265-274.
138. Basford CL, *et al.* (2012) The functional and molecular characterisation of human embryonic stem cell-derived insulin-positive cells compared with adult pancreatic beta cells. *Diabetologia* 55(2):358-371.
139. Jiang W, *et al.* (2008) Differentiation of mouse nuclear transfer embryonic stem cells into functional pancreatic beta cells. *Diabetologia* 51(9):1671-1679.

140. Martens GA, *et al.* (2014) Functional characteristics of neonatal rat beta cells with distinct markers. *J Mol Endocrinol* 52(1):11-28.
141. Jermendy A, *et al.* (2011) Rat neonatal beta cells lack the specialised metabolic phenotype of mature beta cells. *Diabetologia* 54(3):594-604.
142. Hayek A & Beattie GM (1997) Experimental transplantation of human fetal and adult pancreatic islets. *J Clin Endocrinol Metab* 82(8):2471-2475.
143. Castaing M, *et al.* (2001) Blood glucose normalization upon transplantation of human embryonic pancreas into beta-cell-deficient SCID mice. *Diabetologia* 44(11):2066-2076.
144. Gutteridge A, *et al.* (2013) Novel pancreatic endocrine maturation pathways identified by genomic profiling and causal reasoning. *PLoS ONE* 8(2):e56024.
145. Vasir B, *et al.* (2001) Gene expression of VEGF and its receptors Flk-1/KDR and Flt-1 in cultured and transplanted rat islets. *Transplantation* 71(7):924-935.
146. Jansson L & Carlsson PO (2002) Graft vascular function after transplantation of pancreatic islets. *Diabetologia* 45(6):749-763.
147. Zhang N, *et al.* (2004) Elevated vascular endothelial growth factor production in islets improves islet graft vascularization. *Diabetes* 53(4):963-970.
148. Brissova M, *et al.* (2006) Pancreatic islet production of vascular endothelial growth factor--a is essential for islet vascularization, revascularization, and function. *Diabetes* 55(11):2974-2985.
149. Schaffer AE, *et al.* (2013) Nkx6.1 controls a gene regulatory network required for establishing and maintaining pancreatic Beta cell identity. *PLoS Genet* 9(1):e1003274.
150. Gauthier BR, Gosmain Y, Mamin A, & Philippe J (2007) The beta-cell specific transcription factor Nkx6.1 inhibits glucagon gene transcription by interfering with Pax6. *Biochem J* 403(3):593-601.
151. Dobreva MP, Pereira PN, Deprest J, & Zwijsen A (2010) On the origin of amniotic stem cells: of mice and men. *Int J Dev Biol* 54(5):761-777.
152. Fauza D (2004) Amniotic fluid and placental stem cells. *Best practice & research. Clinical obstetrics & gynaecology* 18(6):877-891.
153. Gosden CM (1983) Amniotic fluid cell types and culture. *British medical bulletin* 39(4):348-354.
154. Siegel N, Rosner M, Hanneder M, Freilinger A, & Hengstschlager M (2008) Human amniotic fluid stem cells: a new perspective. *Amino Acids* 35(2):291-293.
155. In 't Anker PS, *et al.* (2003) Amniotic fluid as a novel source of mesenchymal stem cells for therapeutic transplantation. *Blood* 102(4):1548-1549.
156. Zhou Q, Brown J, Kanarek A, Rajagopal J, & Melton DA (2008) In vivo reprogramming of adult pancreatic exocrine cells to beta-cells. *Nature*.
157. Grapin-Botton A, Majithia AR, & Melton DA (2001) Key events of pancreas formation are triggered in gut endoderm by ectopic expression of pancreatic regulatory genes. *Genes Dev* 15(4):444-454.
158. Li WC, Horb ME, Tosh D, & Slack JM (2005) In vitro transdifferentiation of hepatoma cells into functional pancreatic cells. *Mech Dev* 122(6):835-847.
159. Mombaerts P, *et al.* (1992) RAG-1-deficient mice have no mature B and T lymphocytes. *Cell* 68(5):869-877.

160. Hou Y, Huang Q, Liu T, & Guo L (2008) Human amnion epithelial cells can be induced to differentiate into functional insulin-producing cells. *Acta Biochim Biophys Sin (Shanghai)* 40(9):830-839.
161. Wei JP, *et al.* (2003) Human amnion-isolated cells normalize blood glucose in streptozotocin-induced diabetic mice. *Cell Transplant* 12(5):545-552.
162. Portha B & Kergoat M (1985) Dynamics of glucose-induced insulin release during the spontaneous remission of streptozocin diabetes induced in the newborn rat. *Diabetes* 34(6):574-579.
163. Li Y, *et al.* (2007) Generation of insulin-producing cells from PDX-1 gene-modified human mesenchymal stem cells. *J Cell Physiol* 211(1):36-44.
164. Naya FJ, Stellrecht CM, & Tsai MJ (1995) Tissue-specific regulation of the insulin gene by a novel basic helix-loop-helix transcription factor. *Genes Dev* 9(8):1009-1019.
165. Ohlsson H, Karlsson K, & Edlund T (1993) IPF1, a homeodomain-containing transactivator of the insulin gene. *EMBO J* 12(11):4251-4259.
166. Olbrot M, Rud J, Moss LG, & Sharma A (2002) Identification of beta-cell-specific insulin gene transcription factor RIPE3b1 as mammalian MafA. *Proc Natl Acad Sci U S A* 99(10):6737-6742.
167. Zhang H, *et al.* (2009) The LIM-homeodomain protein ISL1 activates insulin gene promoter directly through synergy with BETA2. *J Mol Biol* 392(3):566-577.
168. Sander M, *et al.* (1997) Genetic analysis reveals that PAX6 is required for normal transcription of pancreatic hormone genes and islet development. *Genes Dev* 11(13):1662-1673.
169. Jin T (2008) Mechanisms underlying proglucagon gene expression. *J Endocrinol* 198(1):17-28.
170. Gosmain Y, *et al.* (2010) Pax6 controls the expression of critical genes involved in pancreatic {alpha} cell differentiation and function. *J Biol Chem* 285(43):33381-33393.
171. St-Onge L, Sosa-Pineda B, Chowdhury K, Mansouri A, & Gruss P (1997) Pax6 is required for differentiation of glucagon-producing alpha-cells in mouse pancreas. *Nature* 387(6631):406-409.
172. Wei R, *et al.* (2013) Dynamic expression of microRNAs during the differentiation of human embryonic stem cells into insulin-producing cells. *Gene* 518(2):246-255.
173. Amit M, *et al.* (2000) Clonally derived human embryonic stem cell lines maintain pluripotency and proliferative potential for prolonged periods of culture. *Dev Biol* 227(2):271-278.
174. O'Connor MD, *et al.* (2008) Alkaline phosphatase-positive colony formation is a sensitive, specific, and quantitative indicator of undifferentiated human embryonic stem cells. *Stem Cells* 26(5):1109-1116.
175. Hasegawa K, Fujioka T, Nakamura Y, Nakatsuji N, & Suemori H (2006) A method for the selection of human embryonic stem cell sublines with high replating efficiency after single-cell dissociation. *Stem Cells* 24(12):2649-2660.
176. Watanabe K, *et al.* (2007) A ROCK inhibitor permits survival of dissociated human embryonic stem cells. *Nat Biotechnol* 25(6):681-686.
177. Sun Y, *et al.* (2012) Mechanics regulates fate decisions of human embryonic stem cells. *PLoS ONE* 7(5):e37178.

178. Li D, *et al.* (2010) Integrated biochemical and mechanical signals regulate multifaceted human embryonic stem cell functions. *J Cell Biol* 191(3):631-644.
179. Chen G, Hou Z, Gulbranson DR, & Thomson JA (2010) Actin-myosin contractility is responsible for the reduced viability of dissociated human embryonic stem cells. *Cell Stem Cell* 7(2):240-248.
180. Ellerstrom C, Strehl R, Noaksson K, Hyllner J, & Semb H (2007) Facilitated expansion of human embryonic stem cells by single-cell enzymatic dissociation. *Stem Cells* 25(7):1690-1696.
181. Suemori H, *et al.* (2006) Efficient establishment of human embryonic stem cell lines and long-term maintenance with stable karyotype by enzymatic bulk passage. *Biochem Biophys Res Commun* 345(3):926-932.
182. Denning C, *et al.* (2006) Common culture conditions for maintenance and cardiomyocyte differentiation of the human embryonic stem cell lines, BG01 and HUES-7. *Int J Dev Biol* 50(1):27-37.
183. Draper JS, *et al.* (2004) Recurrent gain of chromosomes 17q and 12 in cultured human embryonic stem cells. *Nat Biotechnol* 22(1):53-54.
184. Werbowetski-Ogilvie TE, *et al.* (2009) Characterization of human embryonic stem cells with features of neoplastic progression. *Nat Biotechnol* 27(1):91-97.
185. Andrews PW, *et al.* (2005) Embryonic stem (ES) cells and embryonal carcinoma (EC) cells: opposite sides of the same coin. *Biochem Soc Trans* 33(Pt 6):1526-1530.
186. O'Connor MD, *et al.* (2011) Retinoblastoma-binding proteins 4 and 9 are important for human pluripotent stem cell maintenance. *Exp Hematol* 39(8):866-879 e861.
187. Vierbuchen T & Wernig M (2012) Molecular roadblocks for cellular reprogramming. *Mol Cell* 47(6):827-838.
188. Lund RJ, Narva E, & Lahesmaa R (2012) Genetic and epigenetic stability of human pluripotent stem cells. *Nat Rev Genet* 13(10):732-744.
189. Ishizaki T, *et al.* (2000) Pharmacological properties of Y-27632, a specific inhibitor of rho-associated kinases. *Mol Pharmacol* 57(5):976-983.
190. Riento K & Ridley AJ (2003) Rocks: multifunctional kinases in cell behaviour. *Nat Rev Mol Cell Biol* 4(6):446-456.
191. Richards M, *et al.* (2003) Comparative evaluation of various human feeders for prolonged undifferentiated growth of human embryonic stem cells. *Stem Cells* 21(5):546-556.
192. Mallon BS, Park KY, Chen KG, Hamilton RS, & McKay RD (2006) Toward xeno-free culture of human embryonic stem cells. *Int J Biochem Cell Biol* 38(7):1063-1075.
193. Xu C, *et al.* (2001) Feeder-free growth of undifferentiated human embryonic stem cells. *Nat Biotechnol* 19(10):971-974.
194. Ludwig TE, *et al.* (2006) Feeder-independent culture of human embryonic stem cells. *Nat Methods* 3(8):637-646.
195. Ludwig TE, *et al.* (2006) Derivation of human embryonic stem cells in defined conditions. *Nat Biotechnol* 24(2):185-187.
196. O'Connor MD, Kardel MD, & Eaves CJ (2011) Functional assays for human embryonic stem cell pluripotency. *Methods Mol Biol* 690:67-80.

197. Caron NJ, Quenneville SP, & Tremblay JP (2004) Endosome disruption enhances the functional nuclear delivery of Tat-fusion proteins. *Biochem Biophys Res Commun* 319(1):12-20.
198. Fujita Y, Asadi A, Yang GK, Kwok YN, & Kieffer TJ (2010) Differential processing of pro-glucose-dependent insulinotropic polypeptide in gut. *Am J Physiol Gastrointest Liver Physiol* 298(5):G608-614.
199. Peerani R, *et al.* (2007) Niche-mediated control of human embryonic stem cell self-renewal and differentiation. *EMBO J* 26(22):4744-4755.
200. Narva E, *et al.* (2010) High-resolution DNA analysis of human embryonic stem cell lines reveals culture-induced copy number changes and loss of heterozygosity. *Nat Biotechnol* 28(4):371-377.
201. Wu H, *et al.* (2008) Copy number variant analysis of human embryonic stem cells. *Stem Cells* 26(6):1484-1489.
202. Spits C, *et al.* (2008) Recurrent chromosomal abnormalities in human embryonic stem cells. *Nat Biotechnol* 26(12):1361-1363.
203. Lefort N, *et al.* (2008) Human embryonic stem cells reveal recurrent genomic instability at 20q11.21. *Nat Biotechnol* 26(12):1364-1366.
204. Desbordes SC, *et al.* (2008) High-throughput screening assay for the identification of compounds regulating self-renewal and differentiation in human embryonic stem cells. *Cell Stem Cell* 2(6):602-612.
205. Stewart MH, *et al.* (2006) Clonal isolation of hESCs reveals heterogeneity within the pluripotent stem cell compartment. *Nat Methods* 3(10):807-815.
206. Zhang JH, Chung TD, & Oldenburg KR (1999) A Simple Statistical Parameter for Use in Evaluation and Validation of High Throughput Screening Assays. *J Biomol Screen* 4(2):67-73.
207. Osafune K, *et al.* (2008) Marked differences in differentiation propensity among human embryonic stem cell lines. *Nat Biotechnol* 26(3):313-315.
208. McKnight KD, Wang P, & Kim SK (2010) Deconstructing pancreas development to reconstruct human islets from pluripotent stem cells. *Cell Stem Cell* 6(4):300-308.
209. Bruin J & Kieffer T (2012) Differentiation of Human Embryonic Stem Cells into Pancreatic Endocrine Cells. *Stem Cells and Cancer Stem Cells, Volume 8,* Stem Cells and Cancer Stem Cells, ed Hayat MA (Springer Netherlands), Vol 8, pp 191-206.
210. Bruin JE, *et al.* (2014) Characterization of polyhormonal insulin-producing cells derived in vitro from human embryonic stem cells. *Stem Cell Res* 12(1):194-208.
211. Cabrera O, *et al.* (2006) The unique cytoarchitecture of human pancreatic islets has implications for islet cell function. *Proc Natl Acad Sci U S A* 103(7):2334-2339.
212. Brissova M, *et al.* (2005) Assessment of human pancreatic islet architecture and composition by laser scanning confocal microscopy. *J Histochem Cytochem* 53(9):1087-1097.
213. Heller RS (2010) The comparative anatomy of islets. *Adv Exp Med Biol* 654:21-37.
214. Kim A, *et al.* (2009) Islet architecture: A comparative study. *Islets* 1(2):129-136.
215. Guo T & Hebrok M (2009) Stem cells to pancreatic beta-cells: new sources for diabetes cell therapy. *Endocr Rev* 30(3):214-227.
216. Ghosh S, *et al.* (2010) Cell density-dependent transcriptional activation of endocrine-related genes in human adipose tissue-derived stem cells. *Exp Cell Res* 316(13):2087-2098.

217. Pfaffl MW (2001) A new mathematical model for relative quantification in real-time RT-PCR. *Nucleic Acids Res* 29(9):e45.
218. Weinberg RA (1995) The retinoblastoma protein and cell cycle control. *Cell* 81(3):323-330.
219. Sela Y, Molotski N, Golan S, Itskovitz-Eldor J, & Soen Y (2012) Human embryonic stem cells exhibit increased propensity to differentiate during the G1 phase prior to phosphorylation of retinoblastoma protein. *Stem Cells* 30(6):1097-1108.
220. Calder A, *et al.* (2013) Lengthened G1 phase indicates differentiation status in human embryonic stem cells. *Stem Cells Dev* 22(2):279-295.
221. Pauklin S & Vallier L (2013) The cell-cycle state of stem cells determines cell fate propensity. *Cell* 155(1):135-147.
222. Sarkar SA, *et al.* (2008) Global gene expression profiling and histochemical analysis of the developing human fetal pancreas. *Diabetologia* 51(2):285-297.
223. Artner I, *et al.* (2010) MafA and MafB regulate genes critical to beta-cells in a unique temporal manner. *Diabetes* 59(10):2530-2539.
224. Becker KA, *et al.* (2010) Cyclin D2 and the CDK substrate p220(NPAT) are required for self-renewal of human embryonic stem cells. *J Cell Physiol* 222(2):456-464.
225. Becker KA, *et al.* (2006) Self-renewal of human embryonic stem cells is supported by a shortened G1 cell cycle phase. *J Cell Physiol* 209(3):883-893.
226. Becker KA, Stein JL, Lian JB, van Wijnen AJ, & Stein GS (2010) Human embryonic stem cells are pre-mitotically committed to self-renewal and acquire a lengthened G1 phase upon lineage programming. *J Cell Physiol* 222(1):103-110.
227. Becker KA, Stein JL, Lian JB, van Wijnen AJ, & Stein GS (2007) Establishment of histone gene regulation and cell cycle checkpoint control in human embryonic stem cells. *J Cell Physiol* 210(2):517-526.
228. Collombat P, *et al.* (2007) Embryonic endocrine pancreas and mature beta cells acquire alpha and PP cell phenotypes upon Arx misexpression. *J Clin Invest* 117(4):961-970.
229. Collombat P, *et al.* (2003) Opposing actions of Arx and Pax4 in endocrine pancreas development. *Genes Dev* 17(20):2591-2603.
230. Sosa-Pineda B, Chowdhury K, Torres M, Oliver G, & Gruss P (1997) The Pax4 gene is essential for differentiation of insulin-producing beta cells in the mammalian pancreas. *Nature* 386(6623):399-402.
231. Lyttle BM, *et al.* (2008) Transcription factor expression in the developing human fetal endocrine pancreas. *Diabetologia* 51(7):1169-1180.
232. Plengvidhya N, *et al.* (2007) PAX4 mutations in Thais with maturity onset diabetes of the young. *J Clin Endocrinol Metab* 92(7):2821-2826.
233. Blyszczuk P, *et al.* (2003) Expression of Pax4 in embryonic stem cells promotes differentiation of nestin-positive progenitor and insulin-producing cells. *Proc Natl Acad Sci U S A* 100(3):998-1003.
234. Liew CG, *et al.* (2008) PAX4 enhances beta-cell differentiation of human embryonic stem cells. *PLoS ONE* 3(3):e1783.
235. Schwitzgebel VM, *et al.* (2000) Expression of neurogenin3 reveals an islet cell precursor population in the pancreas. *Development* 127(16):3533-3542.
236. Apelqvist A, *et al.* (1999) Notch signalling controls pancreatic cell differentiation. *Nature* 400(6747):877-881.

237. Smith SB, *et al.* (2003) Neurogenin3 and hepatic nuclear factor 1 cooperate in activating pancreatic expression of Pax4. *J Biol Chem* 278(40):38254-38259.
238. Brun T, *et al.* (2008) The diabetes-linked transcription factor Pax4 is expressed in human pancreatic islets and is activated by mitogens and GLP-1. *Hum Mol Genet* 17(4):478-489.
239. Brun T, *et al.* (2004) The diabetes-linked transcription factor PAX4 promotes {beta}-cell proliferation and survival in rat and human islets. *J Cell Biol* 167(6):1123-1135.
240. Sosa-Pineda B (2004) The gene Pax4 is an essential regulator of pancreatic beta-cell development. *Mol Cells* 18(3):289-294.
241. Smith SB, Ee HC, Conners JR, & German MS (1999) Paired-homeodomain transcription factor PAX4 acts as a transcriptional repressor in early pancreatic development. *Mol Cell Biol* 19(12):8272-8280.
242. Smith SB, Watada H, Scheel DW, Mrejen C, & German MS (2000) Autoregulation and maturity onset diabetes of the young transcription factors control the human PAX4 promoter. *J Biol Chem* 275(47):36910-36919.
243. Collombat P, *et al.* (2005) The simultaneous loss of Arx and Pax4 genes promotes a somatostatin-producing cell fate specification at the expense of the alpha- and beta-cell lineages in the mouse endocrine pancreas. *Development* 132(13):2969-2980.
244. In't Veld P & Marichal M (2010) Microscopic anatomy of the human islet of Langerhans. *Adv Exp Med Biol* 654:1-19.
245. Dorrell C, *et al.* (2011) Transcriptomes of the major human pancreatic cell types. *Diabetologia* 54(11):2832-2844.
246. Kitamura K, *et al.* (2002) Mutation of ARX causes abnormal development of forebrain and testes in mice and X-linked lissencephaly with abnormal genitalia in humans. *Nat Genet* 32(3):359-369.
247. Miura H, Yanazawa M, Kato K, & Kitamura K (1997) Expression of a novel aristaless related homeobox gene 'Arx' in the vertebrate telencephalon, diencephalon and floor plate. *Mech Dev* 65(1-2):99-109.
248. Du A, *et al.* (2012) Arx is required for normal enteroendocrine cell development in mice and humans. *Dev Biol* 365(1):175-188.
249. Ohira R, *et al.* (2002) Human ARX gene: genomic characterization and expression. *Mol Genet Metab* 77(1-2):179-188.
250. Stromme P, *et al.* (2002) Mutations in the human ortholog of Aristaless cause X-linked mental retardation and epilepsy. *Nat Genet* 30(4):441-445.
251. Shoubridge C, Fullston T, & Gecz J (2010) ARX spectrum disorders: making inroads into the molecular pathology. *Hum Mutat* 31(8):889-900.
252. Itoh M, *et al.* (2010) Partial loss of pancreas endocrine and exocrine cells of human ARX-null mutation: consideration of pancreas differentiation. *Differentiation* 80(2-3):118-122.
253. Engler C, Kandzia R, & Marillonnet S (2008) A one pot, one step, precision cloning method with high throughput capability. *PLoS ONE* 3(11):e3647.
254. Miyata R, *et al.* (2009) Analysis of the hypothalamus in a case of X-linked lissencephaly with abnormal genitalia (XLAG). *Brain Dev* 31(6):456-460.
255. Wilcox CL, Terry NA, & May CL (2013) Arx Polyalanine Expansion in Mice Leads to Reduced Pancreatic alpha-Cell Specification and Increased alpha-Cell Death. *PLoS ONE* 8(11):e78741.

256. Goudet G, Delhalle S, Biemar F, Martial JA, & Peers B (1999) Functional and cooperative interactions between the homeodomain PDX1, Pbx, and Prep1 factors on the somatostatin promoter. *J Biol Chem* 274(7):4067-4073.
257. Brakch N, Galanopoulou AS, Patel YC, Boileau G, & Seidah NG (1995) Comparative proteolytic processing of rat prosomatostatin by the convertases PC1, PC2, furin, PACE4 and PC5 in constitutive and regulated secretory pathways. *FEBS Lett* 362(2):143-146.
258. Furuta M, *et al.* (1997) Defective prohormone processing and altered pancreatic islet morphology in mice lacking active SPC2. *Proc Natl Acad Sci U S A* 94(13):6646-6651.
259. Bersani M, Thim L, Baldissera FG, & Holst JJ (1989) Prosomatostatin 1-64 is a major product of somatostatin gene expression in pancreas and gut. *J Biol Chem* 264(18):10633-10636.
260. Zhu X, *et al.* (2002) Disruption of PC1/3 expression in mice causes dwarfism and multiple neuroendocrine peptide processing defects. *Proc Natl Acad Sci U S A* 99(16):10293-10298.
261. Sussel L, *et al.* (1998) Mice lacking the homeodomain transcription factor Nkx2.2 have diabetes due to arrested differentiation of pancreatic beta cells. *Development* 125(12):2213-2221.
262. Prado CL, Pugh-Bernard AE, Elghazi L, Sosa-Pineda B, & Sussel L (2004) Ghrelin cells replace insulin-producing beta cells in two mouse models of pancreas development. *Proc Natl Acad Sci U S A* 101(9):2924-2929.
263. Mastracci TL, *et al.* (2011) Nkx2.2 and Arx genetically interact to regulate pancreatic endocrine cell development and endocrine hormone expression. *Dev Biol* 359(1):1-11.
264. Kodra JT, *et al.* (2008) Novel glucagon receptor antagonists with improved selectivity over the glucose-dependent insulinotropic polypeptide receptor. *J Med Chem* 51(17):5387-5396.
265. Andersen FG, *et al.* (1999) Pax6 and Pdx1 form a functional complex on the rat somatostatin gene upstream enhancer. *FEBS Lett* 445(2-3):315-320.
266. Andersen FG, *et al.* (1999) Pax6 and Cdx2/3 form a functional complex on the rat glucagon gene promoter G1-element. *FEBS Lett* 445(2-3):306-310.
267. Hussain MA, Lee J, Miller CP, & Habener JF (1997) POU domain transcription factor brain 4 confers pancreatic alpha-cell-specific expression of the proglucagon gene through interaction with a novel proximal promoter G1 element. *Mol Cell Biol* 17(12):7186-7194.
268. Heller RS, *et al.* (2004) The role of Brn4/Pou3f4 and Pax6 in forming the pancreatic glucagon cell identity. *Dev Biol* 268(1):123-134.
269. Wen JH, *et al.* (2009) Paired box 6 (PAX6) regulates glucose metabolism via proinsulin processing mediated by prohormone convertase 1/3 (PC1/3). *Diabetologia* 52(3):504-513.
270. Dorrell C, *et al.* (2008) Isolation of major pancreatic cell types and long-term culture-initiating cells using novel human surface markers. *Stem Cell Res* 1(3):183-194.
271. Petri A, *et al.* (2006) The effect of neurogenin3 deficiency on pancreatic gene expression in embryonic mice. *J Mol Endocrinol* 37(2):301-316.

272. Ragvin A, *et al.* (2010) Long-range gene regulation links genomic type 2 diabetes and obesity risk regions to HHEX, SOX4, and IRX3. *Proc Natl Acad Sci U S A* 107(2):775-780.
273. Braun M, *et al.* (2009) Somatostatin release, electrical activity, membrane currents and exocytosis in human pancreatic delta cells. *Diabetologia* 52(8):1566-1578.
274. Quesada I, Nadal A, & Soria B (1999) Different effects of tolbutamide and diazoxide in alpha, beta-, and delta-cells within intact islets of Langerhans. *Diabetes* 48(12):2390-2397.
275. Hauge-Evans AC, *et al.* (2009) Somatostatin secreted by islet delta-cells fulfills multiple roles as a paracrine regulator of islet function. *Diabetes* 58(2):403-411.
276. Hauge-Evans AC, King AJ, Fairhall K, Persaud SJ, & Jones PM (2010) A role for islet somatostatin in mediating sympathetic regulation of glucagon secretion. *Islets* 2(6):341-344.
277. Rutter GA (2009) Regulating glucagon secretion: somatostatin in the spotlight. *Diabetes* 58(2):299-301.
278. Heinis M, *et al.* (2010) Oxygen tension regulates pancreatic beta-cell differentiation through hypoxia-inducible factor 1alpha. *Diabetes* 59(3):662-669.
279. Miyatsuka T, Kosaka Y, Kim H, & German MS (2011) Neurogenin3 inhibits proliferation in endocrine progenitors by inducing Cdkn1a. *Proc Natl Acad Sci U S A* 108(1):185-190.
280. Hart AW, Mella S, Mendrychowski J, van Heyningen V, & Kleinjan DA (2013) The developmental regulator Pax6 is essential for maintenance of islet cell function in the adult mouse pancreas. *PLoS ONE* 8(1):e54173.
281. Zhang J, McKenna LB, Bogue CW, & Kaestner KH (2014) The diabetes gene Hhex maintains delta-cell differentiation and islet function. *Genes Dev* 28(8):829-834.
282. Dorrell C, *et al.* (2013) Erratum to: Transcriptomes of the major human pancreatic cell types. *Diabetologia* 56(5):1192-1192.
283. Bock C, *et al.* (2011) Reference Maps of human ES and iPS cell variation enable high-throughput characterization of pluripotent cell lines. *Cell* 144(3):439-452.
284. Lumelsky N, *et al.* (2001) Differentiation of embryonic stem cells to insulin-secreting structures similar to pancreatic islets. *Science* 292(5520):1389-1394.
285. Hansson M, *et al.* (2004) Artifactual insulin release from differentiated embryonic stem cells. *Diabetes* 53(10):2603-2609.
286. Rajagopal J, Anderson WJ, Kume S, Martinez OI, & Melton DA (2003) Insulin staining of ES cell progeny from insulin uptake. *Science* 299(5605):363.
287. Halban PA, Kahn SE, Lernmark A, & Rhodes CJ (2001) Gene and cell-replacement therapy in the treatment of type 1 diabetes: how high must the standards be set? *Diabetes* 50(10):2181-2191.
288. Wong AL, Hwa A, Hellman D, & Greenstein JL (2012) Surrogate insulin-producing cells. *F1000 medicine reports* 4:15.
289. Maes E & Pipeleers D (1984) Effects of glucose and 3',5'-cyclic adenosine monophosphate upon reaggregation of single pancreatic B-cells. *Endocrinology* 114(6):2205-2209.
290. Pipeleers D, in't Veld PI, Maes E, & Van De Winkel M (1982) Glucose-induced insulin release depends on functional cooperation between islet cells. *Proc Natl Acad Sci U S A* 79(23):7322-7325.

291. Bosco D, *et al.* (2010) Unique arrangement of alpha- and beta-cells in human islets of Langerhans. *Diabetes* 59(5):1202-1210.
292. Steiner DJ, Kim A, Miller K, & Hara M (2010) Pancreatic islet plasticity: interspecies comparison of islet architecture and composition. *Islets* 2(3):135-145.
293. Brunicardi FC, *et al.* (2001) Immunoneutralization of somatostatin, insulin, and glucagon causes alterations in islet cell secretion in the isolated perfused human pancreas. *Pancreas* 23(3):302-308.
294. King AJ, *et al.* (2007) Normal relationship of beta- and non-beta-cells not needed for successful islet transplantation. *Diabetes* 56(9):2312-2318.
295. Docherty K, Bernardo AS, & Vallier L (2007) Embryonic stem cell therapy for diabetes mellitus. *Semin Cell Dev Biol* 18(6):827-838.
296. Chen X, *et al.* (2010) Investigations into the metabolism of two-dimensional colony and suspended microcarrier cultures of human embryonic stem cells in serum-free media. *Stem Cells Dev* 19(11):1781-1792.
297. Zweigerdt R, Olmer R, Singh H, Haverich A, & Martin U (2011) Scalable expansion of human pluripotent stem cells in suspension culture. *Nat Protoc* 6(5):689-700.
298. Wong AL & Nierras CR (2010) Do stem cell-derived islets represent a commercially viable treatment for Type 1 and 2 diabetes? *Regenerative medicine* 5(6):839-842.
299. Borowiak M, *et al.* (2009) Small molecules efficiently direct endodermal differentiation of mouse and human embryonic stem cells. *Cell Stem Cell* 4(4):348-358.
300. Chen S, *et al.* (2009) A small molecule that directs differentiation of human ESCs into the pancreatic lineage. *Nat Chem Biol* 5(4):258-265.
301. Mohanakumar T, *et al.* (2006) A significant role for histocompatibility in human islet transplantation. *Transplantation* 82(2):180-187.
302. Scharp DW, *et al.* (1990) Insulin independence after islet transplantation into type I diabetic patient. *Diabetes* 39(4):515-518.
303. O'Sullivan ES, Vegas A, Anderson DG, & Weir GC (2011) Islets transplanted in immunoisolation devices: a review of the progress and the challenges that remain. *Endocr Rev* 32(6):827-844.
304. Weir GC (2013) Islet encapsulation: advances and obstacles. *Diabetologia* 56(7):1458-1461.
305. Scharp DW & Marchetti P (2013) Encapsulated islets for diabetes therapy: History, current progress, and critical issues requiring solution. *Adv Drug Deliv Rev*.
306. De Vos P, *et al.* (1999) Why do microencapsulated islet grafts fail in the absence of fibrotic overgrowth? *Diabetes* 48(7):1381-1388.
307. Duvivier-Kali VF, Omer A, Parent RJ, O'Neil JJ, & Weir GC (2001) Complete protection of islets against allorejection and autoimmunity by a simple barium-alginate membrane. *Diabetes* 50(8):1698-1705.
308. Jacobs-Tulleneers-Thevissen D, *et al.* (2013) Sustained function of alginate-encapsulated human islet cell implants in the peritoneal cavity of mice leading to a pilot study in a type 1 diabetic patient. *Diabetologia* 56(7):1605-1614.
309. Hoesli CA, *et al.* (2011) Pancreatic cell immobilization in alginate beads produced by emulsion and internal gelation. *Biotechnol Bioeng* 108(2):424-434.

310. Hoesli CA, *et al.* (2012) Reversal of diabetes by betaTC3 cells encapsulated in alginate beads generated by emulsion and internal gelation. *Journal of biomedical materials research. Part B, Applied biomaterials* 100(4):1017-1028.
311. Ludwig B, *et al.* (2012) Improvement of islet function in a bioartificial pancreas by enhanced oxygen supply and growth hormone releasing hormone agonist. *Proc Natl Acad Sci U S A* 109(13):5022-5027.
312. Rafael E, Wu GS, Hultenby K, Tibell A, & Wernerson A (2003) Improved survival of macroencapsulated islets of Langerhans by preimplantation of the immunoisolating device: a morphometric study. *Cell Transplant* 12(4):407-412.
313. Ludwig B, *et al.* (2013) Transplantation of human islets without immunosuppression. *Proc Natl Acad Sci U S A* 110(47):19054-19058.
314. Lee SH, *et al.* (2009) Human beta-cell precursors mature into functional insulin-producing cells in an immunoisolation device: implications for diabetes cell therapies. *Transplantation* 87(7):983-991.
315. Matveyenko AV, Georgia S, Bhushan A, & Butler PC (2010) Inconsistent formation and nonfunction of insulin-positive cells from pancreatic endoderm derived from human embryonic stem cells in athymic nude rats. *Am J Physiol Endocrinol Metab* 299(5):E713-720.
316. Miyazaki S, Yamato E, & Miyazaki J (2004) Regulated expression of pdx-1 promotes in vitro differentiation of insulin-producing cells from embryonic stem cells. *Diabetes* 53(4):1030-1037.
317. Lavon N, Yanuka O, & Benvenisty N (2006) The effect of overexpression of Pdx1 and Foxa2 on the differentiation of human embryonic stem cells into pancreatic cells. *Stem Cells* 24(8):1923-1930.
318. Bernardo AS, *et al.* (2009) Biphasic induction of Pdx1 in mouse and human embryonic stem cells can mimic development of pancreatic beta-cells. *Stem Cells* 27(2):341-351.
319. Lin HT, *et al.* (2007) Enhancement of insulin-producing cell differentiation from embryonic stem cells using pax4-nucleofection method. *World J Gastroenterol* 13(11):1672-1679.
320. Treff NR, *et al.* (2006) Differentiation of embryonic stem cells conditionally expressing neurogenin 3. *Stem Cells* 24(11):2529-2537.
321. Shiroi A, *et al.* (2005) Differentiation of embryonic stem cells into insulin-producing cells promoted by Nkx2.2 gene transfer. *World J Gastroenterol* 11(27):4161-4166.
322. Kubo A, *et al.* (2011) Pdx1 and Ngn3 overexpression enhances pancreatic differentiation of mouse ES cell-derived endoderm population. *PLoS ONE* 6(9):e24058.
323. Raikwar SP & Zavazava N (2012) PDX1-engineered embryonic stem cell-derived insulin producing cells regulate hyperglycemia in diabetic mice. *Transplantation research* 1(1):19.
324. Marchand M, *et al.* (2009) Mouse ES cells over-expressing the transcription factor NeuroD1 show increased differentiation towards endocrine lineages and insulin-expressing cells. *Int J Dev Biol* 53(4):569-578.
325. Raikwar SP & Zavazava N (2011) Spontaneous in vivo differentiation of embryonic stem cell-derived pancreatic endoderm-like cells corrects hyperglycemia in diabetic mice. *Transplantation* 91(1):11-20.

326. Hockemeyer D, *et al.* (2009) Efficient targeting of expressed and silent genes in human ESCs and iPSCs using zinc-finger nucleases. *Nat Biotechnol* 27(9):851-857.
327. Smith JR, *et al.* (2008) Robust, persistent transgene expression in human embryonic stem cells is achieved with AAVS1-targeted integration. *Stem Cells* 26(2):496-504.
328. Liew CG, Draper JS, Walsh J, Moore H, & Andrews PW (2007) Transient and stable transgene expression in human embryonic stem cells. *Stem Cells* 25(6):1521-1528.
329. Hua H, *et al.* (2013) iPSC-derived beta cells model diabetes due to glucokinase deficiency. *J Clin Invest* 123(7):3146-3153.
330. Micallef SJ, *et al.* (2012) INS(GFP/w) human embryonic stem cells facilitate isolation of in vitro derived insulin-producing cells. *Diabetologia* 55(3):694-706.
331. Pannell D & Ellis J (2001) Silencing of gene expression: implications for design of retrovirus vectors. *Rev Med Virol* 11(4):205-217.
332. Cockrell AS & Kafri T (2007) Gene delivery by lentivirus vectors. *Mol Biotechnol* 36(3):184-204.
333. Stoppie P, *et al.* (2000) R115866 inhibits all-trans-retinoic acid metabolism and exerts retinoidal effects in rodents. *The Journal of pharmacology and experimental therapeutics* 293(1):304-312.

Appendices

Appendix A 96-well Plate Adenoviral Transcription Factor Delivery Map For HCS in hAF cells

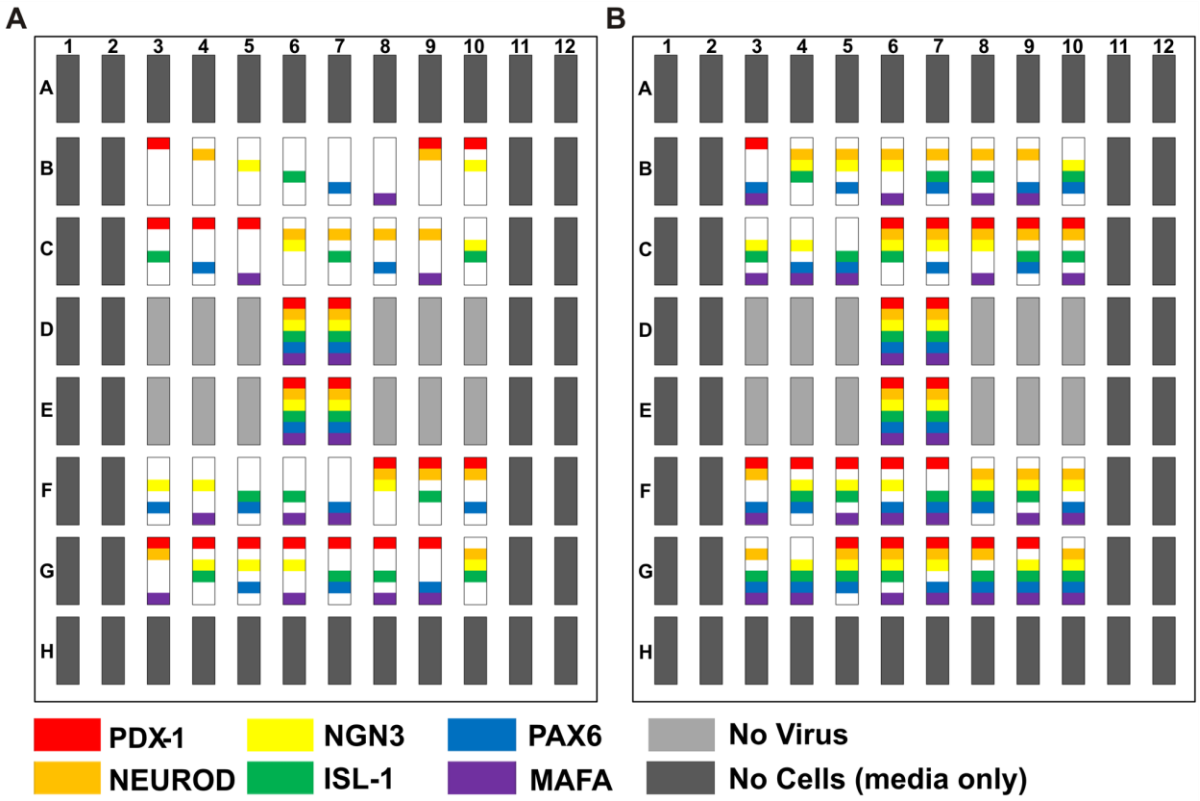

Appendix B Pancreatic Differentiation Conditions Used in Chapter 6 Adapted from Bruin et. al (2014)

B.1 Basal Media Formulations

Stage	Medium Component	Concentration	Cat #	Source
1 - 2 "MCDB-LG"	MCDB131 basal medium	--	10372	Invitrogen
	Fatty acid free bovine serum albumin (FAF BSA)	2%	68700	Proliant
	$NaHCO_3$	2.5 g/L	S233-500	Fisher
	ITS-X (Insulin, Transferrin, Selenium, Ethanolamine Solution)	1:5000	51500	Invitrogen
	GlutaMAX™	1X	35050-061	Invitrogen
	Glucose	7.5 mM	D14-500	Fisher
3 – 7 "MCDB-HG"	MCDB131 basal medium	--	10372	Invitrogen
	BSA	0.1%	11021-037	Invitrogen
	$NaHCO_3$	2.5 g/L	S233-500	Fisher
	ITS-X	1:200	51500	Invitrogen
	GlutaMAX™	1X	35050-061	Invitrogen
	Glucose	25 mM	D14-500	Fisher

B.2 Daily Growth Factor Additions

Stage (# days)	Basal Medium	Day(s)	Compound	Concentration	Source
Stage 1: Definitive Endoderm (4 days)	MCDB-LG	1	GDF8 (Myostatin)	100 ng/mL	Peprotech
			MCX-928 (GSK3β inhibitor; 14-Prop-2-en-1-yl-3,5,7,14,17,23,27-heptaazatetracyclo [19.3.1.1~2,6~.1~8,12~]heptacosa-1(25),2(27),3,5,8(26),9,11,21,23-nonaen-16-one)	2.5 μM	BetaLogics
		2 - 4	GDF8 (Myostatin)	100 ng/mL	Peprotech
Stage 2: Primitive	MCDB-LG	5 - 6	FGF7	50 ng/mL	R&D Systems

Stage (# days)	Basal Medium	Day(s)	Compound	Concentration	Source
Gut Tube (2 days)					(#251-KG)
Stage 3: Foregut Endoderm (4 days)	MCDB-HG	7 – 10	FGF7	50 ng/mL	R&D Systems (#251-KG)
			Activin A	20 ng/mL	R&D Systems (#338-AC)
			SANT-1	0.25 µM	Sigma (#S4572)
			Retinoic acid	2 µM	Sigma (#R2625)
			LDN193189 (BMP receptor antagonist)*	200 nM	Betalogics
Stage 4: Endocrine Progenitors (3 days)	MCDB-HG	11 – 13	SANT-1	0.25 µM	Sigma (#S4572)
			LDN193189*	200 nM	Betalogics
			TBP (PKC activator)*	500 nM	EMD Millipore Chemicals (#565740)
			CYP26A inhibitor (333)	100 nM (in 45% ethanol: 55% PEG 400 solution)	BetaLogics
Stage 5: Pancreatic Endoderm (3 days)	MCDB-HG	14 – 16	LDN193189*	200 nM	StemGent
			ALK5 inhibitor II *	1 µM	Axxora
			CYP26A inhibitor	100 nM (in 45% ethanol: 55% PEG 400 solution)	BetaLogics
Stage 6: Pancreatic Endocrine (3 days)	MCDB-HG	17 – 19	LDN193189*	200 nM	BetaLogics
			ALK5 inhibitor II *	1 µM	Axxora

Stage (# days)	Basal Medium	Day(s)	Compound	Concentration	Source
Stage 7: Polyhormonal Endocrine (7 days)	MCDB-HG	20 - 26	LDN193189*	200 nM	StemGent
			ALK5 inhibitor II *	1 µM	Axxora
			Vitamin A (retinol)*	100 nM	Sigma (#R7632)

* Light sensitive compound; minimize exposure of differentiation culture media to light.